UNIVERSITY OF PALERMO

Department of Civil, Environmental, Aerospace, Materials Engineering

DICAM

PhD IN CIVIL, ENVIRONMENTAL AND MATERIAL ENGINEERING

Transportation Infrastructures Engineering and Geomatics

S.S.D. ICAR/04

PhD THESIS

Calibration of microscopic traffic simulation models for evaluating operation and safety performance at roundabouts

PhD Candidate
Eng. Maria Luisa Tumminello

Coordinator:
Prof. Eng. Antonina Pirrotta

Tutor:
Prof. Eng.Orazio Giuffrè
Prof. Eng. Anna Granà

Co-Tutor:
Eng. Antonino Sferlazza

CICLE XXX

February 2018

UNIVERSITÀ DEGLI STUDI DI PALERMO

Department of Civil, Environmental, Aerospace, Materials Engineering

DICAM

PhD IN CIVIL, ENVIRONMENTAL AND MATERIAL ENGINEERING

Transportation Infrastructures Engineering and Geomatics

CICLE XXX – S.S.D. ICAR/04

PhD THESIS

Calibration of microscopic traffic simulation models for evaluating operation and safety performance at roundabouts

PhD Candidate
Eng. Maria Luisa Tumminello

Coordinator:
Prof. Eng. Antonina Pirrotta

Tutor:
Prof. Eng. Orazio Giuffrè

Prof. Eng. Anna Granà

Co-Tutor:
Eng. Antonino Sferlazza

ACKNOWLEDGEMENTS

TABLE OF CONTENTS

CHAPTER THREE:

Uncertainty in capacity estimation at roundabouts

1. Introduction

2. Preliminary hypothesis

3. Monte Carlo simulation

4. Uncertainty analysis with Crystal Ball Software

CHAPTER FOUR:

Genetic algorithm-based calibration of microscopic traffic simulation model. Application for single-lane and double-lane roundabouts

1. Introduction

2. Traffic flow modelling

3. Microscopic behavioural models

4. Modelling single-lane and double-lane roundabouts in AIMSUN

CHAPTER FIVE:
Estimation of Passenger Car Equivalents for single-lane and double-lane roundabouts

CHAPTER SIX:
Surrogate safety measures at roundabouts in AIMSUN and VISSIM environment

CONCLUSION
Findings and Future Developments

FOREWORD

I.1 THE BACKGROUND

Microscopic traffic simulation models have become increasingly useful tools for the advanced analysis of transport systems and have proven to be an active field of research in computer science and transportation engineering. Advances in research and current application to road and highway planning and design over the last few years have outlined their great potential to assess operational performances and safety effects on road facilities, since they can support the evaluation of road policy and infrastructure changes before implementing them in the real world.

Differently from analytical approaches, microscopic traffic simulation models capture road traffic interactions through a combination of complex algorithms which take into consideration car following, lane changing and gap acceptance describing real-world driving behavior. Thus, microsimulation enables the analyst to develop increasingly higher levels of complexity and uncertainty in operations of road networks and single installations. However, concerns are often expressed by practioners about the possible misuse of traffic microsimulation. In simulation studies, indeed, model calibration is a very crucial task, since reliable results must be obtained from the analysis that is made. Results of several applications, as the technical literature in the road engineering sector refers, show that simulation-based optimization methods can be usefully applied in the calibration process of microscopic traffic simulation models. Incorporating the optimization problem within the model calibration, the iterative process of manually adjusting the model parameters, that users and practioners are required to perform, can be automatized. However, in order to automate the iterative process of manually adjusting the model parameters, some microscopic traffic simulation models have to be still enhanced with custom models and/or have be equipped with various APIs (if available) to remotely control the simulation. Now for practical implications, the question is how to provide integrated software solutions, user-friendly for practioners and transportation engineers which use microsimulation for real world case studies in the professional sphere. In this regard, engineers often need an analytical aid to develop their own codes and adapt the objective function to the specific requirements of the problems that are often encountered in their professional practice.

Besides, despite several microscopic traffic simulation models are capable of modeling road networks and single road entity, transportation engineers often lack proper knowledge of the performance of different simulation tools in modeling the same (safety or operational) problem of practical relevance that needs to be solved.

I.2 THE AIMS OF THIS PHD THESIS AND ITS ARTICULATION

Starting from above considerations, this PhD thesis focuses on the use of microscopic traffic simulation models as useful tools to evaluate operational and safety performances at roundabouts. Case studies of roundabouts are selected and then built in AIMSUN in order to perform the calibration process appropriately.

Roundabouts are selected among road entities since they have become an important component in urban transportation system and have been widely selected in many cities as the preferred traffic control mode due to their convenience for operations with less conflict points, slower speeds and better landscape. Roundabouts can represent an effective engineering solution in a wide array of possible applications with respect to operations, safety, and geometric design; thus, there are many reasons for selecting a roundabout as the preferred alternative over other forms of at-grade intersections, with each reason carrying its own considerations and trade-offs. Turbo roundabouts are also examined and studied since several turbo installations have already been implemented around the world.

In this PhD thesis issues related to the estimation of the behavioral parameters on which gap-acceptance capacity modeling is based and uncertainty in capacity estimates are preliminarily studied. The calibration problem in AIMSUN is explored and then solved by optimization. In this case genetic algorithms have been used. Based on the calibrated model, the passenger car equivalents for heavy vehicles driving roundabouts are calculated. Finally, the use of surrogate safety measures produced by microsimulation is introduced; a comparison between two microscopic traffic simulation models (i.e. AIMSUN and VISSIM) is performed to evaluate the their effect on the determination of traffic conflicts and other surrogate measures that can be useful in safety analysis of roundabouts.

At last findings and possible future work directions are presented.

Based on the general aims as above explained, this PhD thesis is articulated as follows.

Chapter 1 summarizes the geometric and functional features of modern and alternative roundabouts, and presents some roundabout layouts and the main characteristics of their geometric design. Focus is also made on modeling methods for roundabout capacity analysis, especially capacity evaluation based on gap-acceptance theory and capacity formulae currently used by engineers and practitioners, as well as on safety issues of driving roundabouts.

Chapter 2 introduces the gap-acceptance parameters which explain the traffic interaction of a minor street vehicle when enters the roundabout, merging into or crossing one or more circulating (major) streams. Considering that several studies and researches provide measurements of critical and follow-up

headways from real data at roundabouts, in this chapter the objective of achieving a meta-analytic estimation of the critical and the follow up headways to be used for entry capacity estimation at roundabouts is pursued. Thus, issues on summarizing the data from series of selected studies to interpret variation across the studies are preliminarily described; based on several studies and researches developed worldwide a systematic literature review on estimations of critical and follow-up headways at roundabouts is then presented. At last, the summary effect for each of the parameters under examination is computed both for single-lane and double-lane roundabouts, as well as for turbo roundabouts. The results are then used in the further applications with AIMSUN.

In turn, the purpose of Chapter 3 is to study how to derive the entry capacity distribution which accounts for the variations of the contributing (random) variables and suggest how to consider this issue in the operational analysis of roundabouts. Monte Carlo simulation is applied to get the distribution of entry capacity; Crystal Ball software is found effective for performing the random sampling from the probability density functions of each contributing parameter. A steady-state model of capacity is used for performing many runs; in each run, the values of each contributing parameter are randomly drawn from the corresponding distributions. First simulations and the entry capacity distributions at roundabouts are presented once the probability distributions of the headways are assumed. A comparison of the capacity values based on a meta-analytic estimation of critical and follow-up headways and the capacity functions based on the probability distributions of the model parameters is performed to gain insights in developing an appropriate approach to capacity estimation at roundabouts.

In turn, Chapter 4 presents a genetic algorithm-based approach to calibrate microscopic traffic simulation models. The genetic algorithm tool in MATLAB® and AIMSUN micro-simulator were used. A subroutine in Python implemented the automatic interaction of AIMSUN with MATLAB®. Focus is made on two roundabouts selected as case studies. Empirical capacity functions based on meta-analytical estimations of critical and follow up headways are used as reference for calibration purposes. Objective functions are defined to minimize the difference between the empirical capacity functions and simulation output data. Some model parameters in AIMSUN, which can significantly affect the simulation outputs, are selected. A better match to the empirical capacity functions is reached with the genetic algorithm-based approach compared with that obtained using the default parameters of AIMSUN and the values of the model parameters derived from manual calibration. The GA-calibrated model is the starting point for performing the research activities described in chapter 5.

Chapter 5 introduces a criterion to find the passenger car equivalents that reflect traffic conditions at roundabouts, where the capacity is typically

estimated for each entry lane. This research activity was performed since the calculation of passenger car equivalents for heavy vehicles represents the starting point for the operational analysis of road facilities and other traffic management applications.

Based on the equivalence defined by the proportion of capacity used by vehicles of different classes, the criterion implies a comparison between the capacity that would occur with a traffic demand of passenger cars only and the capacity reached beginning from a demand with a certain percentage of heavy vehicles. A preliminary activity, as introduced in chapter 4, consisted of the comparison of the empirical capacity functions - based on a meta-analytical estimation of critical and follow up headways - and simulation output data obtained - for two roundabouts built in AIMSUN – by using the default values, the manually calibrated values and GA calibrated values of the model parameters. Differently from methods that propose constant values for the passenger car equivalents, the passenger car equivalents at single-lane and double-lane roundabouts vary when the circulating flow varies, and a higher effect is obtained when the traffic streams include a higher number of heavy vehicles.

At last Chapter 6 introduces issues on safety analysis through microscopic traffic simulation models and use of surrogate safety measures. The Surrogate Safety Assessment Model (SSAM) is used as a post-processor to analyze the batch of TRJ files from two microscopic traffic simulation models (i.e. AIMSUN and VISSIM); it is used to analyze vehicle-to-vehicle interactions, identify conflict events and then catalog all events found. SSAM is also used to calculate several surrogate measures of safety as time to collision (TTC), post-encroachment time (PET), deceleration rate (DR), maximum speed (MaxS), and so on.

Since safety assessment of any road entity can be very different depending on the micro-simulator which is applied, the objective of exploring the safety performance of different roundabout layouts through surrogate measures of safety is pursued. AIMSUN and VISSIM are used to built, for each roundabout layout, their own calibrated model which fits the same empirical capacity function (one for each roundabout here examined). Thus, SSAM is able to perform the corresponding output data which are compared and then discussed. Implications of various traffic scenarios on the safety performance of the examined roundabouts are also discussed.

CHAPTER ONE:

Functional aspects of roundabouts: capacity and safety

1. Introduction

The roundabout as a particular intersection configuration was born in the early twentieth century in Paris, France, without any success: poor operating conditions occurred due to a traffic regulation giving priority to entering flows. In turn, at the end of the eighties, the yield-rule changed: the circulating flow on the ring was considered to be the priority stream over the entering flows; thus, operating conditions have been considerably improved. Henceforth, this type of intersection became increasingly used for new installations or converting existing ones [1].

Roundabouts have become an important component in urban transportation system and have been widely selected in many cities as the preferred traffic control mode due to their convenience for operations with less conflict points, slower speeds and better landscape. Roundabouts can represent an effective engineering solution in a wide array of possible applications with respect to operations, safety, and geometric design; thus, there are many reasons for selecting a roundabout as the preferred alternative over other forms of at-grade intersections, with each reason carrying its own considerations and trade-offs.

Roundabouts may better handle traffic problems at two-way stop-controlled intersections with high volume of left turns from major streets, since they offer a more effective treatment to left turns than other control modes; they may represent a favourable alternative even under situations with low minor street volume. Roundabouts that operate within their capacity usually produce lower delays than similarly sized signalized intersections that operate with similar traffic volumes and right-of-way limitations. In comparison to signalized intersections, roundabouts eliminate dangerous situations, such as red-light running, and remove some of the most serious conflict points, including angle, left-turn, and head-on crashes. Roundabouts are also an effective alternative to signalized control for closely spaced intersections, because they better manage vehicle queues between successive intersections. Improved capacity at roundabouts is due to the continuously flowing nature of yielding only until a gap is available, versus waiting at a traffic signal. Roundabouts also encourage motorized users to slow down, especially when the constraints of the built environment limit their size [2, 3].

Typically, modern roundabouts are classified according to the number of circulating lanes and the width of the central island diameter; in turn, the "alternative" ones are characterized by their specific geometric design. The most classic example for modern roundabouts is represented by single-lane layout, having one-lane entries and exits and one-lane circulatory roadway on the ring. When traffic volumes are very high, the number of circulating lanes needs to be increased by modifying the "single-lane" roundabout to the "multi-lane"

roundabout to improve entry capacity. Standards and guidelines used worldwide distinguish further roundabout categories within the single-lane and multi-lane roundabouts based on the key dimensions of geometric design; for instance, within the multi-lane roundabouts one can identify the double-lane roundabouts having a circulatory roadway that can accommodate two vehicles travelling side-by-side and double-lane entries and exits. However, geometric design and operations at double-lane roundabouts are more complex than single-lane roundabouts. Using the double-lane roundabout layout as a design solution to increase entry capacity, the same level of safety as single-lane roundabouts cannot be maintained. Indeed, when the circulatory roadway of a roundabout is composed by more than one lane, vehicles weaving and merging among circulating lanes cause large traffic and safety problems. Thus, passing from single-lane roundabouts to double-lane roundabouts, entry capacity increases but safety decreases because the number of conflict points grows. The issue could be solved by using "alternative" multi-lane roundabouts, as turbo-roundabouts, rather than modern ones, that make it possible to improve operating conditions without compromising safety [4]. The turbo-roundabout was introduced in the Netherlands by Fortuijn [5] in the late 1990's and it is characterized by a spiralling traffic flow and physical barriers among lanes, i.e. curbs prevent the possibility of moving between adjacent circulating and entry lanes; in turn, Tollazzi [4] patented and then introduced other alternative schemes of roundabout (e.g. the flower roundabout) [4]. Thus, considering an alternative solution of roundabout, conflict points can be reduced [1].

It must be said that in a general way any safety improvement on a roundabout involves not only an effective reduction of conflict points (as it will be explained in more detail below), but modest driving speeds allow longer reaction and perception times by drivers, who can therefore better handle complex situations at a potential point of conflict; moreover, low driving speeds in the proximity of any road intersection reduce the severity of a possible crash. In a nutshell, higher safety at roundabouts is attributable to: i) fewer conflict points; ii) no left-turn crashes; iii) simple decision-making at the entries; iv) slow relative speeds of all vehicles in the conflict area; v) splitter islands providing refuge for pedestrians and permit them to cross one direction of traffic at a time. Furthermore, roundabouts also show benefits about sustainable design: no power consumption by signal indicators; less pavement; and lower vehicle speeds and consequentially lower employment of energy and emissions [1].

Thus, roundabout intersections for their advantages are today the kind of intersection preferred by many road designers and they are therefore subject to continual study by many road and transportation engineers.

In this chapter, single-lane, double-lane and turbo roundabouts are described, firstly from a geometric and functional point of view; in this regard, geometric features and operating principles for each scheme are presented, and the main

models of capacity for roundabout intersections available in the literature are also provided. At last, the safety of these roundabout layouts is also explored.

2. Roundabout layouts

Three basic categories of roundabouts are usually distinguished according to the size and the number of entry and circulating lanes: mini roundabouts, single-lane roundabouts and multi-lane roundabouts.

As introduced above, standards and guidelines used worldwide further distinguish roundabout categories within the single-lane and multi-lane roundabouts based on the key dimensions of the roundabout geometric design. Without being exhaustive, the following Table 1 offers a comparison of roundabout categories used in many countries worldwide.

2.1. Mini roundabouts

Due to smaller design vehicles and greater constraints of the built environment, mini-roundabouts - usually identified for urban areas - require smaller outer diameters than single-lane and multi-lane roundabouts. One of the main design characteristics that distinguish mini- from single-lane roundabout is the fully traversable central island, also making it possible to accommodate large vehicles. Since mini-roundabouts require a minimal additional pavement, they are considered relatively inexpensive; furthermore, because they are small, mini roundabouts are perceived as pedestrian-friendly with short crossing distances and very low vehicle speeds on approaches and exits.
However, the use of mini-roundabouts is limited because in some cases their installation may be inappropriate due to the reduced ability to control speeds on the traversable central island, so that the trade-off of using mini-roundabouts versus single-lane roundabout should be based on site conditions [1, 4]. As an example, Figure 1 shows the typical layout of mini-roundabouts and the main geometric features.

Table 1. Roundabout category comparison

Country & roundabout layout	outer diameter [m] min	max	circulatory roadway width [m] min	max	entry width [m] min	max	exit width [m] min	max	area (type of roundabout)
Australia [6]									
single-lane	-	80.0	4.60	7.60	4.00	5.00	4.00	5.00	urban and rural
double-lane	-	80.0	8.40	10.30	7.00	8.00	7.00	8.00	urban and rural
France [7]									
mini	15	24	6.0	9.50	2.50	3.50	2.75	3.50	urban
single-lane	30	-	6.0-7.0	9.0	2.5-3	4.0	4.0	4.50	urban
	24	30	6.0	9.0	4.0	4.0	4.0	5.00	rural
double-lane	-	-	7.0	9.0	6.0	7.0	-	-	urban
	24	50	8.50	10	6-7	9.0	6.0	7.00	rural
Germany [8]									
mini	13	24	4.50	5.00	3.25	3.50	3.50	3.75	urban
compact	26	35	6.50	10.0	3.25	3.50	3.25	3.75	urban (single-lane)
	35	45	5.75	6.50	3.50	4.00	3.50	4.25	rural (single -lane)
	>40	60	-	-	-	-	*	*	urban and rural (double-lane)
large	55.0	80.0	-	-	-	-	*	*	urban and rural
Italy [9]									
mini	14	< 25	7.0	8.0	3.50	-	4.00	-	urban (single-lane)
			8.5	9.0	6.00	-	4.00	-	urban (double-lane)
compact	25	< 40	7.0	-	3.50	-	4.50	-	urban and rural (single-lane)
			8.5-9.0	-	6.00	-	4.50	-	urban and rural (double-lane)
conventional	40	< 50	6.00	-	3.50	-	4.50	-	urban and rural (single-lane)
			9.00	-	6.00	-	4.50	-	urban and rural (double-lane)
large	50	-	6.00	-	3.50	-	4.50	-	urban and rural (single-lane)
			9.00	-	6.00	-	4.50	-	urban and rural (double-lane)
Netherlands [10]									
single -lane	32	32	5.50	-	3.5 [a]	4	4	4.50	urban
	36	36	5.25	-	3.5 [a]	4	4	4.50	rural
double-lane	20	38	8	10[c]	3.5 [a]	4	4	4.50	urban
	20	38	8	10[c]	3.5 [a]	4	4	4.50	rural
Sweden [11]									
mini	28	28	12	12	≥3.50	-	≥3.50	4.50	urban
single -lane	30.8	90	5[c]	10.4[c]	3.5	3.5	3.5	4.5	urban and rural
double-lane	30.8	90	5[c]	10.4[c]	7	7	7	7	urban and rural
UK [12]									
single-lane	28	36	**	-	3.0[d]	4.5[d]	7.0-7.50		urban and rural
double-lane	28	100	**	-	7.0[d,e]	9.0[d,e]	10.0-11.0		urban and rural
US [1]									
Mini	14	27	-	-	***	***	-		urban
Single-lane	27	46	4.8	6.1	4.2	5.5	-		urban and rural
Double-lane	46	67	8.5	9.8	7.3	9.1	-		urban and rural
Tree-four-lanes	61	91	12.8	14.6	11.00	13.7	-		urban and rural
Slovenian [13]									
Single lane [f]	27	100	5.4	16.2	3.0	7.3	-		urban and rural
Single lane [g]	27	172	4.5	25.0	2.75	12.5	-		

Note: [a] with splitter island; [b] with splitter island; [c] note that the minimum width of the circulatory lane corresponds to the maximum outer diameter; [d] it is assumed in the UK that it is the entry width rather than the number of lanes that affects capacity; [e] entry width was calculated based on each lane width without entry flaring; [f] recommended dimensions; [g] Border dimensions;* double-lane exit not recommended unless roundabouts are signalized; ** 1.0-1.2 x maximum entry width, *** entry lane and splitter island by inscribed circle diameter or by swept path of large vehicles.
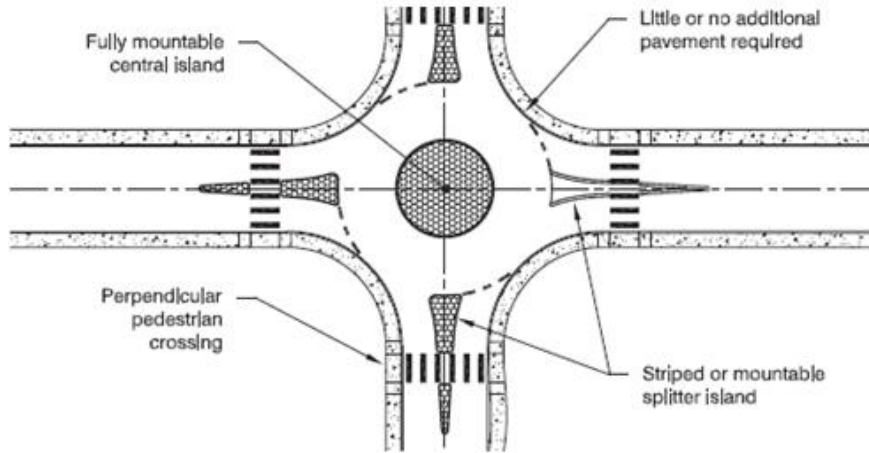
Figure 1 Features of atypical mini roundabout [1]

2.2. Single-lane roundabout

Single-lane roundabouts are distinguished from mini roundabouts by their larger inscribed circle diameters and non-traversable central islands. This allows slightly higher speeds at entry, on the circulatory roadway, and at the exit, than mini roundabouts. It is characterized as having a single-entry lane at all legs and one circulatory lane. The geometric design typically includes raised splitter islands, a non-traversable central island, crosswalks, and a truck apron. The size of the roundabout is largely influenced by the choice of design vehicle and available right-of-way [1]; see Figure 2 for an example layout of single-lane roundabout and Figures 3 and 4 for examples from Google.
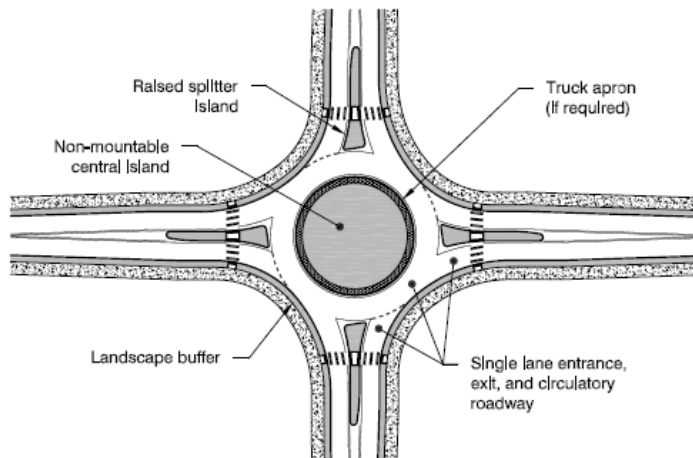
Figure 2 The example layout of the single-lane roundabout.

Figure 3 An example of single-lane roundabout located in Mazara Del Vallo, Trapani, Italy, from Google
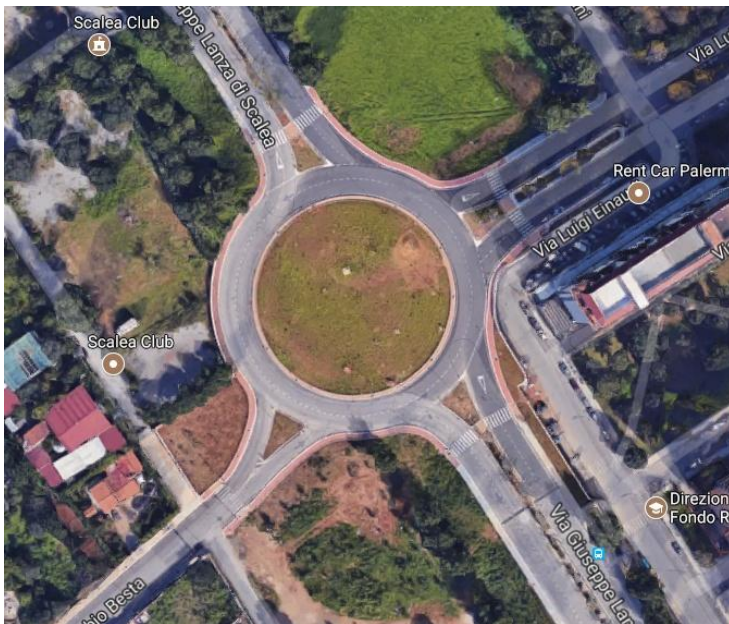
Figure 4 An example of single-lane roundabout located in Palermo, Italy, from Google

2.3. Double-lane roundabout

Multilane roundabouts have at least two or more lanes on the circulatory roadway, while at least one entry approach has the same number of lanes which characterize the circulatory roadway. In some cases, roundabouts may have a different number of lanes on one or more approaches (e.g., two-lane entries on the major road and one-lane entries on the minor road. The speeds at the entry, on the circulatory roadway, and at the exit are similar or may be slightly higher than those for single-lane roundabouts; see Figure 5 for an example of double-lane roundabout.

As introduced above, within multi-lane roundabouts, one can identify double-lane roundabouts, having double-lane entries and exits, and a circulatory roadway that can accommodate two vehicles travelling side-by-side. The most critical design objective, common to all roundabout categories, is to maintain low and consistent speeds at the entries and through the roundabout. The geometric design and operations at double-lane roundabouts, however, are a more complex issue than single-lane roundabouts [2]. In general, double-lane design should address:

a) appropriate lane arrangements to ensure lane continuity, so that drivers select the correct lane before entering and navigate within the same lane through the roundabout to the desired exit, without competing for the same space;

b) adequate alignment of the approaches so that vehicles are accommodated in adjacent lanes at the entrance line and through the roundabout, without path overlap;

c) entry speed control through adequate deflection;

d) more extensive pedestrian and cyclist's features, and so on.

Traffic patterns and gap acceptance behaviour have been shown to influence the capacity mechanisms and determine the efficiency with which a roundabout operates [3]. In general, as best practices and design principles suggest for roundabouts, the number of entry, circulating and exit lanes should be limited to the minimum number that achieves the desired capacity, as well as safety and operating requirements for the projected future traffic volumes. For this reason, lane assignment should be identified on the preliminary design in order to retain information about the lane configuration through the various design iterations.

To maximize the level of safety and efficiency during the early years of operation, a single-lane roundabout may be the interim configuration, initially built to serve the near-term traffic volumes; the entries and the circulatory roadway can be cost-effectively expanded within a horizon of 10 to 15 years from the present to

accommodate the future traffic volumes [1]. Fugal et al. [14] explored the features of a good expandable roundabout design and proposed two alternative approaches to convert an initial single-lane layout to a future double-lane roundabout: one alternative requires building the full outside footprint and widening inward, whereas the other alternative involves building the central island and splitter islands in the ultimate configuration and widening outward. Expansion from a single-lane roundabout to a double-lane roundabout can be driven by the long-range volume forecasts that exceed single-lane roundabout capacity and needs of higher capacity and improved traffic performances, especially for urban roads and arterials [15].
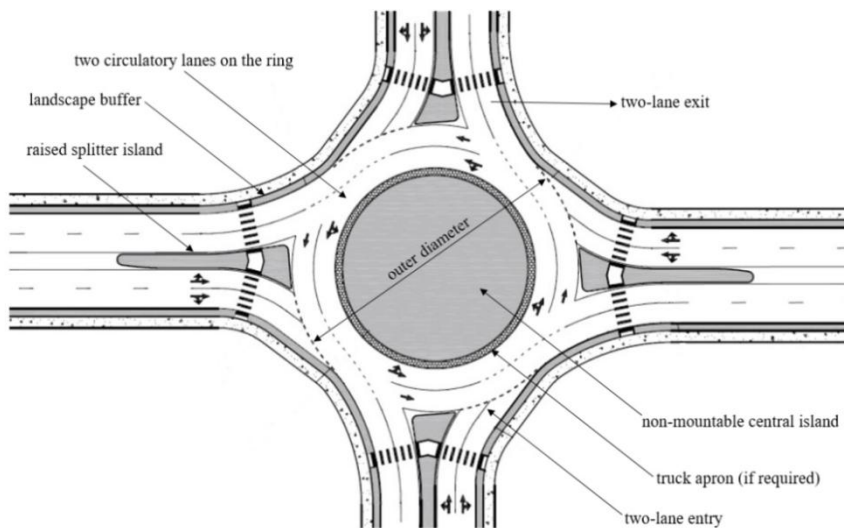
Figure 5 The example layout of the double-lane roundabout.

It is noteworthy that double-lane roundabouts that operate within their capacity may represent a favorable alternative to signalized control for closely spaced intersections; indeed, double-lane roundabouts provide better operational performance in terms of stops, delays, vehicle queues between successive intersections, safety and pollutant emissions than signalized intersections.

Double-lane roundabouts also require less footprint of space than signalized intersections, since they reduce lane requirements between intersections and may not need more area on the approaches. Improved capacity at double-lane roundabouts is due to the continuously flowing nature of yielding only until a gap is available, versus waiting turns at a red light. However, the double-lane design produces patterns of conflict at entries with one or two conflicting traffic streams; this should be taken into consideration when analysts have to calculate entry capacity especially under heterogeneous traffic conditions and assess the different degrees of traffic functionality through level-of-service determinations.

2.4. Turbo roundabout

Turbo roundabouts belong to a particular type of roundabout intersection, called "alternative", because they provide a valid and effective design solution to overcome the limitations related to the use of the multi-lane roundabouts [5].

Alternative types of roundabouts typically differ from "standard" ones - or two-lane roundabouts in one or more design elements; some of them are already in frequent use all over the world (hamburger, dumb-bell…), while some of them are recent and have only been implemented within certain countries (turbo, dog-bone, compact semi-two-lane circle…) or are still at the development phase (turbo-square, flower, target, with segregated left-turn slip-lanes…)[4]. Among all these alternative types of roundabouts mentioned above, turbo-roundabouts are surely the most popular and attractive all over Europe.

The turbo-roundabout was developed in 1996 by Fortuijn [5], and is considered a special type of two-lane roundabout, where some traffic flows are separated physically due to curbs, thus eliminating necessity of weaving.
The central island of the turbo roundabout is composed by multiple centers of the outer and inner diameters; thus, it seems to be a spiral or "turbine." Due to its particular configuration, all entry flows at a turbo-roundabout require a pre-selection of the direction, or of the entry lanes, since these run separately at the entry, throughout the roundabout and at the exit from this; the physical separation of traffic flows is interrupted only at entry into the inner circulatory roadway. In this regard, traffic signs should be quickly and easily intelligible, designed and presented so that their message is comprehended by all users that are approaching the intersection; see Figure 6 for an example of turbo roundabout on real world.

Figure 6 An example of turbo roundabout located in Slovenia [4]

Thanks to their geometric configuration, turbo roundabouts are distinguished from double-lane ones because they manage to overcome several problems

linked to the need to reach a better safety level and high entry capacity. Indeed, turbo roundabouts, with respect to multi-lane roundabouts, provide:

- reduction of the number of conflicts, including complete elimination of weaving and cut-in conflicts through the presence of curbs that also produce some benefit for control speeds;

- inhibition of the possibility of crossing the annular roadway according to the median trajectories that produce partial employment of both circulating lanes;

- a positive effect on the capacity, because the disadvantages of using the inner circulatory lane are removed thanks to the spiral lane marking and the presence of curbs; so, one can conclude that a turbo roundabout makes it possible to distribute the traffic flow better over the different lanes, which makes the entry capacity higher.

According to Fortuijn [5], turbo-lane roundabouts can be classified depending on the number of lanes on the access and exit legs as follows:

- Egg roundabout in which the minor road is composed by a single-lane; it is also nevertheless classified as a main turbo roundabout type, since it is widely used;
    - (Three or four legs) Egg roundabout (in essence a reduced form of the basic turbo roundabout);
    - Basic turbo roundabout;
    - Spiral roundabout;
    - Knee roundabout;
    - Rotor roundabout;
- Three legs only:
    - Stretched-knee roundabout;
    - Star roundabout;

The following Figures 7-12 show examples of roundabout layouts as classified above and reported by [5].

"Egg" turbo roundabout layouts	
Four legs	Three legs
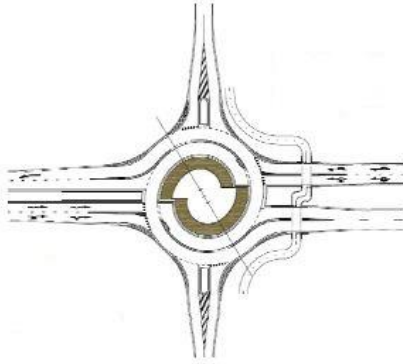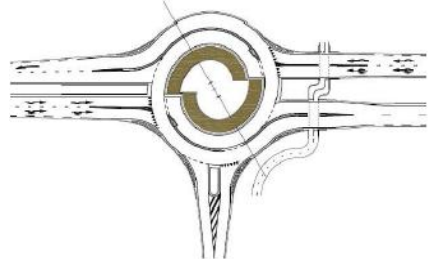
Figure 7 Examples of Egg roundabout layouts

"Basic" layouts of Turbo roundabouts	
Four legs	Three legs
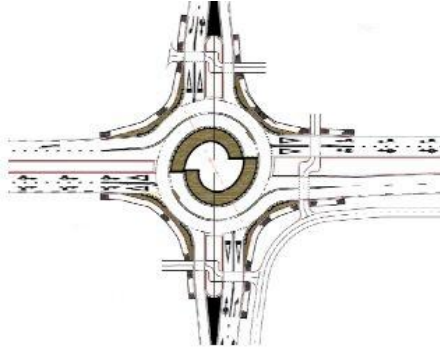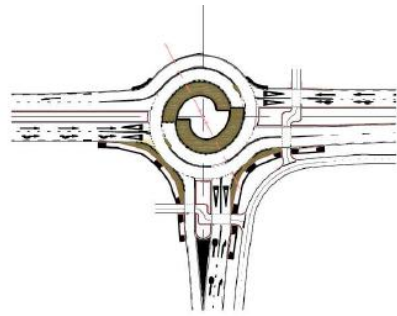
Figure 8 Examples of Basic roundabout layouts

"Spiral" turbo roundabout layouts	
Four legs	Three legs
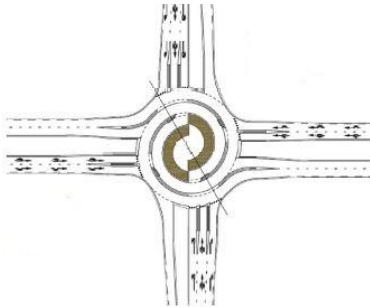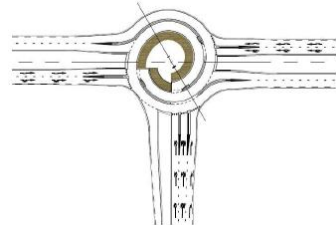
Figure 9 Examples of Spiral roundabout layouts

21

"Rotor" turbo roundabout layout	
Four legs	Three legs
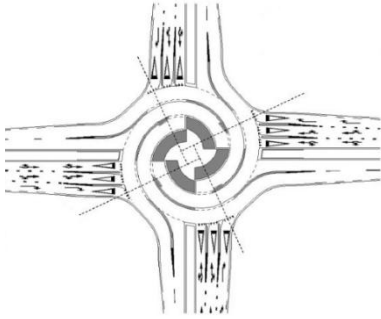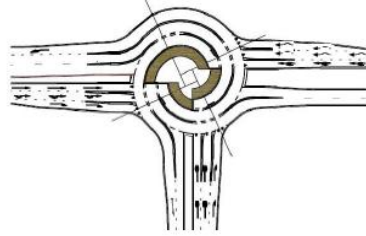
Figure 10 Examples of Rotor roundabout layouts

"Star" turbo roundabout layout	
Four legs	Three legs
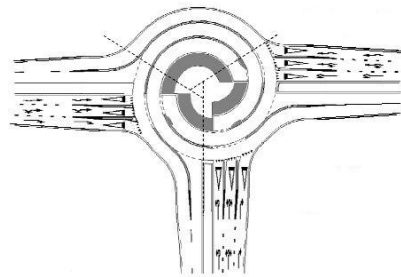
Figure 11 Examples of Star roundabout layouts

Knee turbo roundabout layout	
Four legs	Three legs
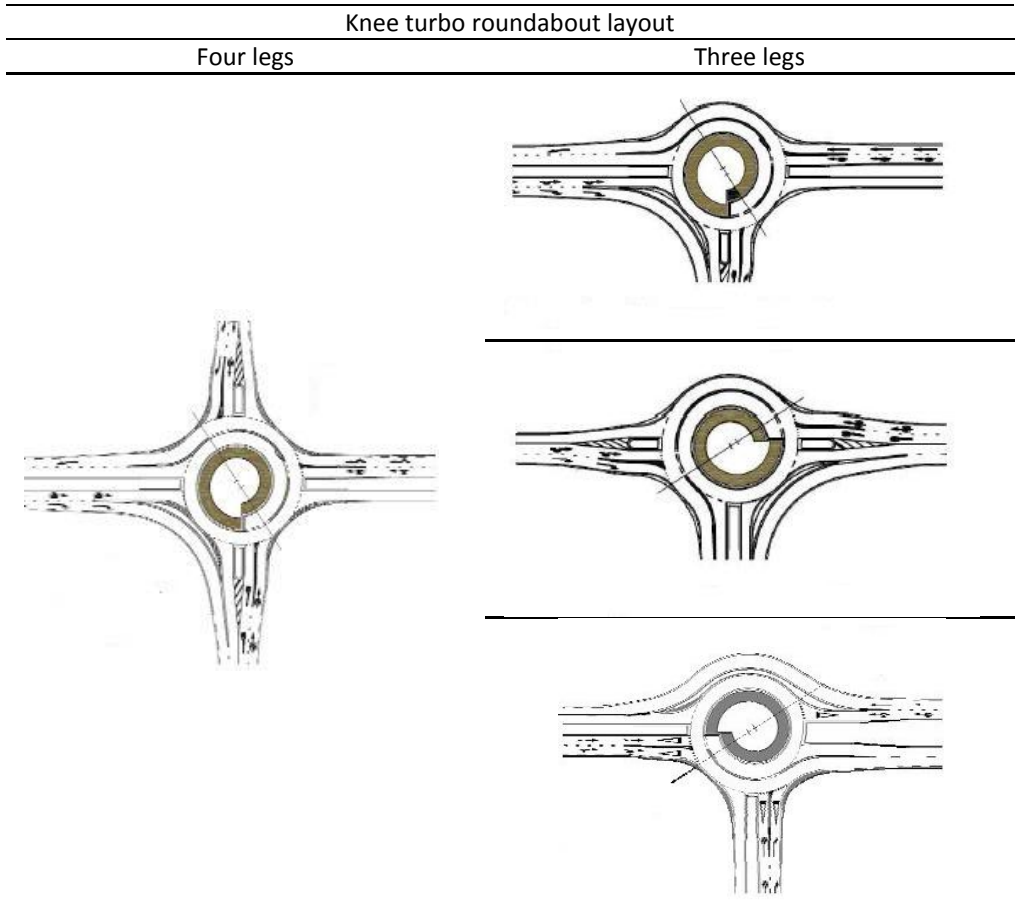
Figure 12 Examples of Knee roundabout layouts

The most used roundabout type, among the aforementioned, is certainly the basic turbo roundabout, which is the subject of this research study.

To better understand its operation, it was considered appropriate to show the following Figure 13, which represents the geometric layout of the turbo roundabout used in this research study. In this scheme it is possible to recognize a basic turbo roundabout formed by two circulating lanes and by four legs, in which one can distinguish a main road (west-east direction) and a minor road (north-west direction). The main road is composed by two entry lanes and two exit lanes; in this case the entry flow only crosses one circulating flow, hence these entry lanes work like that of a single-lane roundabout. By contrast, the minor road is composed by the only one exit lane and by two entry lanes -right and left - whose operation is the same as that of a double-lane roundabout.
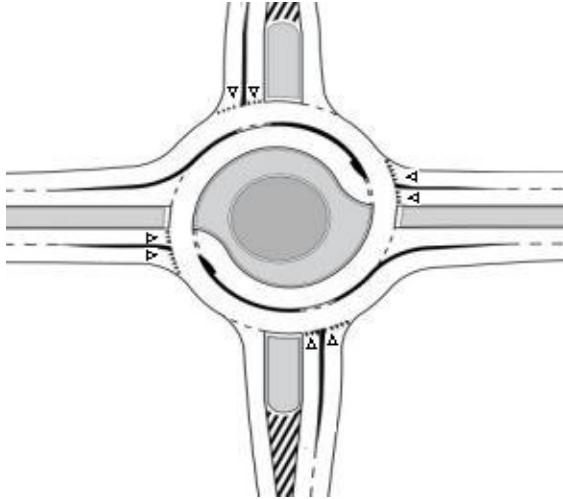
Figure 13 The example layout of the Basic Turbo-roundabout

A geometrical form of the turbo-roundabout is a little complicated as it is formed by the so-called turbo block in Figure 14. This is a formation of all the necessary radii, which must be rotated in a certain way, thereby obtaining traffic lanes or driving lines
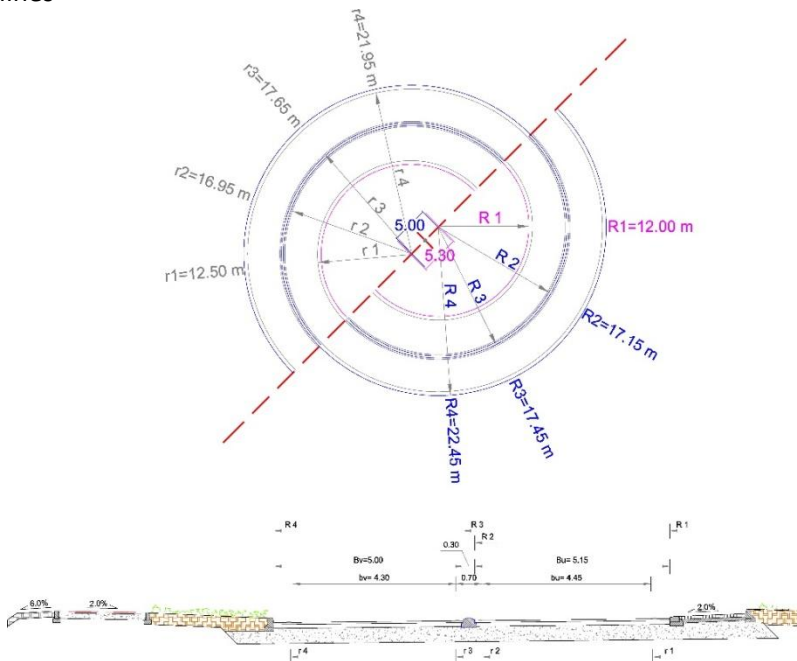
Figure 14 A turbo block with a translator axle

The center of a turbo block must be located in such a way that a radial connection of all entries into the roundabout with a spiral course of a circulatory carriageway is possible. The turbo block also contains (besides all radii) the so-called

24

"*translator axle.*" A translator axle is an axle, where a shift (movement) of different radii occurs. A shift of radii depends on the width of the circulatory traffic lane and on the locations of the verges.

The best position of the translator axle is as if the clock hands pointed to "five minutes to five o'clock" (see Figure 15) in the case of a four-arm or "ten minutes past eight o'clock" in the case of a three-arm turbo-roundabout [4, 5].

The size of the radii of a turbo-roundabout and the width of the circulatory carriageway must be selected in such a way that the driving speed through the roundabout does not exceed 40 km/h (see Table 2 for roundabouts).
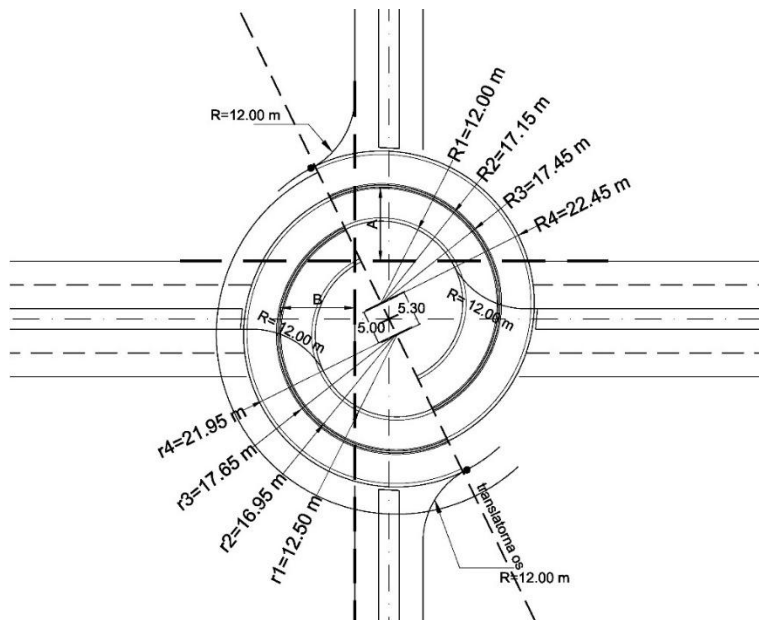
Figure 15 The best position of the translator axle in the four-arm turbo-roundabout (normal size) [4]

As current practice suggests, experiences differ from country to country but, in general, a turbo-roundabout is conditionally an appropriate solution in the cases of:

- an existing single lane roundabout in an over-saturation condition; the size of the outer diameter enables implementation of an additional circulatory lane inwards or with enough space for the implementation of another circulatory lane outwards;
- an existing two-lane roundabout in an over-saturation condition;
- existing traffic not safe enough at two-lane roundabouts;
- reconstruction of a classic intersection with a predominant main traffic direction and with a heavy traffic flow.

In all these cases, the selection of the turbo-roundabout type also depends on the predominant direction of the main traffic flow. Namely, the predominant direction

of the main traffic flow is a criterion for the selection of the turbo-roundabout type. Consequently, different types of turbo-roundabout have been developed for specific combinations of traffic volumes and directions [4, 5].

Table 2 The size of radii of a turbo-roundabout [4]

Size of the turbo roundabouts elements [m]			
Element	Mini	Normal	Medium	Large
R_1	10.45	12.00	14.95	19.95 (21.70)
R_2	15.85	17.15	20.00	24.90 (27.10)
R_3	16.15	17.45	20.30	25.20 (27.40)
R_4	21.20	22.45	25.25	29.95 (32.80)
r_1	10.95	12.50	15.45	20.45
r_2	15.65	16.95	19.80	24.70
r_3	16.35	17.65	20.50	25.40
r_4	20.70	21.95	24.75	29.45
B_v	5.05	5.00	4.95	4.75 (5.40)
B_u	5.40	5.15	5.05	4.95 (5.40)
b_v	4.35	4.30	4.25	4.05
b_u	4.70	4.45	4.35	4.25
D_v	5.75	5.30	5.15	5.15 (5.50)
D_u	5.05	5.00	4.95	4.75 (5.50)

3. Analysis of Operational condition

The process of designing roundabouts, more so than other intersection layouts, requires iteration among geometric layout, operational analysis, and safety evaluation; thus, the designer often needs to revise and refine the initial layout attempt to improve its capacity and safety.

However, modelling of real-world performances can result in a complex action, especially when one has to evaluate:

1) the effect of exiting vehicles on an entering driver's decision (e.g., one can be uncertain of the intentions of the exiting or turning vehicles);
2) conditions of capacity constraint for one or more entries (with the consequent circulating flow downstream of the constrained entry less than the demand);
3) origin–destination patterns, which may influence the capacity of a given entry;
4) differences in vehicle fleet mixes, and so on.

Thus, the operational performance of roundabouts can be influenced by the traffic volume desiring to enter a roundabout at a given time, the vehicle flow rate on the ring and the arrival headway distributions, as well as geometric design, vehicle and environment characteristics that affect each individual gap acceptance behaviour. Geometry also plays a significant role in evaluation of operational performance at roundabouts: the angle at which a vehicle enters can affect the

speed of circulating vehicles; the entry widths can determine the number of side-by-side vehicle streams at the yield line and can affect the rate at which the circulatory roadway may accommodate the vehicles; lane alignment can determine imbalanced lane flows on an entry and thus can influence entry capacity, etc. Thus, the geometric characteristics have an impact on the gap acceptance decision-making and then the capacity [1, 3].

In general, the operational conditions of a roundabout may be studied as a succession of states with a probability associated.
In order to characterize these states, it is important to know the probability associated with each state of the system. Thus, if the probability for a same state varies any time, then the system is in a transient condition. In turn, if the probability of each state remains constant over time, the system is in a steady-state condition.
In turn, the system reaches a statistical equilibrium (i.e., the system is in a steady-state condition) when the probabilities of the states remain constant over time. According to Mauro [3], rather than evaluating the time-invariant state probability distribution, the finding that a steady-state condition exists relies on evaluation of the time invariance of some appropriate statistical values for one or more variables, which evolve randomly, and which are deemed to be related to the operating conditions of the system. Thus, a roundabout can be considered at steady-state condition when entering traffic demand does not change over time and its entries are characterized by under-saturated conditions. In practical terms, a steady-state condition is reached, the entries being under-saturated, when the traffic demand is constant for a finite time interval T which must be:

$$T > max\left[\frac{1}{\left(\sqrt{\frac{C_i}{3600}} - \sqrt{\frac{Q_{ei}}{3600}}\right)^2}\right] \tag{1}$$

where:

- C_i is capacity of entry i;
- Q_{ei} is demand volume of entry i;

The expression (1) is well known as Morse's inequality [16].
This condition can only be applied if the capacity of entry i, C_i and the relative demand volume, both expressed in hourly volumes, can be assumed constant during T, the entries are under-saturated at time T, and the degree of saturation is strictly smaller than unity. Morse's inequality [16], in fact, should make it possible to stabilize the traffic conditions of the roundabout around constant mean values

27

of the state variables (i.e. queue lengths and waiting times). If Morse's inequality is not fulfilled, time-dependent solutions should be used. In other terms, the non-steady-state situations (characterized by the variability of Q_{ei} and/or the over-saturation of the entry under examination having the degree of saturation not sufficiently greater than one) cannot be evaluated through probabilistic and deterministic approaches.

It is noteworthy that this formula can be applied only when the ratio (Q_{ei}/C_i) <1. Besides, it must be said that the steady-state models of entry capacity are only a useful approximation if the duration of the analysis period is considerably greater than the duration calculated using Morse's expression.

3.1. Modeling methods for roundabout capacity analysis

Capacity is commonly defined as the maximum number of entry vehicles that has, under specific geometric and traffic condition, sufficient likelihood of not being exceeded, in a given period of time; it is a determinant parameter for other performance measures such us delay, queue length and portion queued, and waiting time.

In general, the roundabout entry capacity can be expressed by the following formula [3]:

$$C = C(\tilde{G}; Q_d; \tilde{\tau}; \tilde{S}) \qquad (2)$$

where:

- $\tilde{G}$ is a set of variables referred to the geometric characteristic of layout (e.g. number of entries and circulating lanes, central island and entry lane width and so on);
- Q_d is the antagonist traffic flow;
- $\tilde{\tau}$ is a set of psycho-technical times, i.e. critical headway and follow-up headway;
- $\tilde{S}$ is a set of numerical constants that result from the calibration process of the capacity formula.

Based on the formula given above, three types of capacity formulas are distinguished:

- expressions of capacity in which a roundabout is characterized only by its layout, i.e. the number of circle lanes and leg lanes;
- capacity formulas in which geometry is taken into account in a somewhat detailed way;
- capacity expressions that take into account geometric aspects and at the same time users' behaviour.

In general way, the evaluation of operating performances at roundabouts is based on the methods applicable to controlled intersections. These models are generally divided into two categories:

- empirical regression models that are generated from field data and establish relationships between capacity (and/or delay) and geometry;

- gap-acceptance models that are based on the queuing theory.

Empirical models correlate geometric features and operating performance and generate a relationship generally linear or exponential between the entering flow and the antagonist circulating flow. By contrast, gap-acceptance models are used to describe traffic conditions at "give-way" intersections taking into account any driver's behaviour parameters through the queuing theory.

3.1.1. The capacity evaluation based on Gap-acceptance theory

The aim of the gap acceptance theory is to be able to represent as faithfully as possible the behavior of users in those intersections where a traffic flow hierarchy is established. Thus, capacity models based on this theory make it possible to calculate the capacity of secondary currents, taking into account the characteristic behavioral parameters of the users. Indeed, the main capacity models, based on the gap acceptance theory, consider the so-called psycho-technical times, which represent the behavior of the user at the intersection and probabilistic models representing conditions of the vehicle outflow on the main flows. It is noteworthy that behavioral parameters are related to a specify population of users, and represent the behavior enacted in a given intersection scheme and for a specific maneuver, i.e. entry, diversion, crossing, etc. The main behavioral parameters used in the gap-acceptance theory are critical headway, follow-up headway and minimum headway, of which only a short definition will be given here as a wider discussion of these parameters is given in the second chapter.

Roundabout capacity can be studied starting from the capacity model used for two-way-stop-controlled intersections. In effect, driver's behavior at Two-Way-Stop-Controlled (TWSC in the following) intersections and roundabouts is the same: the driver, coming from a secondary flow, can enter an intersection, only when she/he evaluates a sufficiently large gap or headway in the major stream, to consider her/his maneuvers safe. Thus, in the same way, a driver that is at the entry lane of a roundabout looks for a safe gap on the circulatory flow, to make a crossing or turning maneuver. Therefore, critical headway is defined as the minimum time gap in the main flow which the driver in the minor flow is ready to accept for crossing or entering the main flow; in turn, follow-up headway is the gap time between two successive vehicles in the minor flow that entering the conflict area of the intersection exploit the same gap in the main flow.

Capacity calculation for a roundabout in steady-state condition can result from the simple queuing model – in which a single minor traffic stream crosses a single major traffic flow - by specifying the arrival headway distribution in the major stream of volume Q_c(veh/h) and the gap-acceptance function which expresses the number of minor stream vehicles that can depart during an acceptable headway of size τ.

However, an understanding of the interaction of two traffic streams can represent the basic sources of knowledge about capacity estimation for unsignalized intersections and roundabouts with more than two traffic streams. Usually, $n(\tau)$ denotes the number of the minor stream vehicles which can enter the roundabout using time headway of size τ and $f(\tau)$ denotes the probability function of all headways in the major circulating stream. Based on the assumptions about user behaviour at unsignalized intersections and roundabouts as introduced in the previous sections, a biunique correspondence exists between $n(\tau)$ and τ. This is why $f(\tau)$ can be also viewed as the probability distribution of $n(\tau)$ [3]; then the mean value $\bar{n}$ can be calculated as follows:

$$\bar{n} = \int_{\tau=0}^{\infty} n(\tau) \cdot f(\tau) d\tau \tag{3}$$

When one divides this mean value $\bar{n}$ to the average size of headways τ, clearly equal to $\bar{\tau} = \frac{1}{Q_c}$, one can get:

$$C = \frac{\bar{n}}{\bar{\tau}} = Q_c \int_{\tau=0}^{\infty} n(\tau) \cdot f(\tau) d\tau \tag{4}$$

Equation (4) gives the mean number of minor vehicles, which perform their maneuvering in the time unit, i.e., the entry capacity. This equation for the entry capacity of unsignalized intersections and roundabouts forms the foundation of the gap acceptance theory; indeed, most of the analytical capacity models found in literature are based on this concept.

The capacity provided by τ headways per hour is then $Q_c \cdot f(\tau) \cdot n(\tau)$; thus, the capacity is a function of the circulating flow *(Q_c, veh/h)*, which is synthesized by *f(τ)*; in turn, *n(τ)* takes into account the users' psycho-technical attitudes, which are synthesized by the critical headway and the follow-up headway.

The capacity of the simple two-stream situation, and therefore also of the roundabouts, can be calculated by methods based on the elementary probability theory if the following assumptions are used:

1. constant values for the critical headway and the follow-up headway that it means suppose a driver population homogeneous and consistent;

2. negative exponential distribution for major stream headways;
3. each traffic stream is characterized by constant values of the traffic volumes.

Considering constant values for the critical headway and the follow-up headway, two different types of capacity equations can be distinguished based on two different formulations for $n(\tau)$: the first type of capacity equations assumes a stepwise (constant) function for $n(\tau)$ [17], whereas the second type of capacity equations assumes a continuous linear function for $n(\tau)$ [18]. It is noteworthy that when one models the capacity of entries conflicted by two (or more) circulating lanes, the conflicting flow rate is the total of all major streams [19]; thus, all major streams are combined as one traffic stream and examined by using proper multi lane stream parameters. The headway distribution in the major traffic stream can be dealt by using appropriate values of the minimum headway and the bunching parameters.

Some hints about modelling are provided in the following paragraphs.

3.1.2. Counting and Headway Distributions

In general, modeling arrivals of vehicles at a road cross-section is a fundamental step in traffic flow theory. An important application concerns traffic flow simulation in which vehicle generation has to represent vehicles arrivals. However, the vehicle arrival is a random process since several vehicles can come together, or vehicle arrivals can be rare events. Modeling vehicle arrivals means modeling how many vehicles arrive in a given interval of time, or modeling what is the time interval between two arrivals of successive vehicles. In the first process, the random variable is the number of vehicle arrivals observed in a given interval of time; it takes some integer values. Thus, the process can be modelled by a discrete distribution. In the second process, the random variable is represented by the time interval between successive arrival of vehicles and it can be any positive real values; thus, some continuous distributions can be considered to model the vehicle arrivals. It is noteworthy that, being these processes correlated, the distributions that describe them should be also inter-related for better explaining this traffic phenomenon [16].
Bearing in mind the objective to estimate entry capacity at roundabouts, in the following, some discrete distributions are show, which account for traffic counts and are used to model the vehicle arrivals; then, some continuous distributions used for (time) headway modelling are presented.
The derivation of models that take into account the non-uniformity in traffic flow is based on the assumption that vehicle arrivals, at a specified cross section, correspond to some random process [20]. Thus, one should select a probability distribution suitable to represent the observed patterns of traffic arrivals. Among the counting distributions, one can remember the Poisson distribution; the corresponding probability mass function is given as follows:

$$P(n) = \frac{(\lambda \cdot t)^n \cdot e^{-\lambda t}}{n!} \tag{5}$$

Where *P(n)* is the probability of having n vehicle arrivals in the time interval *t*, λ is the average vehicle flow (i.e., the arrival rate in vehicles per unit time), and *t* stands for the duration of the time interval over which vehicles are counted.

Based on the statistical assumptions concerning the derivation of Poisson distribution, the model lends itself well as arrival model in a single lane (or two or more adjacent lanes) when steady-state conditions persist over the analysis time period, and the arrival of one vehicle is independent of the arrival of another vehicle (i.e., no interaction is experienced between the arrivals of two successive vehicles). Empirical observations have shown that the assumption of Poisson-distributed traffic arrivals is most realistic in lightly congested traffic conditions; thus, the model can be consistent with experimental data when the flow is rare and, hence, it can be used when flow rates up to 400–500 veh/h are accommodated.

The Poisson distribution cannot be used without a steady-state condition or when traffic flows reach heavily congested conditions; in these cases, other traffic flow distributions can be considered more appropriate [3].

Another limitation of Poisson model is that the mean of the observations equals the variance [20]. However, many real count data do not adhere to the assumption that the mean and the variance are equal, and another distribution should be used. When the variance exceeds the mean of the counts, the negative binomial distribution can be used; it captures over dispersion, which can take place in various contexts [21]. When, in turn, the mean of the counts exceeds the variance the choice of the probability distribution can fall on the binomial distribution; however, it should be particularized with the measured data [22]. Such distributions are discussed in more specialized sources. The criterion for choosing alternative traffic counting models has been exposed by Mauro & Branco [23]; the same source shows the theoretical probability distributions of arrivals (namely, the binomial, Poisson, and negative binomial distribution) and their expressions as a function of the sample statistics.

Besides counting distributions, suitable for describing counts of discrete units, such as cars, under various conditions of occurrence, another class of distributions is that of interval distributions, which describe the probability of intervals (headways) of different sizes between events and need to be characterized statistically. However, counts of cars deal with discrete events, whereas headways can be measured on a continuous scale. For purely random events, arrival headways are described by the negative exponential distribution; when drivers are forced into non-random behaviour as during congested traffic conditions, other distributions can result more appropriate.

In generally, two types of headway distributions for the major flow are use in gap acceptance models: the negative exponential distribution (M1), and Cowan's M3 distribution [24, 25].

The negative exponential distribution (M1) has been extensively used in literature and it is used for population whose counts are described by the Poisson distribution; it is based on the assumption that each vehicle arrives at random without dependence between successive vehicle arrivals. The probability density function of the negative exponential distribution is given by the following formula:

$$P(h > t) = \lambda e^{-\lambda t} \tag{6}$$

where h stands for the headway between events and $\lambda = Q_c/3600$ is the average arrival rate in the opposing stream expressed in *veh/s*. The cumulative probability function of headways is given by:

$$F(h \leq t) = 1 - e^{-\lambda t} \tag{7}$$

However, the M1 distribution allows unrealistic short headways and does not describe platooning. When traffic volume is so high that each car tends to follow the car ahead, M1 distribution may be unsuitable to describe the headways between cars and can be considered realistic for a very low traffic flow rate (about less than 150 *veh/h*). Thus, the shifted negative exponential distribution (M2) can result more suitable. Indeed, M2 distribution represents the probability that the headway h is less than t with a prohibition of headways less than Δ, that is the shifted exponential distribution assumes that there is a minimum headway between vehicles. The cumulative probability distribution of headways may be stated as follows:

$$F(h \leq t) = 1 - e^{-\lambda(t-\Delta)} \tag{8}$$

Where Δ is the amount of the shift since short headways are prohibited, $\tau \geq \Delta$ and λ is a model parameter calculated as $\lambda = \frac{q}{(1-\Delta q)}$.

Although, the negative and the shifted negative exponential distribution (M1 and M2) are widely used as headway distribution models, the bunched exponential distribution of arrival headways (M3) improves the representation of inter-vehicular time intervals in the (major) circulating stream, and gives a more accurate prediction of arrival headways about up to 12 *s*, that is particularly useful to analyse urban roads and streets.

Modifying the negative exponential distribution by introducing a "bunching" factor α, it is obtained the Cowan's M3 distribution that represents the probability of a headway less than t seconds and may be stated as follows:

$$f(t) = \begin{cases} 1 - \varphi \cdot e^{-\lambda \cdot (t-\Delta)}, & t \geq \Delta \\ 0, & t < \Delta \end{cases} \tag{9}$$

where Δ in this case is the average intrabunch (minimum) arrival headway, φ is the proportion of unbunched (free) vehicles, and λ is a model parameter calculated as $\lambda = \frac{q}{(1-\Delta q)}$, where q is the arrival flow rate which is definite, in vehicle per second, as $q \leq 0.98/\Delta$. The intrabunch headway (or the headway within each bunch equal to the minimum arrival headway Δ) and the proportion of unbunched (free) vehicles (with randomly distributed headways) are related to the distribution of the circulating stream headways.

The average intra-bunch headway corresponds to the average headway at capacity ($\Delta = 3600/C$, where C is the capacity in *veh/h*).

The M3 distribution explicitly takes into account the number of bunched vehicles through the φ parameter representing the proportion of free vehicles. Application of the M3 parameters to each circulating lane of the roundabouts allows to use capacity formulas for n-lanes, each having different Cowan M3 parameters. The M1 and the M2 distributions can be derived from the M3 distribution by assuming *Δ=0* and *φ=1* (and therefore *λ=q*) for the M1 distribution and *φ=1*, and therefore *λ=q/(1-Δq)*, with *q≤0.98/Δ*, for the M2 distribution. One can observe that both distributions assume no bunching, whereas the M3 distribution model can be applied by estimating φ or using a bunching model, which estimates φ as a function of the opposing flow. In practical application, indeed, only the traffic flow is known, not the headway distribution; thus, it is necessary to relate φ or Δ with the opposing flow. Further discussions on the M3 model and gap acceptance models can be found in more specialized sources [26-33].

The arrival headway distribution models can be used together with gap acceptance parameters to derive the capacity models. As above introduced, gap acceptance models are (macroscopic) analytical models, which express the capacity in an exponential function of the circulating flow; thus, the rate of reduction in capacity decreases as the circulating flow increases.

3.1.3. Capacity formulas

The arrival headway distribution models can be used together with gap acceptance parameters to derive the capacity models. As above introduced, gap acceptance models are (macroscopic) analytical models, which express the

capacity in an exponential function of the circulating flow; thus, the rate of reduction in capacity decreases as the circulating flow increases.

Based on the gap acceptance process, for the simple two-stream situation entry capacity can be estimated by elementary probability theory methods; using Eq. 4 and combining a stepwise constant function for the number of minor stream vehicles $n(\tau)$ and the M1 distribution for headways in the major circulating stream, one can obtain the Harders's formula [17]:

$$C_e = \frac{\lambda \cdot e^{-\lambda \tau_c}}{1 - e^{-\lambda \tau_f}}$$

(10)

where:

- $\lambda = q_c/3600$;
- τ_c is the critical gap;
- τ_f is the follow up time.

Assuming a continuous linear function of $n(\tau)$, Siegloch [18] first derived another capacity formula, resulting in a relation of capacity versus conflicting flow $Qc = \lambda \cdot 3600$, that is the following:

$$C_e = \frac{3600}{\tau_f} \cdot e^{-\lambda \cdot \tau_0}$$

(11)

where $t_0 = t_c - t_f/2$.

More recently, this capacity model was revised in the National Research Council and Transportation Research Board [21] as follows:

$$C_e = \frac{3600}{t_f} \cdot e^{-Q_c \cdot \left(\frac{t_c - 0.5t_f}{3600} \right)}$$

(12)

The above capacity model is an exponential regression model based on a gap acceptance theory [16]; this model can be calibrated by using site-specific values for the critical headway and the follow-up headway. Geometry is classified in terms of the numbers of circulating lanes and entry lanes. In this model, shorter critical headways were used for a multilane roundabout than a single-lane roundabout.

More general solutions for the capacity models have been obtained by replacing the M1 distribution with the more realistic M2 and M3 distributions. For instance,

a more general capacity formula is derived by using a dichotomized distribution as follows:

$$C_e = \frac{\varphi \cdot Q_c \cdot e^{-\lambda \cdot (\tau_c - \Delta)}}{1 - e^{-\lambda \cdot \tau_f}}$$

(13)

where $\lambda = (\varphi \cdot Q_c)/(3600 - \Delta \cdot Q_c)$.

If $\varphi = 1 - \lambda \cdot \Delta$ the capacity equation derived by Tanner [34] is obtained with a step function for n(τ), whereas, using the linear relationship for *n(τ)*, the capacity equation derived by Jacobs [35] is given:

$$C_e = \frac{\varphi \cdot Q_c \cdot e^{-\lambda \cdot (\tau_0 - \Delta)}}{\lambda \cdot \tau_f}$$

(14)

The following capacity formula developed by Brilon [28], takes into account the geometric features - i.e. number of entry and circulating lanes - and user's behavior -i.e. the critical headway T_c and follow-up headway T_f .
This capacity formula is based on Tanner's equation [34] and it is expressed as:

$$C = 3600 \cdot \left(1 - \frac{t_{min} \cdot q_k}{n_c \cdot 3600}\right)^{n_c} \cdot \frac{n_e}{t_f} \cdot e^{-\frac{q_k}{3600} \cdot \left(t_g - \frac{t_f}{2} - t_{min}\right)}$$

(15)

where:

- C = capacity of entry lane;   [pcu/h]
- q_k = traffic volume on the circle;   [pcu/h]
- n_c = number of circulating lanes;   [-]
- n_e = number of entry lanes;   [-]
- t_g = critical gap;   [s]
- t_f = follow-up time;   [s]
- t_{min} = minimum gap between vehicles on the circle;   [s]

Capacity formula written above, depends on the circulating traffic flow (q_k) and on the number of circulating and entry lanes. Initially this formula was used by with the values for parameters t_g= 4,1 s, t_f = 2,9 s, t_{min} = 2,1 s from observations by Stuwe [31, 36]. Then, since these parameters were not of a general nature but were derived for a specific type of intersection, Brilon & Wu [33], proposed new values for these parameters depending on the diameter of the roundabout.

The following table shows values for the three parameters t_g, t_f, and t_{min}. It is noteworthy that for the capacity calculation of roundabouts with an inscribed

circle diameter greater than 26 m, i.e. for compact and large roundabouts, a new formula is provided depending only on traffic circulating flow.

Table 3 Capacity formulas for different width of splitter island

Type of roundabout		n_e	n_k	Critical gap t_g [s]	Follow up time t_f [s]	Minimum gap t_{min} [s]
Mini	13≤d≤26 [1]	1	1	$t_g = 3{,}86 + \dfrac{8{,}27}{d}$	$t_f = 2{,}84 + \dfrac{2{,}07}{d}$	$t_{min} = 1{,}57 + \dfrac{18{,}6}{d}$
Compact	26≤d≤40 [2]	1	1			
	40≤d≤60 [3]	1	2	$C = 1440 \cdot e^{-\frac{q_k}{1180}}$		
	40≤d≤60 [4]	2	2	$C = 1642 \cdot e^{-\frac{q_k}{1180}}$		
Large	d>>60 [1][4]	2	2	$C = 1926 \cdot e^{-\frac{q_k}{1180}}$		

[1] d = inscribed circle diameter [m]
[2] for d≥40 m has to be used
[3] if d>60 m but all other characteristics of a compact two lane roundabout according to the guideline are fulfilled, then d =60 m should be used
[4] plus 2 complete and separate lanes (with lane marking) plus full-capacity exits

In the equations above, the entry capacity is measured in passenger car units (pcu) considering: 1 truck equal to 1.5 pcu, 1 motor bike equal to 1 pcu, and 1 bicycle corresponding to 0.5 pcu.

More recently additional studies focusing on the empirical regression approach have been performed by Brilon & Wu [33]. Therefore, the previus entry capacity formula (see equation 15) was recomanded only for the case of roundabouts with a single-lane circle and single-lane entries, whereas when roundabout is composed by more than one lane, a simplified form of the previous capacity equation derived from the Siegloch's capacity equation [18] was provided:

$$C = 3600 \cdot \frac{n_e}{t_f} \cdot e^{-\frac{q_k}{3600}\cdot\left(t_g - \frac{t_f}{2}\right)} \tag{16}$$

where:

- Q_c = circulating flow in front of the entry (pcu/h);
- n_e = parameter related to the number of entry lanes; it is equal to 1 for single-lane
- entries and 1.4 for double-lane entries;
- t_g = critical gap value of 4.3 s;
- t_f = follow-up time equale to 2.5 s.

It should be noted that eq. 15 and 16 are originally obtained from gap acceptance theory, and regression analysis was used only for the parameters (t_g and t_f) that were estimated from data points using minimization for the sum of quadratic deviations.

Whereas Brilon and Geppert [30] developed a capacity estimation method for turbo-roundabouts. This solution distinguishes between the different kinds of lane configurations at the entry. For the turbo roundabout composed by two entry lanes and by only one circle lane, the psycho-technical parameters were calibrated and were resulted equal to 4.5 s for the critical gap, 2.5 s for the follow-up time, and 1.9 s for the minimum gap. The values of these parameters were applied for each of the two entry lanes.

In this regard the distribution of arriving traffic by lanes used by authors is shown:

$$q_{left} = max \begin{cases} q_{left,0} \\ q \cdot \left(0.5 - \dfrac{C_{reserve}}{6670}\right) \end{cases}$$

(17)

$$q_{right} = q - q_{left}$$

where:

- q = total flow on entry [pcu/h];
- q_{left} = traffic volume on the left entry lane [pcu/h];
- $q_{left,0}$ = traffic flow turning on the left [pcu/h];
- q_{right} = traffic volume on the right entry lane [pcu/h];
- $C_{resesrve}$ = $2 \cdot C - q$ = reserve capacity of the entry [pcu/h]; where C is computed by equation 15.

The HCM 2000 [37] provide a capacity formula depending on circulating flow Q_c is in front of the considered entry and on the critical gap and the follow up time; it is also limited to schemes with one lane in the circle and one lane at the entries and with circulating flow Q_c not greater than 1200 pcu/h. The expression of capacity is the following:

$$C = \frac{Q_c \cdot e^{-Q_c \cdot T_c/3600}}{1 - e^{-Q_c \cdot T_f/3600}} \qquad (pcu/h)$$

(18)

where:

- Q_c is circulating flow on front of the entry;   [pcu/h]
- T_c is the critical gap;   [s]
- T_f is the follow-up time.   [s]

Hagring [38] derived a more general capacity formula for multi-lane intersections taking into account a behavioural and traffic flow parameters. Hagring indeed

derived the capacity of a minor stream crossing or merging *n* (independent) major streams, by using for each stream a Cowan's M3 headway distribution.

$$C_e = 3600 \cdot \sum_j \frac{\varphi_j \cdot Q_{c,j}}{3600 - \Delta_j \cdot Q_{c,j}} \prod_k \left(\frac{3600 - \Delta_k \cdot Q_{c,k}}{3600} \right) \cdot \frac{\exp\left[-\Sigma_l \frac{\varphi_l \cdot Q_{c,l}}{3600 - \Delta_l \cdot Q_{c,l}} \right] \cdot (T_{c,l} - \Delta_l)}{1 - \exp\left[-\Sigma_m \frac{\varphi_m \cdot Q_{c,m}}{3600 - \Delta_m \cdot Q_{c,m}} \right] \cdot T_{f,m}} \quad (19)$$

where:

- C_e = entry lane capacity [pcu/h];
- φ = Cowan's M3 parameter representing the proportion of free traffic within the major stream;
- Q_c = conflicting traffic flow [pcu/h];
- T_c = critical gap for circulatory lane, [s];
- T_f = follow-up time,[s];
- Δ = minimum headway of circulating traffic [s];
- j,k,l,m, = indices for conflicting lanes.

The Hagring model in equation (19) was specified both in relation to the antagonist circulating flow values ($Q_{c,i}$ or $Q_{c,e}$) faced by drivers coming from the considered entry approach and in relation to T_c, T_f and Δ values. Thus, right-lane capacity and left-lane capacity of major entries, and right-lane capacity of minor entries were estimated as a function of the only one circulating traffic flow in the outer circle lane in front of the considered entry approach ($Q_{c,e}$); therefore, the capacity formula depends by the critical headway of the external circulating flow (T_{ce}) and by the follow-up headway of the approach considered. These capacities can be computed using the following equation:

$$C_e = Q_{c,e} \cdot \left(1 - \frac{\Delta \cdot Q_{c,e}}{3600} \right) \cdot \frac{exp\left(\frac{-Q_{c,e}}{3600} \cdot (T_c - \Delta) \right)}{1 - exp\left(\frac{-Q_{c,e}}{3600} \cdot T_f \right)} \quad (20)$$

In turn, left-entry capacity of minor road was calculated considering both outer circulating traffic flow ($Q_{c,e}$) and the inner circulating flow ($Q_{c,i}$). Thus capacity formula was based on critical gaps of both circulating lanes and the follow-up time of considered entry lane. The left-entry capacity formula was the following:

$$C_e = \left(Q_{c,e} + Q_{c,i} \right) \cdot \left(1 - \frac{\Delta \cdot Q_{c,e}}{3600} \right) \cdot \left(1 - \frac{\Delta \cdot Q_{c,i}}{3600} \right) \cdot \frac{exp\left(\frac{-Q_{c,e}}{3600} \cdot \left(T_{c,e} - \Delta \right) \frac{-Q_{c,i}}{3600} \cdot \left(T_{c,i} - \Delta \right) \right)}{1 - exp\left(\frac{-\left(Q_{c,e} + Q_{c,i} \right)}{3600} \cdot T_f \right)} \quad (21)$$

The capacity of roundabouts can also be evaluated based on an empirical regression without any consideration about queueing theory. This method was used, in the first time in the United Kingdom by Kimber [39] and by Kyte [40] applying this to a simple intersection with one priority stream and one non priority stream.

An example of empirical capacity model, expressed in linear form, is the following:

$$C = b - c \cdot Q \tag{22}$$

where b and c are constants of regression.
Otherwise the expression, written below, could be used as well:

$$C = A \cdot e^{-B \cdot Q} \tag{23}$$

In the apacity formula written above, the parameter A and B , could be stimate using a liner regression, only after a logathmic transformation of this equation.

The Highway Capacity Manual 2000 [37] proposed several empirical regression models to reflect the capacity of roundabouts with up to two lanes. The entry capacity of a roundabout with only one circulating lane, is the following:

$$c_{e,pce} = 1.130 \cdot e^{(-1.0 \cdot 10^{-3}) \cdot v_{c,pce}} \tag{24}$$

where:

- $c_{e,pce}$ is the lane capacity, adjusted for heavy vehicles, pc/h;
- $v_{e,pce}$ is the conflincting flow, pc/h

whereas the entry capacity of a roundabout with one entry lane opposed by two circulating lanes is computed as:

$$c_{e,pce} = 1.130 \cdot e^{(0.7 \cdot 10^{-3}) \cdot v_{c,pce}} \tag{25}$$

Finally, the capacity of the right and left lanes, respectively, of a two-lane roundabout entry opposed by two circulating lanes is:

$$c_{e,R,pce} = 1.130 \cdot e^{(0.7 \cdot 10^{-3}) \cdot v_{c,pce}} \tag{26}$$

$$c_{e,L,pce} = 1.130 \cdot e^{(0.75 \cdot 10^{-3}) \cdot v_{c,pce}} \tag{27}$$

where:

- $c_{e,R,pce}$ is the right lane capacity, adjusted for heavy vehicles, pc/h;
- $c_{e,L,pce}$ is the left lane capacity, adjusted for heavy vehicles, pc/h;
- $v_{e,pce}$ is the conflincting flow, pc/h

The capacity expression formulated by Brilon and Bonzio [32] belongs to empirical capacity models, expressed in linear form, in which roundabout configuration is represented by the number of entry and circulating lanes:

$$C = A - B \cdot Q_c \quad (pcu/h) \tag{28}$$

The capacity formula of entry lane written above, is a simple linear relationship among the circulating flow, Q_c and two parameters, A and B, depending on the numbers of entry and circle lanes. These parameters A and B were estimate with statistical regression techniques from experimental data (see Table 4).

Table 4 Values of the parameters of Brilon & Bonzio formula.

Circle lane number	Entry lane number	A	B	Sample size
3	2	1409	0.42	295
2	2	1380	0.50	4574
2-3	1	1250	0.53	879
1	1	1218	0.74	1504

It is noteworthy that this formula is recommended for roundabouts with external diameters D_{ext} that range from 28 to 100 meters

Bovy et al. as referred by [3] provided capacity formula expressed as follow:

$$C = \frac{1}{\gamma} \cdot \left(1500 - \frac{8}{9} \cdot Q_d\right) \quad (pcu/h) \tag{29}$$

where ϒ is a parameter whose value changes according to the number of entry lanes; thus, it is equal to:

- 1 for one lane;
- 0.6/0.7 for two lanes;
- 0.5 for three lanes.

Q_d is the disturbing traffic determined as:

$$Q_d = \alpha \cdot Q_u + \beta \cdot Q_c \qquad (pcu/h) \qquad\qquad (30)$$

where:

- Q_u is exiting traffic;
- Q_c is circulating traffic in front of the exit being considered (see Figure 16).
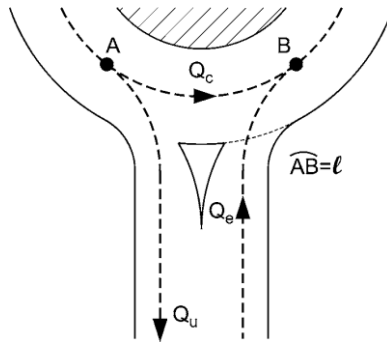
Figure 16 Distance between the exiting conflicting point (A) and entering point (B)

Coefficients α and β are correlated to the geometry of the roundabout and take into account the distance "l" between the exiting conflicting points (A) and entering points (B); see Figure 16. The value of β parameter was derived in function of the number of circulating lanes and consequentially also of conflicting flow caused by the circulating traffic; the values thus obtained are as follows: β = 0.9–1.0 for one lane; β = 0.6–0.8 for two lanes; and β = 0.5–0.6 for three lanes.

An example of expression based on geometrical characteristics of roundabouts, is the formula developed by TRRL (United Kingdom) [39], where the capacity C of a generic entry is determined as a function of the leg and circle geometric parameters and of the circulating flow in the circle (Qc) in front of the entry:

$$C = k \cdot \left(F - (f_c \cdot Q_c)\right) \quad (pcu/h) \qquad\qquad (31)$$

where:

- $F = 303 \cdot x_2$
- $f_c = 0.210 \cdot t_D \cdot (1 + 0.2 \cdot x_2)$
- $k = 1 - 0.00347 \cdot (\phi - 30) - 0.978 \cdot (1/r - 0.05)$
- $t_D = 1 + \dfrac{1}{2 \cdot [1 + exp\,((D - 60)/10)]}$
- $x_2 = v + \dfrac{(e - v)}{(1 + 2 \cdot S)}$
- $S = 1.6 \cdot (e - v)/l' = (e - v)/l$

The following Figures 17-19 show the geometrical construction of the parameters in the capacity formula (26) written above, whereas Table 5 provides the meaning and the range values of these parameters.

Table 5 Values of parameters used into TRRL formula

Parameter	Description	Range values
e	Entry with. It is determined along the perpendicular line traced from point A to the external edge	3.6 - 16.5 m
v	Lane With. It is calculate upstream of the leg widening next to the entry along the perpendicular line traced from the axis of the roadway to the external edge.	1.9 - 12.5 m
u	Circle width: is the distance among the splitter island at legs (point A) and the central island.	
r	Entry bend radius: is the smallest bend radius of the external edge next to the entry.	3.4 - ∞ m
e'	Previous entry with	3.6 - 15.0 m
v'	Previous lane with	2.9 - 12.5 m
l	Flare mean length. Referring to figure 4, the length l corresponds to the segment CF, determined along the perpendicular line that passes through C (mean point of segment BD) of segment AB.	1 - ∞ m
l'	Flare mean length. Referring to figure 4, length l' corresponds to segment CF' along a curve parallel to the external edge BG and passing through C	1 - ∞ m
S	Sharpness of the flare	0 - 2 - 9
W	Exchanges section width: is the shortest distance between the central island and the external edge in the trait between an entry and the following exit.	7.0 - 26.0 m
L	Exchanges section length: is defined as the shortest distance between the splitter islands at the legs of two successive entries.	9.0 - 86.0 m
ϕ	Entry angle. It corresponds to the conflicting angle between the entering flows and the circulating flows, and it must be determined as is shows in figure 6.	0 -77°
$D=D_{ext}$	Inscribed circle diameter	13.5 - 171.6 m
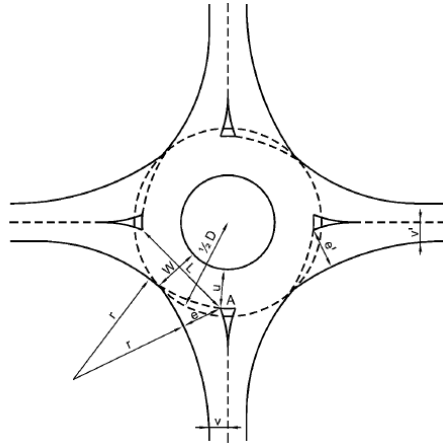
Figure 17   Geometric elements used in the TRRL formula
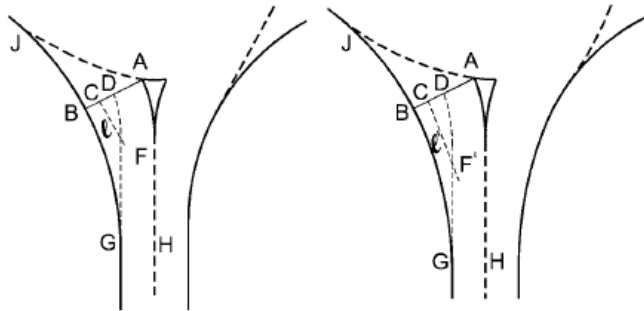
Figure 18   Geometric construction for the determination of l and l'.
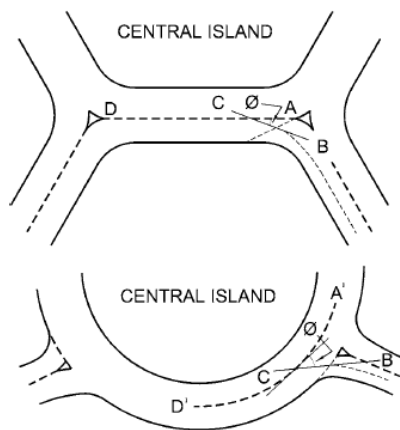
Figure 19   Geometric construction for the determination of the entry angle ϕ

4. About safety on roundabouts

As is well-known, the benefits of installation of a roundabout are related to the improvement in overall safety: the fact is that roundabouts have fewer vehicular conflict points in comparison to conventional intersections. Moreover, the low speed through roundabouts and on each approach allows drivers more time to react to unexpected situations and potential conflicts; consequently, crash severity can be reduced compared to some traditionally controlled intersections. The potential for high-severity conflicts, such as right angle and left-turn head-on crashes, is greatly reduced in roundabout intersections both for urban and for rural settings [41-48]. A summary of safety studies taken to evaluate crash reductions at modern roundabouts compared to other intersection types is shown in Table 6 as reported by [49].

International experience shows that alignment of approaches can play a decisive role in the occurrence of certain crash types: an entry tangential to the circular roadway decreases both the opportunity to deflect entering vehicles into a proper entry path and to reduce entry speeds, resulting in more loss-of control and entering-circulating crashes (entering drivers will be less inclined to yield); tangential exit can increase vehicles exit speeds and the risk for pedestrians on crosswalks [48]. Moreover, an almost centered alignment at the roundabout can generate rear-end and loss of control crashes in relation to any abrupt braking. In order to ensure consistent speeds for circulating and entering vehicles, as well as decreasing speed differentials with other road users, trade-off considerations can interest size and position of splitter islands, entry approach alignment and angle between legs without compromising sight distances and the opportunity to accommodate trucks due to severe curvature of the entry path; see e.g. [1]

Table 6. Summary of safety studies at roundabouts.

Country	reference	method	results
Australia	AUSTROADS [6]	Before-and-after	Crash reduction after roundabout installed*: − 74 % in the casualty crash rate − 32 % in property damage only − 68 % in pedestrian casualty crashes per year. *control before roundabout: give way to the right – stop – give way*
the Netherlands	Schoon and Van Minnen [50]	Before-and-after without control	crash reduction at single-lane roundabouts: − 73% in all pedestrian injury crashes − 89 % for pedestrian fatality; − 63% for moped injuries; − 30% for cycle injuries.
France	Guichet [44]	Comparisons with rural intersections controlled traditionally	− less than 25% of serious injury crashes or fatalities at roundabouts; − 38 fatal or serious type injuries for every 100 crashes at roundabouts vs 55 injury or fatal crashes for every 100 crashes at controlled intersections; − crash frequencies 4 times higher at signalized intersections than roundabouts.
Sweden	Brude and Larson [51]	Comparisons with signalized intersections	− vehicle-pedestrian crashes at the single-lane roundabouts were 3 to 4 times lower than predicted crashes at comparable signalized intersections; − for two-lane roundabouts, crash risk was similar to comparable intersections.
USA	Persaud et al. [45]	before-after study	− 39 % overall reduction in crash rates; − 90% reduction in fatal crashes; − 76% reduction in injury crashes; − 30-40% reduction in pedestrian crashes; − 10% in bicycle crashes.
Crashes reported outside the United States	Elvik [52]	meta-analysis of studies (28 studies to obtain estimates of effect on road safety of conversions to roundabouts)	− 30% to 50% reduction in injury crashes; − 50% to 70% reduction in fatal crashes; − the roundabout effect on injury crashes is greater in 4-leg intersections than in 3-leg intersections; − the roundabout effect is greater in intersections previously controlled by yield signs than in intersections previously controlled by traffic signals.

Several studies have been carried out since 1980s with the purpose to develop support tool for planners and engineers in designing safer roundabouts and in optimizing accessibility issues through design features; see e.g. [41, 43, 48, 51, 53, 54]. A comprehensive set of various roundabout design elements having a positive (or not) effect on safety and operations has been summarized in Table 7; Table 8 reports only effects of design elements on safety by roundabout crash category. In order to understand the relationship between roundabout design features and

crash frequency the use of safety models can provide help in quantifying the safety implications of design choices and in determining the effectiveness of roundabout treatments in road constructions.

Table 7. Roundabout design elements affecting safety and operations [1, 49]

element	safety	capacity
angle between entries	++	- -
circulatory roadway	-	+
entry	-	++
entry angle	++	+
entry radius	-	+
flare length	ns	+
inscribed circle diameter	-	+

++	*an increase in this measure represents a significant positive effect*	-	*an increase in this measure decreases positive effects*
- -	*an increase in this measure decreases significantly positive effects*	ns	*the relationship was not specified*
+	*an increase in this measure represents a positive effect*		

A review of safety prediction models that can be done through intersection-level and approach-level analyses is reported by [48]. The intersection level models have been developed for total and injury collisions; the approach-level models have been developed for all severities combined for entering-circulating, exiting-circulating and approaching collision types. According to [1] these models would be included in the second edition of Highway Safety Manual [55]. Note that, despite the number of turbo roundabouts is increasing around the word, the turbo roundabout installations are still recent; thus, adequate evaluation of their safety performance is not yet available, especially because crash trends are still limited. So the choice between modern roundabout and turbo roundabout layouts may be done by evaluating the convenience in terms of performances, when the traffic demand is known [4].

Table 8. Effects of roundabout design elements on safety [48, 49]

Measure	crash category				
	single vehicle	entering - circulating	rear-end crashes on approach	pedestrian	Exiting - circulating
AADT	↑	↑	↑	↑	↑
pedestrian volumes				↑	
number of approaching lanes			↑	↑	
number of circulating lanes		↑		↑	
radius of vehicle path	↓				
entry deflection	↓	↓			↓
percentage of motorcycles		↑			
angle to next approach		↓			
sight distance	↑				
weaving length between splitter islands				ns	
distance to first sight of roundabout				ns	
length of vehicle path	↑				
85th percentile speeds	↑	↑	↑		↑
reduction in 85th percentile speed	↑				
posted speed limit				ns	

↑   an increase in this measure increases crash frequency
↓   an increase in this measure decreases crash frequency
ns   the measure had a significant relationship with crash frequency but the relationship was not specified.

It should be noted that safety performance measures can be obtained either experimentally based on crash data or through simulation (based on well specified or calibrated traffic models). Accurate calibration of traffic models should ensure that simulated measures of safety performance are reflective of "real world" traffic conditions; see e.g. [56]. This issue will be faced later on in this thesis.

In the following sections some methods are presented for safety theoretical assessment at roundabouts; particular references will be made to single-lane, double-lane and turbo roundabouts, which are studied in this dissertation.

4.1. About conflict points at roundabouts

The safety level of an intersection can be examined based on the conflict points which are associated with a particular configuration of the intersection. Whatever the maneuver to be carried out to follow a certain path, one or more

interferences between traffic flows occur. These interferences represent potential collision points among vehicles and are called conflict points. A conflict point is a place where the paths of two road users, (e.g. two vehicles, or a vehicle and a bicycle, or a vehicle and pedestrians), making their maneuvers consisting in diverging, merging or crossing, can collide with each other. The total number of conflict points depends on the number of legs belonging to the node, the type of intersection and the system of traffic control.

According to [1], conflicts can be divided into four basic categories as follows:

1. *Diverging conflicts.* These conflicts are due to the separation of two traffic flows. Some examples include right turns diverging from through movements or exiting vehicles diverging from circulating vehicles. If the speed of the diverging driver is significantly lower than the follower one, this speed differential increases the risk of a rear-end collision.

2. *Merging conflicts.* These conflicts are caused by the joining of two traffic streams. The most common types of crashes due to merging conflicts are side-swipe and rear-end crashes. Merging conflicts can be more severe than diverging conflicts due to the more likely possibility of collisions to the side of the vehicle, which is typically less protected than the front and rear of the vehicle.

3. *Crossing conflicts.* These conflicts occur where the paths of two traffic streams intersect with each other. These are the most severe of all conflicts and the most likely to involve injuries or fatalities. Typical crash types are right-angle crashes and head-on crashes.

Another type of conflict can also be considered, that is the following:

4. *Queuing conflicts.* These conflicts are caused by a vehicle running into the back of a vehicle queue on an approach. These types of conflicts can occur at the back of a through-movement queue or where left-turning vehicles are queued waiting for gaps. These conflicts are typically the least severe of all conflicts because the collisions involve the most protected parts of the vehicle and the relative speed difference between vehicles is usually less than in other conflicts.

Figure 20 shows a comparison regarding the number of vehicle-vehicle conflict points for four-leg intersection vs. single-lane roundabout [1].

● Diverging

◐ Merging
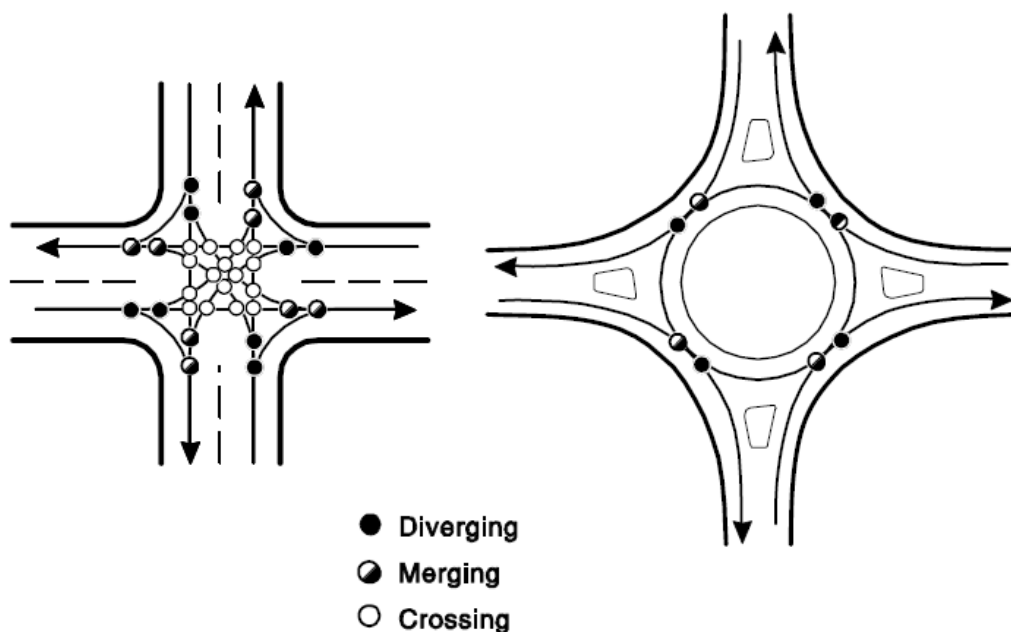
○ Crossing

Figure 20 Number of conflict points at four-leg intersection vs. single-lane roundabout [1]

Although it is possible to reduce conflicts in a controlled intersection, through separate turn lanes, traffic control signals (i.e. stop or give way signals) or by installation of a traffic light, it is proven that drivers are more likely to comply with traffic rules in a roundabout than situations in which there is a traffic control device [1]. Moreover, as already pointed out several times, single-lane roundabouts not only reduce the number of conflict points, and especially the most damaging conflicts (i.e. crossing conflicts), but their safety is also related to the capacity to control the travelling speeds of vehicles, through the physical and geometric features, with a consequential reduction of the severity of crashes.

Multi-lane roundabouts, in turn, cannot normally reach the same level of safety as their single-lane counterpart, because of the increased number of conflict points and then the additional complexity in decision-making due to many movements among interacting users. Indeed, the presence of multi lanes on the ring introduces in the multi-lane roundabouts the possibility for vehicles to move from one lane to another and then the presence of "weaving" conflict points which instead are not present at single-lane roundabouts. These additional conflicts, unique to multilane roundabouts, are generally low-speed side-swipe conflicts that typically have low severity [1, 4]. Therefore, although the number of conflicts increases at double-lane roundabouts, and in general at multi-lane roundabouts, when compared to single-lane roundabouts, the overall severity (and often also the number) of conflicts is typically less than other four-leg intersections.

As introduced above, in this research, in addition to single-lane roundabouts, double-lane roundabouts (i.e. roundabouts with two entry and exit lanes for each approach and two lanes on the ring) as a case of the multi-lane roundabouts were taken into account. Thus, focus will be made on these roundabouts about conflicts points. In the following Figures 21 and 22 the number and classification of the conflict points are shown both for a typical double-lane roundabout and for the case in which the main road approaches have two entry and exit lanes, while the minor road approaches have two entry lanes and only one exit lane.

It should be noted that, although the number of conflict points in the two cases shown below is the same, the types of these conflict points can be different: in the first case (see Figure 21), because there are two exit lanes at each leg, there are no "weaving" conflict points; while, in the second case in Figure 22, since the minor road has one exit lane for each leg, the outgoing vehicles pass from the inner circulating lane to the outer one and thus can create "weaving" conflicts.

It is noteworthy that, even if there are conflict points classifiable as "crossing" at double-lane roundabouts, these conflict points can create traffic situations less severe than four-leg intersections, because the conflict angle is always less than ninety degrees.
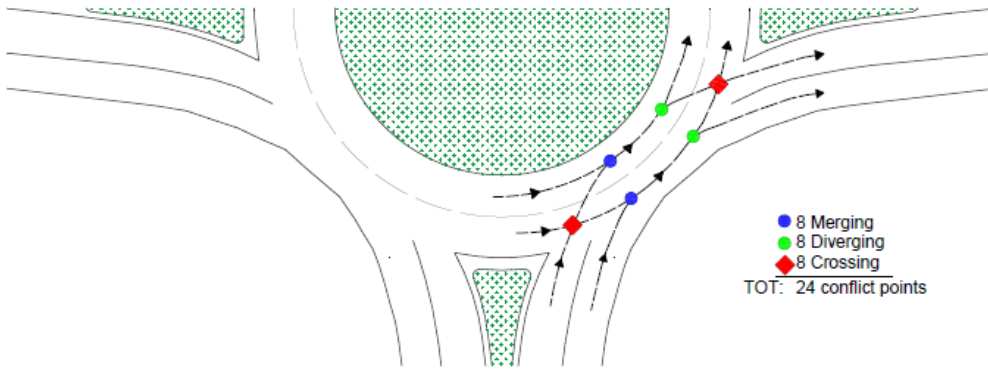
Figure 21 Number of conflict points at double-lane roundabout.
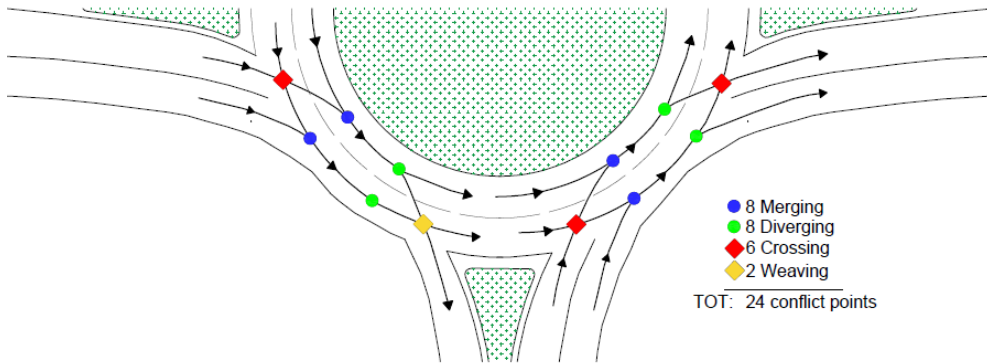
Figure 22 Number of conflict points at multi-lane roundabout having two entry and exit lanes on major road and two entry lanes and one only exit lane on minor road

Finally, as also happens on traditional intersections, at double-lane roundabouts, in addition to the type of conflict mentioned above, crashes could occur due to some wrong maneuvers that drivers make, maybe, because they are unfamiliar with roundabout operation or because of improper roundabout geometry [1, 4]. Figures 23, 24 and 25 show three typical wrong maneuvers made by drivers and in particular related to: maintaining lane position, entering next to an exiting vehicle, and turning from the incorrect lane.
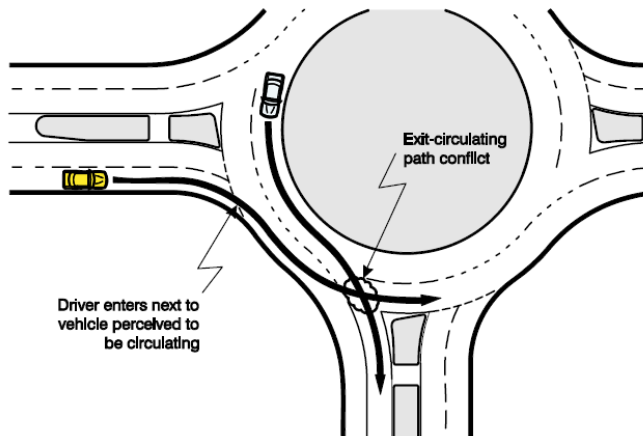
Figure 23 Wrong maneuver entering next to an exiting vehicle at a double-lane roundabout [1]
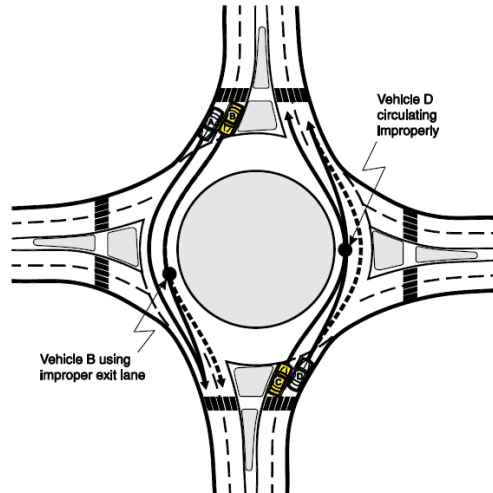
Figure 24 Wrong maneuver: failing to maintain lane position at a double-lane roundabout [1]
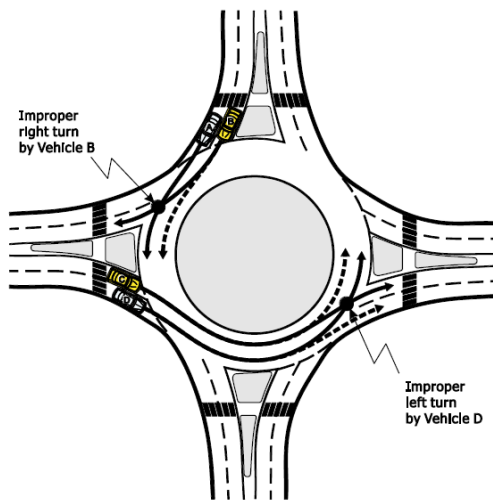
Figure 25 Wrong maneuver: improper turn conflicts at a double-lane roundabout [1]

With regard to turbo-roundabouts a higher level of traffic safety in comparison to typical double-lane roundabouts can be noted. For instance, a lower number of conflict points can be highlighted (see Figure 26). Entering and exiting conflicts are eliminated by directing drivers to the correct lanes before entering a turbo roundabout and introducing spiral lines that guide drivers to the correct exit. A turbo roundabout reduces the number of crossing conflict points (by reducing the number of crossing traffic flows), and eliminates weaving conflict points (by the separate running of individual direction flows). A further benefit is that traffic in the main direction only crosses one circulating lane entering the roundabout.
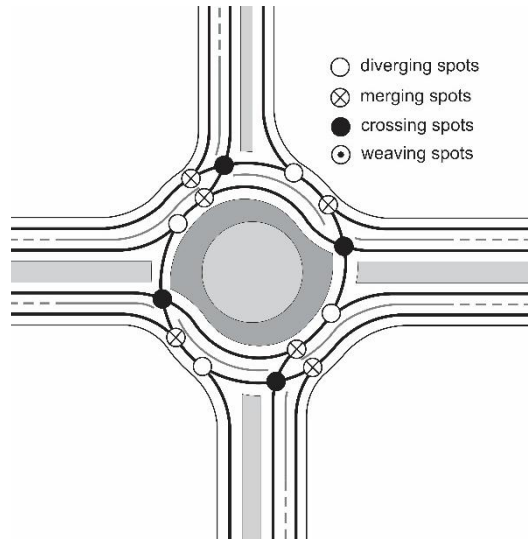
Figure 26 Number of conflict points at a turbo roundabout [4, 5]

Based on current literature on the topic, for the cases of roundabouts presented above, the safety traffic level can be calculated as follows :

$$LOS = \frac{1}{NCP} \qquad (32)$$

where NCP represents the total number of the conflict points for the intersection considered; see e.g. [4] .

4.2. About the maximum number of conflict situations

Conflict analyses should be more than the simple enumeration of the number of conflicts; they should also take into account the severity of the conflicts, for example, based on conflict angle or on the relative speeds of the conflicting vehicles.

According to Tollazzi [4], there are some mistakes related to the "theory of conflict points" (above briefly introduced in section 4.1):

1. when a conflict analysis is conducted at a multi-lane roundabout, it is not well known where the "weaving "conflict point is effectively located or where, more generally, conflict points occur due to failing to maintain circulating lane position by vehicles (see Figure 27). In this case, a conflict section should be considered rather than a single conflict point. In order to understand this issue better, Figures 27 and 28 show two different traffic situation: one can observe that at a turbo roundabout the exact position of the conflict point is known (see Figure 28), unlike at a double-lane roundabout (see Figure 27), where it is difficult to establish in advance the position of the potential conflict points.
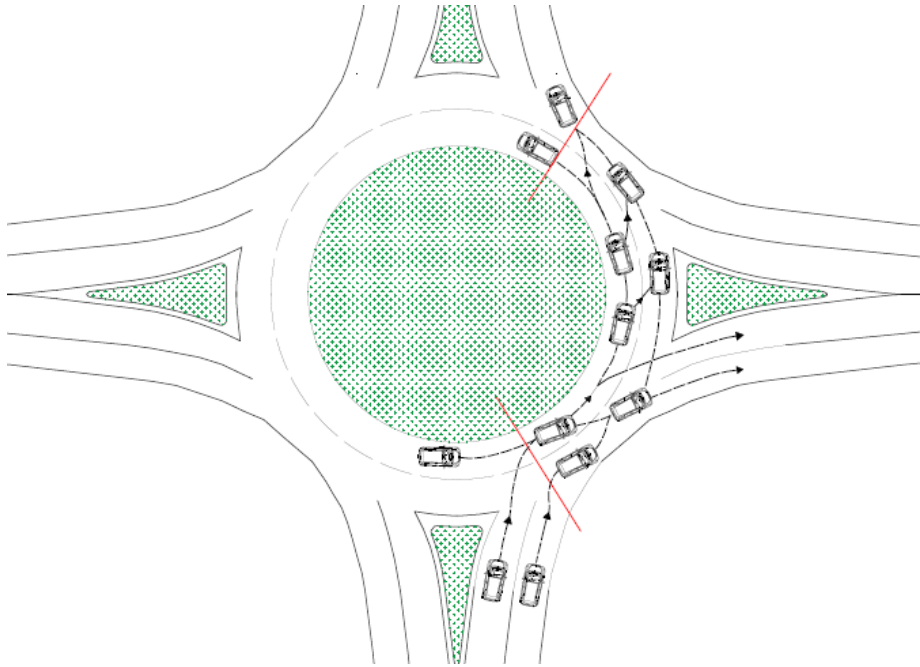
Figure 27 Conflict section at a double-lane roundabout
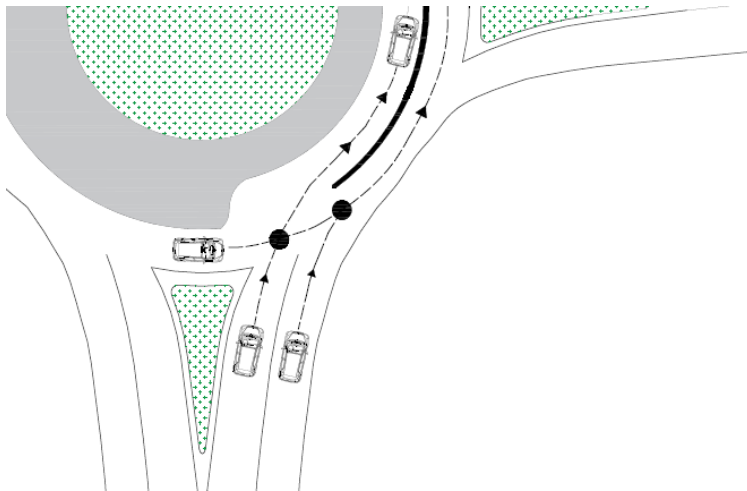
Figure 28 Conflict point at a turbo roundabout

2. Another mistake is related to the belief that separate turn lanes at traditional intersections with traffic control (stop signs or give way signs) can eliminate the number of crossing conflicts, since in reality, it can often reduce, but not completely eliminate, crossing conflict points by means of separation of conflicts in space and/or time.

3. The most important mistake is associated with the incapacity of the "theory of conflicts points" to establish a severity level of crash situations. The question is for example, is a situation more dangerous with 5 "crossing", 10 "merging" and 10 "diverging" conflict points or another situation in which there are 3 "crossing", 10 "merging" and 12 "diverging" conflict points? In these two situations, the total number of conflict points is the same, but it is not possible to be sure on which of the two situations is more dangerous.

Thus, the maximum number of conflict situations can be derived from the sum of all possible conflict situations based on the effective number of vehicles that could collide.

The level of traffic safety, can be calculate by means the following formula:

$$LTS = \sum CTF + \sum MTF + \sum DTF \qquad (33)$$

where:

- *LTS* is the number of traffic danger situations in a time unit (one day);
- *CTF* is the number of crossings of traffic flows;
- *MTF* is the number of merging traffic flows;
- *DTF* is the number of diverging traffic flows.

The calculation makes a comparative analysis of danger situations in order to forecast the level of traffic safety in some intersections.
Equation 33 represents a general formula for determining the maximum possible number of LTS in any type of intersection. The number of LTS depends on the number of conflict points and the average traffic flow in a time unit, e.g. in one day.

For example, analyzing the traffic safety on a four-leg intersection, equation 33 becomes:

$$LTS = \sum_{i=1}^{16}(CTF)_i + \sum_{l=1}^{8}(DTF)_l + \sum_{m=1}^{8}(MTF)_m \qquad (34)$$

Moreover, it is possible to determine which of the two situations with the same number of total conflicts point is more damaging, through a weighted average:

$$\frac{\sum CTF}{\sum CCP} + \frac{\sum MTF}{\sum MCP} + \frac{\sum DTF}{\sum DCP} \qquad (35)$$

where:

- CTF, MTF, DTF are indicated above;
- CCP, MCP, DCP are respectively crossing, merging and diverging conflict points.

References

1. National Academies of Sciences, Engineering, and Medicine, Roundabouts: An Informational Guide, second ed., The National Academies Press, Washington, DC, 2010. https://doi.org/10.17226/22914.
2. Pilko H., Mandžuka S., Barić D. (2017). Urban single-lane roundabouts: A new analytical approach using multi-criteria and simultaneous multi-objective optimization of geometry design, efficiency and safety, Transportation Research Part C: Emerging Technologies 80: 257-271.
3. Mauro R. (2010) Calculation of Roundabouts: Capacity, Waiting Phenomena and Reliability, Springer, Berlin Heidelberg, 2010.
4. Tollazzi T. (2015). Alternative Types of Roundabouts: An Informational Guide, Springer International Publishing, New York, 2015.
5. Fortuijn L.G.H. and Harte V.F. (1997). Multi-lane roundabouts: exploring new models. Traffic engineering working days 1997, CROW, Ede, The Netherlands.
6. AUSTROADS (1993). Guide to traffic engineering Practice; Part 6 – Roundabouts, Sydney, Australia
7. Louah G. (1992). Panorama critique des modeles français de capacité des carrefours giratoires. Actes du séminaire international "Giratoires 92,", Nantes, France, 1992.
8. FGSV Ed. (2015). Handbuch für die Bemessung von Straβenverkehrsanlagen (HBS) Edition 2015 [German Highway Capacity Manual]. Forschungsgesellschaft für Straβen und Verkehswesen (FGSV) [Road and Transport Association]. Cologne, edition 2015.
9. (Norme funzionali e geometriche per la costruzione delle intersezioni stradali) [Functional and geometric standards for the construction of road intersections], 2006
10. CROW (1998). Eenheid in rotondes. CROW publication no.126. Ede, The Netherlands. (Uniform design of roundabouts).
11. Herland L. and Helmers G. (2002). Cirkulationplatser – utformnng och function. Svenska och utlandska rekommendationer och utformingsregler jamte analys och kommentarer. VTI Meddelande 895. Linköpink. [Roundabouts – design and function. Swedish and foreign recommendations and design rules with analyses and comments], in Swedish.
12. DMRB(2007). Design Manual for Roads and Bridges.
13. TSC 03.341: 2011 KROŽNA KRIŽIŠČA, RS Ministry of Transport.
14. Fugal K.J., Dale M. T., Lewis S. J. (2008). Design for single-lane to dual-lane roundabout expandability. National Roundabout Conference 2008, Kansas City, Missouri, US, May, 7- 9, 2008.

15. Troutbeck R.J. and Brilon W. (2016). Chapter 8 revised monograph on traffic flow theory," in Unsignalized Intersection Theory (Federal Highway Administration). Available at: https://www.fhwa.dot.gov

16. Morse PM. (1982). Application of Queuing Theory, 2ndEdn. London: Chapman Hall Ltd.

17. Harders J. (1968). Die Leistungsfähigkeit Nicht Signalregelter Städtischer Verk- shrsknoten [Capacity of Unsignalized Urban intersections]. Bonn: Strassenbau und Strassenverkehrstechnik 76 [Road Construction and Traffic Technology, 76], Bundesministerfür Verkehr [Federal Department of Transport].

18. Siegloch W. (1973). Die Leistungsermittlungan Knotenpunkten Ohne Lichsignalsteuerung (Capacity Unsignalized Intersections. Calculations for Unsignalized Intersections). Bonn: Schriftenreihe Strassenbauand Strassenverkehrstechnik [Road Construction and Traffic Technology, 154].

19. Hilbe J.M.(2008). Negative Binomial Regression. New York: Cambridge University Press.

20. Mannering F.L. and Washburn S.S. (2013). Principles of Highway Engineering and Traffic Analysis, 5th Edn. Singapore: John Wiley & Sons.

21. National Research Council, and Transportation Research Board. (2010). HCM 2010: Highway Capacity Manual. Washington, DC: Transportation Research Board.

22. Devroye L. (1986). Non-Uniform Random Variate Generation. New York: Springer- Verlag.

23. Mauro R. and Branco F. (2013). Update on the statistical analysis of traffic counting on two-lane rural highways. Mod. Appl. Sci. 7, 67. doi: 10.5539/mas.v7n6p67.

24. Cowan R.J. (1975). Useful headway model. Transp. Res. 9, 6. doi:10.1016/0041- 1647(75)90008-8

25. Cowan R. J. (1987). An extension of Tanner's results on uncontrolled intersections. Queuing Syst. 1, 249–263. doi:10.1007/BF01149537

26. Akçelik R.(2011)."An assessment of the Highway Capacity Manual 2010 roundabout capacity model," in International TRB Roundabout Conference, Carmel, Indiana,USA,May2011.

27. Akçelik R., and Chung, E.(1994).Calibration of the bunched exponential distribution of arrival headway. Road Transp. Res. 3, 42–59.

28. Brilon W. (2005). Studies on Roundabouts in Germany: Lessons Learned. National Roundabout Conference, Vail, Colorado, 2005

29. Brilon W. and Vandehey, M. (1998) .Roundabouts–the state of the art in Germany. ITE J. 68: 48–54.

30. Brilon W. and Geppert A. (2010). Verkehrsqualitaet an zweistreifigen Kreisverkehren unter Berücksichtigung der Abbiegebeziehungen und aktueller Grenz- und Folgezeitluecken (Traffic performance at 2-lane roundabouts with respect to turning movements and current critical

headways) research report FE 02.278/2006/ARB for the Federal Highway Agency BASt, Oct. 2010.

31. Brilon W., Stuwe B., Kreisverkehrsplaetze - Leistungsfaehigkeit, Sicherheit und verkehrstechnische Gestaltung. (Roundabouts – Capacity, safety, and design), Strassenverkehrstechnik, vol. 6, 1991

32. Brilon W., Wu, N. and Bondzio, L. (1997). Unsignalized Intersections in Germany – A State of the Art 1997, Proceedings of the Third International Symposium on Intersections Without Traffic Signals, pp. 61–70, Portland, Oregon, USA, July 1997.

33. Brilon W. and Wu N. (2008). Kapazitaet von Kreisverkehren - Aktualisierung, (Capacity of roundabouts – actual solution), Strassenverkehrstechnik, Nr. 5, S. 280 – 288.

34. Tanner, J. C. (1962). A theoretical analysis of delays at an uncontrolled intersection. Biometrica 49, 163–170. doi:10.1093/biomet/49.1-2.163.

35. Jacobs F. (1979). Capacity Calculations for Unsignalized Intersections (Technical Report in German). Institute fur Star Ben Bauund Verkehrswesen, University Stuttgart.

36. Stuwe B.: Untersuchung der Leistungsfaehigkeit und Verkehrssicherheit an deutschen Kreisverkehrsplaetzen. (Investigation of capacity and safety at German roundabouts), Publication of the Institute for Transportation and Traffic Engineering at the Ruhr-University Bochum. No. 10, 1992.

37. Highway Capacity Manual (2000). Transportation Research Board, Washington, D.C. 2000.

38. Hagring O. (1998). A further generalization of Tanner's formula. Transportation Research Part B: Methodological, 32, 423-429.

39. Kimber R.M. and Semmens, M.C. (1977). A track experiment on the entry capacities of offside priority roundabouts -1977- trid.trb.org.

40. Kyte M., Clemow C., Mahfood N., Lall B.K., Khisty C.J. (1991). Capacity and delay characteristics of two-way stop-controlled intersections. Transportation research record 1320: 160-167, available at: http://onlinepubs.trb.org/Onlinepubs/trr/1991/1320/1320-020.pdf

41. Maycock G. and Hall R. D. (1984). Crashes at Four-Arm Roundabouts. Crowthorne, England: Transport and Road Research Laboratory, Laboratory Report LR 1120, 1984.

42. Alphand F., Noelle U. and Guichet B. (1991), Roundabouts and Road Safety: State of the Art in France. Berlin: Springer Verlag.

43. Arndt O. (1998). Road Design Incorporating Three Fundamental Safety Parameters. Technology Transfer Forum 5 and 6, Transport Technology Division, Main Roads Department, Queensland, Australia, August 1998.

44. Guichet B. (1980). Classification of Accidents on Urban Roundabouts. Actes du Seminaire Giratoires 92, Nantes, France, October 14-16.

45. Persaud B.N., Retting R.A., Garder P.E., and Lord D. (2001). Safety effect of roundabout conversions in the United States: empirical Bayes

observational before-after study. Transportation Research Record, 1751: 1-8. http://dx.doi.org/10.3141/1751-01

46. Retting R.A., Persaud B.N., Garder P.E. and Lord, D. (2001). Crash and Injury Reduction following Installation of Roundabouts in the United States. American Journal of Public Health 91:628-31.

47. De Brabander B, Nuyts E. & Vereeck, L. (2005). Road safety effects of roundabouts in Flanders. Journal of Safety Research, 36(3), 289-96. http://dx.doi.org/10.1016/j.jsr.2005.05.001

48. National Academies of Sciences, Engineering, and Medicine. 2007. Roundabouts in the United States. Washington, DC: The National Academies Press. https://doi.org/10.17226/23216

49. Giuffrè O. and Granà A. (2012). Understanding safety-related issues for pedestrians at modern roundabouts. Journal of Sustainable Development 5(4): 23-37. doi:10.5539/jsd.v5n4p23

50. Schoon, C.C., & van Minnen. J. (1994). The safety of roundabouts in the Netherlands. Traffic Engineering and Control 35 (3): 142-148.

51. Brüde U. and Larsson, J. (2000). What roundabout design provides the highest possible safety? Nordic Road and Transport Research, 2000(2), 17-21.

52. Elvik R. (2003), Effects on Road Safety of Converting Intersections to Roundabouts, A Review of Evidence From Non-U.S. Studies. Transportation Research Record 1847, 1-10. http://dx.doi.org/10.3141/1847-01.

53. Service d'Etudes Techniques des Routes et Autoroutes (1988). Accidents at Intersections: The Use of Models to Predict Average Accidents Rates. Memorandum. Bagneux Cedex, France.

54. Daniels S., Brijs T., Nuyts E., & Wets G. (2010). Explaining variation in safety performance of roundabouts. Accident Analysis & Prevention, 42(2), pp. 393-402. http://dx.doi.org/10.1016/j.aap.2009.08.019

55. Highway Safety Manual (2010), American Association of State Highway and Transportation Officials (AASHTO) Washington, DC 20001.

56. Guido G., Astarita V., Giofré V., Vitale A. (2011). Safety performance measures: a comparison between microsimulation and observational data. Procedia - Social and Behavioral Sciences 20: 217-225.

CHAPTER TWO:
Estimation of the Critical and the Follow-up Headways

1. Introduction

Capacity methods for two-way-stop-controlled intersections represent the starting point for evaluating operational performances at roundabouts. According to [1] entry capacity calculations at steady-state conditions can be performed through a variety of capacity formulas incorporating some information on the roundabout configuration, represented by the number of circulating lanes and entry lanes [2, 3], or other formulas incorporating some aspects of the roundabout geometry in a somewhat detailed way [4], as well as formulas incorporating, together with geometric aspects, the users' behaviour through the critical and follow-up headways; for details see Chapter 1.

When capacity estimations are being performed by analytical gap-acceptance models, critical headway and follow-up headway are involved. The accuracy of capacity calculations at roundabouts largely depends on the accurate estimation of critical and follow-up headways [5]. The critical and follow-up headways are the two gap-acceptance parameters which explain the traffic interaction of a minor road vehicle when it enters the roundabout, merging into or crossing one or more circulating (major) streams. Many different methods for estimation of critical and follow-up headways have been published in the international literature; however, estimation of the critical headway represents an average value of all the observed drivers. In turn, the follow-up headway value can be obtained from individual measurements; indeed, it can be measured for individual vehicles whenever two consecutive vehicles in a queue discharge from a minor stream. As a result, capacity estimates based on the values of critical and follow-up headways also reflect average conditions. The same data of critical and follow-up headways included in the recent version of the Highway Capacity Manual [6] are average values representing a range of field data and site characteristics. Since most theories related to gap acceptance behaviour, as employed for unsignalized intersections and roundabouts, presume that drivers are consistent and uniform, capacity estimations are performed assuming constant values for the critical and follow-up headways, whereas these parameters, which are actually stochastically distributed, should be typically represented by a distribution of values.

In order to assess the effect that the range of variation in the input parameters – namely the gap acceptance parameters – has on the estimation of entry capacity at roundabouts, a preliminary collection of measurements of these parameters from real data at roundabouts needs to be performed. Thus, based on the estimations of the critical and follow-up headways proposed in many studies and researches conducted worldwide and already published, the aim of the research activity referred to in this Chapter was to obtain a comprehensive measure, more accurate and reproducible for the parameters of interest at each roundabout

under examination, which could represent a better outcome than can be obtained by each individual reviewed study.

To achieve this goal, a systematic review of empirical studies and researches including estimations of critical and follow-up headways at single-lane, double-lane and turbo roundabouts was conducted. These studies and researches, according to the steps in the systematic review process as is universally recognised, were selected on the basis of criteria established a priori. A statistical and quantitative analysis of the individual studies was then implemented as part of the literature review to assess the consistency of the effect across studies and to compute the summary effect. In other words, a meta-analytic estimation for the critical gap and the follow-up time was performed through the random effect model [7].

Before performing the meta-analysis, the main methods used in literature for estimating the critical and follow-up headways will be outlined in the following sections. The meta-analytic procedure will be then presented starting from the systematic literature review on worldwide studies incorporating estimations of critical and follow-up headways at the three schemes of roundabout, i.e. single-lane, double-lane and turbo roundabouts. After a brief introduction to the meta-analysis principles and models on which the meta-analysis is based on (namely the fixed-effect model and the random-effects model), the statistical approach performed to synthesize the best available empirical data of critical and follow-up headways will be described; finally, the results of the meta-analytic estimation will be presented and discussed.

2. The Gap acceptance parameters

Gap-acceptance models make it possible to evaluate capacity at any entry, when a hierarchy between traffic entry flows is established, taking into account users' behaviour through the so-called psycho-technical parameters, i.e. critical headway, follow-up headway and minimum headway. In order to understand the meaning of these parameters and how they can be estimated, it is necessary to analyze in detail the interactions between users of antagonistic traffic flows. Drivers' behaviour at roundabouts can be studied starting from users' behavior at Two Way Stop Controlled intersections (from now on TWSC). The driver, coming from a secondary flow, arriving at the intersection can enter only when a sufficiently large gap or headway in the major stream occurs, to make safe his/her maneuver. Therefore, the decision to make the desired maneuver is taken by users of the secondary flow on the basis of the subjective estimates of the position and speed of the vehicles belonging to the main stream. At roundabout intersections, drivers approaching the entry execute their manoeuvres when there is an acceptable gap in the circulating traffic flow. Therefore, critical headway is defined as the minimum time gap in the main flow which the driver in the minor

flow is ready to accept for crossing or entering the main flow [8]. By contrast, follow-up headway is the gap time between two successive vehicles in the minor flow that entering the conflict area of the intersection exploit the same gap in the main flow. According to [9], another parameter can be measured as part of the follow-up headway, that is the move-up time. Move-up time is the time that elapses between the departure of one vehicle, from the secondary stream and the arrival at the same stop line of the next vehicle under a condition of continuous queuing [9]. In modeling arrivals of vehicles, a minimum headway between two successive vehicles can also be identified in any (major) traffic flow.

In a general way, the headway is defined as the gap time among the passage of a vehicle from a certain section and the arrival of the successive vehicle from the same section. It is noteworthy that this distance, in terms of time, is calculated from the front bumper of the first vehicle to the front bumper of the next vehicle, while the gap (more used in the past) is computed from the rear bumper of the first vehicle to the front one of the next vehicle [5]. The following Figures 1 and 2 give an idea about the above definition of headways.
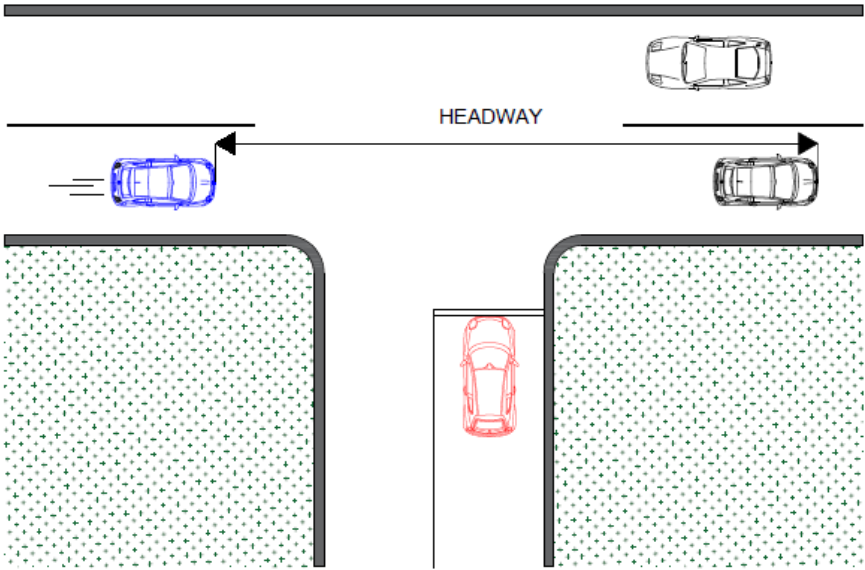
Figure 1 Graphic representation of the headway
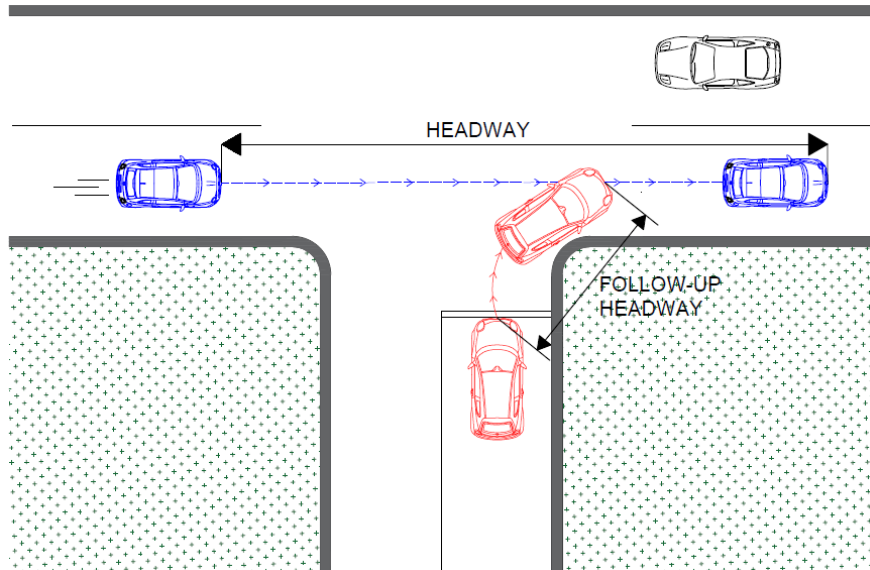
Figure 2 Graphic representation of the follow-up headway

As introduced above, the gap acceptance process is of a stochastic nature and the behavioral parameters (critical and follow-up headways), being related to subjective ratings by drivers, should be treated as random variables.

More detail about estimation of these parameters is provided in the next sections.

2.1. Estimation of Critical Headway

As has already been pointed out, the critical headway, being correlated to totally subjective assessments by drivers, is a random variable. Indeed, critical headways differ from driver to driver, for different types of intersections, the kind of movements and various traffic situations. Furthermore, not only does the critical headway vary from driver to driver, but the same driver can behave differently depending on the traffic situations that can occur. More to the point, drivers' behavior is defined as "inconsistent" since, waiting to make any manoeuvre at the intersection, at first, they could reject a certain gap of a given size, and subsequently accept another gap with a lower size than the one rejected. Therefore, with reference to the behavior of road users at intersection, the population of drivers is defined as non-homogeneous and inconsistent.

In any case, critical gap estimation methods can be based on the observations of two time intervals in the field: the *gap* and the *lag*. *The gap* has been defined in the previous section (it is computed from the rear bumper of the first vehicle to the front one of the next vehicle); in turn, the *lag* is defined as the time interval elapsing from the arrival instant of a driver belonging to the secondary flow to the stop line (or give-way signal) to the arrival instant (in front of it) of the approaching vehicle belonging to the main flow.

65
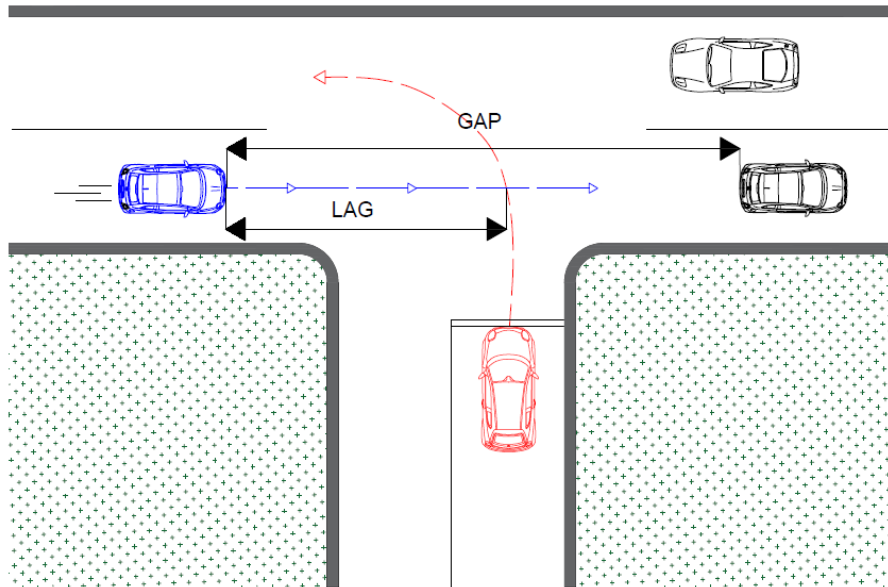
Figure 3 Graphic representation of the lag

These two time intervals are representative of a driver's behavior at the intersection. In fact, when a driver, coming from secondary flow, arrives at the stop line (or give-way signal), before making his/her maneuver, he/she evaluates the *"lag"* interval, defined above. Thus, he/she can make the maneuver basing on the decision of accepting or rejecting this *"lag"*. If this *"lag"* is rejected, then he/she can make the maneuver only when he/she consider a *"gap"* between two successive vehicles coming from major flow big enough to make the maneuver safe. Since it is difficult to evaluate the *"lag"* and especially the instant in which drivers make their decision, models that operate with the gap or headway, which on the contrary is easy to measure, are considered more reliable. Moreover, according to [10], methods for estimating the critical headway, based on "*lag*" evaluation, present some drawbacks related to the long time of the period of observation required in the field to measure these "*lags*". Indeed, if the traffic flow in the main road is low, it takes some time to observe *"lags"* of a small size; by contrast, if the traffic flow in the main road is high, the vehicles in the secondary road could be in a queue and therefore very few *lags* can be observed.

As discussed above, since the critical headway is variable in the population of drivers, it can be treated as a random variable with an unknown distribution. Indeed, some procedures attempt to estimate critical headway distribution, whereas other procedures rather than estimating the distribution of this parameter, more often, assume the form of distribution in advance, and one or more typical parameters of the distribution are sought, like median or variance. It is noteworthy that critical headway cannot be observed directly on the field, thus

it is not possible know a priori its distribution and its relevant parameters. Indeed, measurement in the field makes it possible to establish only if the driver's critical headway is greater than the largest gap rejected and less than or equal to the accepted one; i.e. only the accepted or rejected gaps can be measured.

Hence, although drivers' behavior is inconsistent in reality, an opposite assumption is made when the critical headway is estimated by a probabilistic approach: drivers' behavior is the same every time in all similar situations, i.e. drivers' behavior is consistent. Thus, a driver, coming from a minor flow, with a specific value of critical headway will never accept a headway between vehicles in the main flow less than his/her own critical headway, but will accept only headways larger than his/her own critical headway.

The critical headway can be estimated from on-field observations by employing several techniques which, in general, fall into two classes: the first class of techniques is based on a regression analysis between the number of users, which can enter into a major stream headway and the time duration of this headway; in this case, saturated conditions are required and the queue must have at least one behind the leading vehicle over the observation period. The second class of techniques, in turn, estimates the distribution of the critical headways.

Technical literature presents several methods for the estimation of the critical headway. Siegloch's method [11] belongs to the first class of the abovementioned models: starting from saturated traffic conditions, it uses the regression techniques for estimating the critical headway. In turn, a probabilistic approach is used when the minor stream does not queue continuously. In this regard one can mention Raff's method [12], Ashworth's method [13], and the maximum likelihood technique [14]. Most of these methods require appropriate observation of a minor street driver under unsaturated traffic conditions and his/her gap acceptance decisions at an entry of unsignalized intersections or roundabouts.

2.1.1. Siegloch's method

With reference to regression techniques, Siegloch [11] proposed to observe a condition of continuous queuing on the minor street; thus, one can observe n realizations (that are always integer numbers) for the function $n(\tau)$ by counting the number of the minor stream vehicles that enter the roundabout using major stream headways of size τ (see Figure 4). In order to represent the observed data, one can use the linear regression on the average headway size values (i.e. the dependent variable) against the number of vehicles that enter during this average headway size, $\bar{n}$, or:

$$\tau = a + b \cdot \bar{n} \tag{1}$$

in which the coefficients a and b, have to be estimated.
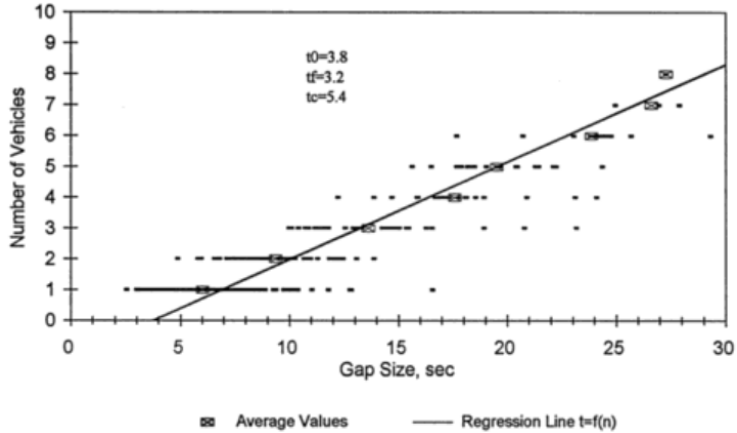
Figure 4 Siegloch method to estimate critical gap and follow up time [11]

However, the average headway size from the observed τ values, for each realization n, should be computed before starting the regression; otherwise the more numerous observations for the smaller *n*, would govern the whole result [10].

The linear regression function in Eq. 1 would be correct if the critical headway and the follow-up headway were constant values; then it can be written as follows:

$$(\tau) = \begin{cases} 0 & for \ \tau < \tau_0 \\ \dfrac{(\tau - \tau_0)}{\tau_f} & for \ \tau \geq \tau_0 \end{cases} \tag{2}$$

where $\tau_0 = \tau_c - \tau_f/2$ represents the intercept of the headway size axis and τ_f the slope of the linear regression above introduced. In this way, the critical headway τ_c can be calculated from the regression technique directly (see Figure 5).
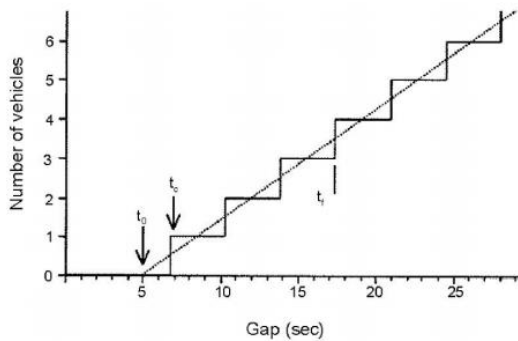
Figure 5 Representation of the linear regression line, the zero value of headway, t_0, given by the line intercepting the x axis, the critical gap t_c, and the follow-up time t_f given by the slope of the line [11].

68

It is important to emphasize that this method can only be applied for saturated conditions, i.e. continuous queuing on the minor street, which are difficult to find in many practical cases [10].

2.1.2. Raff's method

According to Raff and Hart [12] and assuming that lag headways are distributed with an exponential distribution, the critical headway represents that value of τ at which $1-F_r(\tau)=F_a(\tau)$, that is the cross point of the cumulative distribution function $F_r(\tau)$ of the rejected headways ($>\tau$) and the cumulative distribution function $F_a(\tau)$ of the accepted headways ($<\tau$). Thus, the determination of the critical gap graphically is performed, i.e. in a graph, in which x axis represents the time scaling and y axis the number of rejected/accepted lags, two cumulative distribution functions are represented: $F_a(\tau)$ and $F_r(\tau)$ (see Figure 6).
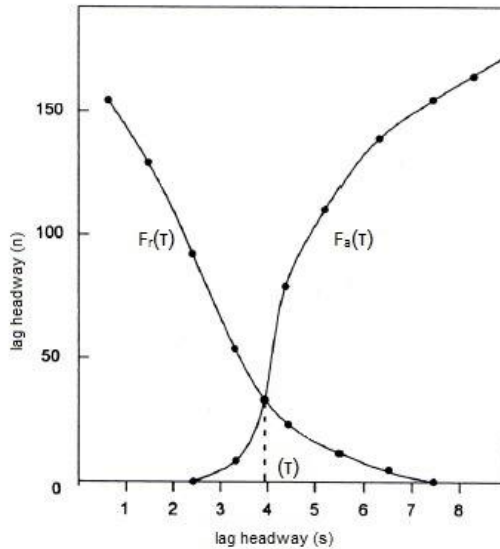
Figure 6 Raff's method to estimate the critical headway [12]

It is noteworthy that the critical headway represents the median value (not the mean value) of the distribution.

2.1.3. Ashorth's method

Differently from Raff and Hart [12], Ashworth [13] found that the critical headway (τ_c) can be estimated from the mean (μ_a) of the accepted headways (τ_a) and the standard deviation SD of the accepted headways (σ_a):

$$\tau_c = \mu_a - q_c \cdot \sigma_a^2 \qquad (3)$$

where q_c stands for major stream traffic volume (in volume per second).
It is noteworthy that the equation above is valid under the assumption of exponentially distributed major stream headways (with statistical independence between consecutive headways) and normal distribution for τ_c and τ_a.

Thus, for the critical headway estimation, Ashworth's method [13] uses only the accepted headways, neglecting the rejected headways. In turn, the maximum likelihood method requires information about the accepted gap and the largest rejected gap for each driver (see next section).

2.1.4. Maximum likelihood method

Troutbeck [14] described in detail this method based on the assumption that a driver's critical headway is larger than the largest rejected headway (τ_r) and smaller than the accepted headway (τ_a).
Thus, the method calculates the probability of the critical headway being between the largest rejected headway (τ_r) and the accepted headway (τ_a).
In order to estimate this probability, the driver's behavior is assumed to be consistent. The likelihood that the driver's critical headway τ_c will be between τ_r and τ_a is given by the difference between the two corresponding cumulative distribution functions:

$$F_a(\tau_a) - F_r(\tau_r) \tag{4}$$

Based on the two vectors of observed $\{\tau_r\}$ and $\{\tau_a\}$, the likelihood L^* for a sample of n observed entering drivers is given by:

$$L^* = \prod_{a,r=1}^{n} [F_a(\tau_a) - F_r(\tau_r)] \qquad (s) \tag{5}$$

whereas the logarithm L of the likelihood L*is given by:

$$L = \prod_{a,r=1}^{n} ln[F_a(\tau_a) - F_r(\tau_r)] \qquad (s) \tag{6}$$

The probabilistic distribution for the critical headways is usually assumed to be log-normal. The likelihood estimators μ and σ^2 the mean and the variance of the critical headway distribution), which maximize L are the solutions to the two equations $\partial L/\partial \mu = 0$ and $\partial L/\partial \sigma^2 = 0$. This leads to a set of two equations, which are depending on the vectors of the observed $\{\tau_r\}$ and $\{\tau_a\}$ and must be solved iteratively by using numerical methods. Troutbeck [14] proposed a solution by using iterative numerical solution techniques; thus the mean critical headway and its variance could be computed by:

$$\bar{\tau}_c = e^{(\mu + 0.5\sigma^2)} \quad \text{and} \quad s^2 = \bar{\tau}_c^2 \cdot \left(e^{\sigma^2} - 1\right) \tag{7}$$

According to Tian et al. [15] the mean critical headway could be calculated and used in various gap acceptance capacity and delay models, since it was an acceptable quantity for representing the average driver behaviour.

2.1.5. Other methods

Other methods for estimating critical headways have been also recommended for practical applications: Harders's method [16] discussed in more detail by Brilon et al. [10], the logit procedures, which provide many similarities to the classical logit models of transportation planning, the probit procedures, having formulations similar to the logit models, and used to estimate the probability that a gap will be accepted; however, in the last flows should be managed a lot more carefully [17]. Wu [18] proposed a method for estimating the distribution function of critical headways at unsignalized intersections based on equilibrium of probabilities; in turn, Hewitt's method [19] enabled the calculation of the probability distribution of the critical headways for entering drivers, which reject the initial lag; the method is based on observations of the time duration of the headways refused and eventually accepted by drivers. Hewitt [20] also performed a comparison between some methods for measuring the critical headway.

More recently, microscopic approaches have been also used to estimate the critical headway at roundabouts. For instance, Vasconcelos et al. [21] proposed an alternative gap-acceptance model that described the interactions on a microscopic level between the entry and opposing vehicles. The model explored the complex interactions between the driver/vehicle dynamics and the intersection geometry; it was calibrated based on a video recording of a Portuguese roundabout, and then validated by using geometric and traffic characteristics of other roundabouts. Since the estimates were close to the results of traditional estimation methods, the proposed model was considered a promising alternative to field observations, particularly for non-standard intersections. In the field of roundabouts, just as for the at-grade intersections, several studies and researches developed worldwide provide measurements of driver's critical headway. In most cases, the maximum likelihood procedure resulted the most promising method for estimating the critical headway at single-lane and multilane roundabouts.

2.2. Estimation of the Follow-up Headway

Differently from the critical headway, the follow-up headway can be estimated directly from on field observations by measuring the difference between the entry departure times of the minor street queued vehicles using the same gap in the major stream [5].

Harders [16] proposed a relation to estimate a n_f observations in order to get an estimate of sufficient reliability (S% probability that the estimate is a range of relative error, r_f, around the true estimate). Thus, assuming the standard deviation δ_f equal to $0.4 \cdot t_f$ (where t_f is the follow-up headway), the necessary number of observation can be calculating by the following equation:

$$n_f = a_f \cdot \frac{1}{r_f^2} \tag{8}$$

where:

- n_f is the necessary number of observations;
- r_f is the relative error, equal to: e_f/t_f;
- e_f is the absolute error;
- δ_f is the standard deviation of the statistical distribution of the t_f;
- a_f is a function of S, and is given as follows:
  - *if S=90%, a_f =0.4;*
  - *if S=95%, a_f = 0.6;*
  - *if S=99%, a_f = 1;*

Rodegerdts et al. [22] observed that vehicles using the same headway usually have the same opposing vehicle time, which may be calculated based on the accepted *lag* or the accepted headway. By using the accepted *lag*, the opposing vehicle time can be calculated by adding the entry arrival time to the accepted *lag*; by using the accepted headway, in turn, the opposing vehicle time can be calculated by adding the entry arrival time to the total rejected headway*s* and *lag*. It is noteworthy that, at multilane sites, the follow-up headway may be also influenced by the dominant and subdominant arrival flows. However, further sites with dominant left-lane arrival flows should be examined to validate the concept; what is more, interdependencies between entering and circulating vehicles at multilane roundabouts can be observed, because of the priority reversal between entering and circulating vehicles [5, 23]; however, the literature may also be consulted for the description and illustration of further details on this last issue.

2.3. Estimation of the Minimum headway

Even the minimum progress is a random variable, being generally tied to the individual user's assessment of the minimum distance to be maintained by two successive vehicles to be able to proceed safely. However, in the literature, as is the case for the follow-up time, the variability of the minimum headway between users is usually neglected, referring to a single value representing the entire population of users, without giving up the probability distribution. This choice is generally made, because there is a very small variability around the average values between the experimental determinations of the minimum headway values; see e.g. [24].

3. Meta-analytic estimate of gap acceptance parameters

Systematic reviews and meta-analysis have their origins around the '90s. Before then a different approach based on narrative review was undertaken by many researchers in several fields in order to combine data from multiple studies, to summarize the findings, and then to arrive at a conclusion. Unlike the classic narrative review, the systematic review is conducted using a clear set of rules to search for studies, and then determining which studies will be included in or excluded from the analysis. A key element in most systematic reviews is the statistical synthesis of the data, or as it is better known, the meta-analysis. In this regard, systematic reviews are part of meta-analysis [7].

Meta-analysis is a statistical technique to formally combine numerical results from different studies. Therefore, meta-analysis differs from traditional literature reviews for:

- systematic and exhaustive research of the results of studies conducted all over the world;
- explaining the criteria for inclusion of the studies considered;
- the statistical analysis of the results of the studies.

Since many studies conducted worldwide provide estimates of the critical and follow-up headways, the aim of the research activity referred to in this Chapter was to obtain a comprehensive measure, more accurate and reproducible for the parameters of interest at each roundabout under examination, through a meta-analysis; thus, a summary effect could represent a better outcome than can be obtained by each individual reviewed study.

The first step was performing the systematic literature review; it makes possible to summarize and evaluate the state of knowledge or practice on measuring critical and follow-up headways at single-lane, double-lane and turbo roundabouts installed both in countries with a longstanding tradition on roundabouts, but where turbo-roundabouts are also in operation, and in other countries where in more recent times modern and/or alternative roundabouts are becoming common as intersection control. This review of existing knowledge represented a preliminary step in a larger research activity aimed at summarizing in some way the collective results and exploring the presence or not of heterogeneity among the examined studies. To do this, the results of the examined studies were sorted into categories based on what the existing studies, researches and published reports had in common, what the studies disagree about, and what they overlooked or ignored. Thus, in order to reach a judgment about the quality of the literature overall, only studies having findings that appeared to be valid for complete information in terms of average values of critical and follow-up headways (with the corresponding values of variance) and sample size were considered. Then a meta-analysis of the individual studies was implemented as part of the literature review to assess the consistency of the effect across studies and to compute the summary effect.

Next sections explain better - step by step- the meta-analysis applied to synthesize measures of critical and follow up headways from observations at single-lane, double-lane and turbo roundabouts as reported by individual reviewed studies.

3.1. Literature review on critical and follow-up headway estimations at roundabouts

The meta-analytical estimation procedure started with a literature review on critical and follow-up headway estimations at single, double lane and turbo roundabout. For the estimation of critical and follow-up headways from observations at roundabouts, a long series of methods has been proposed. Focus is made on studies which have addressed the problems of how to manage the randomness and the variability of values of critical and follow-up headways, and how to depict the distribution of these gap acceptance parameters.

Without expecting to be exhaustive, studies and researches developed worldwide were examined, with reference to the countries (as European countries and Australia) where the roundabouts have an older tradition and schemes of turbo-roundabouts are already in operation. Reference is also made to non-European countries where in more recent times roundabouts are becoming more and more common as intersection control and great emphasis has been given to geometric design and the appropriate use of the many roundabout installations progressively realized.

The reader should be aware that UK and French studies were excluded from investigation despite the important role of the experiences of these countries on improving the roundabout installations. Experiences in United Kingdom were based on a capacity formula which is not a gap acceptance-based model, but the geometric design only is taken into account at a reasonable level of detail. In turn, the French procedure for capacity calculations at roundabouts is based on the exponential regression technique; in this case, it is necessary to determine some geometric values of the roundabout and to use a pre-fixed value of the follow-up headway to implement the formula. Bearing in mind the inclusion criteria that it was established for the analysis, French and UK experiences on roundabouts are not introduced in this literature review on critical and follow-up headway estimations at roundabouts.

3.1.1. European studies

3.1.1.1. German studies

The capacity of roundabouts has been studied over many years by a series of investigations in Germany where for all types of modern roundabouts, except the mini, the capacities of entries have been established as independent from the flow at the other entries. Although both gap acceptance theory and the empirical regression method have been in the scope of these investigations, Brilon [25]

affirmed that the currently established official procedure in the German Highway Capacity Manual [26] is related to gap acceptance theory and uses Tanner's equation [27] in a form which was adjusted to the necessities of roundabout analysis. In order to ease capacity calculations, the computer program KREISEL, which can also apply capacity calculation procedures as they are reported from many other countries, is in frequent use [28].

According to Brilon [29], the values of critical, follow-up and minimum headways at single-lane roundabouts are depending on the inscribed circle diameter ranging from 26 m to 40 m, whereas for multi-lane roundabouts the values of the behavioural parameters could be derived from the capacity formulas calibrated to German traffic conditions. Table 1 shows the minimum and maximum values of the mean critical headway derived from equations proposed by Brilon [29], where the inscribed circle diameter was set equal to 14 m and 40 m, respectively. Within these values of the inscribed circle diameter we could recognize the mini and the compact roundabouts as classified by several international guidelines. The same table shows the minimum and maximum values of the mean follow-up headway; similarly, the minimum headway values resulted ranging from 2.04 s and 2.90 s.

Wu [30] proposed the values of the critical, follow-up and minimum headways to be introduced in the formula for the entry capacity of a roundabout (see Tables 1 and 2); these parameters have been found to represent driver behaviour at roundabouts in Germany and used in the recent edition of German HCM [26]. Wu [31] also estimated the distribution function of critical headways at unsignalized intersections based on equilibrium of probabilities; thus, he presented a solution accounting for different predefined distribution functions of critical headways. To carry out regression analysis, the form of the function was specified; thus, the log-normal distribution and the Weibull distribution were calibrated to the empirical distribution of critical headways. However, the Weibull distribution gave the best results in representing the distribution of critical headways.

Brilon et al. [32] proposed a framework for capacity estimation at turbo-roundabouts entries. Table 3 shows the values of the behavioural parameters depending on the scheme of conflict with one or two circulating streams; the same table shows the mean values of the critical headways for left and right lanes from major entries, where entering vehicles are faced by one circulating stream, and from minor entries, where entering vehicles are faced by two circulating streams.

3.1.1.2.   Swiss studies

An extensive field data collection at 15 double-lane roundabouts with high traffic volume and different geometric characteristics provided a rich database for the analysis of the behavioural parameters [33]. Based on the observations of 2013 gap times of 16 entries, the critical and the follow-up headways were estimated. The maximum likelihood method [15, 34] was applied to measure driver's critical

headways; the logarithmic normal distribution was used as mathematical function for the statistic distribution of these parameters. In turn, follow-up headways were determined with the arithmetic mean of the gap times, which were used for a subsequent entry in the roundabout. The minimum and maximum values of the mean critical and follow-up headways are summarized in Table 2. It should be noted quite large differences among the values of the critical headways (3.22 s for the minimum value and 4.33 for the maximum value), whereas the variability in the measured values of follow-up headway is kept small (about 0.5 s).

3.1.1.3. Danish studies

In a Danish study aimed at estimating entry capacity and delay, a double-lane roundabout in Copenhagen, Denmark, was investigated; data were collected to enables the estimation of critical and follow-up headways [35]. Mean values of critical headways were estimated by using the maximum likelihood methodology [15] for the left- and the right-lane at entries (see Table 2). Critical headway estimates were provided for different levels of circulating flows (low, medium and high) and for the overall circulating flow. Moreover, in the case of the overall circulating flow, the mean critical headways for the left lane at entries resulted higher than the mean critical headways for the right-lane. Estimations of the critical headways were performed also when the headway distributions in each circulating lane were considered separately. Thus, critical headways were also distinguished for the inner and outer circulating lanes; for each entry lane, the values of critical headways for the inner circulating lane resulted lower than the corresponding values for the outer circulating lane, whereas the standard deviation showed the opposite trend. However, in all cases Hagring [35] observed that the values of critical headways resulted stable, from a minimum value of 3.68 s to a maximum of 4.68 s, with a spread of slightly over a second for the various lanes and circulating flow combinations. Follow-up headways were also estimated both considering different types of vehicles (cars and heavy vehicles), and considering all vehicles. Table 2 shows the all vehicles-related values of follow-up headways. It should be noted that follow-up headways did not vary appreciably by entry lane, but there was a noticeable difference between cars and heavy vehicles; however, the sample size for heavy vehicles resulted small, and did not lead itself to statistical testing. Further investigation was conducted in Denmark [36]; based on field measurements, estimations of critical and follow-up headways were done (see Table 2).

3.1.1.4. Dutch studies

Further investigation by Fortuijn [37, 38] covered several types of roundabouts in The Netherlands. An extensive traffic data collection formed the basis for the calibration of gap acceptance parameters for capacity models. Critical headways were derived from the difference between the accepted and rejected gaps. A

maximum likelihood approach based on the assumption that the critical headway distribution is log-normal gave the best results. Follow-up headways were measured; the median value of this headway was selected as a better measure than the mean. The minimum and maximum values of the (mean) critical headway were estimated both for single-lane roundabouts (see Table 1), and for double-lane roundabouts (see Table 2), as well as for turbo roundabouts (see Table 3); the same tables show the values of the follow-up headway. It should be noted that for double-lane roundabouts the mean values of critical and follow-up headways were differentiated by each entry lane (i.e. for the left- and right-lane at entries, where data were available) and distinguished for the inner and outer circulating lanes. Moreover, a further distinction was made between the major road and the minor road at turbo-roundabouts to consider two antagonist traffic streams for the left entry lane of minor roads, and only an antagonist traffic stream for the left- and the right-lane of major roads and for the right entry lane of minor roads. The same tables also show the corresponding values of the standard deviation.

3.1.1.5. Italian studies

The Italian experience on measurement of critical and follow-up headways includes investigations recently conducted by Gazzarri et al. [39] at single-lane and multilane roundabouts. Various well-known techniques for measuring the critical headway using field data were applied, i.e. maximum likelihood method [15], median method [40] and Raff's method [12]; however, the values of the critical headways obtained by the maximum likelihood method represented the best result and they were used in the following statistical analysis (see next section 3). Gazzarri et al. [39] assumed the log-normal distribution for the probabilistic distribution of critical headways and obtained the mean and the variance of the log-normal function by maximizing the likelihood function. The likelihood function was defined as the probability that the critical headway distribution lies between the observed distribution of the largest rejected headways and the accepted headways. Once obtaining the individual follow-up headway, the mean follow-up headway and the standard deviation were calculated from recorded time events at sites under examination. The range of variability of the (mean) critical and the follow-up headways, identified by the minimum and maximum values of these parameters, as well as the corresponding values of the standard deviation, are reported in Tables 1 and 2. Some further indications on the estimations of critical headways were derived from Romano [41] at three multilane roundabouts. For one site, the empirical distribution of critical headways showed two peaks, that characterized two classes of users and a double normal aleatory variable was chosen to fit the empirical distribution. For the other roundabouts the situation resulted more homogeneous and the gamma function was selected to interpret the empirical distributions. Nicolosi et al. [42] investigated three roundabouts: one single-lane roundabouts and two multi-lane roundabouts and measured the

values of critical and follow-up headways; the method proposed by Dawson [43] and the regression method proposed by Siegloch [11] were applied. The analysis of experimental data showed that the hypothesis of Gamma distribution was always verified for the follow-up headway. De Luca et al. [44] investigated four existing rural roundabouts and used real data to calibrate a simulation model. The analysis of the sample allowed to identify the Gumbel distribution as the function that best approximated the observed distribution of the data. Table 2 reports the values of the estimated critical headway and the standard deviation.

3.1.1.6. Portuguese studies

In a Portuguese study a new critical-headway model to describe the gap-acceptance process at microscopic level for roundabouts was proposed [21]. Basing on a data sample collected at a one-lane urban roundabout in Coimbra, Portugal, the model was calibrated and then validated against conventional methods (i.e. such as Raff's method [12], Logit methods [45], maximum likelihood method [15]). The values of critical headways are shown in Table 1. In another study Vasconcelos et al. [46] estimated critical headways and follow-up times basing on observations at six Portuguese roundabouts; gap-acceptance data were collected at each entry, for the left- and right-lanes independently. The Authors applied several estimation methods: Siegloch [11], Raff [12], Wu [31], maximum likelihood [15] and logit method [45]. The results revealed important specificities of the methods with significant effects on the capacity estimates. The comparison of the estimates with values from several countries indicated significant differences among them and suggested the presence of relevant driving style differences; as a consequence, Vasconcelos et al. [46] came to the conclusion that locally calibrated, country-specific, parameters should be preferred for capacity calculations.

3.1.2. Non European studies

3.1.2.1. Australian Research

Various researches and studies were developed in Australia focusing on geometric design, capacity and delays at roundabouts (see e.g. [47-50]). Troutbeck [51] addressed the problem about suitability of the gap acceptance theory to adequately predict the capacity of a roundabout and developed an analytical equation based on gap acceptance characteristics which were measured at roundabouts operating below capacity.
Critical and follow-up headways were related to roundabout geometry and capacity. Based on Troutbeck's studies for the Australian Road Research Board, some changes to the analysis and design of roundabouts were proposed [48, 52]. Troutbeck's critical headway research [48-52] led to the development of a lane-based model that considers the conflicting lane gaps as the combination of gaps

between the vehicles of the circulating streams; thus, for the right entry lane, all conflicting vehicles have an influence on the entering drivers' behavior, which will be true in some cases and generally conservative. If a vehicle in the right entry lane enters at the same time as a vehicle is circulating in the inner conflicting lane, the defined accepted gap may be quite small [22]. Further detailed capacity expressions have been published in Australia; these are most recently available in Akçelik [24, 53] and have been incorporated into the software aaSIDRA [47, 54]. The roundabout capacity is calculated lane-by-lane. An important feature of this method is to treat the lanes at multi-lane entries as dominant and subdominant lanes to which different values of critical and follow-up headways are assigned; the lane with the largest flow rate is called dominant lane and other lanes are called subdominant lanes. The critical and follow-up headways for roundabouts were those predicted by Troutbeck [55]; however, the values adopted in Austroads [56] were modified. In order to prevent the prediction of very low follow-up headways, the maximum value of the inscribed diameter, used in the formula for calculating the follow-up headway in the case of the dominant lane, was limited to 80 m. Furthermore, a maximum follow-up headway of 4 s (applied to dominant lanes only) and a maximum critical headway of 10 s (applied to all lanes) were used; in order to prevent the prediction of very large values of follow-up and critical headways, the inscribed diameter value was limited to 20 m [56]. The minimum and maximum values of the follow-up headway in use into the recent versions of the software aaSIDRA are 1.2 s and 4 s (applied to all lanes), respectively; in turn, the minimum and maximum values of the critical headway are 2.2 and 8 s, respectively. Currently aaSIDRA Intersection offers two roundabout capacity model options: the US HCM 2010 model and the aaSIDRA standard roundabout capacity model; there are various key parameters involved in changing between the two models [57]. The reader is referred to the user guide for any detailed information. Further investigation on five multi-lane roundabouts allowed to measure critical and follow-up headways [58]. The critical headway resulted equal to 3.2 s (ranging from 2.13 s to 4.31 s), while the follow-up headway resulted equal to 2.3 s (with a minimum value of 1.44 s and a maximum value of 3.25 s).

Qu et al. [59] estimated the follow-up headways at a single lane roundabout in Australia during different periods. The mean value of the follow-up headway was found equal to 2.76 s with the standard deviation equal to 0.62 s. In order to obtain the best estimate of the distribution of the follow-up headway, seven continuous distributions were used: inverse Gaussian, exponential, Normal, Lognormal, Gamma, Weibull, Erlang and Kolmongorov-Smirnov test. According to this study the inverse Gaussian distribution gave the best fit. Critical headways were also predicted (see Table 2).

3.1.2.2. US Research

The experience in design practice of modern roundabouts in the United States can be found in the successive editions of Roundabouts: informational guide [5, 60] which provide the most effective approach to the solution of many problems regarding planning, designing, and operational analysis for this kind of intersections. The FHWA Roundabout Guide [60] presents three capacity formulas for estimating the performance of roundabouts. These were intended for use as provisional formulas until further research could be conducted with US data. The FHWA method for urban compact roundabouts is based on German research [10, 32, 34], whereas the method for single-lane is based on the UK's Kimber equations [4] with default values for each of the geometric parameters. The FHWA method for double-lane roundabouts is also based on the Kimber equations [4] with default values for each of the geometric parameters. The NCHRP Report 572 [22] describes some investigations undertaken at a representative sample of single-lane and multi-lane roundabouts for the estimation of the critical headways. Based on a driver's critical headway being larger than the largest rejected headway and smaller than the accepted headway, calculation of critical headways was made using the maximum likelihood method [15]; the log-normal distribution was assumed as the probabilistic distribution of the critical headways. Critical headway estimates at single-lane sites were performed using three different ways of determining the critical headway:

- inclusion of all observations of gap acceptance, including accepted lags s;
- inclusion of only observations that contain a rejected gap;
- inclusion of only observations where queuing was observed during the entire minute the driver rejected a gap.

The critical headway determined using method 1 resulted ranging between 3.9 s and 5.1 s, with a weighted mean of 4.5 s and the mean standard deviation of 1.0 s, while the critical headway determined using method 2 varied between 4.2 s and 5.9 s, with a weighted mean of 5.0 s and the mean standard deviation of 1.2 s; in turn, the critical headway determined using method 3 varied between 4.9 s and 5.6 s, with a weighted average of 5.1 s and the mean standard deviation of 1.3 s. Critical headway estimates at multi-lane sites were done using two different techniques [22]. The first technique assumed each entering lane and conflicting lane separately; vehicles entering from the right entry lane use the gaps in the outer circulating lane (and yield only to conflicting vehicles in the outer lane), whereas vehicles entering from the left entry lane use the combined gaps of the inner and outer circulating lanes. The second alternative technique allowed to estimate the critical headway for the entire approach, combining the entering lanes and conflicting lanes into single entering and conflicting streams, respectively. Lots of investigations have also been made for the purpose of calibrating the existing capacity models for roundabouts [22]; thus, the critical headway was calculated with the original techniques used to develop those

models. The critical headways for the multilane-site data were determined using observations conforming to methods 2 and 3 as described above for single lane critical headway. The critical headways determined using method 2 varied between 3.4 s and 4.9 s in the right lane and 4.2 s and 5.5 s in the left lane (with a weighted mean of 4.3 s and 4.8 s, respectively), while the critical headways determined using method 3 varied between 3.2 s and 4.9 s in the right lane and 3.7 s and 5.5 s in the left lane (with a weighted mean of 4.2 s and 4.6 s, respectively). It is noteworthy that some sites have less than 50 critical headway observations for individual lanes; thus, while the average critical headway of each site could change with a larger sample size, the result was indicative of the average behaviour of the site during those minutes when queuing was observed. Based on a recent analysis of lane-based US field data, HCM [6] proposes a capacity model for single-lane and multi-lane roundabout entries which can be viewed both as an exponential regression model and a gap-acceptance model [57]. The HCM multi-lane capacity model was also developed for the right-lane and the left-lane of a two-lane entry; the behavioural parameters are then related to each specific entry lane [6]. The mean critical and the follow-up headways, as derived from the capacity formula for single-lane roundabouts, are equal to 5.19 s and 3.19 s, respectively. In turn, the mean critical and the follow-up headways for right lane, as derived from the capacity formula for double-lane roundabouts, are equal to 4.11 s and 3.19 s respectively, whereas the mean critical and the follow-up headways for left lane are equal to 4.29 s and 3.19 s, respectively [6].

With regard to the follow-up headway estimations at single-lane roundabouts, calculation was made basing on a value of the move-up time - the time the next vehicle takes to move into entry position - less than 6 s; this value indicates a queued condition. The minimum and maximum values of the mean follow-up headways for the right and the left entry lanes with their standard deviation values are reported in Tables 1 and 2. The HCM 2010 roundabout capacity model [6] is based on research on US roundabouts [22], and is fully integrated into SIDRA intersection software [58].

The values of critical and the follow-up headways above are different from values proposed by the HCM 2000 [61]. Based on background provided by Troutbeck [62], the HCM 2000 [61] introduced the method only for single-lane roundabouts; thus, an upper and a lower bound of 4.1 s and 4.6 s were proposed for the critical headway, whereas an upper and lower bounds of 2.6 s and 3.1 s, respectively, were introduced for the follow-up headway.

Further investigations for the estimation of the critical and follow-up headways were conducted by Zheng et al. [63]. Critical and follow-up headway data were extracted for four roundabouts. The estimation of the critical headways included the mean and the standard deviation, following the current state-of-practice maximum likelihood method [15]; estimation of the follow-up headways included the sample average and standard deviation. Other factors as the consideration of

the adjacent exiting vehicles, vehicle type and queue lengths were also investigated.

The assumption of log-normal distribution for the critical headway was made as suggested by Troutbeck [64] and used in NCHRP Report 572 [22]. Critical and follow-up headways were estimated considering (or not considering) exiting vehicles. For multi-lane roundabouts, engineering judgment was required to examine the different scheme of conflicts with one or two antagonist traffic streams faced by right or left turning vehicles from entries. The minimum and maximum values of the mean critical and follow-up headways at single- and multi-lane roundabouts with their standard deviations are reported in Tables 1 and 2.

Li et al. [65] also estimated the critical headway through the maximum likelihood method [15]; the assumption of lognormal distribution for the critical headway was made. However, they refer only the mean values of the critical and follow-up headways (with the corresponding values of deviation standard) for the most congested entry lane (i.e. the left entry lane) of the double-lane roundabout which was examined (see Table 2).

Xu and Tian [66] collected headway and gap acceptance characteristics, measurement of geometry and vehicle speeds at Californian roundabouts. Critical headways were obtained for single-lane and multi-lane roundabout sites; the maximum likelihood methodology was used to estimate these headways [34]. At single-lane roundabouts the critical headway resulted ranging between 4.5 s and 5.3 s, with a mean value of 4.8 s, while at double-lane roundabouts the critical headway for the left lane varies between 4.4 s and 5.1 s with a mean value of 4.7 s, and the critical headway for the right lane varied between 4.0 s and 4.8 s, with a mean value of 4.4 s. Unlike for critical headway estimation, follow-up headways were obtained directly from recorded time events; the minimum and maximum values of the critical and follow-up headways estimated for the examined sites are shown in Tables 1 and 2. Further field observations were made by Abrams et al. [67]. The Raff's method [12] was used to calculate the critical headway. For the single-lane roundabout a value 2.2 s was found for the critical headway.

Mensah et al. [68] measured the behavioural parameters at two roundabouts in Maryland, US; they collected the accepted and rejected gaps and the follow-up headways. These headways were compared with those obtained in the same sites four year before and the critical headway values resulted reduced, probably due to experience gained by users in the meantime with this type of intersections. The mean values of critical headways were recorded equal to 2.50 s and 2.60 s for the two sites examined, against values of 3.91 s and 3.85 s obtained in 2005.

3.1.2.3.   Canadian Studies

Dahl and Lee [69] observed vehicle movements at 11 roundabouts in Vermont, Wisconsin, and Ontario, Canada, and estimated gap-acceptance parameters for cars and heavy vehicles separately in order to examine the effect of heavy vehicles

on the entry capacity of roundabouts. Two conventional methods were used to estimate the critical headway at all roundabouts. The mean critical headway resulted ranging between 3.9 s and 4.8 s for cars; in turn, the critical headway resulted ranging between 4.5 s and 6.1 s for heavy vehicles. However, as expected, the critical headway for heavy vehicles was longer than that for cars since heavy vehicles require longer headway to enter the roundabout because of their larger size and slower acceleration. The follow-up headways for different vehicle following conditions were also calculated [69]. The follow-up headway resulted longer when a heavy vehicle was a lead vehicle, a following vehicle, or both. The follow-up headway for the heavy vehicle car case was longer than the follow-up headway for the car heavy vehicle case, because it took a longer time for the lead heavy vehicle to enter the roundabout than for the lead car [69]; it was also found that the follow-up headway for the heavy vehicle-heavy vehicle case was the longest due to the lead heavy vehicle's slow entry and the following heavy vehicle's low acceleration.

3.1.2.4.   Chinese studies

In a Chinese study concerning capacity prediction models, the values of critical headways were obtained for a double-lane roundabouts [70]. The values of behavioural parameters both for the right and the left entry lane with two different methods were estimated. Thus, based on the field data, the maximum likelihood method [15] and the Raff's method [12] were used. Assuming that critical headways followed the log-normal distribution, the mean value and the deviation standard of critical headway were obtained. The results of two methods were similar with a maximum difference of about 3.8 %. Further investigations at an existing roundabout were carried out by Guo [71] which estimated the value of mean critical headway using different conventional methods (i.e. maximum likelihood method [15, 34], Raff's method [12], Ashworth's method [13]). The Ashworth's method gave the highest value, while the maximum likelihood method provided the lowest value of critical headway. Despite its simplicity in calculating the critical headway the Ashworth's method assumes the exponential distribution for the headway of circulating stream and the normal distribution for the accepted gaps; this situation is often difficult to satisfy on field because traffic streams can result influenced by upstream traffic conditions or low flow rates in undersaturated conditions.

3.1.2.5.   Japanese studies

In a Japanese study critical and follows up headway measurements were made at a multi-lane roundabout [72]. In order to estimate the behavioural parameters, the accepted and rejected gaps in the circulating stream were collected. Based on these data the cumulative curves of the rejected and accepted gaps were built; mean critical headways were found ranging between 3.00 s and 3.80 s depending

on the entry approach, while the mean follow-up headway ranged between 3.26 s and 4.90 s.

3.2. Statistical treatment of the systematic review on critical and follow-up headways

The above systematic review was completed performing the statistical treatment of data of the individual studies with the objective to summarize the results and to calculate the summary effect; for this purpose, a meta-analysis was implemented as part of the literature review. The following Tables 1, 2 and 3 show the results of the systematic review; each of these tables shows the on-field observations of critical and follow-up headway values referred to a specific roundabout scheme, namely single-lane, double-lane and turbo roundabouts. In particular, one can read, starting from the left: the study name, i.e. the authors of the study taken into account, the country in which parameters were observed, the method applied for estimating parameters and then the mean values of critical and follow-up headways with the relative value of the standard deviation, when this latter was available. It is noteworthy that in these tables is shown only the maximum and minimum values of all observations of the critical and follow-up headways collected for the same study.

Table 1 - Critical and follow-up headways values for single-lane roundabouts

Study name	Country	Estimation method applied	critical headway				follow-up headway			
			mean [s]		St. dev. [s]		mean [s]		St. dev. [s]	
			min	max	min	max	min	max	min	max
Abrams [67]	US	R.M.	2.20	-	-	-	-	-	-	-
Brilon [25, 29]	Germany	n.a.	4.07	4.45	-	-	2.89	2.99	-	-
Dahl & Lee [69]	Canada	R.M., P.E.	3.90	5.30	-	-	2.10	4.20	-	-
Fortuijn [37]	Holland	n.a.	3.16	3.28	0.19	0.28	2.10	-	-	-
Gazzarri et al [39]	Italy	R.M., M.L.M., M.M.	3.54	4.10	0.67	0.95	2.52	2.76	0.68	0.90
Mensah S. et al [68]	US	n.a.	2.50	2.60	-	-	-	-	-	-
Nicolosi et al [42]	Italy	M.L.M., E.R.M.	3.19	3.99	1.13	-	3.15	2.11	0.59	-
Qu X et al [59]	Australia	n.a.	-	-	-	-	2.76	-	0.62	-
Rodegerdts et al [22]	US	M.L.M.	3.90	5.90	0.70	1.80	2.60	4.30	0.80	1.50
Vasconcelos et al [21]	Portugal	R.M., M.L.M., L.M., W.M., P.M.	3.23	4.50	-	-	-	-	-	-
Vasconcelos et al [46]	Portugal	R.M., M.L.M., E.R.M., L.M., W.M.	3.37	4.28	-	-	2.08	2.20	-	-
Wu [30]	Germany	n.a.	4.12	-	-	-	2.88	-	-	-
Xu & Tian [66]	US	M.L.M.	4.50	5.30	0.90	1.10	2.30	2.80	0.30	1.00
Zheng et al [63]	US	M.L.M.	3.80	5.50	1.00	2.00	2.30	3.80	1.00	2.60

According to the meta-analysis principles, the studies included in the analysis were selected through a set of rules. The inclusion criteria, used for the selection of the studies, were consistent with the following objectives:

- to handle the same geometric scheme of roundabouts (i.e. single-lane roundabouts, double-lane roundabouts or turbo-roundabouts);
- to face with comparable estimation methods of headways and/or similar detection techniques;
- to get the entire distribution of the headways (i.e. mean, variance and sample size).

In order to carry on a meta-analysis of the individual studies, a specific software package Comprehensive Meta Analysis V3, was used [73]. This software uses a spreadsheet for data entry, but requires the user to identify specific columns to hold the study names and the effect size data. Thus, once the studies were selected according to the above criteria, the study name and critical and follow-up headway, characterized by mean, sample size and standard deviation, were inserted into specific columns. For each study, a subgroup was created in order to consider all the on-field observations of critical and follow-up headways carried out for the same study. Furthermore, the values of the critical headways considered in the calculations were identified with reference to studies where the maximum likelihood method only was used.

Therefore, once the entry data were inserted inside the spreadsheet of the software, it was possible to launch the analysis.

Before introducing the calculations and the modelling results, a brief overview of the models on which the meta-analysis is based on is described in the following sections.

Table 2 Critical and follow-up headways values for double-lane roundabouts

Study name	Country	Estimation method applied	Entry	critical headway				follow-up headway			
				mean [s]		St. dev. [s]		mean [s]		St. dev. [s]	
				min	max	min	max	min	max	min	max
Dahl & Lee [69]	Canada	R.M., P.E.		3.50	6.10	-	-	1.60	5.00	-	-
De Luca et al [44]	Italy	n.a.		3.22	-	0.80	-	-	-	-	-
Fortuijn [37]	Holland	n.a.	*left*	2.89	3.16	0.04	1.32	2.24	2.26	-	-
Gazzarri et al [39]	Italy	R.M., M.L.M., M.M	*left*	3.59	4.42	0.64	1.14	2.16	3.10	0.49	0.95
			right	3.19	4.33	0.61	1.08	2.44	2.91	0.58	0.76
Greibe et al [36]	Denmark	K.M.	*left*	3.90	4.10	-	-	2.60	-	-	-
			right	3.90	4.20	-	-	2.70	-	-	-
Guo [71]	China	R.M., M.L.M.,R.R.M., A.M.		2.62	3.20	-	-	-	-	-	-
Hagring et al [35]	Denmark	M.L.M.	*left*	4.36	4.68	1.10	1.82	2.79	-	0.87	-
			right	3.68	4.49	1.20	1.68	2.89	-	1.03	-
Leemann & Santel [33]	Switzerland	M.L.M.		3.22	4.33	-	-	2.27	2.63	-	-
Li et al [65]	US	M.L.M.	*left*	4.30	-	1.00	-	3.10	-	1.20	-
Manage et al [72]	Japan	n.a.		3.26	4.90	-	-	-	-	-	-
Nicolosi et al [42]	Italy	M.L.M., E.R.M.		1.87	2.94	0.35	1.01	1.87	2.50	0.42	0.55
Qu Z et al [74]	China	M.L.M. R.M	*left*	4.57	4.85	-	-	-	-	-	-
			right	4.41	4.58	-	-	-	-	-	-
Rodegerdts et al [22]	US	M.L.M.	*left*	3.70	5.50	0.70	2.60	2.90	5.00	1.00	3.90
			right	3.20	4.90	1.00	3.80	2.80	4.40	0.80	2.30
Romano [41]	Italy	n.a.		2.03	3.69	0.24	1.45	-	-	-	-
Vasconcelos et al [46]	Portugal	S.M., R.M., M.L.M., W.M., L.M.		2.56	4.46	-	-	1.94	2.78	-	-
Wu [30]	Germany	n.a.		4.12	-	-	-	-	2.88	-	-
Xu & Tian [66]	US	M.L.M.	*left*	4.40	5.10	0.90	1.10	1.80	2.70	0.60	0.90
			right	4.00	4.80	0.90	1.10	2.10	2.30	0.70	1.00
Zheng et al [63]	US	M.L.M.	*left*	3.30	4.80	0.60	1.40	2.10	3.10	0.70	1.40
			right	3.00	4.40	0.60	1.50	2.20	3.00	0.50	1.20

Table 3 Critical and follow-up headways values for turbo roundabouts

Study name	Country	Entry	Entry lane	Circulating lane	critical headway mean [s]		St. dev. [s]	
					min	max	min	max
Brilon et al [32]	Germany	major	*left*		4.50	-	-	-
Fortuijn [37]	Holland	major	*left*		3.37	3.72	0.36	0.95
Brilon et al [32]	Germany	major	*right*		4.50	-	-	-
Fortuijn [37]	Holland	major	*right*		3.67	4.17	0.85	1.59
Brilon et al [32]	Germany	minor	*left*	inner	4.00	-	-	-
		minor	*left*	outer	4.50	-	-	-
Fortuijn [37]	Holland	minor	*left*	inner	3.15	3.24	0.27	0.47
		minor	*left*	outer	2.79	3.42	0.50	0.80
Brilon et al [32]	Germany	minor	*right*	outer	4.50	-	-	-
Fortuijn [37]	Holland	minor	*right*	outer	3.37	4.93	0.51	2.28

3.3. Fixed-effect model Vs random-effects model

The meta-analyses are based on one of two statistical models, the fixed-effect model or the random-effects model [7].

Under the fixed-effect model, all studies in the analysis share the same true effect size (namely the effect size in the population); all differences in observed effects are due to sampling error. Thus, the summary effect is the estimate of this common effect size. On the contrary, under the random effects model, the true effect varies from study to study and the summary effect is the estimate of the mean of the distribution of effect sizes. Since in this case, studies can differ in the number of observations or some characteristics of the geometric design (e.g. the width of the roundabout ring or the entry lanes, population characteristics, etc.), there may be different effect sizes to the base of each study. It is noteworthy that if it is possible to consider an infinite number of studies, the true effect sizes for these studies would be distributed about the mean. The effect sizes in the studies that were carried out, indeed, are assumed to represent a random sample of these effect sizes; hence the term random effects are used since there is an array of true effects. Furthermore, when setting weights to the different studies in the fixed-effect model, one can largely ignore the information in the smaller studies since one can have better information about the same effect size in the larger studies. This consideration does not apply to random model because, in this case, the objective is to estimate the average effect for the studies considered; since each study provides information about a different effect size, the overall estimate cannot be influenced by a particular study. According to this logic, in a random model, it is not possible to give more weight to a study rather than another. So, in the fixed-effect model the only source of uncertainty is within the studies, while under the random-effects model there is the same source of uncertainty plus an additional source (i.e. between-studies variance). It follows that the variance, standard error, and confidence interval for the summary effect will always be larger in the random effects model than in the fixed-effect model. In general, the fixed-effect model is properly used when two conditions are met:

- all studies included in the analysis are functionally identical;
- the scope is to compute the common effect size for the identified population, and not to generalize to other populations.

By contrast, under the random-effects model, one can allow that the true effect could vary from study to study. Considering that the critical and follow-up headways are country/region-related, and then they can depend on traffic regulation, traffic behavior, age and mentality of drivers population, types of vehicles, tradition of using roundabouts, etc., the effect size might be higher (or lower) in studies where the participants are older, or more educated, or healthier than in others, or when a variant of an installation is used more intensively, and so on. Because studies can differ in the mixes of participants and the implementations of interventions, among other reasons, there may be different effect sizes underlying different studies. Because in the case under examination data were collected from a series of studies conducted by several researchers operating independently, the choice to use the random-effects model was more justified than the fixed-effect model, as further specified in the next section.

3.3.1. The Random-effects model

The random-effect model, discussed above, starts with the assumption that the true effect size is not the same in all studies. Indeed, the effect size might differ from study to study as a consequence of the different sample size, geometric features of the roundabout, the context of insertion, the driver population characteristics, and so on. In order to estimate the mean of the distribution (the summary mean or the summary effect), it needs to take account of two sources of variance: the original variance within-study and the variance between-studies. For the purpose to obtain the most precise estimate of the overall mean, it was compute a weighted mean, where the weight assigned to each study is the inverse of that study's variance:

$$W_i^* = \frac{1}{V_{Yi}^*} \tag{9}$$

where $V_{Yi}^* = V_{Yi} + T^2$, in which V_{Yi} is the variance within for study i and T^2 is the variance between studies. One method for estimating T^2 is the method of moments (or the DerSimonian and Laird) method [7], as follows:

$$T^2 = \frac{Q - df}{C} \tag{10}$$

where:

$$Q = \sum_{i=1}^{k} W_i^* Y_i^2 - \frac{\left(\sum_{i=1}^{k} W_i^* Y_i\right)^2}{\sum_{i=1}^{k} W_i^*} \tag{11}$$

$$df = k - 1 \tag{12}$$

and

$$C = \sum W_i^* - \frac{W_i^{*2}}{W_i^*} \tag{13}$$

in the formulas written above:

- k is the number of studies;
- W_i^* is the weighted mean definite in eq. 9;
- Y_i is the mean for study i;
- the difference (Q–df) represents the dispersion in true effects on a standardized scale.

The weighted mean, M^*, is then computed with the following formula:

$$M^* = \frac{\sum_{i=1}^{k} W_i^* \cdot Y_i}{\sum_{i=1}^{k} W_i^*} \tag{14}$$

in which Y_i is the mean for study i. The variance of the summary effect is estimated as the reciprocal of the sum of the weights:

$$V_{M^*} = \frac{1}{\sum_{i=1}^{k} W_i^*} \tag{15}$$

and the estimated standard error of the summary effects is then the square root of the variance as follows:

$$SE_{M^*} = \sqrt{V_{M^*}} \tag{16}$$

The 95% lower and upper limits for the summary effect are computed as follows:

$$LL_{M^*} = M^* - 1.96 \cdot SE_{M^*} \tag{17}$$

$$UL_{M^*} = M^* - 1.96 \cdot SE_{M^*} \tag{18}$$

Finally, after computing a summary effect, a test of the null hypothesis can be performed. Under random model, the null hypothesis is that the mean effect μ is zero. Thus, a *Z-value* can be calculated as follows:

$$Z^* = \frac{M^*}{SE_{M^*}}$$

(19)

while for a "one-tailed" test, *p-value* can be computed with the following equation:

$$p^* = 1 - \Phi(\pm|Z^*|)$$

(20)

and for a "two-tailed" test, *p-value* is given by:

$$p^* = 2 \cdot [1 - \Phi(\pm|Z^*|)]$$

(21)

3.3.2. Identifying and Quantifying Heterogeneity of studies

Since the random-effects model was used, the true effect size may vary from study to study, thus it must take into account the heterogeneity of studies.
Five ways of measuring heterogeneity are recognized:

1. the *Cochran's Q test* [75], expressed by eq. 11, that is the sum of the squared deviation of each effect size from the mean, weighted by the inverse-variance for each study; i.e. the *Q* index represents the Weighted Sum of Squares (WSS in the following). Thus, introducing the "degree of freedom" *df*, trough the formula 12, it is possible to calculate the expected value of *Q* on the assumption that all studies share a common effect size [7]. Since *Q* is the observed WSS and *df* is the expected WSS, the difference, *Q-df* represent the excess variation, the part that will be attributed to differences in the true effects from study to study.

2. The *p-value*, expressed in (20,21), for any observed value of *Q* (see formula 11). In order to know if the heterogeneity is statistically significant, a hypothesis test can be made. The null hypothesis is that all studies share a common effect size; under this null hypothesis, *Q* will follow a central chi-squared distribution with degrees of freedom equal to k−1, thus one can report a *p-value* for any observed value of *Q* [29].

3. The *between-studies variance (T^2)*. The parameter T^2 represents the estimate value of tau-squared τ^2 parameter. The tau-squared parameter is defined as the variance of the true effect sizes. Since this variance cannot be compute directly, one can estimate it from the observed effects by means T^2 parameter. In other words, τ^2 refers to the actual variance of the true effect sizes while T^2 is its estimate. The T^2 is expressed as the ratio between the difference *Q-df*, which represents the dispersion in true effects on a

standardized scale and the *C* (see expressions 10 and 13). The quantity C, inside the formula T^2, has a dual function: it allows to have the measurements in its original metric, and to make it an average, rather than a sum, of squared deviations [7].

4. The *between-studies standard deviation (T)*; this time, τ refers to the actual standard deviation and T is its estimate. Therefore, the parameter T represents the estimate of the standard deviation and is simply the square root of T^2. Like the standard deviation in a primary study, T can be used to describe the distribution of effect sizes about the mean effect [7].

5. the *Higgin's index I^2*, or the ratio of true heterogeneity to total observed variation [76]. It is computed as:

$$I^2 = \left(\frac{Q - df}{Q}\right) \cdot 100\%$$

in which the quantity *Q* and *df* are described above. This index can be seen as a measure of inconsistency across the findings of the studies. The *Higgin's index* I^2, represents only the proportion of variance that is true, but it says nothing about the absolute value of the variance [7]. In fact the index I^2 allows to discuss the amount of variance on a relative scale: values on the order of 25%, 50%, and 75% might be considered as low, moderate, and high, respectively [76]. These benchmarks refer to the question of what proportion of the observed variation is real, and not to the variation on an absolute scale. Indeed, an I^2 value near 100 % means only that most of the observed variance is real, but does not imply that the effects are dispersed over a wide range.

The flowchart shown in the following figure summarizes the ways of measuring heterogeneity, whereas Table 4 shows the relationship among these measures presented above.
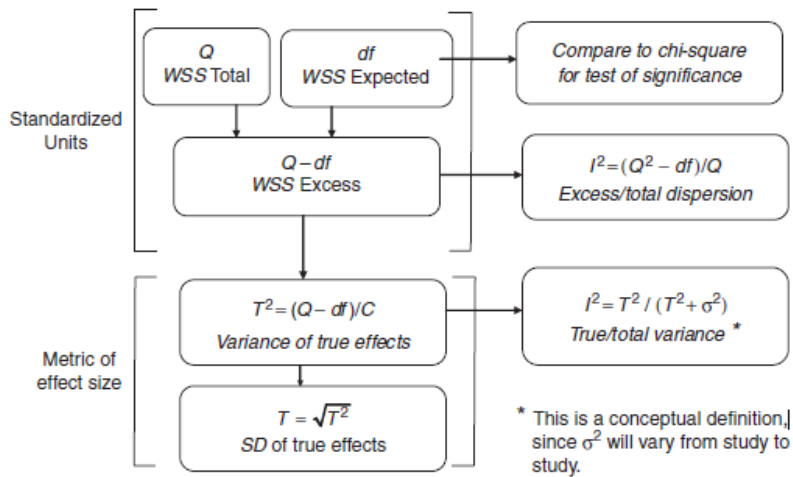
Figure 7 Flowchart showing how T^2 and I^2 are derived from Q and df [7].

Table 4 Factors affecting measures of dispersion [7]

	Range of possible values	Depends on number of studies	Depends on scale
Q	$0 \leq Q$	✓	
p	$0 \leq p \leq 1$	✓	
T^2	$0 \leq T^2$		✓
T	$0 \leq T$		✓
I^2	$0\% \leq I^2 < 100\%$		

Finally, the following considerations can be made (see Table 4):

- the Q statistic and its *p-value* are used for testing significance; they are not depending on number of studies;
- the estimate of τ^2 serves as the between-studies variance in the analysis and the estimate of τ represents the standard deviation of the true effects; furthermore they are not sensitive to the number of studies;
- the Higgs's index, I^2, is the ratio of true heterogeneity to total variation in observed effects. Moreover, as one can see from Table 4, I^2 is not directly affected by the number of studies.

It is noteworthy that T^2 and T on the one hand, and I^2, on the other, have two entirely different functions. The statistics T^2 and T, reflect the amount of true heterogeneity (the variance or the standard deviation) while I^2 reflects the proportion of observed dispersion that is due to this heterogeneity [7].

3.2. Results of Meta-analytic estimation

The cases of single-lane, double-lane and turbo roundabouts were examined separately both for the critical and the follow-up headways. The groups of studies which have been subjected to meta-analysis varied for each case; each of these groups included a variable number of sub-groups (see tables hereinafter). Each

sub-group contained on-field observations characterized by mean, standard deviation, and sample size; these data represented the data input of the meta-analysis.

Tables 5 and 6 show the outputs of the meta-analysis regarding the assessment of the critical and follow-up headways for the single-lane roundabouts; from left to right, one can find the values of the variance that is referred to the summary effect, lower and upper limit, *Z-values* and *p-values*, the values of the *Q* test and the index I^2. In turn, Figures 8 and 9 depict the forest plots corresponding to the random-effect model for the critical headways and follow up headways at single-lane roundabouts, respectively.

It is noteworthy that, for the cases in Tables 6 and 7, the *p-value* is approximately equal to zero, and the *Higgin's index* is around values of 1.2 % for the critical headway and around values of 20.4 % for the follow headway; both parameters confirm poor heterogeneity.

Specifically, Table 8 shows the summary results of the critical headways for right entry lane at double-lane roundabouts, while Table 9 shows the summary results of critical headways for left entry lane at double-lane roundabouts. In turn, by way of example, Figures 10 and 11 depict the forest plots corresponding to the random-effect model for calculating the critical headways for the right entry lane and the left entry lane at double-lane roundabouts, respectively. Finally, Tables 10 and 11 show the summary results for follow – up headways at double-lane roundabouts for the right entry lane and the left entry lane, respectively. The summary results for turbo roundabouts are shown in Table 11. In some case turbo roundabouts revealed moderate or high values of I^2; however, still few empirical studies to estimate the critical headway have been aimed at these roundabouts. Tables 13 and 14 show a comparison between the summary effects and the weighted mean values (with regard to the sample size) of each study considered in the meta-analysis; it can be easily noted that the summary effect can be far from the single study estimate since it is independent and does not account for similar experimental data. Figures 8-11 depict as example the forest plots showing the relative weights for critical headways and follow up headways at single-lane roundabouts and double-lane roundabouts.

Table 5 Summary results for critical headways at single-lane roundabouts

| STUDY NAME	SUBGROUP WITHIN STUDY	MEAN	SAMPLE SIZE	STANDARD ERROR	Z - value	p - value	Q	I^2 (%)
Gazzarri A. et al. [39]	A_1	3.80	71	0.11	35.98	0.00	23.28	1.19
Gazzarri A. et al. [39]	A_2	3.99	98	0.08	50.00	0.00	23.28	1.19
Gazzarri A. et al. [39]	A_3	4.10	47	0.14	29.59	0.00	23.28	1.19
Gazzarri A. et al. [39]	A_4	3.54	61	0.09	41.27	0.00	23.28	1.19
Rodegerdts L. et al. [22]	B_1	4.20	733	0.04	113.71	0.00	23.28	1.19
Rodegerdts L. et al. [22]	B_2	4.90	76	0.15	32.08	0.00	23.28	1.19
Rodegerdts L. et al. [22]	B_3	4.30	1062	0.05	107.47	0.00	23.28	1.19
Rodegerdts L. et al. [22]	B_4	4.20	820	0.02	272.12	0.00	23.28	1.19
Rodegerdts L. et al. [22]	B_5	5.10	98	0.05	85.04	0.00	23.28	1.19
Rodegerdts L. et al. [22]	B_6	4.20	557	0.04	94.21	0.00	23.28	1.19
Rodegerdts L. et al. [22]	B_7	4.60	92	0.10	47.46	0.00	23.28	1.19
Rodegerdts L. et al. [22] *Rodegerdts L. et al. [61]*	B_8	4.40	237	0.03	140.13	0.00	23.28	1.19
Rodegerdts L. et al. [22]	B_9	4.20	1314	0.03	133.63	0.00	23.28	1.19
Rodegerdts L. et al. [22]	B_{10}	4.80	197	0.10	50.49	0.00	23.28	1.19
Rodegerdts L. et al. [22]	B_{11}	4.90	481	0.05	90.11	0.00	23.28	1.19
Rodegerdts L. et al. [22]	B_{12}	4.30	3244	0.07	63.03	0.00	23.28	1.19
Rodegerdts L. et al. [22]	B_{13}	3.90	233	0.12	37.63	0.00	23.28	1.19
Rodegerdts L. et al. [22]	B_{14}	4.10	528	0.03	138.41	0.00	23.28	1.19
Zheng D. et al. [63]	C_1	5.50	548	0.09	64.38	0.00	23.28	1.19
Zheng D. et al. [63]	C_2	4.60	588	0.05	92.95	0.00	23.28	1.19
Zheng D. et al. [63]	C_3	4.80	282	0.08	57.58	0.00	23.28	1.19
Zheng D. et al. [63]	C_4	3.80	318	0.06	67.76	0.00	23.28	1.19
Fortuijn L.G.H. [37]	D_1	3.16	101	0.03	113.42	0.00	23.28	1.19
Fortuijn L.G.H. [37]	D_2	3.28	108	0.02	179.40	0.00	23.28	1.19
RANDOM		**4.27**		**0.11**	**37.46**	**0.00**	**23.28**	**1.19**
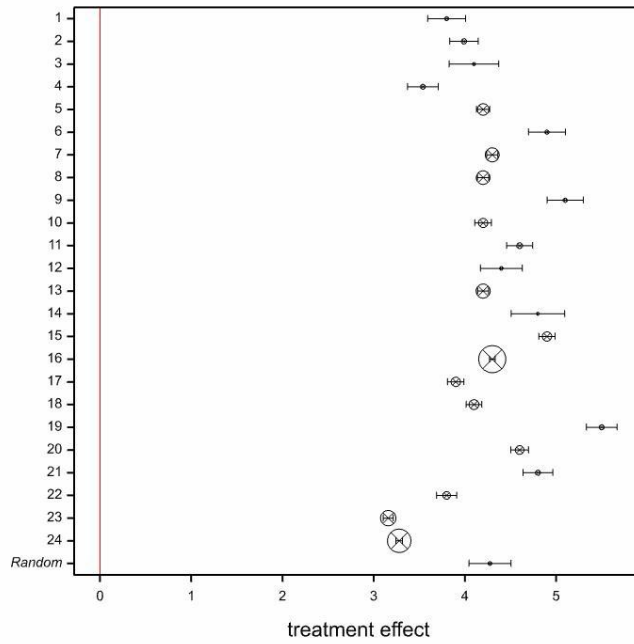
Figure 8 Random-effect model: the forest plot showing the relative weights for critical headways at single-lane roundabouts
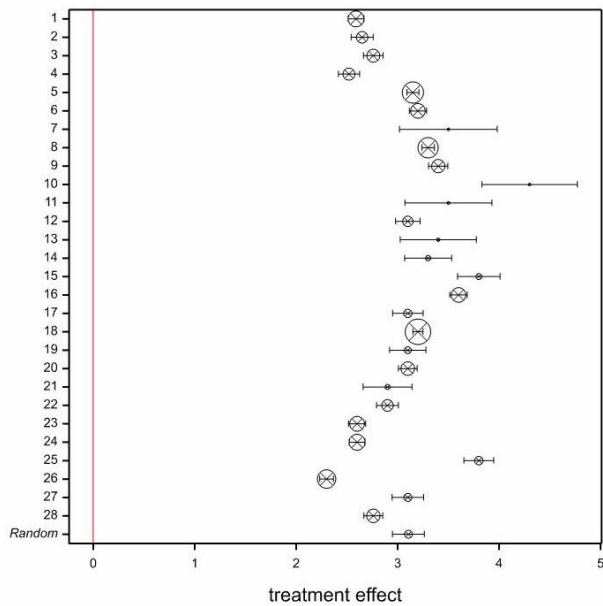
Figure 9 Random-effect model: the forest plot showing the relative weights of the follow up headways at single-lane roundabouts

Table 6 Summary results for follow-up headways at single-lane roundabouts

STUDY NAME	SUBGROUP WITHIN STUDY	MEAN	SAMPLE SIZE	STANDARD ERROR	Z - value	p - value	Q	I² (%)
Gazzarri A. et al. [39]	A_1	2.59	500	0.04	64.35	0.00	33.90	20.40
Gazzarri A. et al. [39]	A_2	2.65	155	0.06	47.81	0.00	33.90	20.40
Gazzarri A. et al. [39]	A_3	2.76	190	0.05	55.95	0.00	33.90	20.40
Gazzarri A. et al. [39]	A_4	2.52	226	0.05	47.35	0.00	33.90	20.40
Nicolosi V. et al. [49]	B_1	3.15	386	0.03	104.89	0.00	33.90	20.40
Rodegerdts L. et al. [22]	C_1	3.20	637	0.04	73.42	0.00	33.90	20.40
Rodegerdts L. et al. [22]	C_2	3.80	28	0.11	35.55	0.00	33.90	20.40
Rodegerdts L. et al. [22]	C_3	3.60	1225	0.04	82.32	0.00	33.90	20.40
Rodegerdts L. et al. [22]	C_4	3.10	522	0.08	40.47	0.00	33.90	20.40
Rodegerdts L. et al. [22]	C_5	3.20	39	0.03	127.39	0.00	33.90	20.40
Rodegerdts L. et al. [22]	C_6	3.10	41	0.09	33.96	0.00	33.90	20.40
Rodegerdts L. et al. [22]	C_7	3.10	262	0.05	65.98	0.00	33.90	20.40
Rodegerdts L. et al. [22]	C_8	2.90	33	0.12	23.58	0.00	33.90	20.40
Rodegerdts L. et al. [22]	C_9	2.90	86	0.06	52.73	0.00	33.90	20.40
Rodegerdts L. et al. [22]	C_{10}	2.60	126	0.04	60.46	0.00	33.90	20.40
Rodegerdts L. et al. [22]	C_{11}	3.50	753	0.25	14.25	0.00	33.90	20.40
Rodegerdts L. et al. [22]	C_{12}	3.30	334	0.03	105.00	0.00	33.90	20.40
Rodegerdts L. et al. [22]	C_{13}	3.40	2282	0.05	70.62	0.00	33.90	20.40
Rodegerdts L. et al. [22]	C_{14}	4.30	120	0.24	17.90	0.00	33.90	20.40
Rodegerdts L. et al. [22]	C_{15}	3.50	453	0.22	16.01	0.00	33.90	20.40
Rodegerdts L. et al. [22]	C_{16}	3.10	80	0.06	50.18	0.00	33.90	20.40
Rodegerdts L. et al. [22]	C_{17}	3.40	400	0.19	17.76	0.00	33.90	20.40
Rodegerdts L. et al. [22]	C_{18}	3.30	438	0.12	27.82	0.00	33.90	20.40
Zheng D. et al. [63]	D_1	2.60	1223	0.04	64.95	0.00	33.90	20.40
Zheng D. et al. [63]	D_2	3.80	1198	0.08	50.59	0.00	33.90	20.40
Zheng D. et al. [63]	D_3	2.30	828	0.03	66.18	0.00	33.90	20.40
Zheng D. et al. [63]	D_4	3.10	768	0.08	39.05	0.00	33.90	20.40
X. Qu et al. [59]	E_1	2.76	171	0.05	58.21	0.00	33.90	20.40
RANDOM		**3.10**		0.07	**41.82**	**0.00**	**33.90**	**20.40**

Table 7 Summary results for critical headways at double-lane roundabouts - outer circulating lane

STUDY NAME	SUBGROUP WITHIN STUDY	MEAN	SAMPLE SIZE	STANDARD ERROR	Z - value	p - value	Q	I^2 (%)
Gazzarri A. et al. [39]	A_1	4.33	59	0.14	30.80	0.00	21.45	20.75
Gazzarri A. et al. [39]	A_2	3.50	36	0.13	26.25	0.00	21.45	20.75
Gazzarri A. et al. [39]	A_3	3.85	56	0.12	32.74	0.00	21.45	20.75
Gazzarri A. et al. [39]	A_4	3.56	43	0.09	38.27	0.00	21.45	20.75
Gazzarri A. et al. [39]	A_5	3.19	69	0.10	33.12	0.00	21.45	20.75
Rodegerdts L. et al. [22]	B_1	4.90	307	0.12	40.88	0.00	21.45	20.75
Rodegerdts L. et al. [22]	B_2	3.40	35	0.20	16.76	0.00	21.45	20.75
Rodegerdts L. et al. [22]	B_3	4.10	813	0.06	73.06	0.00	21.45	20.75
Rodegerdts L. et al. [22]	B_4	4.20	604	0.05	79.40	0.00	21.45	20.75
Rodegerdts L. et al. [22]	B_5	4.00	115	0.11	35.75	0.00	21.45	20.75
Rodegerdts L. et al. [22]	B_6	4.40	182	0.10	42.40	0.00	21.45	20.75
Zheng D. et al. [63]	C_1	3.50	319	0.04	78.14	0.00	21.45	20.75
Zheng D. et al. [63]	C_2	3.80	268	0.07	51.84	0.00	21.45	20.75
Zheng D. et al. [63]	C_3	4.10	194	0.08	51.91	0.00	21.45	20.75
Zheng D. et al. [63]	C_4	4.40	194	0.11	40.86	0.00	21.45	20.75
Zheng D. et al. [63]	C_5	3.00	639	0.02	126.39	0.00	21.45	20.75
Zheng D. et al. [63]	C_6	3.40	670	0.04	88.01	0.00	21.45	20.75
Fortuijn L.G.H. [37]	D_1	3.16	12	0.01	273.66	0.00	21.45	20.75
RANDOM		**3.81**		**0.11**	**35.11**	**0.00**	**21.45**	**20.75**

Table 8 Summary results for critical headways at double-lane roundabouts - inner circulating lane

STUDY NAME	SUBGROUP WITHIN STUDY	MEAN	SAMPLE SIZE	STANDARD ERROR	Z - value	p - value	Q	I^2 (%)
Gazzarri A. et al. [39]	A_1	4.05	62	0.10	39.37	0.00	18.82	0.00
Gazzarri A. et al. [39]	A_2	3.59	53	0.09	40.84	0.00	18.82	0.00
Gazzarri A. et al. [39]	A_3	4.42	51	0.16	27.69	0.00	18.82	0.00
Gazzarri A. et al. [39]	A_4	3.71	54	0.10	36.35	0.00	18.82	0.00
Gazzarri A. et al. [39]	A_5	3.71	82	0.11	33.93	0.00	18.82	0.00
Rodegerdts L. et al. [22]	B_1	5.50	468	0.12	45.76	0.00	18.82	0.00
Rodegerdts L. et al. [22]	B_2	4.20	275	0.14	30.28	0.00	18.82	0.00
Rodegerdts L. et al. [22]	B_3	4.30	17	0.39	11.08	0.00	18.82	0.00
Rodegerdts L. et al. [22]	B4	4.20	99	0.22	19.00	0.00	18.82	0.00
Rodegerdts L. et al. [22]	B_5	4.40	237	0.09	48.38	0.00	18.82	0.00
Rodegerdts L. et al. [22]	B_6	4.30	100	0.09	47.78	0.00	18.82	0.00
Rodegerdts L. et al. [22]	B_7	5.00	73	0.16	30.51	0.00	18.82	0.00
Zheng D. et al. [63]	C_1	4.20	343	0.06	64.82	0.00	18.82	0.00
Zheng D. et al. [63]	C_2	4.10	966	0.03	127.43	0.00	18.82	0.00
Zheng D. et al. [63]	C_3	4.80	492	0.06	76.05	0.00	18.82	0.00
Zheng D. et al. [63]	C_4	3.70	414	0.03	107.55	0.00	18.82	0.00
Zheng D. et al. [63]	C_5	3.30	875	0.02	162.69	0.00	18.82	0.00
Zheng D. et al. [63]	C_6	4.40	490	0.05	88.54	0.00	18.82	0.00
Li et al. [65]	D_1	4.30	648	0.04	109.46	0.00	18.82	0.00
Fortuijn L.G.H. [37]	E_1	2.89	11	0.40	7.26	0.00	18.82	0.00
RANDOM		**4.17**		**0.13**	**32.65**	**0.00**	**18.82**	**0.00**

Figure 10 Random-effect model: the forest plot showing the relative weights of critical headways for right entry lane at double-lane roundabouts
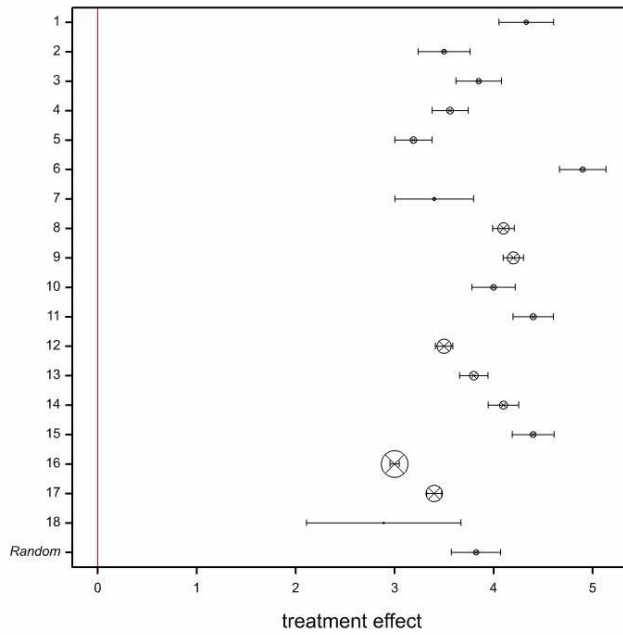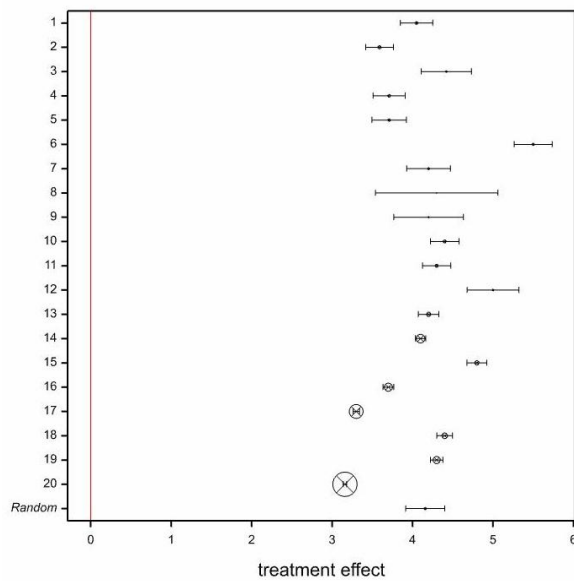

Figure 11 Random-effect model: the forest plot showing the relative weights of critical headways for left entry lane at double-lane roundabouts

Table 9 Summary results for follow – up headways at double-lane roundabouts - right entry lane

Table 9 STUDY NAME	SUBGROUP WITHIN STUDY	MEAN	SAMPLE SIZE	STANDARD ERROR	Z - value	p - value	Q	I² (%)
Gazzarri A. et al. [39]	A_1	2.70	205	0.0	54.4	0.00	17.77	9.98
Gazzarri A. et al. [39]	A_2	2.44	29	0.1	22.7	0.00	17.77	9.98
Gazzarri A. et al. [39]	A_3	2.91	143	0.1	45.8	0.00	17.77	9.98
Gazzarri A. et al. [39]	A_4	2.58	87	0.1	39.5	0.00	17.77	9.98
Gazzarri A. et al. [39]	A_5	2.59	92	0.1	36.0	0.00	17.77	9.98
Rodegerdts L. et al. [22]	B_1	3.10	648	0.1	52.6	0.00	17.77	9.98
Rodegerdts L. et al. [22]	B_2	4.40	2	1.6	2.70	0.00	17.77	9.98
Rodegerdts L. et al. [22]	B_3	3.10	104	0.1	28.7	0.00	17.77	9.98
Rodegerdts L. et al. [22]	B4	2.80	478	0.0	76.5	0.00	17.77	9.98
Rodegerdts L. et al. [22]	B_5	3.10	1340	0.0	94.6	0.00	17.77	9.98
Rodegerdts L. et al. [22]	B_6	3.00	1773	0.0	114.8	0.00	17.77	9.98
Zheng D. et al. [63]	C_1	3.00	425	0.1	51.5	0.00	17.77	9.98
Zheng D. et al. [63]	C_2	2.80	2206	0.0	119.6	0.00	17.77	9.98
Zheng D. et al. [63]	C_3	2.20	22	0.1	20.6	0.00	17.77	9.98
Zheng D. et al. [63]	C_4	2.60	128	0.1	24.5	0.00	17.77	9.98
Zheng D. et al. [63]	C_5	2.20	600	0.0	67.4	0.00	17.77	9.98
Zheng D. et al. [63]	C_6	2.20	17	0.1	18.1	0.00	17.77	9.98
RANDOM		**2.72**		**0.1**	**35.7**	**0.00**	**17.77**	**9.98**

Table 10 Summary results for follow – up headways at double-lane roundabouts - left entry lane

STUDY NAME	SUBGROUP WITHIN STUDY	MEAN	SAMPLE SIZE	STANDARD ERROR	Z - value	p - value	Q	I² (%)
Gazzarri A. et al. [39]	A_1	3.10	145	0.08	39.29	0.00	22.32	19.36
Gazzarri A. et al. [39]	A_2	2.16	57	0.06	33.28	0.00	22.32	19.36
Gazzarri A. et al. [39]	A_3	2.77	59	0.09	29.55	0.00	22.32	19.36
Gazzarri A. et al. [39]	A_4	2.66	82	0.07	39.49	0.00	22.32	19.36
Gazzarri A. et al. [39]	A_5	2.56	124	0.06	43.19	0.00	22.32	19.36
Rodegerdts L. et al. [22]	B_1	3.10	1792	0.03	119.30	0.00	22.32	19.36
Rodegerdts L. et al. [22]	B_2	3.30	315	0.07	48.81	0.00	22.32	19.36
Rodegerdts L. et al. [22]	B_3	4.70	6	0.98	4.80	0.00	22.32	19.36
Rodegerdts L. et al. [22]	B_4	3.20	73	0.13	24.86	0.00	22.32	19.36
Rodegerdts L. et al. [22]	B_5	3.40	85	0.13	26.12	0.00	22.32	19.36
Rodegerdts L. et al. [22]	B_6	3.30	180	0.08	40.25	0.00	22.32	19.36
Rodegerdts L. et al. [22]	B_7	3.50	28	0.28	12.35	0.00	22.32	19.36
Zheng D. et al. [63]	C_1	3.10	698	0.05	63.00	0.00	22.32	19.36
Zheng D. et al. [63]	C_2	2.80	1768	0.03	98.11	0.00	22.32	19.36
Zheng D. et al. [63]	C_3	2.50	142	0.12	21.28	0.00	22.32	19.36
Zheng D. et al. [63]	C_4	2.50	233	0.07	38.16	0.00	22.32	19.36
Zheng D. et al. [63]	C_5	2.20	475	0.03	68.50	0.00	22.32	19.36
Zheng D. et al. [63]	C_6	2.10	100	0.08	26.25	0.00	22.32	19.36
Li et al. [65]	D_1	3.10	638	0.05	65.25	0.00	22.32	19.36
RANDOM		**2.85**		**0.10**	**29.58**	**0.00**	**22.32**	**19.36**

Table 11 Summary results for critical headways at turbo roundabout

	STUDY NAME	SUBGR. WITHIN STUDY	MEAN	SAMPLE SIZE	S.E.	Z - value	p - value	Q	I² (%)
MAIN ROAD									
LEFT	*Fortuijn L.G.H. [37]*	A_1	3.37	253	0.05	61.61	0.00	4.84	37.98
	Fortuijn L.G.H. [37]	A_2	3.62	648	0.04	97.00	0.00	4.84	37.98
	Fortuijn L.G.H. [37]	A_3	3.66	145	0.03	122.42	0.00	4.84	37.98
	Fortuijn L.G.H. [44]	A_4	3.72	269	0.03	135.58	0.00	4.84	37.98
	RANDOM		**3.60**		**0.06**	**61.22**	**0.00**	**4.84**	**37.98**
RIGHT	*Fortuijn L.G.H. [37]*	A_1	3.67	421	0.04	88.59	0.00	1.00	0.00
	Fortuijn L.G.H. [37]	A_2	4.17	273	0.10	43.33	0.00	1.00	0.00
	RANDOM		**3.91**		**0.25**	**15.66**	**0.00**	**1.00**	**0.00**
MINOR ROAD									
LEFT									
- Outer Circ. Lane	*Fortuijn L.G.H. [37]*	A_1	2.79	83	0.05	50.84	0.00	2.91	31.22
	Fortuijn L.G.H. [37]	A_2	3.07	154	0.06	54.43	0.00	2.91	31.22
	Fortuijn L.G.H. [37]	A_3	3.42	35	0.14	25.29	0.00	2.91	31.22
	RANDOM		**3.07**		**0.15**	**20.85**	**0.00**	**2.91**	**31.22**
- Inner Circ. Lane	*Fortuijn L.G.H. [37]*	A_1	3.15	255	0.03	107.02	0.00	1.87	0.00
	Fortuijn L.G.H. [37]	A_2	3.23	54	0.04	87.91	0.00	1.87	0.00
	Fortuijn L.G.H. [37]	A_3	3.24	206	0.03	98.94	0.00	1.87	0.00
	RANDOM		**3.20**		**0.03**	**106.36**	**0.00**	**1.87**	**0.00**
RIGHT	*Fortuijn L.G.H. [37]*	A_1	3.37	69	0.06	54.89	0.00	10.66	81.23
	Fortuijn L.G.H. [37]	A_2	3.48	434	0.04	99.31	0.00	10.66	81.23
	Fortuijn L.G.H. [37]	A_3	4.93	118	0.21	23.49	0.00	10.66	81.23
	RANDOM		**3.83**		**0.20**	**18.70**	**0.00**	**10.66**	**81.23**

As above introduced, it should be noted that, since the methodological diversity will always occur in a meta-analysis, statistical heterogeneity is almost inevitable [7]. Several methods have been developed for quantifying inconsistency across studies: they move the focus away from testing whether heterogeneity is present to assess its impact on the meta-analysis. However, the results in above Tables describe low percentage of variability in the effect sizes, that is due to heterogeneity rather than sampling error (chance). Specially for single-lane roundabouts and double-lane roundabouts, the p-values close to zero and I^2 less than 20% indicated which a low unaccounted variability could be attributable to the residual heterogeneity in the data set. At last, the meta-analytic estimates were found consistent across all the studies; see Tables 12 and 13 for the comparison between summary effect (random) and mean values for critical and follow-up headways, respectively; moreover, they gave a more reliable result for the searched parameters compared to the values of each single study. This can made confident that the results were robust and representative of driver behaviour at the examined roundabouts under heterogeneous traffic conditions.

Table 12 Comparison between summary effect (random) and mean values for critical headways

STUDY NAME	ROUNDABOUT	ENTRY	ENTRY LANE	CIRCULATING LANE	MEAN VALUES [S]
Gazzarri A. et al. [39]	single lane				3.86
Rodegerdts L. et al. [22]	single lane				4.30
Zheng D. et al. [63]	single lane				4.77
Fortuijn L.G.H. [37]	single lane				3.22
Summury effect (random)					**4.27**
Gazzarri A. et al. [39]	double lane			outer	3.69
Rodegerdts L. et al. [22]	double lane			outer	4.26
Zheng D. et al. [63]	double lane			outer	3.49
Fortuijn L.G.H. [37]	double lane			outer	2.89
Summury effect (random]					**3.82**
Gazzarri A. et al. [39]	double lane			Inner	3.88
Rodegerdts L. et al. [22]	double lane			Inner	4.77
Zheng D. et al. [63]	double lane			Inner	4.01
Li et al. [65]	double lane			Inner	4.30
Fortuijn L.G.H. [37]	double lane			inner	3.16
Summury effect (random)					**4.16**
Fortuijn L.G.H. [37]	Turbo	Major	Left		3.60
Summury effect (random)					**3.60**
Fortuijn L.G.H. [37]	Turbo	Major	Right		3.87
Summury effect (random)					**3.91**
Fortuijn L.G.H. [37]	Turbo	Minor	Left	inner	3.19
Summury effect (random)					**3.20**
Fortuijn L.G.H. [37]	Turbo	Minor	Left	outer	3.03
Summury effect (random)					**3.07**
Fortuijn L.G.H. [37]	Turbo	Minor	Right		3.74
Summury effect (random]					**3.83**

Table 13 Comparison between summary effect (random) and mean values for follow-up headways

STUDY NAME	ROUNDABOUT	ENTRY LANE	MEAN VALUES [S]
Gazzarri A. et al. [39]	single lane		2.61
Nicolosi V. et al. [42]	single lane		3.15
Rodegerdts L. et al. [22]	single lane		3.22
Zheng D. et al. [63]	single lane		2.99
X. Qu et al. [59]	single lane		2.76
Summury effect (random)			**3.10**
Gazzarri A. et al. [39]	double lane	Right	2.70
Rodegerdts L. et al. [22]	double lane	Right	3.03
Zheng D. et al. [63]	double lane	Right	2.70
Summury effect (random]			**2.72**
Gazzarri A. et al. [39]	double lane	left	2.72
Rodegerdts L. et al. [22]	double lane	left	3.16
Zheng D. et al. [63]	double lane	left	2.72
Li et al. [65]	double lane		3.10
Summury effect (random]			**2.85**

References

1. Mauro R (2010) Calculation of Roundabouts. Springer-Verlag, Berlin Heidelberg.
2. Brilon W, Wu N, Bondzio L (1997) Unsignalized intersections in Germany—a State of the Art. 3rd International Symposium on Intersections Without Traffic Signals, Portland, Oregon, USA, July 21–23, 1997.
3. Bovy H, Dietrich K, Harmann A (1991) Guide Suisse des Giatoires. Lausanne, Switzerland.
4. Kimber R M (1980) The traffic capacity of roundabouts. TRRL Laboratory Report 942, Berkshire, UK.
5. National Academies of Sciences, Engineering, and Medicine, Roundabouts: An Informational Guide, second ed., The National Academies Press, Washington, DC, 2010. https://doi.org/10.17226/22914.
6. Highway Capacity Manual (2010) Transportation Research Board. Special Report 209. 5th edition.
7. Borenstein M, Hedges LV, Higgins JPT, Rothstein HR (2009) Introduction to meta-analysis. Wiley, Chichester, UK.
8. Tanner, J.C.(1962).A theoretical analysis of delays at an uncontrolled intersection. Biometrica 49, 163–170. doi:10.1093/biomet/49.1-2.163.
9. Kyte, M. (1996) Capacity and Level of Service at Unsignalized Intersections: Final Report Volume 1 - Two-Way-Stop-Controlled Intersections. NCHRP Project 3-46. TRB, National Research Council, Washington, D.C., 1996.
10. Brilon W, Koenig R, Troutbeck RJ (1999) Useful Estimation Procedures for Critical Gaps. Transportation Research Part A: Policy and Practice 33(3–4):161–186. doi:10.1016/S0965-8564(98)00048-2.
11. Siegloch W. (1973). Die Leistungsermittlung an Knotenpunkten Ohne Lichsignalsteuerung (Capacity Unsignalized Intersections. Calculations for Unsignalized Intersections). Bonn: Schriftenreihe Strassenbau and Strassenverkehrstechnik [Road Construction and Traffic Technology, 154].
12. Raff M.S., and Hart J. W. (1950). A Volume Warrant for Urban Stop Signs. Saugatuck, CT:The Eno Foundation for Highway Traffic Control.
13. Ashworth R (1970) The analysis and interpretation of gap acceptance data. Transportation Science 4(3):270–280. doi:10.1287/trsc.4.3.270.
14. Troutbeck R J (1992) Estimating the critical acceptance gap from traffic movements. Queensland University of Technology.
15. Tian Z, KyteW, Vandehey M, Robinson B, KittelsonW, Troutbeck RW, Brilon W (1999). Implementing the maximum likelihood methodology to measure driver's critical gap. Transportation Research Part A 33:187–197.
16. Harders, J. (1968). Die Leistungsfähigkeit Nicht Signalregelter Städtischer Verkshrsknoten [Capacity of Unsignalized Urban Intersections]. Bonn: Strassenbau und Strassenverkehrstechnik 76 [Road Construction and Traffic

Technology, 76], Bundesminister für Verkehr [Federal Department of Transport].

17. Solberg, P., and Oppenlander, J. (1964). Lag and gap acceptances at stop-controlled intersections. Highway Capacity Rec. 118, 48–67.

18. Wu, N. (2012). Estimating distribution function of critical gaps at unsignalized intersections based on equilibrium of probabilities. Transp. Res. Rec. 2286, 49–55. doi:10.3141/2286-06.

19. Hewitt, R.H.(1983).Measuring critical gap. Transp. Sci. 17, 87–109. doi:10.1287/ trsc.17.1.87

20. Hewitt, R.H.(1985).A comparison between some methods for measuring critical gap. Traff. Eng. Control 26, 13–22.

21. Vasconcelos L, Bastos Silva A, Seco Á, Rouxinol G (2012) Estimation of critical headways at unsignalized intersections - a microscopic approach. Advances in Transportation Studies Special Issue 1: 59–72.

22. National Academies of Sciences, Engineering, and Medicine. 2007. Roundabouts in the United States. Washington, DC: The National Academies Press. https://doi.org/10.17226/23216

23. Giuffrè,O.,Granà,A.,Giuffrè,T.,andMarino,R.(2012b).Researchingacapacity modelformultilaneroundaboutswithnegotiationoftheright-of-waybetween antagonisttrafficflows.Mod.Appl.Sci.6,2–12.doi:10.5539/mas.v6n5p2.

24. Akçelik R. (2007). A review of gap-acceptance capacity models. 29th Conference of Australian Institutes of Transport Research (CAITR 2007), University of South Australia, Adelaide, Australia, 5-7 December 2007.

25. Brilon W (2011) Studies on roundabouts in Germany: Lessons Learned. 3rd International TRB-roundabout Conference, Carmel, Indiana, May 2011

26. FGSV: Handbuch fuer die bemessung von Straβen (HBS: German Highway Capacity Manual). Forschungsgesellschaft für Straßenund Verkehrswesen (FGSV). (www.fgsv.de). Cologne, edition 2001

27. Tanner JC (1967) The capacity of an uncontrolled intersection. Biometrica 54(3/4):657–658 Manual for the program KREISEL version 7, (www. bpsverkehr. de), 2011

28. BPS: Manual for the program KREISEL version 7, (www. bpsverkehr.de), 2011.

29. Brilon W (2014) Roundabouts: a state of the art in Germany. 4th International TRB roundabout Conference, Conference, Seattle, Washington, April 2014.

30. Wu N (1997) An universal formula for calculating capacity at roundabouts. Research report of Institute for Traffic Engineering No.13, Ruhr-University Bochum, March 1997.

31. Wu N (2012) Estimating distribution function of critical gaps at unsignalized intersections based on equilibrium of probabilities. Transportation Research Record 2286:49–55. doi:10. 3141/2286-06.

32. Brilon W, Bondzio L, Weiser (2014) Experiences with Turbo- Roundabouts in Germany. 5th Rural Roads Design meeting, Copenhagen. http://nmfv.dk/wpcontent/uploads/2014/04/Experiences-with-Turbo-

Roundabouts-in-Germany-Brilon- Bondzio-Weiser.pdf Accessed April 3–4, 2014.

33. Leemann N, Santel G (2009) Two-lane roundabouts. 9th Swiss Transport Research Conference, Ascona, Sept 9–11, 2009

34. Brilon W (1988) Recent development in calculation methods for unsignalized intersections in West Germany. In: Brilon W (ed)Intersections without Traffic Signals. Springer-Verlag, Berlin Heidelberg, pp. 111–153

35. Hagring O, Rouphail N M, Sørensen H A (2003) Comparison of capacity models for two-lane roundabouts. 82nd TRB Annual Meeting, Washington, DC, USA, January 2003.

36. Greibe P, La Cour Lund B (2010) Capacity of 2-lane roundabouts 4th International Symposium on Highway Geometric Design, Jun 2nd-5th 2010 Valencia, Spain

37. Fortuijn LGH (2009) Turbo roundabout. Estimation of capacity. Transportation Research Record 2130(2009):83–92. doi:10.3141/ 2130-11

38. Fortuijn L.G.H. and Harte V.F. (1997). Multi-lane roundabouts: exploring new models. Traffic engineering working days 1997, CROW, Ede, The Netherlands.

39. Gazzarri A, Martello MT, Pratelli A, Souleyrette R (2013) Gap acceptance parameters for HCM 2010 roundabout capacity model applications in Italy. Wit serifes on Transport systems & traffic engineering 1:1–6

40. Ferrari P, Giannini F (1994) Ingegneria stradale: geometria e progetto di strade [Road engineering: geometry and road geometric design]. ISEDI, pp 228–23

41. Romano E (2004) Driver behaviour at the roundabouts: analysis and simulation. 2nd International SIIV Congress: New technologies and modeling tools for roads, Florence, Italy, October 2004

42. Nicolosi V, Crisalli U, D'Apuzzo M (2008) Le intersezioni a rotatoria: analisi teorico-sperimentale e modelli teorici per la stima della capacità [Roundabouts: theoretical and experimental analysis andmodels for capacity estimation]. 17° Convegno Nazionale SIIV [17th National SIIV Conference], Enna, Italy, September 2008

43. Dawson R F (1969) The hypererlang probability distribution – a generalized traffic headwaymodel. International Symposium on the Theory of Traffic Flow and Transportatio, Karlsruhe, Series Strassenbau und Strassenverkehrstechik 86

44. De Luca M, Grossi R, Petitto S (2002) Studio del funzionamento delle rotatorie mediante la tecnica della simulazione: modello e verifiche sperimentali [Study of roundabout performances by simulation: model and experimental validation]. 1th International SIIV Conference, Parma, Italy, October 2002.

45. Polus A, Shiftan Y, Shmueli-Lazar S (2005) Evaluation of the waiting-time effect on critical gaps at roundabouts by a logit model. European Journal of Transport and Infrastructure Research 5(1):1–12.

46. Vasconcelos L, Seco Á, Bastos Silva A (2013) Comparison of procedures to estimate critical headways at roundabouts. Promet – Traffic & Transportation 25(1):43–53. doi:10.7307/ptt.v25i1.1246.
47. Troutbeck R J (1991) Recent Australian unsignalized intersection research and practices. Intersections without Traffic Signals II. Springer-Verlag (Werner Brilon. ed.): 238–257
48. Troutbeck RJ (1993) Capacity and design of traffic circles in Australia. Transportation Research Record 1398:68–74
49. Troutbeck R J (1990) Traffic interactions at roundabouts. 15th ARRB Conference, Vol. 15-Part 5, Australia, 1990
50. Troutbeck RJ (1984) Capacity and Delays at Roundabouts-A Literature Review. Australian Road Research Board 14(4):205–216
51. Troutbeck R J (1985) Does gap acceptance theory adequately predict the capacity of a roundabout? 12th ARRB Conference, Australia, Vol. 12-Part 4: 62–75
52. Troutbeck R J (1992) Changes to Analysis and Design of Roundabouts Initiated in the Austroads Guide. 16th ARRB Conference, Vol. 16-Part 5, Australia, 1992
53. Akcelik R (2008) Roundabouts in Australia. 2nd International TRB-Roundabouts Conference. Kansas City, MO, USA, 18–21 May 2008
54. Akçelik R, Chung E, Besley M (1998) Roundabouts: Capacity and Performance Analysis, Research Report ARR No 321, 2nd edn ARRB Transport Research Ltd, Australias.
55. Troutbeck RJ (1989) Evaluating the performances of a roundabouts. Special report SR 45 ARRB, Transport Research Ltd, Vermouth South, Australia.
56. AUSTROROADS (1993) Roundabouts. Guide to traffic engineering practice Part 6. Association of State Australian state road and transport authorities, Sidney, Australia
57. Akcelik R (2011) An Assessment of the Highway Capacity Manual 2010 Roundabout Capacity Model. International TRB Roundabout Conference, Carmel, Indiana, USA, May 2011.
58. Akcelik R (2011) Roundabout design and capacity analysis in Australia and New Zealand. International Roundabout Design and Capacity Seminar. 6th International Symposium on Highway Capacity and quality of service, Stockholm, Sweden, 1st July, 2011
59. Qu X, Zhang IJ, Wang S, Liu Z (2014) Modelling follow up time at a single-lane roundabout. Journal of Traffic and Transportation Engineering 1(2):97–102.
60. Robinson B W, Rodegerdts L, Scarbrough W, Kittelson W, Troutbeck R, Brilon W, Bondzio L, Courage K, Kyte M, Mason J, Flannery A, Myers E, Bunker J, Jacquemart G (2000) Roundabouts: An Informational Guide. Report Federal Highway Administration - FHWA-RD-00-067. US Department of Transportation.
61. Highway Capacity Manual (2000) Transportation Research Board Special Report 209, 3th edition.

62. Troutbeck RJ (1998) Background for HCM Section on Analysis of Performance of Roundabouts. Transportation Research Record 1646(1998): 54–6.

63. Zheng D, Chitturi M, Bill A, Noyce D A (2011) Comprehensive evaluation of Wisconsin roundabouts Volume 1: Traffic Operations. Wisconsin Traffic Operations and Safety Laboratory, Wisconsin, US, Available at http://wwwtopslabwiscedu/projects/4-10html Accessed 28 March 2013

64. Troutbeck RJ (1986) Average delay at an unsignalized intersection with two major streams each having a dichotomized headway distribution. Transportation Science 20(4):272–286. doi:10.1287/trsc.20.4.272.

65. Li Z, De Amico M, Chitturi M V, Bill A R (2013) Calibrating Vissim roundabout model using a critical gap and follow-up headway approach. 16th Road Safety on Four Continents Conference, Beijing, China, 15–17 May 2013

66. Xu F, Tian Z (2008) Driver behavior and gap-acceptance characteristics at roundabouts in California. Transportation Research Record 2071(2008):117–124. doi:10.3141/2071-14

67. Abrams D S, Fitzpatrick C D, Tang Y, Knodler M A (2013) A spatial and temporal analysis of driver gap acceptance behavior at modern roundabouts. 92nd Annual Meeting of the Transportation Research Board, Washington, D.C. January, 2013

68. Mensah S, Eshragh S, Faghri A (2009) A critical Gap Analysis for Modern Roundabouts. 89th Annual Meeting of the Transportation Research Board, Washington, D.C. January, 2010.

69. Dahl J, Lee C (2012) Empirical estimation of capacity for roundabouts using adjusted gap-acceptance parameters for trucks. Transportation Research Record 2312:34-45. doi:10. 3141/2312-04.

70. Qu Z, Duan Y, Song X, Hu H, Liu H, Guan K (2014) Capacity prediction model based on limited priority gap-acceptance theory at multilane roundabouts. Mathematical Problems in Engineering 2014:1–12(Article ID 490280)

71. Guo R (2010) Estimating critical gap of roundabouts by different methods. 6th Advanced Forum on Transportation of China, IET publisher, Beijing, October 2010: 84:89. doi:10.1049/cp.2010.1107

72. Manage S, Suzuki K, Nakamura H (2003) Performance analysis of roundabouts as an alternative for intersection control in Japan. Journal of the Eastern Asia Society for Transportation Studies 5: 871–883

73. Comprehensive Meta-Analysis (CMA), software version 3.

74. Qu Z, Duan Y, Song X, Hu H, Liu H, Guan K (2014) Capacity prediction model based on limited priority gap-acceptance theory at multilane roundabouts. Mathematical Problems in Engineering 2014:1–12(Article ID 490280).

75. Cochran WG (1950) The comparison of percentages in matched samples. Biometrika 37(3/4):256–266. doi:10.1093/biomet/37.3-4. 256.

76. Higgins J, Thompson SG, Deeks JJ, Altman DG (2003) Measuring inconsistency in meta-analyses. BMJ 327:557–560

CHAPTER THREE:
Uncertainty in capacity estimation at roundabouts

1. Introduction

The transportation decision-making process about a road facility or a transport system, as a consequence of planning and design activities or operational analysis, often exposes planners and designers to many sources of variability and uncertainty [1, 2]. In transportation engineering, although considerable information can be derived from new technologies and can be incorporated into the traditional performance measurements, the effect on outputs of variability and uncertainty in input parameters is not often taken into account in the capacity analysis of roads and intersections [3, 4]. Assessment of the effects of a design choice on one or more parameters that are used when an operational analysis is being carried out, requires information on the sources of uncertainty that have affected them and the relation among them [5]. Since the variability is a chance-caused variation and depends on the facility or the system that is being considered, while uncertainty is the lack in the analyst's knowledge of the parameters which define the physical system to be modelled, the combination of variability and uncertainty can erode the ability for making predictions about the future [6]; moreover, high levels of uncertainty can characterize long-term predictions [7]. It should be noted that analysts typically produce a single number that explains the performance of the road facility, but they usually do not give a statement of a likely range of variation in the result nor try to quantify the impact of this uncertainty on capacity estimation [8, 9]. In order to characterize any process governing road traffic phenomena, deterministic models are developed and used. However, these models should be applied for many iterations and, for each iteration, rather than selecting the mean or the median value for each parameter, the values of model parameters should be randomly drawn from the corresponding probability distributions. Thus, the results can be expressed in probabilistic terms [10, 11].

Although the tasks required may be more complex, they should at least include the following:
- identifying the possible sources of uncertainty for the problem under consideration;
- determining the main variables involved in the probabilistic analysis;
- assigning the probability distributions to these variables.

The uncertainty analysis, indeed, aims to assess various aspects of a model, such the statistical properties of the outputs when stochastic input parameters are considered [12]. In the case of capacity analysis at intersections and roundabouts, the impact of uncertainty depends on the kind of problem to be faced and/or solved. The analysts may need to identify how many lanes are required for a given

approach of a roundabout, or know which control type (stop or traffic signal) is most appropriate for a given intersection, etc.; see e.g. [8]. According to Kyte et al. [13], the analysts should account for uncertainty when the capacity and level-of-service of a given intersection and/or roundabout is to be estimated, and should explain how this component can affect the problem or decision under consideration. Moreover, the analyst should be aware of the large observed variation in driver behaviour at intersections and roundabouts [14-16].

When a gap acceptance model is going to be developed, assumptions need to be made both for the psycho-technical headways (or the critical headway and the follow-up headway), and for the arrival headway distribution (that is to say the distribution of the gaps between the vehicles in the different circulating streams; see chapter two for more details), as well as for the distribution of traffic flows among the circulating lanes. The accuracy of the capacity estimation is primarily determined by the accuracy of the estimation of the critical headway and the follow-up headway.

Based on the considerations above, the purpose of the research activity described in this chapter was to consider which variables significantly affect entry capacity estimation and suggest how to investigate this question in the operational analysis of roundabouts. It should be noted that, many methods exist for incorporating uncertainty into the quantitative estimates of the performance parameters; in any case, the Monte Carlo simulation is commonly used by researchers and engineers as a method for propagating uncertainties in model inputs into uncertainties in results. Therefore, in order to exploring the uncertainty in capacity estimation at roundabouts, Monte Carlo simulation was performed through the software Oracle Crystal Ball which enabled us to obtain probability distributions of entry capacity, once the probability distributions of the critical headway and the follow-up headway were assumed. Specifically, the use of Oracle Crystal Ball is illustrated with three working examples of roundabout (i.e. the single-lane roundabout, the double-lane roundabout and the turbo roundabout), dealing with a capacity model of non-linear features and the correlated variables. In this regard, before to perform the Monte Carlo simulations with the software above mentioned, some preliminary hypotheses were made; these hypotheses will be better explained in the next section and in general way they regarded mainly the capacity model at steady-state conditions and the distribution function assumed for the critical and follow-up headways. The results of the analysis were expressed probabilistically, meaning that the probability distributions of the capacity at each entry lane rather than the simple point estimates of the performance measure were obtained. Lastly, a comparison was also made between capacity estimations based on meta-analytical estimations of the behavioural parameters (see chapter two), and the capacity functions based on the probability distributions of the model parameters.

2. Preliminary hypothesis

As is well-known, roundabouts produce efficiency through the gap acceptance process. The critical headway and the follow-up headway are two key factors in determining the entry lane capacity which, in turn, depends on the circulating flow under a specified arrival headway distribution. Note that, depending on the roundabout layout and the number of lanes on the ring, the circulating flow can be arranged in a single stream or two streams of vehicles travelling side-by-side. Thus, the critical and the follow-up headways, on which the driver gap acceptance process is based, were differentiated for each entry lane.

A meta-analytic estimation of the gap acceptance parameters as developed in the previous chapter was used to calculate the entry capacity functions. It should be noted that due to its statistically reliable approach, a meta-analysis makes the review process less subject to subjective appraisal than narrative reviews; it also represents a method to synthesize data across studies, since the results may vary from one study to another [17]. Generalizing the results from a meta-analysis makes more sense than from a single empirical study, because a meta-analysis integrates different sets of populations into the analysis and accounts for different variations between different groups which will likely respond differently. Based on the wide application of quantitative methods to summarize the results of several empirical studies in lots of research fields (see e.g. [18]), the mean values of the critical headways and the follow-up headways, previously estimated at observation sites characterized by similar layouts, were collected in order to evaluate their mean effect or the effect size, evaluate the dispersion in these effects and then compute a summary effect for each parameter. Table 1 shows the results of the meta-analysis of effect sizes through the random effect model summarized for the purpose of this research activity.

Table 1 The meta-analytic estimates for critical headway at roundabouts
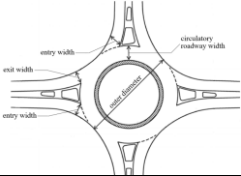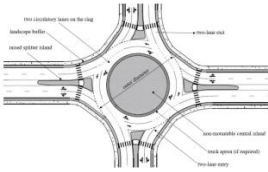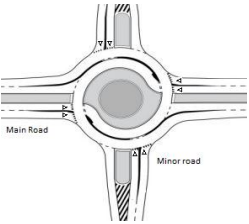
Roundabout	Entry lane	Circulating lane	Random estimate (se)	Random estimate (se)
Single-lane			4.27 (0.11)	3.10 (0.07)
Double lane	Right		3.82 (0.13)	2.85 (0.10)
	Left		4.17 (0.13)	2.72 (0.08)
Turbo (major road)	Left		3.60 (0.06)	
Turbo (major road)	Right		3.91 (0.25)	
Turbo (minor road)	Left	Outer	3.07 (0.15)	
Turbo (minor road)	Left	Inner	3.20 (0.03)	
Turbo (minor road)	Right		3.83 (0.20)	

Once meta-analytic estimates of critical and follow-up headways was known, the next step consisted of estimating the entry capacity functions; for this purpose, a

capacity formula had to be specified for the three roundabout layouts studied here: the single-, the double-double roundabout and the turbo roundabout. In this regard, the general formula proposed by Hagring [19] (see chapter one) was take into account, and it was particularized according to each scheme under examination. The conflict scheme of the right entry lane at double-lane roundabouts is the same as for single-lane roundabouts, since vehicles must yield to only one antagonist stream; in turn, the vehicles entering from the left entry lane at double-lane roundabouts must yield to the two antagonist flows: one of them uses the outer circulating lane close to the entry, and the other uses the inner circulating lane close to the central island of the roundabout. Therefore, by using Hagring's capacity formula [19] one can estimate:

- the capacity of each entry lane at single-lane roundabouts as a function of the circulating flow Q_c, the critical headway (T_c) and the follow-up headway (T_f) (see Eq.1 in Table 2);
- at double-lane roundabout entries:
  - the capacity of the right entry lane as a function of the outer circulating flow Q_{ce}, the critical headway (T_{ce}) and the follow-up headway (T_f) (see Eq. 2 in Table 2);
  - the capacity of the left entry lane as a function of the inner circulating flow Q_{ci}, and the outer circulating flow, Q_{ce}, the critical headways referred to the outer circulating lane (T_{ce}) and the inner one (T_{ci}), and the follow-up headway (T_f)(see Eq. 3 in Table 2);
- at turbo roundabouts, considering the analogies with single- and double-lane roundabout entries:
  - the capacity of the right-lane and left-lane of major entries, and the right-lane of minor entries as a function of the only circulating traffic flow in the outer circle lane in front of the considered entry approach (Q_{ce}), the critical headway of the external circulating flow (T_{ce}) and the follow-up headway for the considered approach (see Eq. 4 in Table 2);
  - the left-entry capacity of the minor road as a function of the outer circulating traffic flow ($Q_{c,e}$) and the inner circulating flow ($Q_{c,i}$), the critical headways of both circulating lanes and the follow-up headway of the considered entry lane (see Eq. 5 in Table 2).

Table 2 Hagring's formula particularized for different roundabout layouts

Roundabout layout	Hagring capacity formula [veh/h]	
Single - lane roundabout		
	$$C_e = Q_c \cdot \left(1 - \frac{\Delta \cdot Q_c}{3600}\right) \cdot \frac{\exp\left(\frac{-Q_c}{3600} \cdot (T_c - \Delta)\right)}{1 - \exp\left(\frac{-Q_c}{3600} \cdot T_f\right)}$$	(1)
Double - lane roundabout		
	Right entry lane	
	$$C_e = Q_{c,e} \cdot \left(1 - \frac{\Delta \cdot Q_{c,e}}{3600}\right) \cdot \frac{\exp\left(\frac{-Q_{c,e}}{3600} \cdot (T_c - \Delta)\right)}{1 - \exp\left(\frac{-Q_{c,e}}{3600} \cdot T_f\right)}$$	(2)
	Left entry lane	
	$$C_e = (Q_{c,e} + Q_{c,i}) \cdot \left(1 - \frac{\Delta \cdot Q_{c,e}}{3600}\right) \cdot \left(1 - \frac{\Delta \cdot Q_{c,i}}{3600}\right) \cdot \frac{\exp\left(\frac{-Q_{c,e}}{3600} \cdot (T_{c,e} - \Delta) \frac{-Q_{c,i}}{3600} \cdot (T_{c,i} - \Delta)\right)}{1 - \exp\left(\frac{-(Q_{c,e} + Q_{c,i})}{3600} \cdot T_f\right)}$$	(3)
Turbo roundabouts		
	Right entry lane and left entry lane, major road - Right entry lane, minor road	
	$$C_e = Q_{c,e} \cdot \left(1 - \frac{\Delta \cdot Q_{c,e}}{3600}\right) \cdot \frac{\exp\left(\frac{-Q_{c,e}}{3600} \cdot (T_c - \Delta)\right)}{1 - \exp\left(\frac{-Q_{c,e}}{3600} \cdot T_f\right)}$$	(4)
	Left entry lane, minor road	
	$$C_e = (Q_{c,e} + Q_{c,i}) \cdot \left(1 - \frac{\Delta \cdot Q_{c,e}}{3600}\right) \cdot \left(1 - \frac{\Delta \cdot Q_{c,i}}{3600}\right) \cdot \frac{\exp\left(\frac{-Q_{c,e}}{3600} \cdot (T_{c,e} - \Delta) \frac{-Q_{c,i}}{3600} \cdot (T_{c,i} - \Delta)\right)}{1 - \exp\left(\frac{-(Q_{c,e} + Q_{c,i})}{3600} \cdot T_f\right)}$$	(5)

In order to reach a broad-based assessment of the variability of the behavioural parameters and incorporate uncertainty into the entry capacity estimation, it was assumed that the critical headway and the follow-up headway could be captured over an observation period short enough to ensure a persistent steady-state condition and long enough to overstep the transient state. Under this hypothesis, the headways experienced by users during the observation period can be considered as sampled from the entire population; in this sense, they assume mean values that are within the distribution of the mean.

Based on the probability theory, if the initial (normal distributed) population (X) has mean μ and variance σ^2, the sampling distribution of the sample mean $\bar{X}$ from samples of size *n* is assumed normally distributed $\bar{X} \sim N(\mu, \sigma^2/n)$.

This is also true for a population that is not normally distributed - namely the sampling distributions may also be assumed approximately normally distributed, regardless of the population distribution that one samples from - if the sample size is not too small (*n*≥30), and the population size, N, is at least twice the sample

size. When the distribution of $\overline{X}$ is unknown or differs from the normal distribution, according to the central limit theorem, $\overline{X}$ assumes a normal asymptotic distribution. In fact, as *n* increases, the density function of $\overline{X}$ approaches a normal distribution very rapidly, although the population distribution is strongly asymmetric, see e.g. [20].

In these applications, independently of the sample size, it was assumed that the sampling distribution of the sample mean $\overline{X}$ is approximately normally distributed.

Based on literature data, Fig. 1 shows the log-normal distribution for the critical headway vs. the normal distribution for the mean of the critical headway. The sample size *n*, as will be better explained below, was obtained under a specific hypothesis on the degree of saturation (namely the ratio of the entry flow to the entry capacity) and the time duration of the observation period.
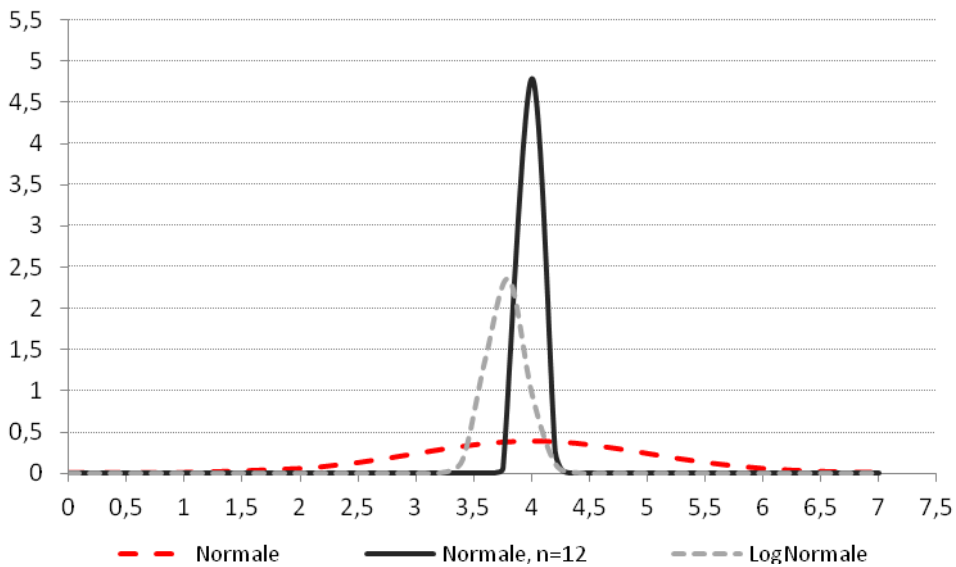

Figure 1 Log-normal distribution of T_c Vs. normal distribution for the mean of T_c

Based on the consideration made above, in order to characterize the sampling distribution of the sample mean $\overline{X}$ from samples of size *n*, the sample size *n* has to be defined. In this regard, according to Mauro [4], the number of entering vehicles during the period of observation will depend on the duration of the steady-state condition, which is not immediately known. By contrast, it is possible to get an appropriate measurement of the time *T* that the system needs in order to move from a steady-state condition to another subsequent steady-state condition. The transient time *T* can be calculated through Morse's inequality [20], which is recalled below (see chapter one for more details):

$$T > \max\left[\cfrac{1}{\left(\sqrt{\cfrac{C_i}{3600}} - \sqrt{\cfrac{Q_{ei}}{3600}}\right)^2}\right] \qquad (1)$$

where:

- C_i is the capacity of entry i;
- Q_{ei} demand volume of entry i.

It is noteworthy that this formula can only be applied when the ratio (Q_{ei}/C_i) <1. Besides, it must be stated that the steady-state models of entry capacity are only a useful approximation if the duration of the analysis period is considerably greater than the duration calculated using Morse's expression [20]. For the application which was performed, an observation period was assumed that was equal to twice the time of the transient phenomenon and the number of entering vehicles over this period was calculated and considered as the sample size. In order to apply the Morse's formula (thereby determining the sample size n), an entering flow rate should be set, or the ratio of the entry flow to the entry capacity (Q_e/C) should be specified upon the condition (Q_{ei}/C_i)<1; this means that only under-saturated conditions are to be considered. Thus, a value of the ratio of the entry flow to the entry capacity equal to 0.50 was considered. Under these hypotheses, the corresponding values of *n* was found equal to 12, where half of this can be considered in steady-state conditions.

Based on the preliminary hypotheses as above defined, in order to find the probability distributions of entry capacity for single-lane, double-lane and turbo roundabouts, a Monte Carlo simulation was performed with Crystal Ball Software [21]. Therefore, in the following sections, after a brief introduction to the principles of the Monte Carlo method, the simulation conducted with Crystal Ball software will be described step by step.

3. Monte Carlo simulation

The simulation, in its most general meaning, is a numerical technique that builds a mathematical model consisting of equations describing, through virtual experiments, the relationships between the components of the system studied, with the aim of reproducing with some accuracy the behavior of the real system. In this sense, the Monte Carlo technique is a particular case of a simulation method that uses a probabilistic approach to solve a specific problem. The Monte Carlo method is defined as representing the solution of a problem as a parameter of a hypothetical population, and using a random sequence of numbers to construct a sample of the population, from which statistical estimates of the parameter can be obtained [23]. In other words, the Monte Carlo method reproduces a sufficiently high number of possible combinations of input variables,

whose probability distribution is known, and calculates outputs based on model equations expressing the relationship between variables. Thus for each of the input variables, a probability distribution must be specified; indeed, for obtaining the N combinations, a value for each of the input variables is randomly extracted from its specified probability distribution. This process of extraction, repeated many times, makes it possible to generate a sample of possible output values; this sample is then analyzed by statistical techniques for estimating the descriptive parameters of its probability distribution. Therefore, the Monte Carlo method makes it is possible to estimate the probability density function of the outputs, starting with the probability functions of the input data.

In general way, a Monte Carlo simulation procedure includes:

− the input parameters specified by the analyst and then controllable;
− input variables, defined as exogenous, because they depend on events that are not under the control of the analyst, whose performance is, however, described in probabilistic terms, that is, by probability distributions;
− the mathematical equations of the model that express the relationships between outputs, parameters of the system and input variables;
− and finally output variables that represent the results of the simulation.

Therefore, a Monte Carlo simulation starts with identification of the parameters and input variables by the analyst; for each input variable, a probability distribution needs to be specified and then the mathematical relationship that makes it possible to determine the output variables according to the input variables and the parameters has to be defined. At this point, before starting the simulation, the number of the trials must be set and the sampling technique, has to be also specified. Regarding the number of trials, one can observe that the more numerous the trials are, the larger is the output sample, and therefore greater precision and accuracy in the estimate of the outputs distribution can be obtained. On the other hand, a very high number of trials could make the simulation process very long. Instead, with regard to sampling techniques, there are several sampling methods used for statistical applications, but the most used in the Monte Carlo simulation are mainly three: Simple Random Sampling (SRS in the follow); Stratified Sampling; Latin Hypercube Sampling. Simple random sampling, is the basic type of sampling, in which extraction of a specific number of elements, from a population, distributed according to its probability density function, is totally random. This technique is characterized by attributing the same probability of extraction to all the elements extracted from the population; it follows that each element of the population has the same probability of being part of the sample. Finally, with this sampling technique, it is possible to choose whether each element can be extracted several times, that is, one can choose extraction with or without replacement. It should be noted that although the SRS method is one of the simplest sampling methods, sometimes it could be considered inefficient since, especially for small samples, the extracted elements

may fail to cover the entire range of variation of the random variable. Instead, stratified sampling is a sampling method that consist of dividing the population into homogeneous subgroups, according to the variable for which the value has to be estimated. Each subgroup represents a stratum from which a sample is extracted through simple random sampling; then all samples extracted from each stratum are put together, thus obtaining a global sample. This method, compared to simple random sampling, makes it possible to entirely represent the range of variation of the random variable and consequentially it generates a greater accuracy in output estimation. Furthermore, using the stratified sampling method, the values of variance is lower than with simple random sampling; indeed, it is considered as a sampling method for reducing the variance of the estimator. Therefore, on the one hand stratified sampling, for the reason explained above, is a more efficient method than simple random sampling; on the other hand, stratified sampling method has a more complex structure, since subpopulations, i.e. homogeneous stratums, within population, must be identified. A particular case of stratified sampling is Latin Hypercube sampling, which is an extension of the d-dimensional case of the stratified sampling method. This method works exactly like the stratified sampling method. Thus, it reduces the variance of the estimator and makes it possible to represent in more efficiently the d-dimensional definition set of the random variable.

4. Uncertainty analysis with Crystal Ball Software

To understand uncertainty in roundabout capacity estimation, the probability distributions of the random variables of the capacity model had to be identified.
For this purpose a Monte Carlo simulation was performed using specific software namely Crystal Ball developed by the Oracle Corporation [22]. This software consists of a suite of applications based on Microsoft Excel software that make it possible to create predictive models exploiting the Monte Carlo simulation technique. In this case, Crystal Ball software was used to find the probability distributions of each parameter contributing to the entry capacity of the three working examples of roundabout, i.e. the single-lane roundabout, the double-lane roundabout and the turbo roundabout.
As described in the previous section, building a model characterized by definition of input parameters, input variables with their distributions, and mathematical equations, represents the first step of Monte Carlo simulation procedure. Building a model in Crystal Ball means putting input data into three types of cells - *assumption*, *decision* and *forecast* cells. *Assumption cells* are related to input random variables, i.e. the cells within which the distributions of such random variables must be specified. In this regard, the software provides a "Gallery" of all possible distributions available, such as Normal distribution, Gamma distribution, Log-Normal distribution, Poisson distribution, etc. of which the statistical parameters, according to the type of distribution chosen, (e.g. mean, standard deviation, etc..) must be specified [23]. In this study case, random input variables

were the critical and follow-up headways; for each of them a probability distribution and its statistical parameters had to be assumed. For this purpose, literature data sources were used to hypothesize the probability distributions of each contributing parameter, as described in the previous section. Indeed, for each roundabout and each contributing parameter, normal distribution best seemed to fit the data; the (random) summary effect, or the meta-analytic estimation for each headway, is the mean of the distribution, whereas the standard deviation σ is weighted with regard to the sample size, as reported in the different primary studies.

With reference to this case study in which $Q_e/C = 0.5$ (n = 12/2 = 6), Table 3 shows the parameters of the sampling distribution for the critical headway and the follow-up headway for the single-lane roundabout, the double-lane roundabout and the turbo roundabout.

Instead, the decision-making variables that are controllable by the analyst can be introduced within *decision cells*. Decision-making variables are not mandatory for simulation models, but may be useful for comparing and optimizing alternative scenarios. Therefore, since no scenarios were compared, no decision-making variable was taken into account, for all the cases studied.

Finally, the output forecasts in the model can be defined in a *Forecast cell* in which an equation or a function must be inserted. Thus, for each roundabout scheme studied here, a formula for entry capacity estimation, i.e. Hagring's formula (see previous section for more details), was inserted into a cell and then defined as the *Forecast cell*.

Table 3 The parameters of the sample distribution for the critical and the follow-up headways (Qe = 0.5·C)

Roundabout	Entry	Entry lane	Circulating lane	Mean	$\sigma/\sqrt{n}$
Critical headway					
Single-lane				4.27	0.43
Double-lane		Right		3.82	0.49
		Left	Inner	4.17	0.49
			Outer	3.81	0.49
Turbo	Major	Left		3.60	0.31
Turbo	Major	Right		3.91	0.47
Turbo	Minor	Left	Inner	3.20	0.18
			Outer	3.07	0.27
Turbo	Minor	Right		3.83	0.41
Follow-up headway					
Single-lane				3.10	0.53
Double-lane		Left		2.85	0.45
Double-lane		Right		2.72	0.44

Once the model was built in Crystal Ball, the next step was to set the number of trials and the simulation technique used. In this regard, the software refers to two types of sampling: Monte Carlo sampling, which is simply random sampling, and Hypercub Latin sampling (for more details see previous section). In all cases under study, Monte Carlo sampling was chosen, while the major task in this application was to perform preliminary simulations in order to know how many iterations were needed. Thus, quite a high number of iterations was tried until very slight differences in the outputs led to the distributions sought; lastly, the decision was taken to do 10,000 trials. In addition, an option in the simulation preferences was set, which provided for stopping of simulations when a predetermined reliability level of 95% was reached.

After defining the hypothesis and prediction cells and, optionally, the decision-making cells in the spreadsheet, the simulation started. Thus Crystal Ball software, according to the Monte Carlo method, selected a random set of input data values drawn from their individual probability distributions, and using these values in the simulation model some output values were obtained. Indeed, during the simulation, the software creates a prediction chart for each forecast cell using frequency distributions to see the range of possible results.

The final step was to interpret the resulting forecast chart and the corresponding statistic generated after running the simulation; in this regard the Crystal Ball software provided, for each type of roundabout, the "overlay" graph which depicts, in a single graph, the probability distributions of entry capacity when varying the circulating flow. Based on such output, one can analyze variations in capacity and then make a comparison with the results given by the deterministic model. In detail, Fig. 2 depicts the probability distributions of capacity at single-lane roundabouts, where eight values of the circulating flow from 0 to 1400 veh/h with step 200 veh/h were considered in the single circulating lane.
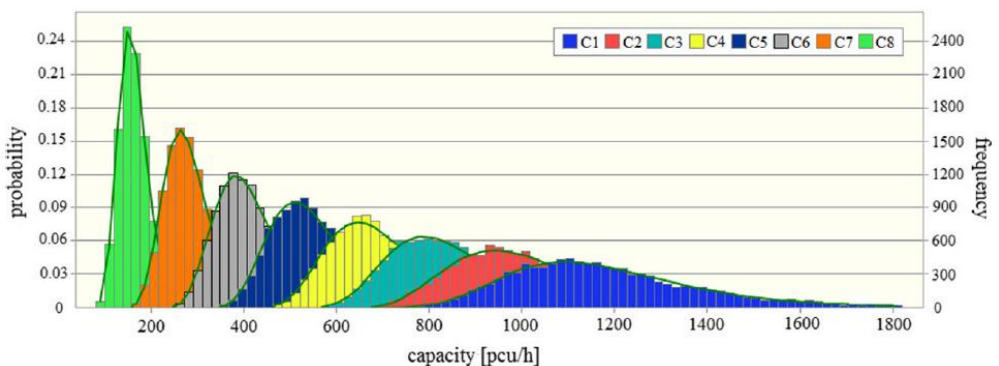

Figure 2 Probability distributions of entry capacity at single-lane roundabouts.

Note that C1–8 are the probability distributions of entry capacity where each of them is corresponding to a value of the circulating flow around the ring ranging from 0 to 1400 pcu/h with step 200 pcu/h

117

In the same way, Fig. 3 contains the probability distributions of the left-lane capacity for double-lane roundabouts; the probability distributions of the right-lane capacity for double-lane roundabouts are shown in figure 4.
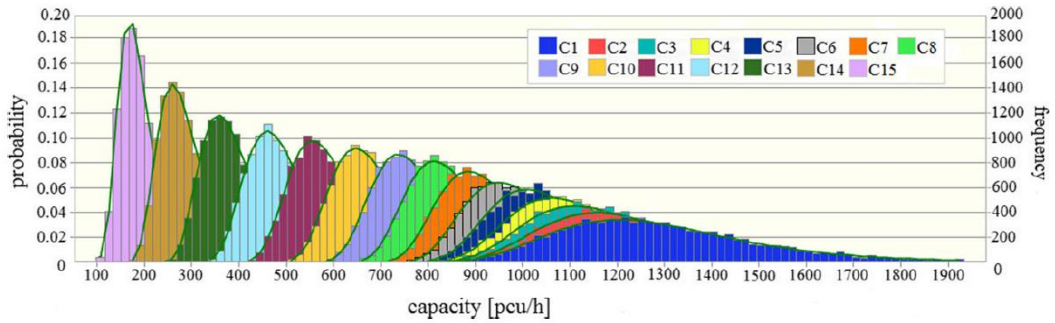

Figure 3 Probability distributions of entry capacity for the left-lane at double lane roundabouts

Note that C1–15 are the probability distributions of entry capacity where each of them is corresponding to a value of the circulating flow around the ring (where $Q_{c,i}= Q_{c,e}$) ranging from 0 to 2800 pcu/h with step 200 pcu/h
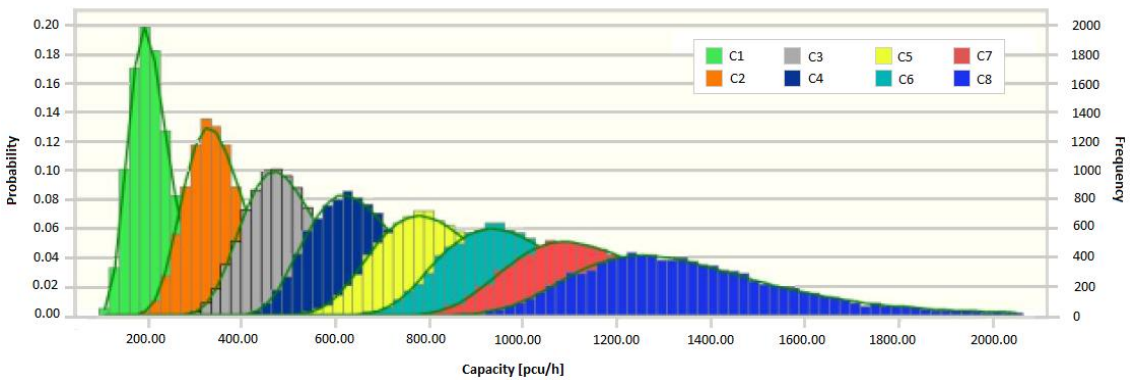

Figure 4 Probability distributions of entry capacity for the right-lane at double lane roundabouts

Note that C1–8 are the probability distributions of entry capacity where each of them is corresponding to a value of the circulating flow around the ring ranging from 0 to 1400 pcu/h with step 200 pcu/h

Figure 5 shows the probability distributions of the left-lane capacity for major entries at turbo roundabouts, whereas Fig. 6 shows the probability distributions of entry capacity only for the left lane on minor entries at turbo roundabouts; in this case entering vehicles face two antagonist traffic streams for which the assumption was made that $Q_{ce}= Q_{ci}$.
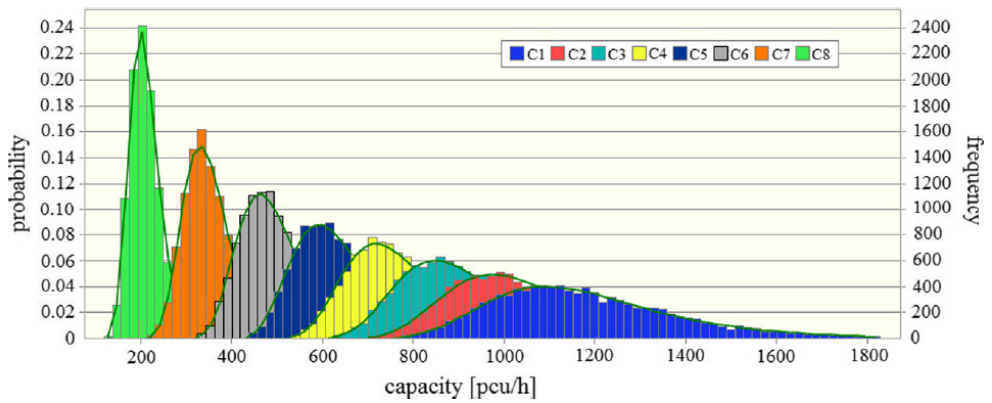
Figure 5 Probability distributions of entry capacity for the left-lane on major entries at turbo roundabouts.

Note that C1–8 are the probability distributions of entry capacity where each of them is corresponding to a value of the circulating flow around the ring ranging from0 to 1400 pcu/h with step 200 pcu/h

Figure 6 Probability distributions of entry capacity for the left-lane on minor entries at turbo roundabouts.

Note that C1–15 are the probability distributions of entry capacity where each of them is corresponding to a value of the circulating flow around the ring (where Qc,i=Qc,e) ranging from 0 to 2800 pcu/h with step 200 pcu/h

Finally Figures 7 and 8 depict the probability distribution of entry capacity for right-lane on both minor and main road at turbo roundabout.

Figure 7 Probability distributions of entry capacity for the right-lane on main entries at turbo roundabouts

Note that C1–8 are the probability distributions of entry capacity where each of them is corresponding to a value of the circulating flow around the ring ranging from0 to 1400 pcu/h with step 200 pcu/h
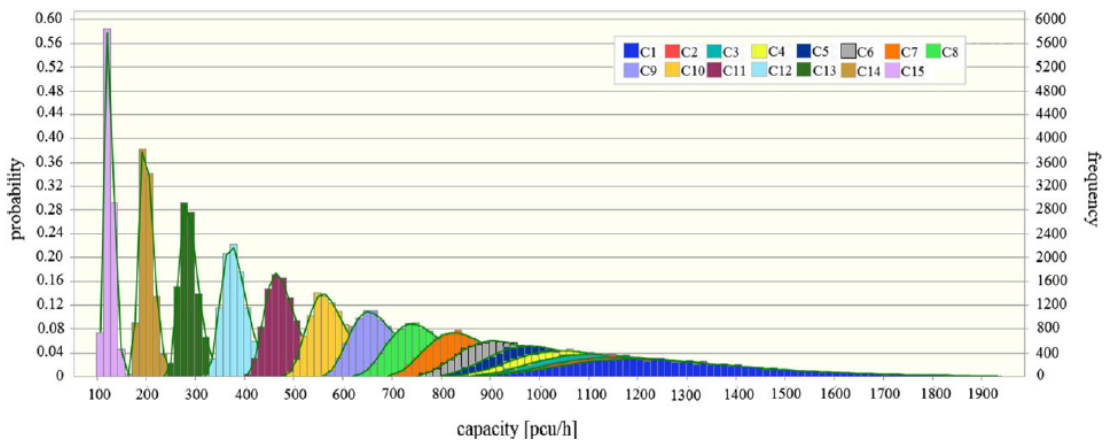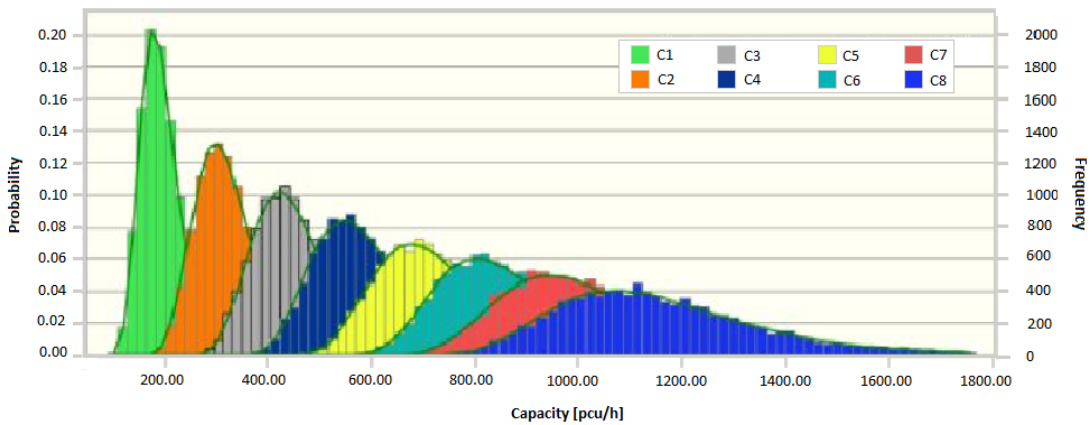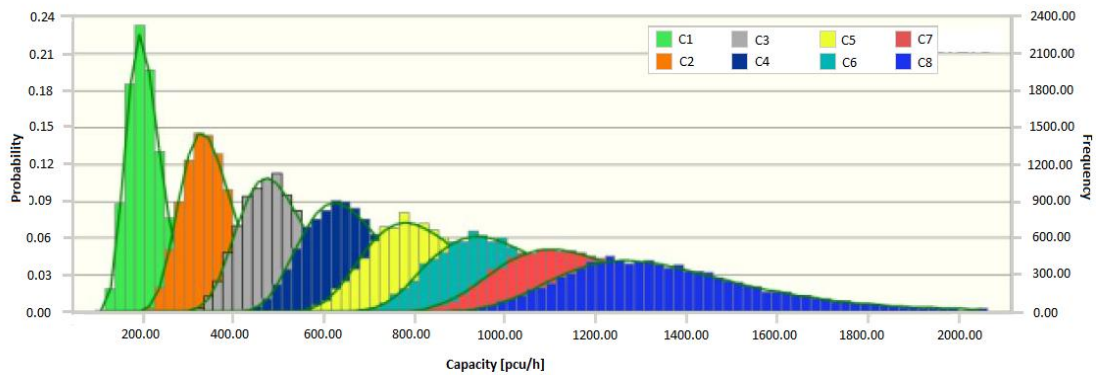

Figure 8 Probability distributions of entry capacity for the right-lane on minor entries at turbo roundabouts

In any overlay graph, regardless of the scheme of the roundabout examined, the vertical symmetrical histograms show the frequency of a particular capacity value occurring out of the total number of the trials, while the cumulative frequency represents the total probabilities of all values capacity occurring in the forecast. Moreover, from these bell-shaped curves, one can see the central column represents the (mean) capacity corresponding to a specified value of the circulating flow; more numerous measures around the mean value can be observed. It should be noted that, when the circulating flow is low, the capacity distribution turns out to be "squashed" with respect to the abscissa axis. Such distribution is characterized by a high variance, or values highly dispersed, so that the degree of uncertainty of the output in this case is of some importance. It

120

should be noted again that, if one considers gradually higher values in the circulating flow, the distribution of capacity takes a higher and narrow shape, with values quite concentrated around the mean; so the result is found to be more stable.

Figures from 9 to 15 show the capacity functions which incorporate the mean values of the critical headway and the follow-up headway, as derived from the meta-analysis, for each type of roundabout under study. In the same figures one can also see the 5th and 95th percentiles that, for a specified set of values, represent a measure that expresses what percent of the total frequency is falling below that measure. The capacity functions which were based on the adopted capacity model matched the median function or the 50th percentile below which 50% of the resulting measures of capacity falls below. As one can expect, for all the cases the capacity functions - built running the steady-state model and assuming for each behavioural parameter a single (mean) value representative of the entire population - tend to overlap with the 50th percentile curve
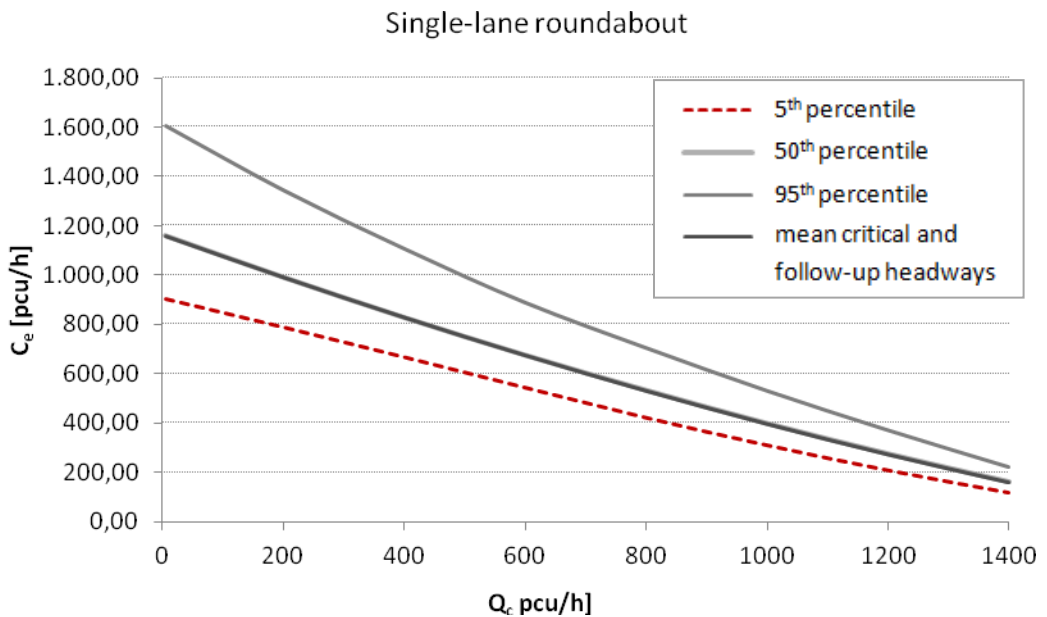
Figure 9 Entry capacity function for single lane roundabout
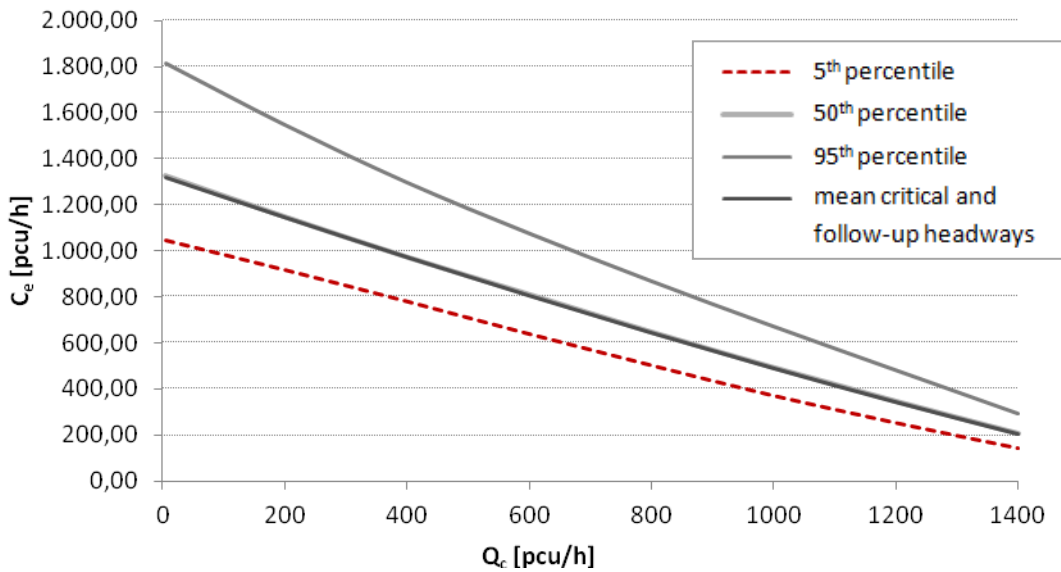
Figure 10 Entry capacity function for the right lane at double-lane roundabout
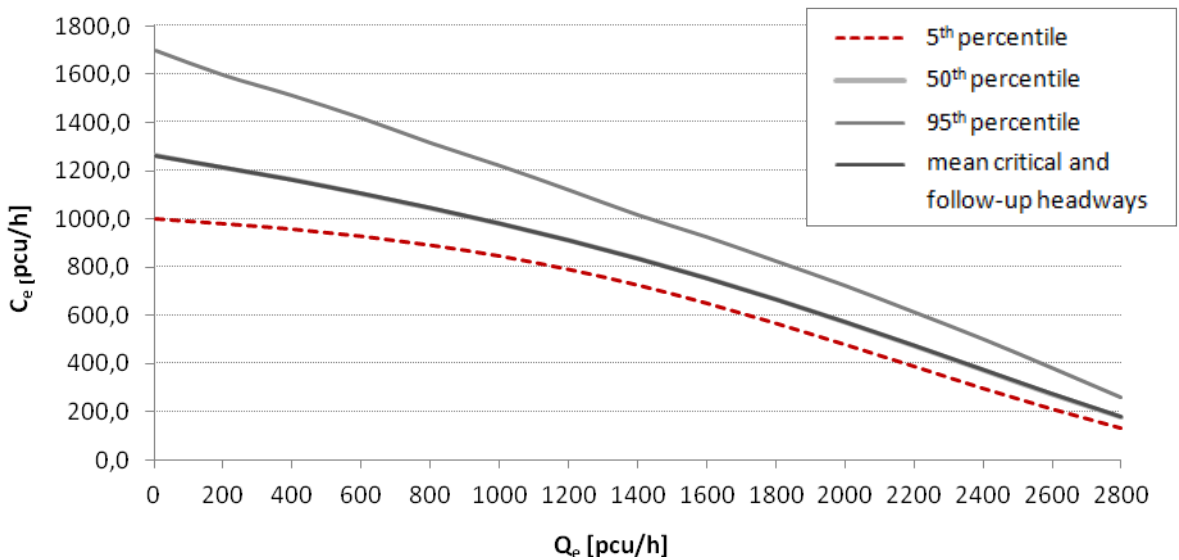
Figure 11 Entry capacity function for the left lane at double-lane roundabout
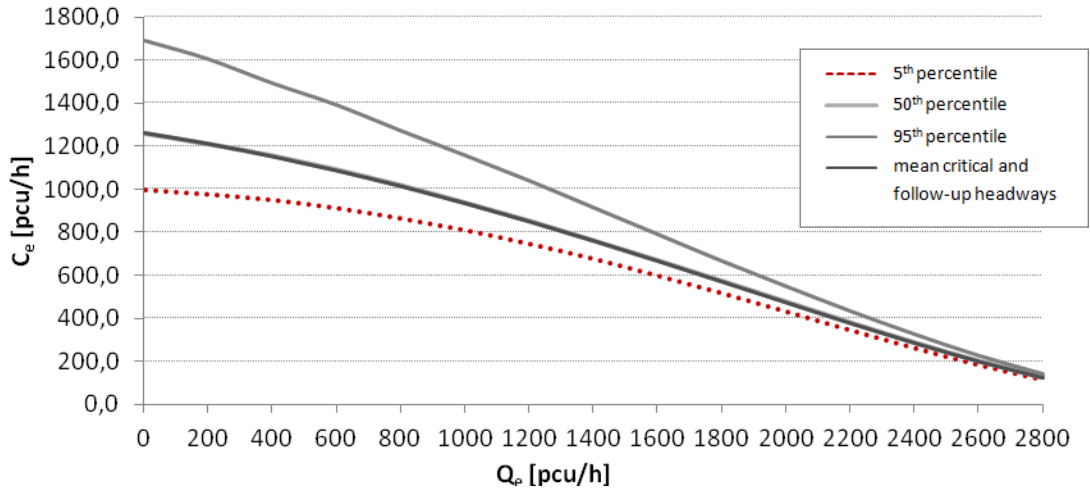
Figure 12 Entry capacity function for the left lane on minor entries at turbo-roundabout

Figure 13 Entry capacity function for the left lane on major entries at turbo-roundabout

Turbo roundabout - Right lane on Minor entry
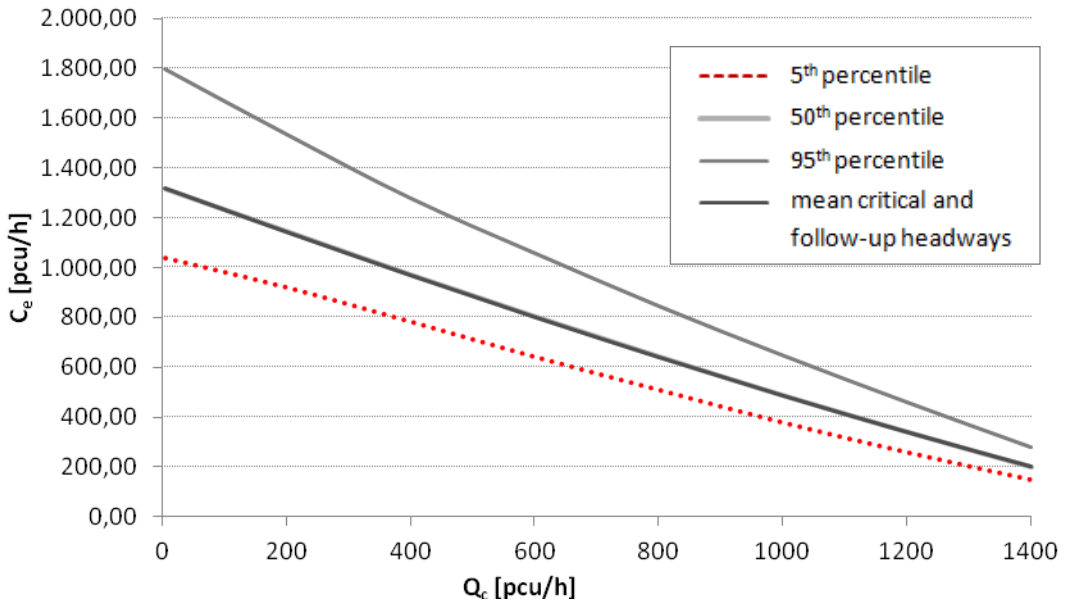
Figure 14 Entry capacity function for the right lane on minor entries at turbo-roundabout

Turbo roundabout- Right lane on major entry
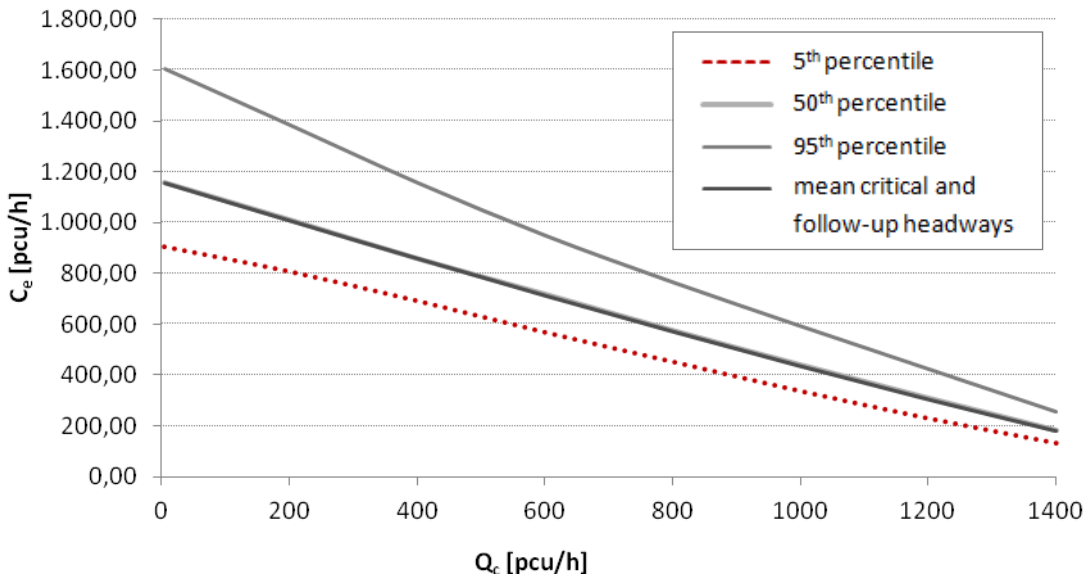
Figure 15 Entry capacity function for the right lane on major entries at turbo-roundabout

The results of the simulations indicated that the uncertainty in capacity estimation could be high, especially when the opposing flow is low; in these cases, estimation

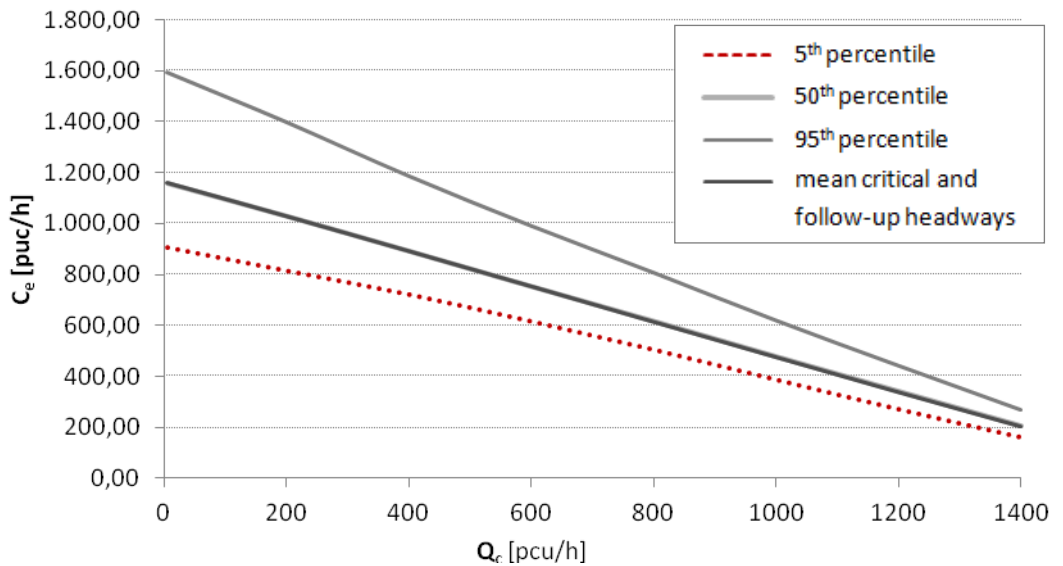through the mean values of the individual parameters can be far from the real value, providing a rough underestimation/overestimation of the latter value. The results indicated, indeed, that the actual capacity of the roundabout may be, with a probability of about 50%, higher than the capacity which can be estimated deterministically; based on this result, the traffic conditions could be better than the expected conditions.

At the same time, however, with the same probability, capacity estimation based on the deterministic model may be an overestimation of the actual capacity, with the result that, for a given traffic demand, the oversaturated conditions at entries are not highlighted. Based on the results obtained, the deterministic estimation of capacity is not cautionary, but rather the risk of poor performances at roundabouts, especially when the circulating flow is low, is quite significant. However, the conclusions that were drawn could be affected by the choice of one or another capacity model. The use of other models that incorporate different processes could probably further improve understanding of uncertainty in capacity estimation at roundabouts.

References

1. Grayman WM (2005) Incorporating uncertainty and variability in engineering analysis. J Water Resour Plan Manag 131(3):158–160. doi:10.1061/(ASCE)0733-9496(2005)131:3(158)

2. Uusitalo L, Lehikoinenb A, Hellec I, Myrberga K (2015) An over- view of methods to evaluate uncertainty of deterministic models in decision support. Environ Model Softw 63:24–31. doi:10.1016/j.envsoft.2014.09.017

3. Ameri M, Moayedfar R, Jafari F (2013) Determination the capacity of two-lane suburban roads with neural networks and effect of speed on level of service. Eur Transp Res Rev 5(4):179–184. doi:10.1007/s12544-013-0096-y

4. Mauro R (2010) Calculation of roundabouts. Springer-Verlag, Berlin Heidelberg

5. Gao Y, Rong G, Yang L (2015) Analysis of order statistics of un- certain variables. J Uncertain Anal Appl 3:1. doi:10.1186/s40467- 014-0025-1

6. Vose D (2008) Risk analysis: a quantitative guide. John Wiley & Sons, Inc., New York, USA

7. Matas A, Raymond JL, Ruiz A (2012) Traffic forecasts under un- certainty and capacity constraints. Transportation 39(1):1–17. doi:10.1007/s11116–011–9325-1

8. Bie J, Lo HK, Wong SC (2010) Capacity evaluation of multi-lane traffic roundabout. J Adv Transp 44(4):245–255. doi:10.1002/atr.124

9. Tarko A, Tian Z (2003) Example analysis and handling of uncertainty in the highway capacity manual with consideration of traffic diversion. Transp Res Rec 1852:40–46. doi:10.3141/1852-06

10. Iman RL, Helton JC (1988) An investigation of uncertainty and sensitivity analysis techniques for computer models. Risk Anal 8(1):71–90. doi:10.1111/j.1539-6924.1988.tb01155.x

11. Cullen AC, Frey HC (1999) Probabilistic exposure assessment: a handbook for dealing with variability and uncertainty in models and inputs. Plenum press; New York, USA

12. Bulleit WM (2008) Uncertainty in structural engineering. Pract Period Struct Des Constr 13(1):24–30. doi:10.1061/(ASCE)1084-0680(2008)13:1(24)

13. Kyte M, Dixon M, Basavaraju P (2003) Why field measurements differ from model estimates analysis - framework for capacity and level-of-service analysis of unsignalized intersections. Transp Res Rec 1852:32–39. doi:10.3141/1852-05

14. Mukherjee A, Majhi S (2016) Characterisation of road bumps using smartphones. Eur Transp Res Rev 8:13. doi:10.1007/s12544-016- 0200-1

15. Wu J, Liu P, Tian ZZ, Xu C (2016) Operational analysis of the contraflow left-turn lane design at signalized intersections in China. Transp Res Part C: Emerg Technol 69:228–241. doi:10.1016/j. trc.2016.06.011

16. Schnebele E, Tanyu BF, Cervone G, Waters N (2015) Review of remote sensing methodologies for pavement management and as- sessment. Eur Transp Res Rev 7:7. doi:10.1007/s12544-015-0156-6

17. M. Borenstein, L.V. Hedges, J.P.T. Higgins, Rothstein H.R. (2009). Introduction to Meta-analysis, John Wiley & Sons, Ltd Chichester, UK.

18. Elvik R. (2017). Road safety effects of roundabouts: A meta-analysis, Accident Analysis and Prevention 99:364–371. https://doi.org/10.1016/j.aap.2016.12.018

19. Hagring, O. 1998. A further generalization of Tanner's formula. *Transportation Research Part B: Methodological* 32(6): 423–429.

20. Morse PM (1982) Application of queuing theory, 2nd edn. Chapman Hall, London.

21. OracleCrystal Ball._ Users guide, avaialble at: https://docs.oracle.com/cd/E52437_01/it/crystal_ball_users_guide/frame set.htm?index.html

22. Gravetter FJ, Wallnau LB (2013) Statistics for the behavioral sciences, 9th edn. Cengage Learning, Boston, US

23. Halton J. H. (1960). Numerische Mathematik - On the efficiency of certain quasi-random sequences of points in evaluating multi-dimensional integrals. 2 84-90 - 1970 Siam Rev. 12 1-63

CHAPTER FOUR

Genetic algorithm-based calibration of microscopic traffic simulation model. Application for single-lane and double-lane roundabouts

1. Introduction

Microscopic traffic simulation models have become an increasingly important tool to assess not only operational performances but also safety aspects of any road facilities. Indeed, a microscopic traffic simulation model is able to reproduce the operating conditions of a road or intersection, exploiting the simulation technique that can be seen as a sampling experiment on a dynamic real system through a computer model that formally represent it [53]. Therefore, microscopic traffic simulation models represent for researchers and practioners the favourite methods for analysing operations of road networks or single road infrastructures, and taking decisions on their geometric design and layout development; simulation models, indeed, allow the accurate modelling of some transportation planning and design problems. Nowadays, there are several micro-simulators that can be used to build traffic simulation models, such as VISSIM, PARAMICS, AIMSUN, and so on [1, 2, 3]. Regardless of the software being used, microscopic simulation models can be built using a large number of independent parameters that describe traffic flow characteristics, geometric features of the modelled network or driver behaviour. Even though these microscopic simulation models provide default values for these parameters, a simulation under default values often produces unreliable results. Therefore, the values of these parameters need to be adjusted in order to accurately represent the traffic conditions of the system being examined. This adjusting process, better known as calibration, has the objective of finding the values of the model parameters in order to minimize the difference between microscopic model and real system. In turn, validation is a process carried out after calibration and consists in determining whether the simulation model can be considered as a good representation of real traffic conditions. In other words, validation compares the simulation model output with other measured data (i.e. data different from data used for calibration); this implies an iterative process since it may occur that the simulation model is rejected and the input data need to be revised or changed.

Therefore, the ability to produce a simulation model that represents the system's behaviour closely enough, depends on the choice of value parameters that affect the output of traffic simulations. For these reasons calibration and validation of micro-simulation models are some very crucial tasks, since reliable results must be obtained from the analysis that we perform.

A calibration process can be carried out through several procedures, but model calibration as an optimization problem is perhaps the most recommended practice [6]. In general, the optimization problem is expressed by an objective function that minimizes the "distance" between an observable traffic variable and its simulated value, which in turn depends on the set model parameters and their values.

Calibration of any traffic micro-simulation model, formulated as an optimization problem, can be performed by applying an optimization algorithm which searches for an optimum set of model parameters for automatically determining the calibrated model. In other words, incorporating the optimization problem within the model calibration, the effort of users and practioners is reduced, since the iterative process of manually adjusting the model parameters is now automatized.

In order to provide a valid microscopic simulation model to evaluate operation and safety performance at roundabouts, AIMSUN micro-simulator was used to model two case studies of single-lane and double-lane roundabouts; for both roundabouts the calibration was implemented through a genetic algorithm.

The modelling started by drawing the layouts of the single-lane and double-lane roundabouts and including supply and demand data input required for building the network models of the roundabouts. Before starting the calibration process, the most sensitive parameters for each roundabout model under examination were identified. In order to carry on the analysis, the roundabout capacity functions were calculated by using the Hagring formula [4]; it was implemented by using the meta-analytic estimation of the critical and the follow-up headways as presented in Chapter 2. For each roundabout case study, the genetic algorithm tool in MATLAB® [5] was applied, in order to minimize the differences between the empirical capacity functions and the corresponding simulation outputs. The automatic interaction of MATLAB with AIMSUN was implemented through an external Python script that was specially written. The goodness of the fitting between the empirical capacities and simulation outputs of the calibrated models was also tested.

After some references to microscopic simulation models in a general way and the description of AIMSUN modelling for the single-lane roundabout and the double-lane roundabout selected as case studies, the GA-based calibration procedure of a microscopic traffic simulation model will be introduced. Based on this premise, it was also considered appropriate to describe a brief review about genetic algorithm applications to transportation engineering.

2. Traffic flow modelling

The dynamism of traffic flows in traffic simulation models can be modelled in three different ways: macroscopically, microscopically and mesoscopically.

Macroscopic modelling of traffic flows takes into account an aggregate viewpoint, in that the traffic flow, based on hydrodynamic analogy, can be seen as particular fluid characterized by aggregate macroscopic variables such as density, volume

and speed. Thus, in this regard, the evolution of the variables characterizing macroscopic flows are defined at each time instant and each point in space.

Traffic flow can also be modelled microscopically, assuming instead a disaggregated point of view considering the dynamics of the individual particles, that are vehicles. Thus, the description of the movement of each vehicle that compose the flow involves modelling of its dynamic characteristics such as acceleration, deceleration and also lane change. Finally, as mentioned before, traffic flows can be modelled in mesoscopic way, which means an intermediate manner between microscopic and macroscopic modelling of traffic flows.

At the road network level, one can use a microscopic approach if one wants to simulate the behaviour of small road networks such as single nodes, or intersections; on the contrary when the size of a road network expands to an entire urban area, it is recommended to use a mesoscopic approach; macroscopic modelling is generally used at strategic planning level for vast area networks.

In the research studies that were carried out and described in the following sections, since the operating performance of a specific intersection scheme (i.e. a single roundabout and a double-lane roundabout) was analysed, a microscopic approach was adopted. Without being exhaustive, microscopic behavioural models are introduced in the next section.

3. Microscopic behavioural models

The level of detail that can be achieved by using micro-simulation to represent the evolution of vehicular traffic on a road network depends essentially on the attributes that users put into the micro-simulation traffic models.

These attributes reflect the geometric and functional characteristics of a road facility, the kinematic features of moving vehicles on the network and their dimensions, and the behavioural attitudes of users, which are influenced by the characteristics of their vehicle and those of other vehicles near them in the network.

Simulation of a traffic model in AIMSUN is performed step by step, each step having a fixed duration; in these simulation steps, each vehicle's state, having behavioural attributes assigned when it enters the system, is updated according to a specific algorithm. It is noteworthy that a simulation step may affect not only the computing performance, but also some simulation outputs. The differences between mesoscopic, microscopic and macroscopic models relate to the level of abstraction and the process employed to update each vehicle's status.

When a microscopic approach is used to simulate a traffic model built in AIMSUN, each vehicle's position travelling in the road network is updated according to two driver behaviour models named "car following" and "lane changing." A gap-acceptance model is also used to simulate give-way behaviour at any intersection.

Since the research presented in this thesis focused on microscopic modelling through AIMSUN, in the next sections the fundamental microscopic behavioural models are briefly presented: car following, lane changing and gap-acceptance models.

3.1. Car following model

In car following models the behaviour of each user belonging to a traffic flow is influenced by the behaviour of the driver of the vehicle that precedes it. Specifically, in such models one can recognize two types of driver behaviour: the "follower", that is a driver who tends to adapt his/her driving to that of the previous vehicle, therefore named "leader".

The car-following model implemented in AIMSUN is based on the Gipps model, that considers the speed of vehicles mainly depending on speed limit acceptance of the vehicle and geometry of the section (speed limit on the section, speed limits on turnings, etc.). It basically consists of two components, acceleration and deceleration, the respectively expressions of which are given below:

$$V_a(n, t + T) = V(n, t) + 2.5 \cdot a(n) \cdot T \cdot \left(1 - \frac{V(n, t)}{V^*(n)}\right) \cdot \sqrt{0.025 + \frac{V(n, t)}{V^*(n)}} \quad (1)$$

where:

- $V(n, t)$ is the speed of the vehicle n at the time t;
- $V^*(n)$ is the desired speed of the vehicle *(n)* for the current position;
- $a(n)$ is the maximum acceleration for the vehicle *n*;
- T is the reaction time.

$$V_b(n, t + T) = d(n) \cdot T + \sqrt{d(n)^2 \cdot T^2 - d(n) \left[2 \cdot \{x(n-1, t) - s(n-1) - x(n, t)\} - V(n, t) \cdot T - \frac{V(n-1, t)^2}{d^2(n-1)}\right]} \quad (2)$$

where:

- $d(n)(< 0)$ is the maximum deceleration desired by vehicle n;
- $x(n, t)$ is the position of the vehicle n at time t;
- $x(n - 1, t)$ is the position of the preceding vehicles (n-1) at the time t;
- $s(n - 1)$ is the effective length of the vehicle (n-1);
- $d^2(n - 1)$ is an estimation of the vehicle (n-1) desired speed.

The acceleration component represents the propensity of a vehicle to achieve a certain desired speed, i.e. the speed in free flow conditions in the time interval (t,

131

t+T); the deceleration component, on the other hand, reproduces the limitations imposed by the leader vehicle in an attempt to reach the desired speed; the last one represents the maximum speed that the vehicle n can reach in the time interval (t, t+T) due to the presence of the leading vehicle, indicated by (n-1).

Considering the two components of vehicle speeds above, the vehicle speed (n) and its position at the time (t, t+T), can be calculated as follows:

$$V(n, t + T) = min \ \{V_a(n, t + T), V_b(n, t + T)\} \qquad (3)$$

$$x(n, t + T) = x(n, t) + V(n, t + T) \cdot T \qquad (4)$$

In order to simulate traffic flows as close as possible to real ones, a modification to the classic Gipps's model was implemented in the AIMSUN software: namely, the so-called "Sensitivity Factor" was introduced. Thus, the leader's deceleration can be calculated with the following formula in which the parameter α, defined for the vehicle type, represent the above sensitivity factor:

$$d'(n - 1) = d(n - 1) * \alpha \qquad (5)$$

The sensitivity factor can assume a higher or lower value than the unit. In the first case, the vehicle underestimates the deceleration of the leader, and thus the following vehicle becomes more aggressive, decreasing the distance from the leader. In the second case, the vehicle overestimates the deceleration of the leader and thus moves away from the vehicle that precedes it.
The minimum headway between leader and follower can also be calculated as a restriction of the deceleration component.
This Minimum Headway constraint is defined as:

$$If \ x(n - 1, t + T) - [x(n, t) + V(n, t + T)T] < V(n, t + T) \cdot MinHW(n) \qquad (6)$$

$$then \ \ V(n, t + T) = (x(n - 1, t + T) - x(n, t))/(MinHW(n) + T) \qquad (7)$$

where:

- $x(n,t)$ is the position of vehicle *n* at time *t*;
- $x(n-1,t)$ is the position of preceding vehicle *(n-1)* at time *t*;
- *MinHW(n)* is the minimum headway of vehicle *(n)* respect to its follower.

In the car-following model, the leader vehicle, not having any interference with other vehicles, could reach his/her maximum desired speed. The maximum desired speed is calculated using three parameters: two are related to the vehicle and one to the section as follows:

1. Maximum desired speed of the vehicle i: $V_{max}(i)$;
2. Speed acceptance of the vehicle i: $\theta(i)$;
3. Speed limit of the section or turning s: $S_{limit}(s)$.

In this regard, it is to be remembered that speed acceptance in a section can assume values:

- equal to zero, meaning that a driver travelling in the road network reaches the speed limit in a section;
- ≥1 means that the vehicle will achieve a maximum speed greater than the speed limit;
- ≤ 1 means that the vehicle will travel with a speed lower than the limit one.

In order to calculate the maximum desire speed, the speed limit of vehicle *i*, travelling on section *s*, must to be calculated with the following expression:

$$S_{limit}(i,s) = \theta(i) \cdot S_{limit}(s) \qquad (8)$$

Then the maximum desired speed of vehicle *i* on a section *s* is calculated as follows:

$$V_{max}(i,s) = \min\ [S_{limit}(i,s); V_{max}(i)\ ] \qquad (9)$$

Thus, as one can observe from equations written above, the maximum desired speed is calculated as the minimum value between the speed limit, $S_{limit}(i,s)$, which represents the limit of the maximum speed for a vehicle *i* on a section, and the value of the maximum desired speed $V_{max}(i)$ that can be reached by a vehicle i on a section.

The AIMSUN software makes it possible to consider not only a one-dimensional model, but also the "two lane car-following model." Indeed, Gipp's car-following model [6] was developed considering only interactions, along the same lane, between the leader vehicle and the follower vehicle. The car-following model implemented in AIMSUN software also considers the influence that a vehicle can receive from other vehicles travelling in adjacent lanes. In this regard, two different situations can be distinguished: the adjacent lane is an on-ramp one; the adjacent lane is any other type of lane. Thus, the software first calculates the number of vehicles travelling in the adjacent lane, downstream of the current vehicle (i.e. the one subject to that influence), within a certain distance defined as "Maximum Distance"; thus, for the vehicles falling in the maximum distance, it calculates the average speed, i.e. "Mean Speed Vehicles Down." In the Figure 1, one can better understand how the variables just described are calculated. One can define two additional parameters, Maximum Speed Difference and Maximum

Speed Difference On-Ramp that represent the maximum speed difference (in km/h) between one lane and the adjacent lane and maximum speed difference (in km/h) between the main lane and an on-ramp lane in the two-lane car-following model, respectively.
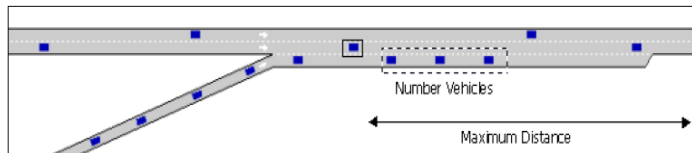

Figure 1 AIMSUN Two lane car-following model [1]

3.1. Lane change model

"Lane change" models are mainly used to model vehicle flows in two-lane roads, where there is a need for drivers to outmatch a slower vehicle and reach their desired speed; or when, for example, there is a need to change the lane to follow a certain path. Lane changing is modelled as a decision process; indeed, this manoeuvre is based on assessments by drivers about traffic conditions i.e. speed of vehicles, queue lengths and then gap between two successive vehicles driving in the desired lane (i.e. the lane into which one wants to move). Specifically, lane changing occurs only when the driver feels that this manoeuvre is really advantageous and safe. In the logic of the lane-change models implemented in AIMSUN, this is equivalent to answering three specific questions. The first one: is it necessary to change lanes? To answer this question, the traffic conditions of lanes are measured in terms of speed and queue lengths. If the answer to this question is affirmative, to successfully change lanes, it is necessary to answer two other questions: is there a benefit to changing lane? and is it possible to change lanes safely? In the first case, it will be assessed whether, by changing lanes, there will be an improvement in traffic conditions, i.e. the driver intending to change lanes will evaluate whether the speed in the adjacent lane is higher than that of his/her own lane, or if the number of vehicles queued in the desired lane is small enough to consider the lane changing manoeuvre advantageous. In the second case, he/she will verify if there is a large enough gap between two subsequent vehicles travelling in the lane one wants to enter, such as to make sure the lane change manoeuvre is safe.

In order to better understand driver's behaviour in the lane-changing decision process, three different zones are considered (see Figure 2):

- Zone 1: In this zone the necessity of lane changing is not yet taken into account. At this time several parameters such as position and speed of the vehicles in the current and adjacent lanes are considered in order to

evaluate a possible improvement that the driver will get from changing lanes.

- Zone 2: in this area, the decision to change lanes has not yet been taken. Vehicles look for a gap between vehicles in adjacent lanes, but at this time their driving behaviour does not affect that of other vehicles.
- Zone 3: lane changing happens in this zone; vehicles driving in the adjacent lane are influenced by vehicles wishing to change lanes, because they may also slow down, in order to provide a big enough gap for the vehicle entering the flow.
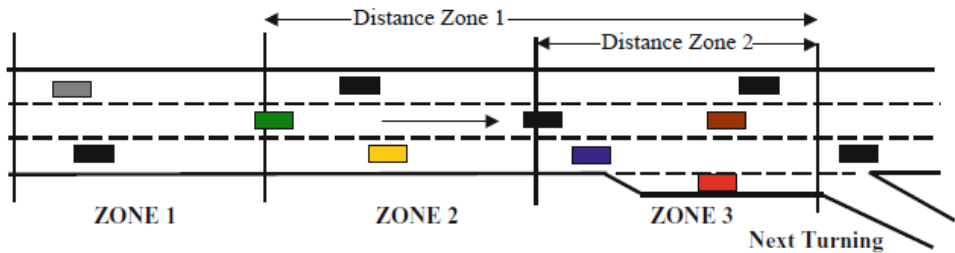

Figure 2 Lane change zone [1]

Finally, the zone is modelled depending on type of entity (central lane, off-ramp lane, junction, on-ramp, etc) in which the manoeuvre is carried out.

Figure 3 explains better how the lane change model works.
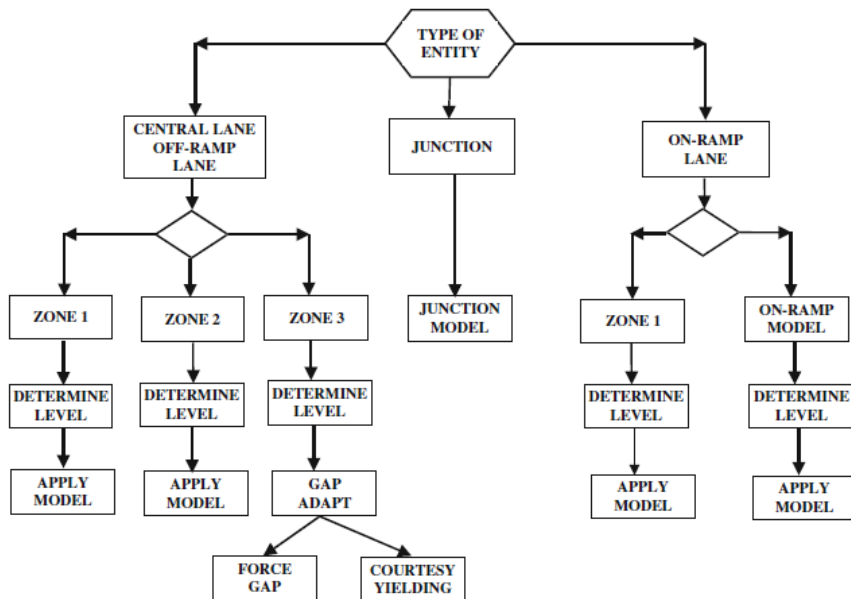
Figure 3 - lane changing logic model [1]

135

3.2. Microscopic Gap-Acceptance Model

The gap acceptance model implemented by AIMSUN applies the gap acceptance theory, discussed in the previous chapters, essentially at intersections. This model, in fact, according to the rank of priority, simulates give-way behaviour by users at any intersections. For each couple of vehicles entering the intersection and approaching the intersection area with different ranks of priority, the software calculates the relative speed, position and acceleration rate, and then determines the time needed by the vehicles with a lower priority to cross the intersection safely. Among the main parameters of the models one can remember the "Give-way time", defined as the maximum time which a vehicle approaching the intersection is willing to wait in order to comply with the priority rules, before it becomes "aggressive" and reduces the acceptance safety margins. Other parameters taken into account by microscopic gap-acceptance models are: Maximum Gap, Minimum Gap, Gap Reduction Factors, and Visibility Distances at the intersection, and so on.

In order to determine if a vehicle with a lower priority can or cannot cross an intersection, the following algorithm, is applied by the model [1]. If a vehicle VEHY reaches a junction where it must give priority (see Figure 4):

a) determine the closest higher priority vehicle (VEHP);
b) determine the Theoretical Collision Point (TCP);
c) calculate the time (TP1) needed by VEHY to reach TCP;
d) calculate the estimated time (ETP1) needed by VEHP to reach TCP;
e) calculate the time (TP2) needed by VEHY to cross TCP;
f) calculate the estimated time (ETP2) needed by VEHP to clear the junction;
g) If TP2 is less than ETP1, vehicle VEHY has enough time to cross; therefore, it will accelerate and cross;
h) Else, if ETP2 is less than TP1, vehicle VEHP will have already crossed TCP when VEHY reaches it, then search for the next closest vehicle with a higher priority, which becomes VEHP, and go to step 2;
i) Else, vehicle VEHY must give way, decelerating and stopping if necessary.

Figure 4 Give Way Gap Acceptance Model by AIMSUN software [1]

Note that the algorithm only considers vehicles with a higher priority within 100 m of the intersection.

4. Modelling single-lane and double-lane roundabouts in AIMSUN

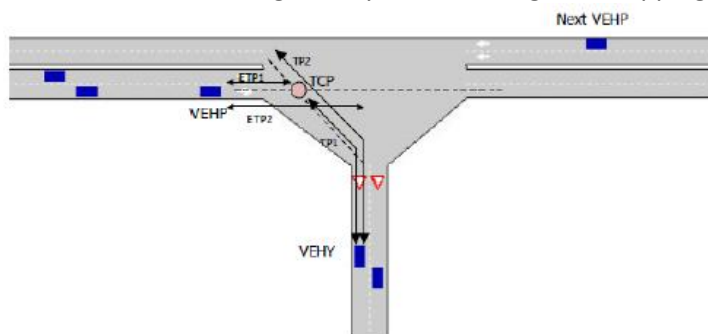Nowadays traffic simulation is increasingly used to assess the operational conditions of any intersection scheme existing or being designed. However, a great number of parameters, that any traffic simulation software makes it possible to use, should be considered in order to create a model that is adherent to reality. On the other hand, in order to obtain reliable results, it is necessary to know the meaning of each parameter and how each parameter acts on the model and affects the results of the simulation. In fact, the quality of the model is highly dependent on the availability and accuracy of the input data. And not least, the values that these parameters can assume are not absolute, but of course depend on the model to be built. As previously mentioned, these model parameters do not only refer to the traffic rules or the geometric design of the intersections or road network, but are also inherent to the type of model chosen for simulation, user behaviour and so on. For these reasons, when one uses microscopic simulation as a technique for evaluating traffic condition at a whole road network, but specially at a lower level (nodes or intersections), the sensitivity analysis and calibration of the model parameters is a key step.

Based on the objectives of the research, the following sections will describe step by step the modelling and then calibration process for the two roundabouts built in AIMSUN.

4.1. A preliminary consideration

As introduced in Chapter 1, the principles of roundabout design suggest that roundabout treatments for at-grade intersections simplify conflicts, reduce vehicle speeds and provide a clearer indication of the driver's right of way than other treatments for at-grade intersections. However, geometric design and operations at double-lane roundabouts are more complex than single-lane roundabouts [7]. Single-lane roundabouts have one circulatory lane and a single-lane entry at all legs, while double-lane roundabouts have double-lane entries and exits; two vehicles travelling side-by-side can be accommodated within the circulatory roadway. To maximize the level of efficiency and safety during the early years of traffic operations, a single-lane roundabout may be the interim configuration, initially built to serve the near-term traffic volumes. Expansion from a single-lane roundabout to a double-lane roundabout can be driven by needs of higher capacity and improved traffic performances especially for urban roads and arterials [7]. Since so many conditions may (or may not) preclude installing a roundabout and so many factors have to be considered, it is not easy to specify

whether a site could or could not be appropriate for a specified roundabout treatment.

As introduced above, in this study two roundabout layouts were selected: a single-lane roundabout and a double-lane roundabout. It is noteworthy that no roundabout treatment with a modern design was installed in our City when this study was carried out. However, different signalized and unsignalized at-grade intersections in operation had been identified in the urban road network. Due to comparable size, some of them were likely to be converted into the single-lane roundabout or the double-lane roundabout chosen for calibration purposes. By way of example, Figure 5 exhibits an isolated signalized intersection, installed (at the intersection of S. Lorenzo Street and G. Spadolini Street) along a corridor in the in the Palermo City road network, Italy, where other roundabouts are currently in operation. Traffic data required for the model were collected from 7:30 to 8:30 am and 5:30 to 6:30 pm on weekdays last winter. On field observations revealed that these periods were the rush hours of the intersection; heterogeneous traffic was observed with a percentage of heavy vehicles never more than 30%. In Figure 6 the truck percentage versus time throughout a study period (7:30 to 8:30 am) is given as an example.

Based on the above, the following sections describe step-by-step the modelling and calibration process of the single-lane roundabout and the double-lane roundabout built in AIMSUN.

Figure 5 - Map of the case study from Google.
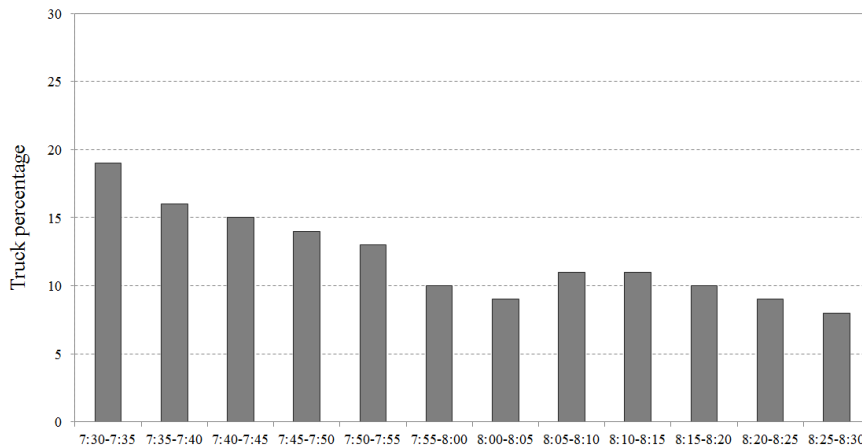
Figure 6 Truck percentage vs. time throughout a study period given as an example.

4.2. The single-lane roundabout case study

4.2.1. Single-lane roundabout geometric configuration

Single-lane roundabouts are distinguished from mini-roundabouts by their larger outer diameters (alias the inscribed circle diameters) and non-traversable central islands; their geometric design typically includes raised splitter islands, crosswalks (such that pedestrians cross one lane of traffic at a time), and a truck apron (which is part of the central island). Speeds at the entry, on the circulatory roadway, and at the exit are a little higher than on mini-roundabouts [7].

For the first case study, the choice of the scheme fell on this type of roundabout, since single-lane, four-leg roundabouts are designed for low-speed operations and they represent one of the safest treatments for at-grade intersections. Moreover, operational analysis at single-lane roundabouts is relatively simple, since drivers have no lane use decisions to make; in turn, driver decisions are more complex at multi-lane sites, where drivers have to perform proper lane selection before entering the intersection. Figure 7 exhibits the sketch of the at-grade single-roundabout having one circulatory lane and a single-lane entry at all legs, features of which comply with the instructions by the Italian standards on geometric design of compact roundabouts; see [9].
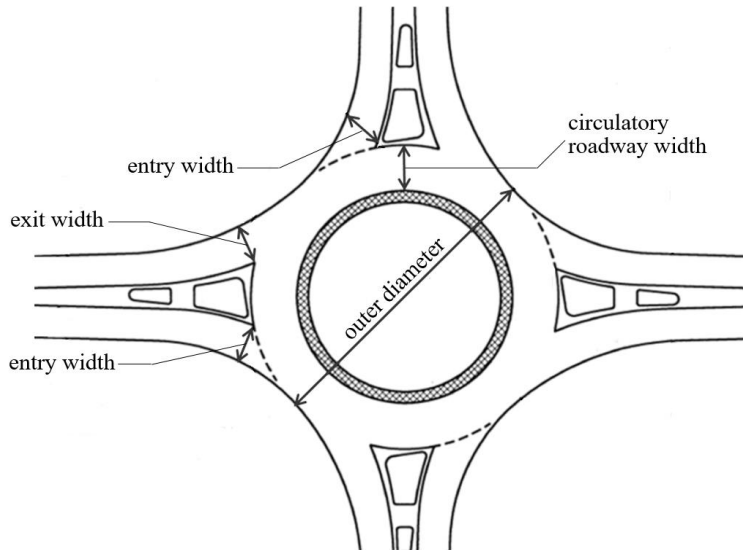
Figure 7 Single lane roundabout sketch

Based on the definitions of the geometric design elements proposed by international guidelines and manuals on modern roundabouts, the geometric design of the roundabout that was selected included:

a) the outer diameter (that is the basic parameter used to define the size of a roundabout and measured between the outer edges of the circulatory roadway) of 39.0 m;

b) the circulatory roadway width (or the roadway width for vehicle circulation around the central island which is measured between the outer edge of the circulatory roadway and the central island) of 7.0 m (without including the width of the mountable apron);

c) the entry width (where the entry meets the inscribed circle) of 3.75 m; it can be measured perpendicularly from the right edge of the entry to the intersection point of the left edge line and the inscribed circle;

d) the exit width (where the exit meets the inscribed circle) of 4.50 m, which can be measured perpendicularly from the right edge of the exit to the intersection point of the left edge line and the inscribed circle;

e) the length of legs reaching the roundabout of 35 m without parking possibilities for vehicles from 20 m up to the approach zones.

4.2.2. Single lane roundabout AIMSUN modeling

The microscopic simulation package AIMSUN (version 8.1) was used for microscopic modelling of the single-lane roundabout.

The roundabout model building in AIMSUN consisted of developing the link-node diagram, coding links and nodes, creating the link geometries, assigning traffic demand data, and then choosing the model parameters.

Generally, the intersection layout is built in AIMSUN using sections (one-way links) connected to each other through nodes (intersections), which may contain different traffic features. In the specific case of roundabouts, AIMSUN is able to build such intersections with a specific "roundabout" tool. Each section is characterized by its width and length; for each of these it is possible to set the type of road (roundabout, arterials, street, freeway, etc) with maximum speed allowed. In this case, the geometric design drawn in AIMSUN is consistent with the single-lane roundabout layout described in the previous section. The legs of roundabout were connected to the circulatory roadway through nodes. AIMSUN distinguishes two types of nodes: junction and join. The main difference among the two nodes is that in a junction there is a space between the origin and destination sections and they are often used on arterials and streets; while in the join node there is no space between these two sections and they are generally used on roads and highways, and the number of origin lanes equals the number of destination lanes.

Figure 8 shows the single-lane roundabout model built in AIMSUN, where, as for all modern roundabouts, no priority was created for the legs approaching the roundabout, but priority to vehicles moving anticlockwise on the ring was established. AIMSUN provides output data through detectors that can be positioned at any point in a section. Indeed detectors, during simulation, record vehicle counts, presence, speed, occupancy, density, headways etc., and they return such data either in tabular form or with graphs that depict the variation of the said values during the entire duration of the simulation. Detectors were located so that they could replicate the possible location of field detectors, that is at each entry/exit and upstream/downstream of each entry.

As mentioned above, traffic operations at roundabouts are typically ruled by the gap acceptance process, which specifically for single-lane sites is also facilitated by speeds moderated by the particular geometric design. The driver approaching a roundabout must give way to vehicles on the circulating roadway, and once they have stopped at a yield lane they must look for and accept gaps as they appear and then enter the roundabout. In order to reproduce priority to circulating vehicles the yield-at-entry rules were assigned at each entry.

Indeed, in the AIMSUN software, through the editing node folder, it is possible to assign priority rules or a stop signal to any movement.
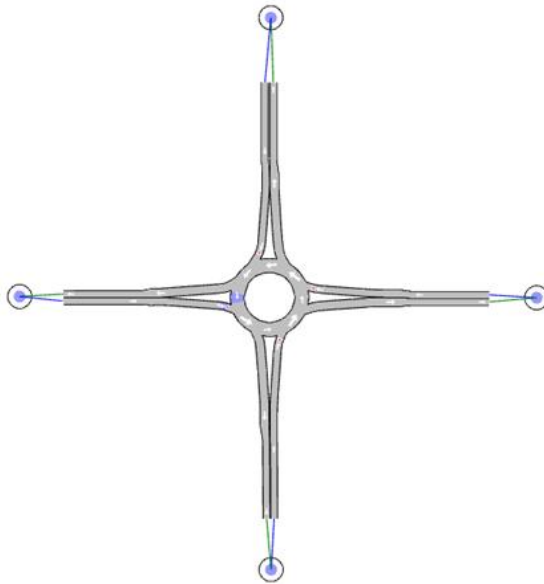
Figure 8 The single-lane roundabout model in AIMSUN

As far as the traffic demand, in AIMSUN is possible to insert these data in the form of either (time-dependent) O/D matrices based on routes or paths, or traffic states, based on input traffic flows and turning percentages; this latter is valid only in the microscopic model. O/D matrices were used with due consideration for the direction of turn; thus, the positioning of the centroids was indispensable and they were located appropriately upstream of each leg of the roundabout. In order to reproduce the traffic demand and represent realistic traffic conditions on the roundabout, O/D matrices were assigned by reproducing the circulating flow Q_c, from 0 veh/h to 1400 veh/h with a step of about 200 veh/h and a high and fixed values for entry flows were imposed at each entry in such a way as to guaranteed saturation conditions. In this regard, several simulations were carried out to find the maximum flow rate that would ensure reaching the capacity at each entry. The entire simulation runs for eight hours with a simulation step of 15 minutes; therefore, these matrices guaranteed saturation conditions at entries, so that the number of vehicles entering the roundabout was the capacity for the specific entry considered each time.

4.2.3. Calibration of the single lane roundabout model

Considering that every traffic simulator (like AIMSUN) has a lot of parameters inside the model and they must be calibrated so as to reproduce the real phenomena, the calibration parameters were preliminarily identified using a sensitivity analysis.

Indeed, outputs from trial simulation runs are usually not good enough to represent the traffic conditions of the system of streets and roads around the

intersection area (or where the selected layout of single-lane roundabout could be installed) when the default values for the model parameters of AIMSUN are used. Calibration of a traffic micro-simulation model, indeed, requires that some model parameters are changed and adjusted in an iterative way until model outputs are close to empirical data, based on a predefined level of agreement between the two data sets.

Thus, before applying the optimization procedure that automated the calibration process:

- variables with low influence on entry capacity were excluded;
- for the particular model, the influence of some important parameters on the entry capacity was established;
- a manual calibration was performed running the simulation many times and iteratively adjusting the model parameters that were taken into account for the single-lane roundabout built in AIMSUN.

Specifically, the following activities were performed:

- one-parameter sensitivity analysis; for this purpose, the reaction time [s], minimum headway [s], the max acceleration [m/s^2] and speed acceptance were singly tested using different parameter values;
- two-parameter manual calibration; for this purpose, pairs of two parameters (i.e. reaction time [s] and minimum headway [s]; reaction time [s] and speed acceptance) were tested, together with their combinations of values;
- three-parameter manual calibration; a set of three parameters was considered (i.e. reaction time [s], minimum headway [s] and speed acceptance) were tested, together with their combinations of values.

A set of three parameters was identified (see Table 2). More specifically the driver's reaction time or more easily the reaction time, as used in the car-following model of AIMSUN, is the time in seconds that it takes a driver to react to the speed changes in the preceding vehicle. The reaction time assigned to a vehicle, moreover, is a global parameter of AIMSUN, which means during each trip it is constant. In each simulation run, the parameter was set as fixed and equal to the simulation step, that is the same value for all vehicles. Moreover, the reaction time may influence the computing performance and some simulation outputs, such as the section capacities: in general, the lower the reaction time is, the higher capacity values can be obtained. The reason for this is that if drivers are more skilful they have shorter reaction times; they can drive closer to the preceding vehicles, they can find gaps more easily, they have more opportunities to enter the network, and so on. The minimum headway is primarily a lane-changing model parameter; setting this parameter ensures the minimum headway

(minimum time in seconds) between the leader and the follower. The AIMSUN traffic simulation model includes the minimum headway between leader and follower as a restriction of the deceleration component in the car following model and applies this constraint before updating the position and the speed of the vehicle (i.e. the leader) with respect to its follower.

At last, the speed acceptance ($S_{acc} \geq 0$) represents the level of goodness of the drivers or the degree of acceptance of speed limits:

- $S_{acc} \geq 1$ means that the vehicle will take, as maximum speed for a section, a value greater than the speed limit;
- $S_{acc} \leq 1$ means that the vehicle will use a lower speed limit.

In the AIMSUN car-following model speed acceptance, together with other parameters such as the target speed and the section speed limit, helps to define the desired speed for each vehicle on each section. The Speed acceptance may, moreover, influence the behaviour of the gap-acceptance model; several vehicle parameters (i.e. speed acceptance, turning speed, desired speed and so on), influencing all vehicles of a particular type when driving anywhere in the network, also have an influence on the output of the model.

Sensitivity analysis was conducted comparing, from time to time, the simulation outputs with the parameters manually adjusted and the values of empirical capacity computed by applying the Hagring model [4] in which the meta-analytical estimation of the critical and the follow-up headways was introduced. In this regard, Table 1 shows synthetically the meta-analytic estimates of critical and follow-up headways used to implement the Hagring capacity model; see equation 10.

Table 1 Meta-analytic estimates for gap acceptance parameters and Hagring's capacity formulae for single-lane roundabout

Statistics	Headway [s]		Hagring capacity formula [veh/h]	
	Critical	Follow up		
random estimate (s.e.)	4.27 (0.11)	3.10 (0.07)	$C_e = Q_{c,e} \cdot \left(1 - \frac{\Delta \cdot Q_{c,e}}{3600}\right) \cdot \frac{\exp\left(\frac{-Q_{c,e}}{3600}(T_c - \Delta)\right)}{1 - \exp\left(\frac{-Q_{c,e}}{3600} T_f\right)}$	(10)

The GEH index was used as a criterion for acceptance (or otherwise rejection) of the model, i.e. its ability or otherwise to reproduce the empirical capacities (see Table 1). This index is a global indicator widely used in practice for validating traffic micro-simulation models, especially when only aggregated values are available as flow counts at detection stations aggregated to the hour and entry capacity values [8].

The GEH statistic calculates the index for each counting station *i* as follows:

$$GEH_i = \sqrt{\frac{2(x_i - y_i)^2}{(x_i + y_i)}} \qquad (11)$$

where x_i is the ith simulated capacity and y_i is the ith empirical capacity. Based on this criterion the model is accepted if the deviation of the simulated values with respect to the measurement is smaller than 5 in (at least) 85% of the cases. Note that the maximum acceleration that a vehicle can achieve under any circumstances was excluded from manual calibration (see Table 2). This parameter is required by the car-following model and usually influences speed, travel time, queue discharge, lane changing, etc. However, significant benefits in GEH values were not found when the maximum acceleration was combined with other parameters.

Table 2 Results of the sensitivity analyses and manual calibration.

AIMSUN parameter	Default		Levels											
	Value	GEH	Value	GEH	Value	GEH	Value	GEH	Value	GEH	Value	GEH	Value	GEH
One-parameter sensitivity analysis														
Reaction Time [s]	0.80	56.25	0.85	68.75	0.90	75.00	1.00	78.13						
Min. headway [s]	0.00	56.25	1.00	50.00	1.50	59.38	2.0	62.50						
Max acc. [m/s^2]	3.00	56.25	2.6	46.88	2.80	43.75	3.40	37.50						
Speed acceptance	1.10	56.25	0.90	84.34	1.00	75.00	1.20	41.00						
Two-parameters sensitivity analysis														
Reaction Time [s]			0.85	68.75	0.85	62.50	0.90	75.00	0.90	65.63	1.00	75.00	1.00	71.88
Min. headway [s]			1.50		2.00		1.50		2.00		1.50		2.00	
Reaction Time [s]			0.85	81.25	0.85	87.50	0.90	87.50	0.90	84.38	1.00	84.38	1.00	75.00
Speed acceptance			0.90		1.00		0.90		1.00		1.00		0.90	
Three-parameters sensitivity analysis														
Reaction Time [s]			0.85		0.90		0.90		1.00		1.00			
Min. headway [s]			1.50	87.50	1.50	81.25	1.50	81.25	1.50	81.25	2.00	75.00		
Speed acceptance			1.00		0.90		1.00		1.00		1.00			

Note: the set of three parameters [reaction time = 1.50 s; min headway = 1.50 s; speed acceptance = 1.00] was also explored and returned a GEH > 85 %. However, for 0 ≤ Qc < 200 veh/h, it was obtained higher GEH i than those produced with the set of three parameters [reaction time = 0.85 s; min headway = 1.60 s; speed acceptance = 1.00] selected for the application of the GA-based procedure.

Figure 9 shows the plot of simulated capacities with the default and manually calibrated parameters Vs empirical capacities. Note that the simulated capacities were obtained using initially the AIMSUN default parameters (named in this figure "AIMSUN default parameters") and then inserting into AIMSUN the parameters derived from manual calibration as reported in Table 2 (named the "AIMSUN manually calibrated parameters"). As mentioned above, the empirical capacities were computed applying the Hagring model with the meta-analytical estimation of the critical and the follow-up headways.
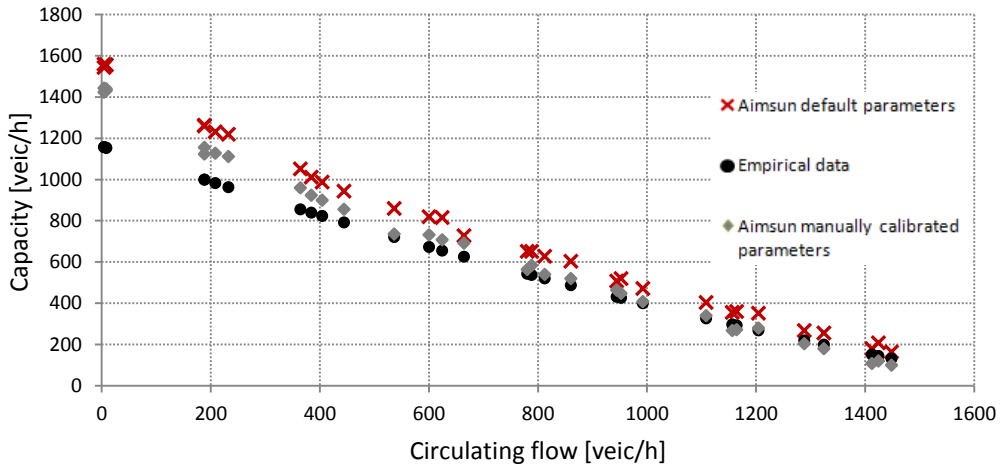
Figure 9 Entry capacity: Empirical capacities Vs. AIMSUN simulation

4.3. The double-lane roundabout case study

4.3.1. Double-lane roundabout geometric configuration

The double-lane roundabout selected as the second study was designed with an outer diameter of 41 m, measured between the outer edges of the circulatory roadway; it was expected to be an appropriate design solution to keep circulating speeds adequate to accommodate mixed fleets of passenger cars and heavy vehicles also in urban area. The other geometric design elements of the double-lane roundabout selected as case study included: the circulatory roadway width for vehicle circulation around the central island of 9.0 m, measured between the outer edge of the circulatory roadway and the central island; the width of the double-lane entry (where each entry meets the outer diameter) and the width of the double-lane exit (where each exit meets the outer diameter) of 6.0 m; the length of legs of 35 m without parking from 25.0 m to the approaches. Crosswalks and splitter islands were present at each entry and exit, whereas the distance of crosswalks from the yield line of 6 m is hypothesized to accommodate one passenger car. Figure 10 shows an example sketch of double-lane roundabout.
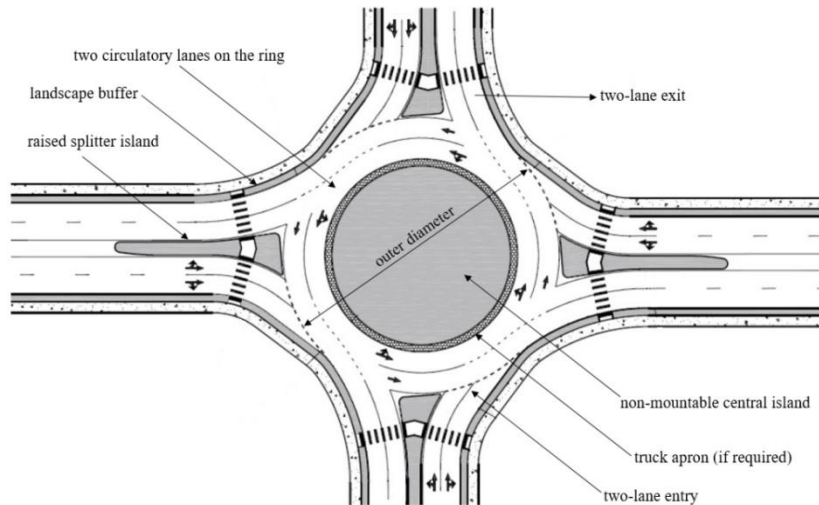
Figure 10 The example sketch of the double-lane roundabout.

However, Italian standards on geometric design of modern roundabouts published in 2006 [9] include exit always arranged on a single lane; despite double-lane roundabouts are widespread around the world, this explains the failure to introduce typical double-lane roundabouts in the Italian territory, and the need of gap acceptance parameters appropriate for the purpose of this study.

4.3.2. Double-lane roundabout AIMSUN modeling

The calibration process that was applied at the double-lane roundabout is almost the same as the single-lane roundabout study case.

Again, traffic conditions on the roundabout were reproduced in the AIMSUN micro-simulation model (version 8.1.3) using the default parameters. Vehicle traffic flows were assigned from all entries; the eastbound approach was assumed to be the subject entry for observing each entry lane capacity. Thus, O/D matrices were assigned on the roundabout built in AIMSUN with due consideration to the direction of turn, in such a way as to reproduce a circulating flow (facing the subject entry) from 0 veh/h to 1400 veh/h, with a step of 200 veh/h. A saturated condition was reached at each entry lane; the corresponding maximum number of vehicles approaching the roundabout gave the entry lane capacity.

The double-lane roundabout model layout built in AIMSUN is shown in Figure 11, where priority was given to traffic approaching from the left; priority rules were established to model the right of way and reduce the opportunities for collisions among turning vehicles.
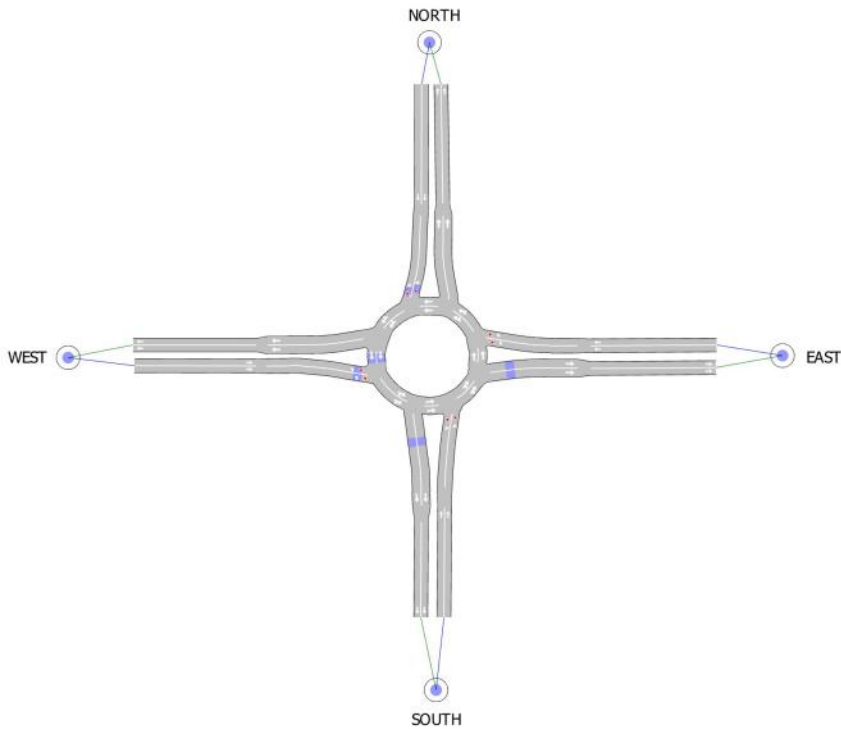
Figure 11 The AIMSUN model of the double-lane roundabout.

1.1.1. Calibration of the double lane roundabout model

A sensitive analysis of the AIMSUN parameters was conducted also in this case as for the single-lane roundabout; it was the preliminary activity to exclude the parameters without any influence on entry lane capacity and, in turn, identify those that may best reproduce empirical capacities. Thus, the simulation outputs were recalculated under different alternative assumptions in order to determine the impact of the explored variables on the capacity of entry lanes. A manual calibration was then performed by running AIMSUN many times and iteratively adjusting the model parameters that were identified until the model outputs tended to stay close to the empirical capacities.

The general formula proposed by Hagring [4] was used to calculate entry capacity also in this case. According to the schemes of conflict at entries, two critical headways were attributed to the left entry lane opposed by two circulating streams, while one value of critical headway was considered for the right entry lane faced by one antagonist traffic stream in the outer lane of the ring. A meta-analytic estimation of the gap acceptance parameters was used to calculate the capacity functions according to the results reported in chapter two.

Specifically, the left lane capacity was calculated using equation 12 in Table 3 as a function of the inner Q_{ci} and the outer Q_{ce} circulating flows, whereas the right lane capacity was calculated using equation 13 in Table 3 as a function of the

circulating traffic flow Q_{ce} in the outer lane of the ring; according to literature, a minimum arrival headway Δ of 2.10 s was used.

Table 3 Meta-analytic estimates for gap acceptance parameters and Hagring's capacity formulae

Statistics	Headway [s]			Hagring capacity formula [veh/h]	
	Critical gap		Follo w up		
	Tci	Tce	Tf		
left entry lane					
random estimate (s.e.)	4.16 (0.13)	3.82 (0.13)	2.85 (0.10)	$C_e = (Q_{c,e} + Q_{c,i}) \cdot \left(1 - \frac{\Delta \cdot Q_{c,e}}{3600}\right) \cdot \left(1 - \frac{\Delta \cdot Q_{c,i}}{3600}\right) \cdot \dfrac{\exp\left(\frac{-Q_{c,e}}{3600} \cdot (T_{c,e} - \Delta) \frac{-Q_{c,i}}{3600} \cdot (T_{c,i} - \Delta)\right)}{1 - \exp\left(\frac{-(Q_{c,e} + Q_{c,i})}{3600} \cdot T_f\right)}$	(12)
right entry lane					
random estimate (s.e.)	-	3.82 (0.13)	2.72 (0.08)	$C_e = Q_{c,e} \cdot \left(1 - \frac{\Delta \cdot Q_{c,e}}{3600}\right) \cdot \dfrac{\exp\left(\frac{-Q_{c,e}}{3600} \cdot (T_c - \Delta)\right)}{1 - \exp\left(\frac{-Q_{c,e}}{3600} \cdot T_f\right)}$	(13)

Accuracy in the calibration process means that the simulation model replicates as closely as possible the empirical data set, based on a specific level of agreement between the empirical data and simulation outputs.

In this study, first some model parameters were singly tested using different values and then two parameters or three parameters were tested every time together with their combinations of values. At last, the set of the calibration parameters of AIMSUN included the driver reaction time R_T, minimum gap G_{min} (that means the same as the minimum headway used before for the single-lane roundabout) and speed acceptance S_{acc}; note that the meaning of these terms has already been specified above.

However, vehicle parameters may influence the output of the model; for instance, in the car-following model of AIMSUN, speed acceptance, together with other parameters, may have an effect on the desired speed of the vehicles on a section and gap-acceptance behaviour.

Other model parameters were excluded from manual calibration because they did not provide further benefit to the process of manually adjusting the model parameters.

The results of the sensitivity analyses and manual calibration are shown in Table 4; also in this case one can see that a GEH index was used (see equation 11) to quantify the deviation of each simulated value with respect to the measurement for each entry lane.

In any case, the calibration described was not enough and the objective of finding the values of the parameters which will produce a valid model was pursued through formulation of the model's calibration process as an optimization problem (see next section).

Table 4 Results of the sensitivity analyses and manual calibration

AIMSUN parameter	default value	GEH* [%]	Levels											
			value	GEH	value	GEH	value	GEH	value	GEH	value	GEH	value	GEH
right entry lane														
one-parameter sensitivity analysis														
reaction time [s]	0.80	78.10	0.85	100	0.90	100	0.95	100	1.00	93.80	-	-	-	-
min gap [s]	0.00	78.10	1.00	78.10	1.5	81.30	2.00	90.60	-	-	-	-	-	-
max acc. [m/s²]	3.00	78.10	2.60	18.80	2.80	84.40	3.40	84.40	-	-	-	-	-	-
speed acceptance	1.10	78.10	0.90	93.80	1.00	90.60	1.30	65.60	-	-	-	-	-	-
two-parameters manual calibration														
reaction time [s]			0.85	100	0.85	100	0.85	96.90	0.95	100	0.95	100	0.95	96.90
min gap [s]			1.00		1.50		2.00		1.00		1.50		2.00	
reaction time [s]			0.85	100	0.85	100	0.95	96.90	0.95	93.80				
speed acceptance			0.90		1.00		0.90		1.00					
three-parameters manual calibration														
reaction time [s]			0.85	96.90	0.85	100	0.85	96.90	0.85	96.90	0.95	90.60	0.95	96.90
min gap [s]			1.00		1.00		1.50		1.50		1.00		1.50	
speed acceptance			0.90		1.00		0.90		1.00		0.90		0.90	
left entry lane														
one-parameter sensitivity analysis														
reaction time [s]	0.80	78.10	0.85	100	0.90	90.60	0.95	96.9	1.00	93.80	-	-	-	-
min gap [s]	0.00	78.10	1.00	78.10	1.50	81.30	2.00	81.30	-	-	-	-	-	-
max acc. [m/s²]	3.00	78.10	2.60	0.00	2.80	84.40	3.40	81.30	-	-	-	-	-	-
speed acceptance	1.10	78.10	0.90	87.50	1.00	87.50	1.30	40.60	-	-	-	-	-	-
two-parameters manual calibration														
reaction time [s]			0.85	81.30	0.85	84.40	0.85	100	0.95	100	0.95	96.90	0.95	96.90
min gap [s]			1.00		1.50		2.00		1.00		1.50		2.00	
reaction time [s]			0.85	90.60	0.85	87.50	0.95	96.90	0.95	96.90				
speed acceptance			0.90		1.00		0.90		1.00					
three-parameters manual calibration														
reaction time [s]			0.85	90.60	0.85	100	0.95	100	0.95	100	0.95	100	0.95	100
min gap [s]			1.50		2.00		1.00		1.00		1.50		1.50	
speed acceptance			0.90		0.90		0.90		1.00		0.90		1.00	

Thus, in the context of micro-simulation based modelling, in order to automate the iterative process of manually adjusting the model parameters, the calibration of the microscopic traffic simulation model was formulated both for the single-lane roundabout and the double-lane roundabout as an optimization problem

through a genetic algorithm; it searched for an optimum set of model parameters through an efficient search method. After a brief overview of genetic algorithm applications, the structure of the GA-based method will be described in next section.

5. Calibrating a microscopic traffic simulation model using genetic algorithms

5.1. A brief review of genetic algorithm applications

Genetic algorithms are search algorithms inspired by the principles of Darwinian evolution and form part of the broader class of evolutionary algorithms [66]. As it is known, evolutionary algorithms are population-based meta-heuristic optimization algorithms that make use of the bio-inspired mechanisms and the theory of species survival (known colloquially as "survival of the fittest") for tuning a set of solution in an iterative way [68]. In order to develop a robust search algorithm, the concept of the survival of the fittest is used in a structured (but randomized) information exchange. Genetic algorithms are usually applied in complex non-linear process controllers for the optimization of parameters. Optimization is, indeed, the process of modifying the inputs (or the characteristics of process) to obtain the minimum or maximum of the output. It is well-known that the input to the optimization process is represented by the cost function (or the objective function or the fitness function), while the output consists of the fitness function of the system. Very briefly, in a genetic algorithm an initial population of individuals is generated randomly; each individual obtains a (numerical) fitness value via a fitness function which is used to obtain multiple copies of higher-fitness individuals and delete lower-fitness individuals. Thus, several genetic operators (e.g. mutation and crossover) are applied probabilistically to population to give the next generation of individuals. Based on the selected method of generation (i.e. the synchronous or asynchronous method), the new generation replaces or overlaps the previous generation. The genetic algorithm can be considered successful when a population with highly fit individuals evolves as the result of iterating this procedure; thus, in the context of an optimization procedure, success is obtained when an optimum (or near optimum) of the given function is reached [69].

However, several issues, (i.e. deciding of population size, mutation rate, selection method for selecting good chromosomes, crossover rate to manage convergence problems, and so on), have already been widely discussed for the appropriate implementation of genetic algorithms to optimization problems. It should be noted that attention has to be put on the major tasks corresponding to the major phases (i.e. pre-processing, running optimization, post-processing) of the simulation-based optimization studies. By way of example, in the optimization phase, analysts must monitor convergence of the optimization and detect errors which may occur. On this regard, a convergent optimization process does not

necessarily mean the global minimum (or minima) has been found; indeed, genetic algorithms may suffer from the problem of premature convergence due to improper selection of some operators [68,71]. However, convergence behaviours of different optimization algorithms are not trivial and still represent a crucial research area of computational mathematics. In the last decade, due to the development of computer technology, advances in the use of genetic algorithms to solve optimization problems have allowed widespread diffusion of these optimization techniques into real world design challenges even in transportation engineering. Several studies have demonstrated, indeed, how the genetic algorithms could be adapted for use in computer aided design software mainly to serve as an analytical aid in adapting the objective function to the user's requirements. Among the applications for geometric design one can cite Ahmad Al-Hadad et al. [72] that have applied a genetic algorithm-based approach to generate highway alignments of different configurations by using station points along the centre line of the alignment; thus, they developed a two-dimensional highway alignment optimization model that encouraged further investigations for better solutions. In turn, Ahmad Al-Hadad & Mawdesley [73] proposed a genetic algorithm-based technique for optimizing a highway alignment in a three-dimensional space; they used station points to simultaneously configure both horizontal and vertical alignments rather than considering the alignments in two different design stages. However, also in this case more specific genetic operators still needed to be tested to generate more realistic alignments and include earthwork in optimization problems. Rubio Martín et al. [57] developed a heuristic procedure based on a real-code genetic algorithm for optimizing speed consistency in the geometric design of single-lane roundabouts with any number of intersection legs and any angle between legs. Moreover, further advances have already been made to develop integrated models that combine the capabilities of the GA and the GIS to optimize the highway alignments. Chan et al. [66] also demonstrated the applicability of genetic algorithms, as an optimization tool to resolve the road-maintenance problems at the network level. Fwa et al. [74] used the computer model named Pavenet which was formulated on the operating principles of genetic algorithms; they presented examples to explain how this program can be used to formulate a maintenance strategy to regulate the long-term maintenance demand.

The application of genetic algorithms for the solution of the problems inherent in the calibration of microscopic traffic simulation models is a fact even more recent. The integration of genetic algorithms with the traffic simulation software is, moreover, an open research field.

A brief overview of some studies that have used a genetic algorithm procedure to calibrate the parameters of a traffic simulation model and enhance the correlation between simulated and observed data, will be presented below.

In this regard it is worth mentioning Wonkyu et al. [75] that compared calibration methods based on the application of some optimization tools (among which the

genetic algorithms) for determining an optimal set of the parameter values of two microscopic traffic simulation models (i.e. AIMSUN and Paramics); they observed that genetic algorithms were faster than other algorithms to converge the optimal solution. Mathew & Radhakrishnan [76] developed a methodology for the calibration of a microsimulation model for highly heterogeneous traffic at signalized intersections and searched for the optimum values for the model parameters by minimizing the error between the field and simulated delay by using genetic algorithms. Other interesting results were obtained in the context of road safety studies. In order to investigate the relationship between field measured and simulated conflicts at signalized intersections, Essa & Sayed [77] used a genetic algorithm procedure to calibrate the parameters of the microsimulation model and enhance the correlation between the two-data set. Ghods & Saccomanno [78] calibrated, in turn, the model parameter values by applying a genetic algorithm to different car-following models for safety performance analysis by using vehicle trajectory data.

Despite several encouraging results already obtained from studies on the specific topic, it is noteworthy that commercial traffic simulation software, specially formulated on the operating principles of genetic algorithms are not yet available. Thus, engineers often need an analytical aid to develop their own codes and adapt the objective function to the specific requirements of the problems that are often encountered in professional practice. However, it is now possible to use software packages with specific optimization tools as for example MathWorks's® proposes. In this regard, based on a large set of traffic data collected from the A22 Freeway, Italy, Chiappone et al. [21] applied the genetic algorithm tool in MATLAB® to reach convergence of the outputs from AIMSUN microscopic simulator to the empirical data (that is to minimize the differences between the field measurements observed in the speed-density diagram and the simulator's outputs obtained for a selected freeway segment); the automatic interaction with AIMSUN software was achieved through an external Python script, so that the data transfer between the two programs could automatically happen.

5.2. Structure of the GA-based Method

First of all, one introduces the formal interpretation of the problem and, subsequently one describes the solution by applying genetic algorithms.

Let $\{u_k\}_{i=1...N}$ and $\{y_k\}_{i=1...N}$ be two input-output sequences of observed data acquired during suitable traffic measurements; they are the "experimental surveys". One wants to reproduce the same output sequence corresponding to the same input sequence by simulation. In order to obtain the simulated output, denoted with $\{\hat{y}_k\}_{i=1...N}$, the model has to be calibrated; this means to find values for the model parameters such that the simulated output $\{\hat{y}_k\}_{i=1...N}$, is as close as possible the observed output $\{y_k\}_{i=1...N}$ given the same input $\{u_k\}_{i=1...N}$.
The optimization problem is formulated as:

$$j(\beta) = \frac{1}{N}\sum_{i=1}^{q} w_i \left[\sum_{k=1}^{N} g\left(y_{i,k} - \hat{y}_{i,k}(u_k, \beta) \right) \right] \qquad (14)$$

where

- k = the discrete time instant;
- N = the number of measures (each one at each time instant);
- q = the number of outputs considered for the identification procedure;
- w_i = the weight associated with the error on the ith variable (the generic i^{th} variable will be specified for the problem under study in the next section);
- $g(\cdot)$ = either the square or the absolute-value function;
- $y_{i,k}$ = the experimental value of the ith variable at the instant k;
- $\hat{y}_{i,k}(u_k, \beta)$ = the corresponding simulated value that is a function of the input u and the parameter vector β.

In this application the "experimental surveys" consist of entry capacity values calculated by using the Hagring model [4] as a function of the meta-analytic estimation of the critical and the follow-up headways (see Chapter 2); this estimation was based on a systematic literature review on measurements of the two gap-acceptance parameters from real data at single-lane and double-lane roundabouts in operation worldwide. The estimated output was generated by means of AIMSUN software which ran with a fixed model corresponding to the model under study, and tuned with a suitable set of parameters. It is obvious that if the selected parameters are incorrect, then the estimated capacity values do not coincide with the experimental survey. For this reason, let us select the objective function (14) as follows:

$$J(\beta) = \frac{1}{N}\sum_{i=1}^{N} \left[\left(C_k - \hat{C}_k(\beta) \right)^2 \right] \qquad (15)$$

where N = 32, since it was considered observations distributed over eight hours, in each of them it was ran four simulations (one every fifteen minutes).

In the case of the AIMSUN traffic simulation model, the model behaviour depends on a wide variety of model parameters. In general, if one considers the model to be composed of entities, (i.e. vehicles, sections, intersections, and so on), each of them described by a set of attributes, (i.e. parameters of car following, lane change, gap acceptance, speed limits and speed acceptance, and so on), the model behaviour is determined by the numerical values of these parameters.
As part of the calibration process, one evaluates beforehand the calibration parameters by using a sensitivity analysis, or re-calculating the simulation outputs under different alternative assumptions to determine the impact of the explored variables on the entry capacity. Thus, the objective of finding the values of the parameters which were able to produce a valid model was pursued (see Tables 2 and 4).

The solution of the calibrating problem will be the parameter vector β^* that minimizes the objective function (see equation 15), that is to say:

$$\beta^* = \arg \min_\beta j(\beta) \tag{16}$$

Equation 16 can be solved iteratively. However, two further problems have to be solved. The first problem involves the initial condition to be chosen, whereas the second problem is represented by the stopping criteria. The problem of the initial condition should not be undervalued. It should be noted that most algorithms only search for local minima; when one faces multiple minima (non-convex problem), the algorithm usually converges only if the initial guess is already somewhat close to the final solution. However, this problem is avoided if genetic algorithms are used, since they are robust evolutionary optimization algorithms with respect to the initial condition. The second problem, instead, can be easily solved by selecting a maximum number of iterations. That is to say, the algorithm can be stopped when:

$$\left| \frac{j(\beta)_k - j(\beta)_{k-1}}{j(\beta)_{k-1}} \right| < \varepsilon \tag{17}$$

where ε = the error stop quantity; $j(\beta)_k$ and $j(\beta)_{k-1}$ = the values of $j(\beta)$ computed at the iterations k and $k-1$, respectively.
This stopping criterion means that the algorithm will be stopped when the objective function variation, between two consecutive instants, is less than a quantity ε, freely chosen.

The problem expressed in Equation 16 can be solved iteratively by implementing the genetic algorithm tool in MATLAB®.

This tool has been applied in order to minimize the differences between the two sets of capacities: the set of empirical capacities or the entry capacity values calculated using the Hagring model based on the meta-analytic estimation of the critical and follow-up headways - and the set of simulated capacities - or the entry capacities that were simulated setting the AIMSUN parameters based on the results derived from the three-parameter manual calibration (see Tables 2 and 4). The automatic interaction with AIMSUN was implemented through an external Python script.

Starting from a generic initial condition, the genetic algorithm generates a set of parameters β, and then the AIMSUN software runs with the parameters β. AIMSUN is attached to MATLAB® via a Python subroutine that allows the data transfer between the two programs. Thus, AIMSUN provides a set of estimated outputs (one for each β) and the algorithm computes the objective functions (see equation 15) associated with each β. Lastly, the algorithm selects the best parameter β and generates a new set of parameters β that is the new generation. The cycle goes on and on until the predefined stopping criterion is met.

A stopping criterion was chosen with a specified, fixed, maximum number of iterations (50 generations). The initial population that was used to seed the genetic algorithm was composed of 20 individuals, by using the default setting of AIMSUN as the first individual. Moreover, it was thought that a further increase in the population size would increase the structural bias of the GA.

With reference to the other GA parameters, the following options were used:

a) mutation function: constraint dependent;
b) crossover function: scattered;
c) selection function: stochastic uniform;
d) elite count: 2;
e) crossover fraction: 0.8.

Based on these assumptions, the computational time lasted for about four hours; an Intel(R) Core (TM) 2 Quad CPU Q9300 2.50 GHz and 8Gb of RAM were used. The algorithm was stopped after 50 iterations so that the value of the cost function in Eq. 15 could reach a steady-state and the algorithm could be stopped. Figure 12 shows the outline of GA calibration process.
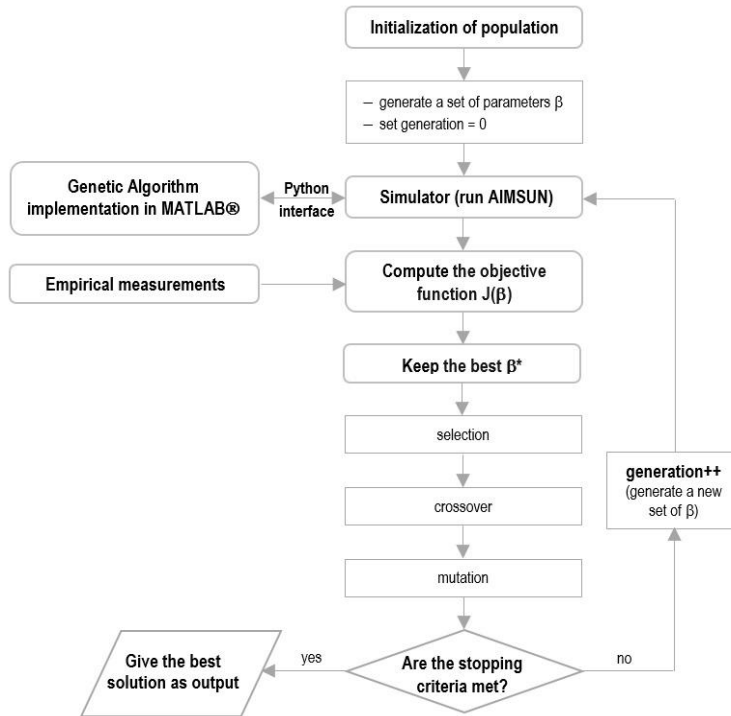
Figure 12 The GA calibration process

An upper bound β'' and a lower bound β' for β were introduced to restrict the search domain. Restrictive values were set for these bounds, since this choice was based on the outcome of the manual calibration. Thus, the condition β'≤β≤β'' was established to avoid generating parameters without physical meaning (i.e. negative reaction time, negative distance among vehicles, etc.). The best $β^*$ that is obtained by solving the optimization problem can only represent the best value of the model parameters such that the simulated values of capacity track as well as possible the empirical capacities. This gives an efficient automated calibration procedure for simulation with AIMSUN.

The optimization problem was solved by applying the algorithm illustrated before. In order to show the sequence of steps needed for the problem under examination, the pseudo code of the Python script is given in the following:

```
 1: procedure Python script file (pseudocode)
 2: inputFilePath ← path of the .txt file where MATLAB writes the values of
    reaction time, minimum gap and speed acceptance at each iteration.
 3: networkFilePath ← path of the Aimsun file where the network is modeled;
 4: outputFilePath ← path of the .txt file where Aimsun will write the
    results of the simulation carried out with the parameters' value given
    in inputFile;
 5: replicationID ← ID replication number indicated in the Aimsun file;
 6: detectorID ← ID detector number indicated in the Aimsun file;
 7: carID ← ID car number indicated in the Aimsun file;
 8: experimentID ← ID experiment number indicated in the Aimsun file;
 9: inFile ← open(inputFilePath,"reading")
    ▷ open the file inputFilePath in reading mode.
10: outFile ← open(outputFilePath,"writing")
    ▷ open the file outputFilePath in writing mode.
11: reactionTime ← takes the value from the file in inFile;
12: minGap ← takes the value from the file in inFile;
13: speedAcc ← takes the value from the file in inFile;
    ▷ In the following is shown the Pyton code which runs the Aimsun file
    of the network in consol mode, using the parameters of reaction time,
    minimum gap and speed acceptance indicated in inFile. It gives as
    output the values of capacity.
14: if console.open(networkFile) then
15:    plugin ← GKSystem.getSystem().getPlugin("GGetram")
16:    model ← GKSystem.getSystem().getActiveModel()
17:    simulator ← plugin.getCreateSimulator(model)
18:    experiment ← model.getCatalog().find(experimentID)
19:    simTime ← model.getColumn("GKExperiment::simStepAtt")
20:    experiment.setDataValue(simTime, reactionTime)
21:    carType ← model.getCatalog().find(carID)
22:    carType.setDataValueByID(GKVehicle.minimunGapMean, minGap)
23:    carType←model.getCatalog().find(carID)
24:    carType.setDataValueByID(GKVehicle.speedAcceptanceMean,speedAcc)
25:    if simulator.isBusy() == False then
26:     replication ← model.getCatalog().find(replicationID)
27:     if replication!= None and replication.isA("GKReplication")then
28:        simulator.addSimulationTask(GKSimulationTask(replication,
          GKReplication.eBatch))
29:        simulator.simulate()
30:        detector ← model.getCatalog().find(detectorID)
31:        counts ←model.getColumn("DYNAMIC::SRC_GKDetector_count_0")
32:        capacities←model.getColumn("DYNAMIC::SRC_GKDetector_flow0")
33:        ts1←detector.getDataValueTS(counts)
34:        ts2←detector.getDataValueTS(capacities)
35:        numValues←ts1.size()
36:        for j←0, numValues do
37:          outFile.write(j,ts1.getValue(GKTimeSerieIndex(j)),
          ts2.getValue(GKTimeSerieIndex(j)));
38:            j = j + 1;
39:         end for
40:      end if
41:    end if
42:  end if
43: outFile.close()                              ▷ close outFile.
44: inFile.close()                               ▷ close inFile.
45: end procedure
```

5.3. Application of a genetic algorithm for calibrating AIMSUN single-lane roundabout model and simulation results

With reference to the case study of single-lane roundabout described in section 4.2, the following parameters were selected for the GA-based optimization:

$$\beta = \left[R_T, H_{\min}, S_{acc} \right] \tag{18}$$

where R_T= reaction time; H_{min} = minimum headway; S_{acc}= speed acceptance (see previous section for the meaning of these parameters).

The upper bound β" and the lower bound β' of the calibration parameters were introduced to restrict the search domain; for the single-lane roundabout, these bounds were equal to β": [R_T = 0.86; H_{min} = 1.7; S_{acc} = 1.1] and β': [R_T = 0.82; H_{min} = 1.5; S_{acc}= 1.0], respectively. As above introduced, restrictive values were set for these bounds, since this choice was based on the outcome of the manual calibration. Thus, the condition β'≤β≤β" was established to avoid generating parameters without physical meaning; the best β* that is obtained by solving the optimization problem represented the best value of the AIMSUN parameters (i.e. the reaction time; the minimum headway; the speed acceptance) such that the simulated values of capacity track as well as possible the empirical capacities. This gave an efficient automated calibration procedure for simulation with AIMSUN.

The optimization problem was solved by applying the genetic algorithm illustrated above. According to the convergence condition, after 50 generations (approximately 4 h of computing time), the algorithm converged on the optimal solution. For the single-lane roundabout the best combination of the values for the simulation parameters included the following:

   − for the reaction time the value of 0.86 s instead of the default value of 0.80 s;
   − for the minimum headway the value of 1.58 s instead of the default value of 0 s;
   − for the speed acceptance the value of 1.0, instead of the default value of 1.1.

These values were different both from values obtained with the three-parameter manual calibration, and from the AIMSUN default values used to perform the one-parameter sensitivity analysis (see Table 2).
Figure 9 shows the series of simulated and empirical data of capacity:

   • the simulation outputs of entry capacity obtained with default AIMSUN parameters;

- the simulated capacity obtained with the GA-optimized parameters;
- the simulation outputs in term of capacity, obtained with the three-parameter manual calibration (see Table 2);
- the empirical capacities based on the meta-analytic estimation of the critical and follow-up headways (see Chapter 2).

Figure 13 shows that simulation outputs which were generated using the GA-optimized parameter set are very close to the simulation outputs which were obtained using AIMSUN with the manually calibrated parameters; nevertheless, the capacity curve from the GA-calibrated model better fits the empirical capacity data than the capacity curve obtained with the manually calibrated parameters (named "AIMSUN manually calibrated parameters"). In fact, the statistical GEH index (see equation 10) resulted:

- equal to 56.25% in the case when the comparison was made between empirical capacity data and simulation outputs obtained with the AIMSUN default parameters;
- equal to 87.5% in the case when the comparison was made using empirical capacity vs. AIMSUN simulation outputs obtained with the manually calibrated parameters;
- finally, GEH index was equal to 88 % by comparing the capacity simulated with the GA-optimized parameters and empirical capacity data.

It should be noted that the GEH index value was about the same in the latter two cases. However, the parameter set derived from GA-based optimization gave the lowest value for each single GEH_i; thus, based on the parameter set derived from GA-based optimization, the simulated curve of capacity gave the best fit to the empirical capacity data. Besides, since the deviation of each simulated value with respect to the measurement for each entry was smaller than 5 in 88% of the cases (however, smaller than 8 in the remaining cases), the model could be considered "calibrated" in terms of its ability to reproduce the empirical capacities at entries of the examined single-lane roundabout. Thus, the model was seen as significantly able to reproduce local conditions and traffic behaviour in a satisfactory way.
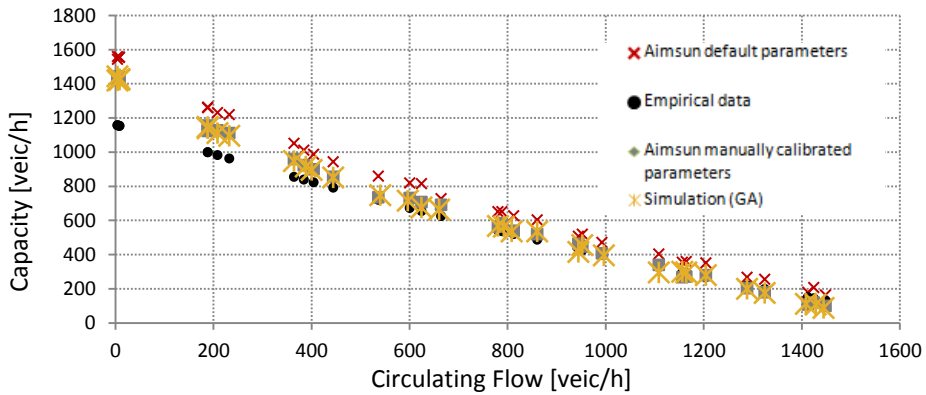
Figure 13 Comparison between different entry capacity

Figure 14 shows the values of the fitness function or the cost function J(β) in Eq. 15 during the optimization period, and the corresponding value of the same function computed using the default parameters. The cost function resulted equal to J(β)= 126.8 for the optimized parameters and equal to J(β)= 135 for the parameters derived from manual calibration ("AIMSUN manually calibrated parameters"). It should be highlighted that the benefit in tuning the model parameters would have been greater if one had used the default parameters of AIMSUN as the initial condition; indeed, the cost function resulted equal J(β) = 159.04 for the AIMSUN default parameters.

Figure 14 Values of the cost function *J(β)* during the optimization period.

The graph in Fig. 14 also plots the mean score of the population at every generation: the mean best fit is the mean value of the cost functions calculated for all individuals of the same generation; the best fit is, in turn, the cost function of the best individual within the generation. Because the GA finds the minimum of the fitness function, the best fitness value for a population is the smallest fitness value for any individual in the population. It is useful to note that t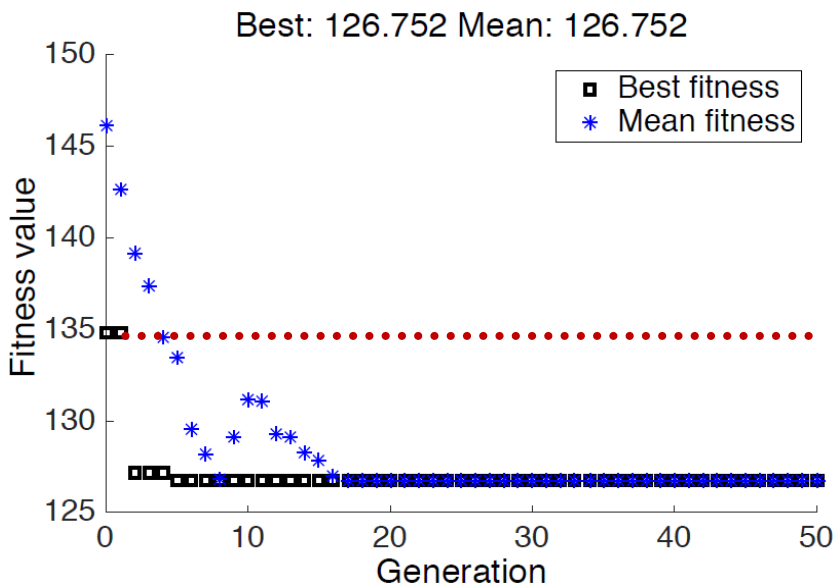he algorithm was not stopped when it reached the steady-state (iteration 20), but ran for 30 more iterations (totally 50 generations, approximately 4 hours of computing time). This is useful in order to be sure about the accuracy of the estimation. In fact, Fig. 14 shows that the value of the algorithm reached the steady-state in 20 iterations, but 50 iterations were done. This means that during the last 30 iterations the algorithm generated randomly 20 individuals at each iteration, totally 600 sets of possible parameters generated randomly, but belonging to the compact sets bounded from the upper and the lower bounds given before. However, among all these 600 sets of possible parameters "randomly generated", none gives a smaller cost function than the set of parameters generated at the 20th iteration. This can also be seen from Fig. 14 , since the cost function is constant during the last 30 iterations. Moreover, one would like to underline that a genetic algorithm allows to avoid the problem of the choice of the initial condition, since it is robust with respect to the latter choice. This means that whatever the initial condition is, it will converge towards the global minimum. Note that for the examined roundabout the root mean squared normalized error, which provides information on the magnitude of the errors relative to the average measurement, proved to be less than 0.10, while the mean absolute percent error, also calculated as a supplemental parameter to measure the size of the error in percentage terms, proved to be less than 5%. At last, Fig. 15 depicts the scattergram analysis developed to compare empirical versus GA-optimized capacities at entries of the single-lane roundabout taken into consideration. The regression line of empirical versus simulated capacity was plotted along with the 95% Prediction Interval (95% PI). Based on the R^2 value of 0.9919 and the fact that most of points were within the confidence band of the regression lines, the conclusion was reached that the model could be accepted as significantly close to the reality.
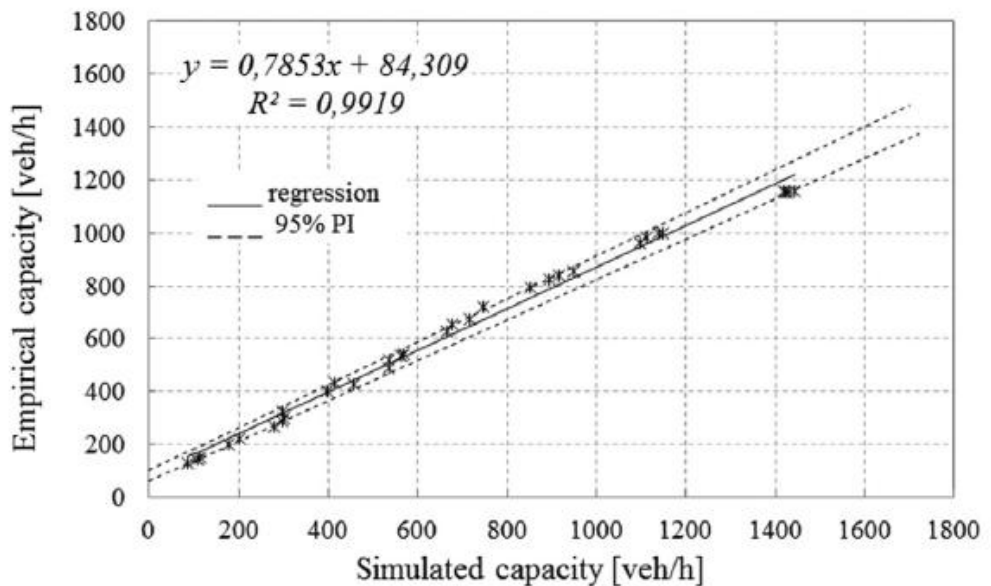
Figure 15 Simulated and empirical relationship with 95% confidence limits.

5.4. Application of a genetic algorithm for calibrating AIMSUN double-lane roundabout model and simulation results

In order to determine the most likely model parameters for the case study of the double-lane roundabout built in AIMSUN and the bounds of the intervals of potential variation of their values, a calibration process as an optimization problem was carried out; the selection of an objective function was therefore needed to measure the degree of closeness between the empirical values and simulated outputs.

As for the study case of single-lane roundabout, the experimental values of capacity were calculated using the Hagring model [4] on the basis of the meta-analytic estimation of the critical headways and the follow-up headways (see Chapter 2); however, differently from the single-lane roundabout study case, now capacity was calculated for each entry lane. In turn, the simulation output was generated by using AIMSUN which ran with a fixed model (i.e. the model taken into consideration), and tuned with a suitable set of model parameters. If the selected model parameters were incorrect, then the simulated values of entry lane capacity would not tend to stay close to the empirical capacities.

Objective function choose for this study case is the same used for single-lane roundabout case; see equation 15 in section 5.2.

In the objective function to be optimized, N was set equal to 32, since the observations were distributed over eight hours; in each of them four simulations

163

ran (one every fifteen minutes). Each hour corresponded to an antagonist traffic volume so that the capacity function could be plotted.

The solution of the calibration problem was given by the parameter vector (18), that minimized the objective function in equation 15. Once again the problem of searching for β* was solved iteratively; thus, for the selected double-lane roundabout, the problem of searching for β* was solved in the same way as in the previous case study regarding the single-lane roundabout.

To minimize the fitness function using the GA function, a number of variables were specified, as well as lower and upper bounds for the model parameters; the maximum number of iterations was fixed equal to 50 generations. Since a further increase in the population size could increase the structural bias of GA, the initial population used to seed the genetic algorithm was composed by 20 individuals. For the other GA parameters, the options included a mutation function, which was constraint dependent; a crossover function, which was scattered; a selection function, which was stochastic uniform; an elite count of 2 and the crossover fraction of 0.8. Based on the outcome of the manual calibration in Table 4, for each parameter the following bounds were set:

- the lower bound *β':* [$R_T = 0.85$; $G_{min} = 1.00$; $S_{acc} = 0.90$];
- the upper bound *β''*: [$R_T = 0.95$; $G_{min} = 1.50$; $S_{acc} = 1.10$].

Note that R_T stands for the driver reaction time, G_{min} stands for the minimum gap, and S_{acc} means the speed acceptance; see for details see section 4.3.3. The lower and upper bounds were introduced, here again, in order to restrict the search domain and avoid generating negative parameters or parameters without physical meaning. The algorithm after 50 iterations was stopped when the cost function *J(β)* reached a steady state. The vector β* achieved by solving the optimization problem represented the best value of the driver reaction time, the minimum gap and the speed acceptance such that the simulated values of entry lane capacity were as close as possible to the values of empirical capacity on each entry lane of the roundabout approaches.

Table 5 shows the results of the ultimate manual calibration and the GA-based optimization; the same table reports the measures of goodness-of-fit used to compare the simulated and empirical values of entry lane capacity that supported the decision to accept or otherwise reject the model. According to Barceló [8] the measures used were both the root mean squared normalized error (RMSE), which provides information on the magnitude of the errors relative to the average measurement, but in general heavily penalizes large errors, and the mean absolute percent error (MAPE) also calculated as a supplemental parameter to measure the size of the error in percentage terms. Despite recognizing the significance of individual measurements, the Theil's indicator *U* and the *GEH* index

were also used as joint measures that provide an overall view. The Theil's indicator *U* gives a normalized measure of the relative error that smoothes out the impact of large errors; the global index *U* is bounded, *0 ≤U≤ 1: U = 0* indicates a perfect fit, while *U=1* indicates the worst fit; the closer the values are to 0, the better. For *U ≤ 0.2*, the simulated series can be accepted as replicating the observed series acceptably well, whereas for values greater than 0.2, the simulated series should be rejected. In this table the GEH index is also shown; its meaning was discussed extensively in section 4.2.3.

Table 5 Results of manual calibration vs. GA-based optimization and goodness of fit.

AIMSUN parameter	values by entry lane					
	default values		manual calibrated		GA-optimized	
	left	right	left	right	left	right
driver reaction time R_t [s]	0.80	0.80	0.95	0.95	0.95	0.94
minimum gap G_{min} [s]	0	0	1.50	1.50	1.33	1.00
speed acceptance S_{acc}	1.10	1.10	0.90	0.90	0.97	0.95
fitness function $J(\beta)$	129.16	117.63	61.61	74.20	57.03	60.52
goodness of fit						
$RMSNE = \sqrt{\dfrac{1}{N}\sum_{i=1}^{N}\left(\dfrac{x_i - y_i}{y_i}\right)^2}$	0.12	0.10	0.10	0.10	0.09	0.08
$MAPE = \dfrac{100}{N}\sum_{i=1}^{N}\left|\dfrac{x_i - y_i}{y_i}\right|$	12.94	8.53	9.34	7.40	10.00	6.94
$U = \dfrac{\sqrt{\frac{1}{N}\sum_{i=1}^{N}(x_i - y_i)^2}}{\sqrt{\frac{1}{N}\sum_{i=1}^{N}(x_i)^2} + \sqrt{\frac{1}{N}\sum_{i=1}^{N}(y_i)^2}}$	0.07	0.07	0.07	0.07	0.06	0.06
$GEH = \dfrac{100}{N}\sum_{i=1}^{N}\sqrt{\dfrac{2(x_i-y_i)^2}{(x_i+y_i)}}$ [%]	78.10	78.10	100.00	96.90	93.80	96.90

Note that N is the number of measurements; x_i and y_i are the ith simulated and empirical value of entry lane capacity, respectively.

In order to be sure about the accuracy of the estimation, the GA ran for 50 generations in total; i.e. about 4 hours as amount of computational time. However, GA reached the steady state just under the 20th generation for both lanes, but it ran for the other generations, during which the algorithm generated randomly 20 individuals at each generation; thus, more than 600 sets of potential parameters by lane within the sets bounded from the upper and the lower bounds were randomly generated. In Figure 12, indeed, the fitness value is constant during the remaining generations for both the lanes of double-lane roundabouts.

Figure 16 shows the values of the fitness function *J(β)* during optimization for the left lane and the right lane of entries. The best fit is the fitness function or the cost function of the best individual within the generation. The graphs in Figure 16 also plot the mean best fit, that is the mean value of the cost functions calculated for

all individuals of the same generation. Since the GA finds the minimum of the fitness function, the best fitness value for a population is the smallest fitness value for any individual in the population. With reference to the optimized parameters, *J(β)* proved to be equal to 57.03 for the left lane and 60.52 for the right lane, whereas *J(β)* resulted equal to 61.61 for the left lane and 74.20 for the right lane when the parameters derived from manual calibration were used as the initial condition. Parameter tuning would bring significant benefits if the default parameters of AIMSUN were used as the initial condition (*J(β)* =129.16 and 117.63 for the left lane and the right lane, respectively).
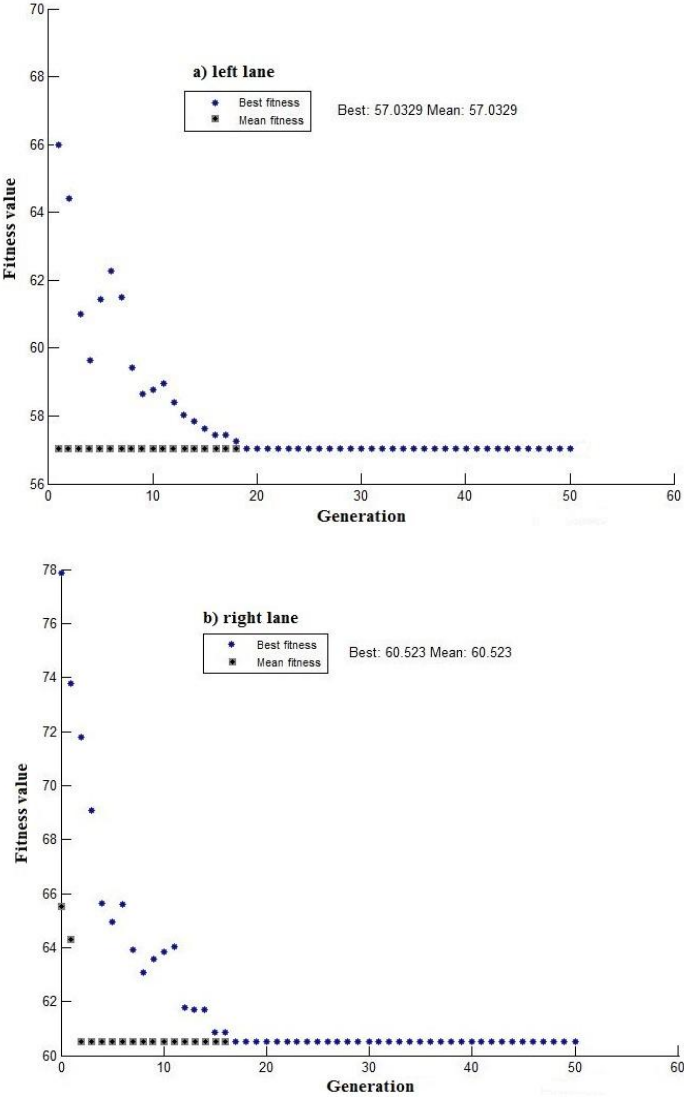
Figure 16 Values of the cost function *J(β)* during the optimization period for: a) the left entry lane; b) the right entry lane

Once again, the decision was taken to represent the scattergram analysis of empirical versus simulated capacities of the entry lanes; see Figures 17 and 18. Both graphs show the regression lines of empirical versus simulated capacity plotted along with the 95% prediction interval. Based on the R^2 and most of the points within the confidence band of the regression lines, one can observe that the model can be accepted as able to reproduce the empirical data.
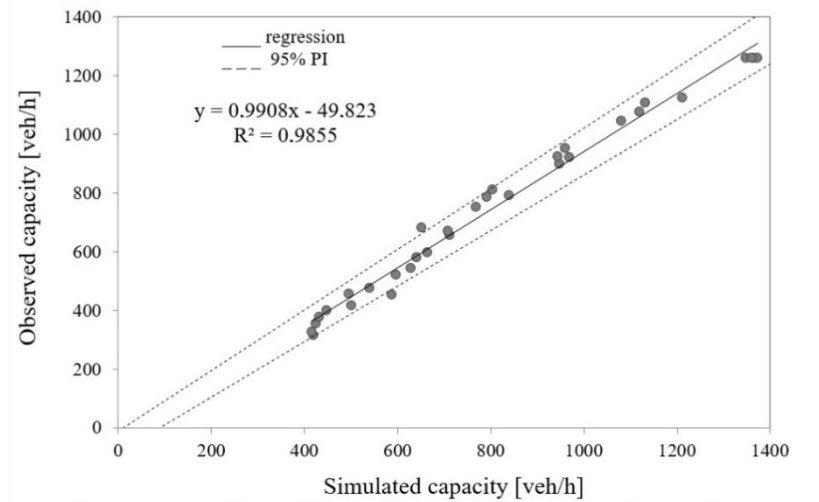
Figure 17 Simulated and observed relationship with 95% confidence limits for the left entry lane
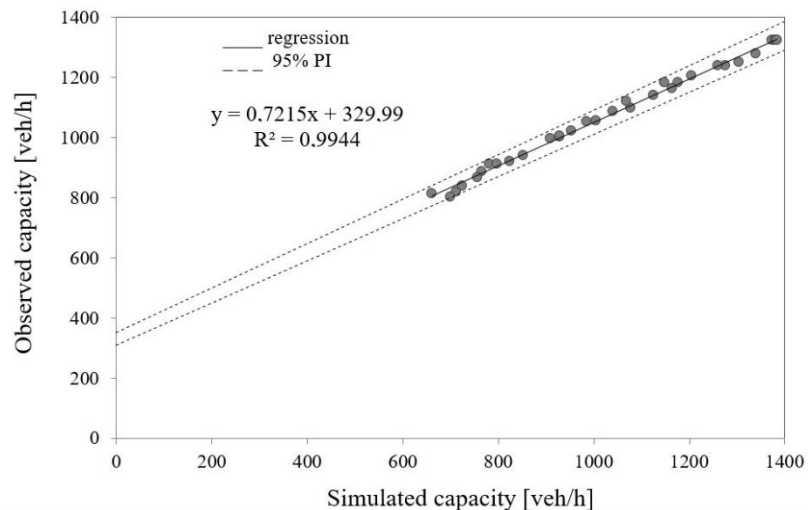
Figure 18 Simulated and observed relationship with 95% confidence limits for the right entry lane

References

1. AIMSUN Dynamic Simulator User Manual, Transport Simulation System (TSS) version 8, Barcelona, 2011.
2. VISSIM PTV Verkehr In Städten – SIMulationsmodell. software package. PTV Planung Transport Verkehr AG in Karlsruhe, Germany, 2015.
3. Paramics Microsimulation, SYSTRA Limited. www.paramics.com, 2016.
4. O. Hagring, A further generalization of Tanner's formula, Transportation Research Part B: Methodological 32(6) (1998) 423–429
5. MathWorks®, Documentation on genetic algorithms [Online]. Available: https://www.mathworks.com/help/gads/geneticalgorithm.html, 2015
6. Gipps, P.G.: A behavioural car-following model for computer simulation. Transp. Res. B 15B, 105--111 (1981)
7. National Academies of Sciences, Engineering, and Medicine, Roundabouts: An Informational Guide, second ed., The National Academies Press, Washington, DC, 2010. https://doi.org/10.17226/22914]
8. Barceló, J.: Fundamentals of Traffic Simulation. Springer, Heidelberg (2010)
9. Italian Minister of Infrastructure and Transport, http://www.mit.gov.it/mit/site.php?p=normativa&o=vd&id=1735&id_cat=&id_dett=0
10. Akcelik, R. 2004. aaSIDRA user Guide. Akcelik and Associates Pty ltd, Melbourne, Australia.
11. Arasan, V. T., Arkatkar, S.S. 2010. Microsimulation study of effect of volume and road width on PCU of vehicles under heterogeneous traffic. *Journal of Transportation Engineering* 136(12), 1110–1119.
12. Aumann, P., Whitehead, M. 2015. Austroads Guide to Road Design Part 4b - Roundabouts. Sydney, N.S.W. Austroads, December 2015. pp. 84.
13. AUSTROADS. 2011. VicRoads Supplement to Austroads Guide to Road Design – Part 4B roundabouts.
14. AUSTROADS 1993. Guide to traffic engineering Practice; Part 6 – Roundabouts, Sydney, Australia.
15. Barceló, J. 2010. *Fundamentals of Traffic Simulation*. London: Springer.
16. Bell, M.C., Galatioto, F., Giuffrè, T., Tesoriere, G. 2012. Novel application of red-light runner proneness theory within traffic microsimulation to an actual signal junction. *Accident Analysis & Prevention* 46, 26-36.
17. Borenstein, M., Hedges L.V., Higgins, J.P.T., Rothstein, H.R. 2009. *Introduction to Meta-analysis*. Chichester, UK: John Wiley & Sons, Ltd.
18. Bovy, P.H. 1991. Zusammenfassung des Schweizerischen Kreiselhandbuchs *[Summary of Swiss Roundabout Guide]*, In: Straße und Verkehr 3/1991, S. 129-139, *in German*.

19. Brilon, W. 2014. Roundabouts: A State of Art in Germany. In 4th International Conference on Roundabouts. Transportation Research Board, Seattle, April 2014.

20. Brilon, W., Stuwe, B. 1993. Capacity and design of traffic circles in Germany. *Transportation Research Record* 1398, 61-67.

21. Chiappone, S., Giuffrè, O., Granà, A., Mauro, R., Sferlazza, A. 2017. Traffic simulation models calibration using speed-density relationship: An automated procedure based on genetic algorithm. *Expert Systems with Applications* 44, 147-155.

22. Cao, N.Y., Sano, K. 2012. Estimating capacity and motorcycle equivalent units on urban roads in Hanoi, Vietnam. *Journal of Transportation Engineering* 138(6), 776-785.

23. CERTU 1999. Carrefours urbains Guide, Lyon France 1999.

24. Coifman, B. 2015. Empirical flow-density and speed-spacing relationships: Evidence of vehicle length dependency. *Transportation Research Part B: Methodological* 78, 54-65.

25. CROW 1998. Eenheid in rotondes. CROW publication no.126. Ede, The Netherlands. (Uniform design of roundabouts).

26. Daganzo, C.F., Lehe, L.J. 2016. Traffic flow on signalized streets. *Transportation Research Part B: Methodological* 90, 56-69.

27. Dahl, J., Lee, C. 2012. Empirical estimation of capacity for roundabouts using adjusted gap-acceptance parameters for trucks. *Transportation Research Record* 2312, 34–45.

28. Design Manual for Roads and Bridges (DMRB). 2007. Volume 6, Section 2, Part 3. TD 16/07. Geometric design of roundabouts. London: The Stationery Office Ltd. On-line available at: http://www.standardsforhighways.co.uk/ha/standards/dmrb/index.htm

29. Dowling, R., Skabardonis, A., & Vassili, A. (2004). Traffic Analysis Toolbox Volume III: Guidelines for Applying Traffic Microsimulation Software. Report No. FHWAHRT-04-040. Washington DC: Federal Highway Administration-United States Department of Transportation, on-line available http://ops.fhwa.dot.gov/trafficanalysistools/tat_vol3.

30. Egger, M., Davey Smith, G. 1997. Meta-analysis: Potentials and promise. *British Medical Journal* 315(7119), 1371-1374.

31. Elvik, R. 2011. Publication bias and time-trend bias in meta-analysis of bicycle helmet efficacy: a re-analysis of Attewell, Glase and McFadden 2001. *Accident Analysis and Prevention* 43(3), 1245-1251.

32. FGSV Ed. 2015. Handbuch für die Bemessung von Straβenverkehrsanlagen (HBS) Edition 2015 [*German Highway Capacity Manual*]. Forschungsgesellschaft für Straβen und Verkehrswesen (FGSV) [*Road and Transport Association*]. Cologne, edition 2015.

33. Fugal, K. J., Dale, M. T., Lewis, S. J. 2008. Design for single-lane to dual-lane roundabout expandability. National Roundabout Conference 2008, Kansans City, Missouri, US, May, 7- 9, 2008.

34. Gautam, A., Das, K.A., Rao, R., Tiwari, G. 2016. Estimation of PCE values for hill roads in heterogeneous traffic conditions. *Journal Transportation Letters: The International Journal of Transportation Research*, June 2016, 1-9.

35. Giuffrè, O., Granà, A., & Tumminello, M.L. 2016b. Gap-acceptance parameters for roundabouts: a systematic review. *European Transport Research Review* 8(1):2, 1-20.

36. Giuffrè, O., Granà, A., Giuffrè, T., Marino, R. 2012. Researching a capacity model for multilane roundabouts with negotiation of the right-of-way between antagonist traffic flows. *Modern Applied Science* 6(5), 2-12.

37. Guichet, B. 2005. Roundabouts in France and new use. TRB Transportation research, National Roundabout Conference proceedings 2005, Vail Colorado, USA, 22-25 May, 2005.

38. Hamadi, Y., Monfroy, E. Saubion, F. 2011. Autonomous search. Heidelberg: Springer. Chapter 2.

39. Highway Capacity Manual. (2010). *Transportation Research Board*. (5th ed). Washington DC: Transportation Research Board.

40. Herland, L. and Helmers, G. 2002. Cirkulationplatser – utformnng och function. Svenska och utlandska rekommendationer och utformingsregler jamte analys och kommentarer. VTI Meddelande 895. Linköpink. [*Roundabouts – design and function. Swedish and foreign recommendations and design rules with analyses and comments*], *in Swedish*.

41. Hollander Y, Liu, R. 2008 The principles of calibrating traffic microsimulation

42. Kimber, R.M. 1989. Gap-Acceptance and Empiricism in Capacity Prediction. *Transportation Science* 23(2), 100-111.

43. Kiran, S., Verma, A. 2016. Review of Studies on Mixed Traffic Flow: Perspective of Developing Economies. *Transportation in Developing Economies*, 2:5.

44. Lenters, M., Rudy, C. 2010. HCM Roundabout Capacity Methods and Alternative Capacity Models. *ITE Journal 80(7)*, 22-27.

45. List, G. F., Yang, B., Schroeder J.B. 2015. On the treatment of trucks in roundabout analyses. *Transportation Research Record* 2483, 140–147.

46. Louah G. 1992. Panorama critique des modeles français de capacité des carrefours giratoires. Actes du séminaire international Giratoires '92 [*Roundabouts, 1992*], Nantes, France, 1992.

47. Mauro, R., Giuffrè, O., Granà, A., Chiappone, S.n2014. A statistical approach for calibrating a microsimulation model for freeways. *WSEAS Transactions on Environment and Development* 10/2014, 497-508.

48. Mauro, R. 2010. *Calculation of Roundabouts: Capacity, Waiting Phenomena and Reliability*. Berlin Heidelberg: Springer.

49. Mohan, M., Chandra, S. 2016. Concept of queue clearance rate for estimation of equivalency factors at priority junctions. *Canadian Journal of Civil Engineering* 43(7), 593-598.

50. Norme funzionali e geometriche per la costruzione delle intersezioni stradali [*Functional and geometric standards for the construction of road intersections*]. 2006. Ministero Infrastrutture e Trasporti [Minister of Infrastructure and Transport], *in Italian*.

51. Otković, I. Tollazzi, T., Šraml, M. 2013. Calibration of microsimulation traffic model using neural network approach. *Expert Systems with Applications* 40(15), 5965-5974.

52. Pilko, H., Mandžuka, S., Barić, D. 2017. Urban single-lane roundabouts: A new analytical approach using multi-criteria and simultaneous multi-objective optimization of geometry design, efficiency and safety. *Transportation Research Part C: Emerging Technologies* 80, 257-271.

53. Piotrowski, A.P., Napiorkowski J.J. 2016. Searching for structural bias in particle swarm optimization and differential evolution algorithms. *Swarm Intelligence* 10(4), 307–353.

54. Robinson, B. W., Rodegerdts, L., Kittelson, W. et al. 2000. Roundabouts. An informational Guide. Federal Highway Administration. United States Department of Transportation, Publication No. FHWA-RD-00-067 FHWA.

55. Rodegerdts, L., Bansen, J., Tiesler, C., et al. 2010. Roundabouts: An informational guide (2nd ed.). Washington, DC: Federal Highway Administration. United States Department of Transportation, NCHRP REPORT 672.

56. Roess, R.P., Prassas, E.S. 2014. *The Highway Capacity Manual: A Conceptual and Research History Vol. 1*. Springer Tracts on Transportation and Traffic 5. London: Springer.

57. Rubio-Martín, J.L., Jurado-Piña, R., Pardillo-Mayora, J.M. 2015. Heuristic procedure for the optimization of speed consistency in the geometric design of single-lane roundabouts. *Canadian Journal of Civil Engineering* 42(1), 13-21.

58. Tollazzi, T. 2015. Alternative Types of Roundabouts: An Informational Guide. Springer International Publishing. 206 p. http://doi.org/10.1007/978-3-319-09084-9

59. Troutbeck, R.J. (1988). Current and future Australian practice for the design of unsignalised intersections. In: W. Brilon (ed.) Intersections Wthout Traffc Signalis, Proceedings of an International Workshop, Bochum, West germany, Srnger-Verlag, Berlin, pp. 1-19.

60. Valdez, M., Cheu, R.L., Duran, C. 2011. Operations of modern roundabout with unbalanced approach volumes. *Transportation Research Record* 2265, 234–243.

61. Vasconcelos, L., Seco, Á., Silva, A.B. 2014. Hybrid calibration of microscopic simulation models. *Advances in Intelligent Systems and Computing 262*, R. Rossi and J. F. de Sousa, Editors. Springer International Publishing.

62. VSN International 2016. GenStat for Windows 17th Edition. VSN International, Hemel Hempstead, UK. Web page: GenStat.co.uk

63. Wu, N. 2001. A universal procedure for capacity determination at unsignalized (priority-controlled) intersections. *Transportation Research Part B: Methodological* 35(6), 593–623.

64. Yap, Y.H., Gibson, H.M., Waterson, B. J. 2013. An international review of roundabout capacity modelling. *Transport Reviews* 33(5), 593-616.

65. Zhen (Sean), Q., Jia, L., Li, X., Zhang, M., Wang, H. 2017. Modeling heterogeneous traffic flow: A pragmatic approach. *Transportation Research Part B: Methodological* 99, 183-204.

66. Chan, W.T., Fwa, T.F. & Tan, C.Y. 1994. Road-maintenance planning using genetic algorithms. I: Formulation. Journal of Transportation Engineering 120(5): 693-709.

67. Chan, W.T. & Tao, F. 2003. Using GIS and genetic algorithm in highway alignment optimization. Intelligent Transport System 2:1563–1567.

68. Malhotra, R., Singh, N. & Singh, Y. 2011. Genetic algorithms: concepts, design for optimization of process controllers. Computer and Information Science 4(2): 39-54.

69. Mitchell, M., Forrest, S. & Holland, J.H. 1991. The royal road of genetic algorithms: fitness landscapes and GA performances. Francisco J. Varela and Paul Bourgine (ed). Toward a Practice of Autonomous Systems; Proc. First European Conference on Artificial Life. Cambridge, MA: MIT Press.

70. Mitchell, M. 1996. An Introduction to Genetic Algorithms. Cambridge, MA: MIT Press.

71. Nguyen, A.T., Reiter, S. & Rigo P. 2014. A review on simulation-based optimization methods applied to building performance analysis. Applied Energy 113 (2014) 1043–1058

72. Ahmad Al-Hadad, B.M. & Mawdesley, M. 2010. A genetic algorithm approach to a 3D highway alignment development. Evolutionary Computation (ICEC 2010), part of the International Joint Conference on Computational Intelligence (IJCCI 2010)); Proc. inter. conf., Valencia, Spain, 24–26 October, 2010.

73. Ahmad Al-Hadad, B., Mawdesley, M.J. & Stace, R., 2010. A genetic algorithm approach to highway alignment development. In Tizani W. (ed.), Computing in Civil and Building Engineering; Proc. inter. conf. Nottingham, UK30 June-2 July, 2010. Nottingham: Nottingham University Press.

74. Fwa, T.F., Tan, C.Y. & Chan, W.T., 1994. Road-maintenance planning using genetic algorithms. II: Analysis. Journal of Transportation Engineering 120(5): 710-722.

75. Wonkyu, K., Jaesung, P., Youn-Soo, K., Pyo, K.G., Hyeonmi, K. 2010. Comparing calibration methods for microscopic traffic simulation models. 17th World Congress on Intelligent Transport Systems, ITS 2010. Busan, South Korea, 25-29 October 2010.

76. Mathew, T.V. & Radhakrishnan, P. 2010. Calibration of microsimulation models for nonlane-based heterogeneous traffic at signalized intersections. Journal of Urban Planning and Development 136 (1): 59-66.

77. Essa, M. & Sayed T. 2016. A comparison between PARAMICS and VISSIM in estimating automated field-measured traffic conflicts at signalized intersections. Journal of advanced transportation 50: 897–917.

78. Ghods, A.H & Saccomanno, E.F. 2010. Comparison of carfollowing models for safety performance analysis using vehicle trajectory data. Annual Conference of the Canadian Society for Civil Engineering 2010 (CSCE 2010), Winnipeg, MB, Canada,June 9-12, 2010. Volume 2: 13391348.

CHAPTER FIVE

Estimation of Passenger Car Equivalents for single-lane and double-lane roundabouts

1. Introduction

The traffic flows observed in any road facilities are generally heterogeneous, since different categories of vehicles compose them and affect traffic conditions in different ways due to their specific operating performance. In order to adequately analyze traffic conditions, heterogeneous traffic must be converted into homogenous stream in which it is assumed that only passenger cars are travelling; Passenger Car Equivalents (hereinafter PCEs) are usually used to perform this conversion. It is well known that the passenger car equivalency of a particular category of vehicles represents the number of passenger cars that would have an equivalent effect on traffic flow quality [1].

A wide variety of heavy vehicles, such as trucks (single-unit trucks and combinations trucks with one, two or three trailers), recreational vehicles, buses, tractors and other farm machinery in agricultural areas, oversized trucks in manufacturing areas and so on, operate on highways and roads, and interact with the geometric features that affect the operational quality and road safety. Besides, the static and dynamic characteristics of heavy vehicles operating on various road entities make their impact on traffic performance quite different than the passenger cars: heavy vehicles occupy more roadway space per vehicle due to their dimensions, take longer to accelerate and/or decelerate due to their weight and horsepower, and maintain greater spacing from a lead vehicle than a passenger car specially on grades; moreover, heavy vehicles can limit the field of vision of drivers behind and in the adjacent lanes, and they can affect in some way the driving abilities of car drivers in front of them, and so on.

Despite in usual operational conditions heavy vehicles can generally amount to less than 30% of all vehicles of a traffic mix, they produce a significant effect on performance of the mixed traffic streams for a great variety of road entities. Thus, passenger car equivalents for heavy vehicles are used for the capacity calculation and operational analysis of any road entity (roadway segments or intersections). Notwithstanding the use of PCEs represents the starting point for the operational analysis of roads and intersections and other traffic management applications, very few studies have looked at the effect of heavy vehicles on traffic operations at roundabouts. Indeed, the constraints to the vehicular trajectories imposed by the curvilinear geometric design of roundabouts and drivers' gap acceptance behavior are expected to produce an impact of the heavy vehicles on the quality of traffic flow different from that produced on freeways and two-lane highways or other at-grade intersections. This is also because entering flow is opposed by the circulating flow which has priority and travels in an counter clockwise direction

around the central island. Besides, the entering flow is highly depending on the drivers' gap acceptance behavior, when deciding on the time gap within the circulating flow to accept or reject. This acceptance process by drivers becomes more complicated when a roundabout is composed by more than one circulating lanes, since the drivers are called to decide on more gaps according to the number of the antagonist circulating flows.

Therefore, based on the belief that the constraints to the vehicular trajectories imposed by the curvilinear design of roundabouts imply an impact of heavy vehicles on the traffic flow quality, capacity determination should be based on the effects of heavy vehicles on roundabout operations, and the values of PCEs should depend on the amount of the circulating flow and the percentage of heavy vehicles in the traffic mix.

The purpose of this research activity was to explore the mechanism through which the heavy vehicles driving roundabouts can be converted into Passenger Car Equivalents. This research starts from the assumption that the highly curvilinear nature of the roundabout design has significant effects on the paths that heavy vehicles would travel; as a consequence, the interaction between the physical and performance characteristics of heavy vehicles and the geometric features of the roundabouts produce higher impacts on traffic operations than other at-grade intersections. However, it is noteworthy that the HCM [2] proposes constant values for PCEs regardless the roundabout layout and number of heavy vehicles.

The PCEs for heavy vehicles driving two case studies of roundabouts (i.e. a single-lane roundabout and a double-lane roundabout) were estimated as a function of different percentages of heavy vehicles that characterized the traffic demand. The criterion proposed in this research activity implies a comparison between the capacity that would occur with a traffic demand of passenger cars only and the capacity reached beginning from a traffic demand with a certain percentage of heavy vehicles. Estimation of PCEs for each entry lane was based on the above-mentioned comparison of entry capacities calculated for a fleet of passenger cars only and mixed vehicle fleets, each of them including different percentages of heavy vehicles. The entry capacity of the single-lane roundabout and capacities for each entry lane of the double-lane roundabout were determined based on a calibrated microscopic traffic simulation model, by varying the percentage of heavy vehicles in the traffic demand. For this purpose, AIMSUN software [3] was used to replicate traffic conditions difficult to identify during field surveys and account for a wide range of traffic conditions on the roundabouts selected as case studies. In other words, traffic microsimulation was used to evaluate the variation of traffic flow conditions at roundabouts in presence of mixed fleets, varying the percentage of heavy vehicles in the traffic demand. A preliminary activity consisted of the comparison of the empirical capacity functions based on a meta-analytical estimation of critical and follow up headways (see Chapter 2), and simulation output data derived for the two case studies of roundabout built in AIMSUN.

After a brief introduction to the literature on PCEs, the procedure carried out to calculate PCEs for heavy vehicles driving the single-lane and the double-lane roundabouts selected as case studies will be presented in the next sections.

2. Literature Review on PCEs

Traffic conditions are usually far from ideal due to the heterogeneous structure of traffic patterns [4]. The presence of a heterogeneous mix of vehicles in traffic streams affects the level of service of any road entity and has effects on the accuracy of whatever traffic management application. In capacity and level of service analyses, heavy vehicles are usually modelled by means of the car equivalents for individual types of vehicles. Different size vehicles have different impacts on entry capacity; the passenger cars are used as the basis for the comparison: an equivalent coefficient for a particular type of vehicle expresses the number of passenger cars (termed the car equivalent) which affects the traffic conditions similarly to the analysed vehicle. In other words, the PCEs are generally defined as the number of passenger cars (i.e. the base unit) displaced from the traffic stream by one heavy vehicle of a specific class under prevailing conditions and then expressed as multiples of the effect of an average passenger car (see e.g. [1]). Calculation of PCEs builds upon a wide literature which initiated several decades ago. Most of the studies on this domain of science have revealed that the methodological approaches to PCEs vary per type of road entity. There are many studies and researches in the literature on this topic which present the PCEs for individual type groups of vehicles on freeway and highways, or signalized intersections [5-9]. Individual groups of vehicles affect the conditions of traffic streams to different extent. However, car equivalents can vary with a number of conditions as the proportion of heavy vehicles in the traffic stream, the type of facility and conditions of uninterrupted flow or interrupted flow, the directional traffic distribution, the category of heavy vehicles, the level of service, speed or density of a prevailing traffic stream. Traditionally, for freeways and two-lane highways passenger car equivalents vary for trucks, buses, and recreational vehicles, while for signalized intersections through-vehicle equivalents vary for left and right turns. To name but a few for signalized intersections, Benekohal and Zhao [10] found values of PCEs for trucks increasing from 1.0 to 2.18 when the traffic intensity and the proportion of heavy vehicles increased. There are several methods of evaluation of the PCEs, and various criteria of equivalence based on the heavy vehicle effect on different traffic parameters (see e.g. [1]). In this regard, Huber [11] calculated the flow rate of a base stream of passenger cars and the flow rate of a mixed stream including both the share of passenger cars and the share of heavy vehicles. The ratio between the two flow rates characterized by the same level of a measure of impedance, or the density of the two streams, addressed the PCE calculation.

The determination of equivalent coefficients may be based on statistical methods and/or traffic simulation; however, the method of determination has effects on

PCEs [12, 13]. Specifically, macroscopic approaches assume as equivalent the traffic streams which operate at the same speed or the same density, whereas latest microscopic approaches need to consider the behaviour of individual vehicles or pairs of vehicles. In turn, the definitions of equivalence may be related to the number of passing maneuvers of one class of vehicles by another class, the delay that one class of vehicles causes to other vehicles, the headway between vehicles of different classes and for different road entities, the proportion of capacity used by vehicles of different classes (or under different geometric conditions), and so on. In this regard, some Authors based the PCE calculations on flow rates and density (see e.g. [11-18]), whereas Anwaar et al. [5] used lagging headways to estimate PCEs. In turn, further methods for calculating PCEs were based on queue discharge flow (see e.g. [19]), vehicle-hours, and travel time (see e.g. [20]), delay (see e.g. [6]), volume/capacity ratio and platoon formation (see e.g. [19]). However, the results found in studies on mixed traffic flows for different road entities cannot be considered generalizable because PCEs depend on various vehicular, geometric and control conditions, but all were not at the same time regarded [21].

Most of guidelines propose constant values for PCEs for heavy vehicles (see e.g. [1, 23]), but a single value or a single set of PCE values can result inappropriate especially under heterogeneous traffic conditions [4]. With regard to the equivalent factors suggested by the HCM (2010)[2], although they are not sensitive to the performance of heavy vehicles or traffic level, they have been applied to develop traffic analyses for many road entities from free-flow to congested-flow conditions. However, PCEs for use in undersaturated conditions may underestimate the effect of heavy vehicles when congestion is being reached [24]. Some studies and researches also proposed that PCEs for heavy vehicles during congestion should be considered as random variables generally following the normal distribution. In this regard, it was found higher effects of heavy vehicles for congested traffic conditions than free-flow conditions and recommended higher PCEs in oversaturated traffic conditions. In turn, Geistefeldt [25] proposed that PCEs should be approached based on stochastic variation in capacity due to variation in percentage of heavy vehicles; for traffic conditions less congested, the Author found a higher variation in flow rate as heavy vehicle percentage decreased. Many studies applied microscopic traffic simulation to derive PCEs, or estimated PCEs through nonlinear programming using queue discharge flow as equivalency criterion. Despite the results were consistent with on-field observations, it is worth noting that in more cases studies on PCEs were far from a generalization in the results.

2.1. PCE Calculation on Roundabouts

Many studies carried out elsewhere in the world have already focused on roundabout capacity modelling through analytical models, gap acceptance and

traffic simulation (see e.g. [26-31]). However, little is known about the complex behavioral and physical processes involved in roundabout entries in presence of mixed fleets. For demonstration purposes, Dahl and Lee [29] applied the Troutbeck's model [32] to understand the effect of the truck percentage on the capacity trend at two large roundabouts; the results showed that the capacity decreased as truck percentage increased, but there was lower capacity reduction at higher circulating flows. However, very few studies have looked at the effect of heavy vehicles on roundabout performance and/or have calibrated PCEs specifically for roundabouts. Field based studies often require great efforts to collect data on roundabouts; in turn, the number of roundabouts to be surveyed is often insufficient. Thus, experiments are preferably performed with microscopic traffic simulation models in order to have different combinations of approach volumes and obtain equivalent flows under a wide range of traffic and geometric conditions (see e.g. [33-35]). Although the impact of heavy vehicles on the performance of a roundabout is expected that varies with the traffic demand, the operational effect of a high vehicular volume coming from one direction (i.e. the ring) and that of heavy vehicles are unclear and still leave room for further detailed study. It is worth noting that the PCEs at roundabouts can be affected by numerous and specific factors, which include geometric properties (e.g. outer diameter, width of the circulatory roadway), traffic properties (e.g. traffic intensity in the circular roadway and at each entry) and other factors (e.g. location and environment, driver behaviour), the effect of which can be significant under conditions of unlimited traffic with high saturation degrees of the traffic streams. In HCM [2], the impact of heavy vehicles on entry capacity at roundabouts is considered through a heavy vehicle adjustment factor; it includes the heavy vehicle percentage and the passenger car equivalent set as 2.0 (i.e. a heavy vehicle is assumed to be equivalent to two passenger cars regardless of the vehicle type, the percentage of heavy vehicles and the performance of heavy vehicles or traffic level). However, nothing is proposed for specific roundabout layouts (i.e. mini roundabouts, single-lane or multi-lane roundabouts). Other studies have also proposed a single and constant value for the heavy vehicle equivalent at roundabouts, which was estimated based on several considerations (i.e. entry capacity and move-up time), however influenced by local driver behaviour and geometric conditions (see [36, 37]). In turn, Lee [31] observed that there was a lack of study on the prediction of the entry capacity based on the difference in driver's gap acceptance behaviour between cars and heavy vehicles. Lee [31] observed the headways of various following sequence of passenger cars and heavy vehicles and then investigated whether the PCEs were able to represent specific traffic characteristics at roundabouts compared with other road entities. Based on the analysis of three large roundabouts located in a separate site and accommodating large trucks, the PCEs for roundabouts were based on variations in the entry capacity for various mixed fleets of cars and heavy vehicles. Determination of a constant value of PCE, but different for each roundabout, led

the Author to conclude that the generalization of the results of the study would have been obtained after conducting some more research.

Other studies gave great insight into this issue. To name but a few, Macioszek [38] investigated the effect of the traffic intensity on the value of car equivalents for heavy vehicles on circular intersections and determined higher PCEs at higher traffic intensities. In another study Macioszek [39] analysed the effect of some geometric parameters (i.e. width of entry and circulatory roadway, outer diameter) on the vehicle speed through roundabouts. Based on the available measurements of the velocity quantises, the Author then calculated the PCEs for heavy vehicles. Despite the proposed correlations resulted only approximate, PCEs rose from 1.92 to 2.25 when the velocity of vehicles on the circulatory roadway varied. In turn, Tanyel et al. [40] investigated the effect of heavy vehicles, particularly buses, on traffic conditions at five roundabouts (with an outer diameter ranging from 46 m to 140 m). The results showed that different PCE values should be used for minor and major flows; otherwise, the same value may lead engineers to overdesign roundabouts. Table 1 depicts a systematic review of PCEs for heavy vehicles on roundabouts based on field data or capacity analysis performed through an analytical technique.

Academics and practitioners during the last decade have been using microscopic traffic simulation to estimate entry capacity and calculate the PCEs on roundabouts. Kang and Nakamura [36] estimated roundabout capacity considering the impact of buses and trucks on operations of a four-leg, single lane roundabout (with a diameter of 27 m). Specifically, they used VISSIM software for exploring some traffic scenarios under Japanese conditions. Their main results included a reduction in entry capacity when the heavy vehicle percentage increased and an increase in the PCE value when the circulating flow increased, but with a lower increase rate for high levels of the circulating flow. Since the effect of other geometric and traffic-related determinants was neglected in this phase of the study, they are expected to be examined through some experiments in future. In another study, List et al. [41] refined the PCE values used to convert trucks into car equivalents at entries, calibrated the capacity equations so that it more appropriately accounts for trucks, and estimated truck speeds so that travel times through the roundabout could be determined.

Table 1 Systematic review of studies on PCEs for heavy vehicles driving roundabouts.

Study name	country	Subject type of roundabout	Method of capacity calculation	PCE
Lee [31]	US	outer diameter > 50.0 m	Vehicle counts at each entry and circulatory roadway were on-field collected; entry capacity was observed in 1-min (fully saturated) periods, counting the entering vehicles until the last queued vehicle entered the roundabout.	1.5 or 2.5 (heavy truck) 1.0, 1.2 or 1.5 (light truck)
Rodegerdts et al. [22]; Lenters & Rudy [42]	US	outer diameter of 35.0 m to 65.0 m for two-lane.	The multi-lane capacity empirical regression model was calibrated to US conditions using local data for the critical and follow-up headways.	2.0
Robinson et al. [43]	US	The outer diameter of 40.0 m to 60.0 m used for design templates of rural and urban double-lane roundabouts	The capacity forecast was based on British regression formula [44]; it may be also derived using a gap-acceptance model by incorporating limited priority behaviour.	1.5 (single-unit trucks) 2.0 (trucks with trailer)
Overton [45]	US	The restrictions of the data collection to only a single location is prohibitive to the validity of the results.	Based on the 15-min period with the highest vehicles entering, a comparison is made between the total flow rate (veh/h) and the maximum flow rate of passenger cars (i.e. obtained removing the minutes with trucks from vehicle counts) entering the roundabout. An overall weighted average PCE was estimated.	3.37
Louah [46]; CERTU [47], Guichet [48]	France	All types of layouts from small to large (single-lane and multi-lane) roundabouts in urban and rural areas with entry width 3-11 m; splitter island width 0-70 m; exit width 3.5-10.5 m; circle width 4.5-17.5 m; central island radius 3.5-87.5 m	Capacity formula is developed through statistical regression techniques; GIRABASE software's empirical regression equations are based on the counting of 63,000 vehicles during 507 saturated operation periods of 5-10 min in 45 different roundabout entries.	2
Aumann & Whitehead [49]; Akcelik [50]; AUSTROADS [15 - 16]	Australia	Central island radius from 8 m to 80 m is used to determine vehicle path at double-lane roundabouts. Swept paths of the design vehicle for the through and the right-turn movements do not necessarily coincide within the circulatory width as the standard proposes.	The capacity analysis is performed through an analytical technique and is based on the assumption that capacity of a roundabout is influenced by its geometry through the gap acceptance parameters	2 (single-unit trucks)* 3.0 (articulated trucks)*
Bovy [51]	Switzerland	The outer diameter of the roundabouts varies from 24.0 m to 34.0 m for design templates used in urban and suburban double-lane roundabouts	The capacity formula proposed by the Swiss standard takes into account the roundabout geometry in somewhat detailed way through the number of lanes at entries and in the circle, whereas the disturbing flow is a linear combination of the circulating flow and exiting flow.	2.0
Brilon [51]; Wu [52]	Germany	Geometric details are incorporated into the German HCM [23]	The total capacity of each approach is depending on the total traffic intensity in the ring and gap acceptance parameters; the last values were measured at single-lane and double-lane roundabouts; see also Brilon [53].	2.0

(*) for truck volumes greater 5%, the truck flows should be converted to passenger car units as referred by VicRoads [15]

3. A Criterion for PCEs calculation

With the aim of estimating the PCEs that reflect the traffic conditions at single- and double-lane roundabouts, a criterion to find the PCEs needs to be introduced; the criterion was based on equivalence between the proportions of capacity used by vehicles of different classes, i.e. passenger cars and heavy vehicles. As before introduced, the criterion proposed to find the PCEs implies a comparison between the entry lane capacity that would occur with a traffic demand composed only of passenger cars and the entry lane capacity reached beginning from a traffic demand with a certain percentage of heavy vehicles. This key concept was based on the Huber's [11] study, where a model is proposed for estimating the PCE values for vehicles under free-flowing, multi-lane conditions; the model was based on the ratio between two traffic flow rates characterized by the same level of a measure of impedance, or the density of the two streams. The way to address the problem both for the single-lane and the double-lane roundabouts selected as case studies was to compare the capacity C_{car} which was simulated for a traffic demand made only of passenger cars and the capacity C_p which was simulated for a traffic demand with a p percentage of trucks. Thus, based on Huber's [11] study the two capacities ware compared as below:

$$C_{car} = (1 - p) \cdot C_p + p \cdot C_p \cdot E_t \qquad (1)$$

where:

- C_{car} = the entering heterogeneous flow in saturation conditions (or the capacity that would occur in presence of a traffic demand only made of passenger cars);
- p = the percentage of heavy vehicles;
- C_p = the capacity corresponding to a traffic demand characterized by a percentage p of heavy vehicles;
- $(1 - p) C_p$ = the share of passenger cars;
- $p \cdot C_p$ = the share of heavy vehicles;
- E_t = the equivalent factor.

Since there were questions of homogeneity, the last share of heavy vehicles was multiplied by the equivalent factor E_t. In turn, the equivalent factor could be determined using the equation below:

$$E_t = \frac{1}{p}\left(\frac{C_{car}}{C_p} - 1\right) + 1 \qquad (2)$$

In this regard, being the passenger car the base vehicle, the capacity function C_{car} was the base curve, while C_p represented the capacity function for a mixed fleet

with a *p* percentage of trucks. The base curve function was calibrated setting the AIMSUN parameters on the basis of the solution of the GA-based optimization problem (see chapter 4). Generation of the C_{car} and C_p functions required that O/D matrices were assigned to the roundabouts built in AIMSUN. To generate some traffic scenarios, different mixed fleets (i.e. 100% passenger cars, 10%, 20%, 30% up to 100 % heavy vehicles) entering the roundabouts were produced.

Given as an example only, Figure 1 depicts the criterion of PCE calculation through the plots of the base curve C_{car} and the mix curve C_p for a heterogeneous driver population corresponding to whatever mixed fleet; specifically, the base curve C_{car} corresponds to the traffic scenario with 100% passenger cars (i.e. *p* = 0%) and the mix curve is corresponding to the traffic scenario with a certain percentage *p* of heavy vehicles. It should be noted that a reduction in capacity could be observed with a rise in circulating flow; however, the reduction in capacity is more significant with a rise in the percentage *p* of heavy vehicles.

$$C_{car} = (1-p)\,C_p + p\cdot C_p\cdot E_t$$
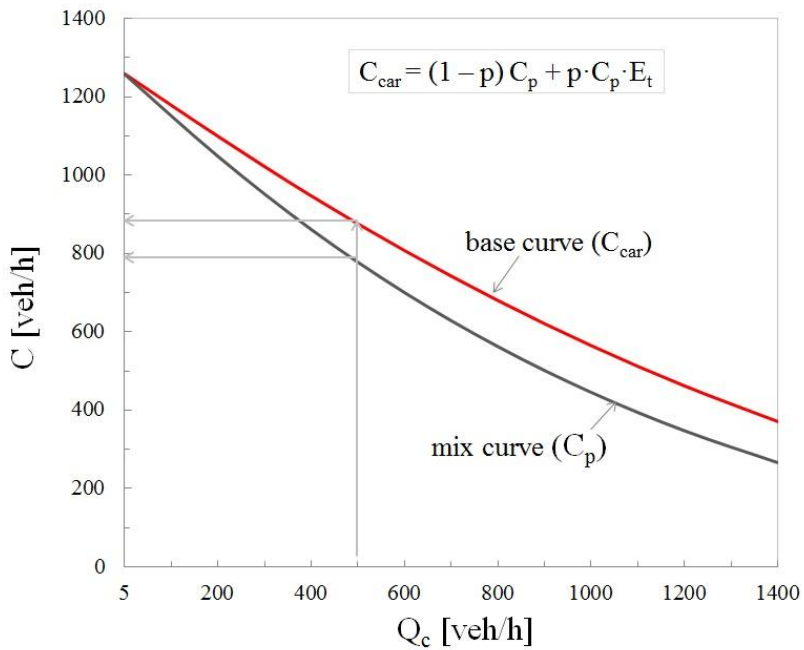
Figure 1 Criterion of PCE calculation

In order to obtain the passenger car equivalent at single-lane and double-lane roundabouts by using Eq. 2, the knowledge of a capacity functions for the base curve C_{car} and the mix curves C_p was needed. Based on the results of the GA-based procedure (see Chapter 4), the capacity functions for the base curve C_{car} and the mix curves C_p were calibrated. The passenger car equivalents that reflect the traffic conditions at the examined roundabouts were calculated on the basis of

different percentages of heavy vehicles that characterized the traffic demand. In this regard AIMSUN software was used to isolate traffic conditions difficult to observe on field, to replicate them, and to have a significant amount of data, i.e. entry capacity values at the roundabout case studies.

To produce the capacity functions C_{car} and C_p, O/D matrices were assigned in AIMSUN so that the traffic demand was, each time, composed of different mixed fleets. In other words, O/D matrices were assigned in AIMSUN so that the traffic demand was composed by a percentage of heavy vehicles p = 0 % (i.e. 100% passenger cars) for obtaining C_{car} (i.e. the base curve) and by different percentages of heavy vehicles (i.e. p = 10%, 20%, 30% up to 100 % heavy vehicles) for obtaining the respective C_p functions (i.e. the mix curves).

In order to deal with the impacts of heavy vehicles operating within mixed traffic streams, the effect of a single class of heavy vehicles (i.e. trucks) was evaluated. The dimensional and operational features of the trucks, as proposed by AIMSUN, included a length ranging from a minimum of 6.00 m to a maximum of 10.00 m, a width ranging from a minimum of 2.00 m to a maximum of 2.80 m, the maximum desired speed of 85 km/h within the range 70–100 km/h, the maximum acceleration of 1 m/s^2 within the range 0.6–1.80 m/s^2, the maximum deceleration of 5 m/s^2 ranging from 4 to 6 m/s^2.

The objective to calculate E_t at single-lane and double-lane roundabouts through equation (2) was then pursued. In order to calculate E_t for each entry lane of the selected roundabouts, the plots of the C_{car} and C_p functions were obtained; they were based upon regressions on simulated data. The critical headways and follow-up headways for each entry lane of the roundabouts selected as case studies were the model parameters to be estimated from the data; they were fitted for heterogeneous populations of vehicles (i.e. different percentages of trucks).

For this purpose, the Hagring's model [54](see Chapter 1) was chosen as the best functional form to perform the regression on simulation output data. A nonlinear regression was then needed to estimate the critical and follow-up headways; they represented the model parameters to be fitted were for the assumed mixed fleets. A specific software, namely Genstat 17.0, was used [55].

Note that in order to carry out statistical regressions, once again Hagring's model [54] was particularized according to the scheme of roundabout (i.e. single-lane or double-lane layout); for the double-lane case study it is obvious that each lane at double lane roundabout entries (i.e. right lane or left lane) was considered.

For completeness of information, the capacity formulas are listed below: equation 3 was used for calculating the capacity of each one-lane entry at the single-lane roundabout and the entry capacity of each right lane at the double-lane approaches; in turn, equation 4 was used for computing the entry capacity of each left lane at the double-lane roundabout approaches. In any case, for more details about these formulas, one can refer to chapter 1.

$$C_e = Q_c \cdot \left(1 - \frac{\Delta \cdot Q_c}{3600}\right) \cdot \frac{exp\left(\frac{-Q_c}{3600} \cdot (T_c - \Delta)\right)}{1 - exp\left(\frac{-Q_c}{3600} \cdot T_f\right)} \tag{3}$$

$$C_e = (Q_{ce} + Q_{ci}) \cdot \left(1 - \frac{\Delta \cdot Q_{ce}}{3600}\right) \cdot \left(1 - \frac{\Delta \cdot Q_{ci}}{3600}\right) \cdot \frac{exp\left(\frac{-Q_{ce}}{3600} \cdot (T_{c,e} - \Delta) \frac{-Q_{ci}}{3600} \cdot (T_{ci} - \Delta)\right)}{1 - exp\left(\frac{-(Q_{ce} + Q_{ci})}{3600} \cdot T_f\right)} \tag{4}$$

where:

- C_e = entry lane capacity;
- Q_c = the circulating traffic flow at single lane roundabout;
- Q_{ce} = the outer circulating traffic flow at double-lane roundabout;
- Q_{ci} = the inner circulating traffic flow at double-lane roundabout;
- T_c = the critical gap for circulating flow at single-lane roundabout;
- T_{ce} = the critical gap for outer circulating flow at double-lane roundabout;
- $T_{,i}$ = the critical gap for inner circulating flow at double-lane roundabout;
- T_f = the follow-up time;
- Δ = the minimum headway of circulating traffic.

Note that the following combinations of circulating flows:

- Q_{ci}/Q_{ce} = 0.25;
- Q_{ci}/Q_{ce} = 0.5;
- Q_{ci}/Q_{ce} = 1;
- Q_{ci}/Q_{ce} = 1.50.

were examined for the double-lane roundabout, in order to examine possible distributions of the circulating flows on the two lanes of the circulatory roadway.

Table 2 and 3 show the results for the critical and follow-up headways on the single-lane entries, while Tables 4, 5 and 6 depict the results of the statistical regressions of the model parameters for the right lane and the left lane at the entries of the double-lane roundabout selected as case study. Note that nonlinear regressions were performed by using Genstat 17.0 software [54]. It is well known that in statistics nonlinear regression is a form of regression analysis where observational data can be modeled by a function which represents a nonlinear combination of the model parameters and depends on one or more independent variables. However, this section did not introduce the theory on the nonlinear regression, but it focuses on the application of this form of regression analysis for estimating the behavioral parameters; for more details on regressions see e.g. [56].

For the case study of single-lane roundabout, Tables 2 and 3 show the estimated values of critical headway and follow up headways with reference to the mixed fleets with the specified (more realistic) percentages of heavy vehicles (i.e. p = 10%, 20%, 30% of heavy vehicles). One can observe that an increase in the percentage of heavy vehicles caused an increase in estimated values of the model parameters.

Table 2 Results of regressions for critical headways on the single-lane roundabout.

Estimation	Fleet			
	10% hv	20% hv	30% hv	100% pc
est [s]	5.13	5.43	5.87	4.85
s.e.	0.06	0.09	0.09	0.05
R^2	0.99	0.99	0.99	0.99
t	92.32	61.71	68.46	88.87
p-value	<.001	<.001	<.001	<.001
UL [s]	5.24	5.60	6.03	4.96
LL [s]	5.02	5.26	5.70	4.75

Note that hv stands for heavy vehicles; pc stands for passenger cars; UL stands for 95% Upper Limit of the confidence interval (α = 0.05) and LL stands for Lower Limit of the 95% confidence interval (α = 0.05); t stands for the t-statistic testing the significance of each regression coefficient; the t-statistic is the ratio of the estimated coefficient (est) to its standard error (s.e.); p-value was obtained in the t-test (α= 0.05).

Table 3 Results of regressions for follow-up headways on the single-lane roundabout.

Estimation	Fleet			
	10% hv	20% hv	30% hv	100% pc
est [s]	2.64	2.78	2.87	2.54
s.e.	0.02	0.03	0.03	0.02
R^2	0.99	0.99	0.99	0.99
t	151.10	100.48	100.28	150.41
p-value	<.001	<.001	<.001	<.001
UL [s]	2.68	2.84	2.92	2.58
LL [s]	2.61	2.73	2.82	2.51

Note that hv stands for heavy vehicles; pc stands for passenger cars; UL stands for 95% Upper Limit of the confidence interval (α = 0.05) and LL stands for Lower Limit of the 95% confidence interval (α = 0.05); t stands for the t-statistic testing the significance of each regression coefficient; the t-statistic is the ratio of the estimated coefficient (est) to its standard error (s.e.); p-value was obtained in the t-test (α= 0.05).

Tables 4, 5 and 6 depict the results of the statistical regressions of the model parameters for the right lane and the left lane at the entries of the double-lane roundabout. According to the Hagring's model [54] particularized for double-lane roundabouts (see Eq. 3 and 4), two critical headways, T_{ce} and T_{ci}, were estimated for the left entry lane of the double-lane roundabout.

Note that the estimated values of critical headways and follow up headways in Tables 4 and 6 are related to the mixed fleets with the specified (more realistic) percentages of heavy vehicles (i.e. p = 10%, 20%, 30% of heavy vehicles); however, the percentage of 100 % of heavy vehicles was also introduced to have some

further insights on the truck behaviour at double-lane entries. Table 5 shows the results of the statistical regressions of the model parameters for the right lane of the double-lane entries for the percentage of heavy vehicles from 40% to 90%; the same results for the left entry lane were omitted for reasons of synthesis.

Table 4 Results of regressions for critical and follow up headways on the double-lane roundabout (right entry lane) in usual operational traffic conditions.

Estimation	Fleet									
	10% hv		20% hv		30% hv		100% pc		100% hv	
	T_c	T_f	T_c	T_f	T_c	T_f	T_c	T_f	T_c	T_f
est [s]	5.19	2.77	5.57	2.90	6.11	2.98	4.54	2.67	9.38	3.61
s.e [s]	0.04	0.01	0.05	0.01	0.05	0.01	0.04	0.01	0.07	0.02
t	137.35	269.28	104.90	195.95	123.27	219.25	121.77	256.36	138.79	213.39
p-value	<.001	<.001	<.001	<.001	<.001	<.001	<.001	<.001	<.001	<.001
UL [s]	5.27	2.79	5.68	2.93	6.21	3.01	4.62	2.69	9.51	3.64
LL [s]	5.12	2.75	5.47	2.87	6.02	2.96	4.47	2.65	9.25	3.57
R^2	0.99		0.99		0.99		0.99		0.99	

Note that hv stands for heavy vehicles; pc stands for passenger cars; UL stands for 95% Upper Limit of the confidence interval ($\alpha = 0.05$) and LL stands for Lower Limit of the 95% confidence interval ($\alpha = 0.05$); T_c stands for critical headway and T_f means follow up headway; t stands for the t-statistic testing the significance of each regression coefficient; the t-statistic is the ratio of the estimated coefficient (est) to its standard error (s.e.); p-value was obtained in the t-test ($\alpha = 0.05$).

Table 5 Results of regressions for critical and follow up headways on the double-lane roundabout (right entry lane).

Estimation	Fleet											
	40% hv		50% hv		60% hv		70% hv		80% hv		90% hv	
	T_c	T_f	T_c	T_f	T_c	T_f	T_c	T_f	T_c	T_f	T_c	T_f
est [s]	6.57	3.08	6.91	3.19	7.43	3.27	7.79	3737	8.29	3.46	8.98	3.51
s.e [s]	0.05	0.01	0.05	0.015	0.06	0.01	0.06	0.01	0.06	0.01	0.08	0.02
t	114.25	196.38	131.94	218.86	117.39	200.74	124.96	198.46	133.82	210	103.59	105.07
p-value	<.001	<.001	<.001	<.001	<.001	<.001	<.001	<.001	<.001	<.001	<.001	<.001
UL [s]	6.68	3.11	7.02	3.22	7.56	3.30	7.92	3.41	8.42	3.50	9.15	3.56
LL [s]	6.46	3.05	6.81	3.17	7.31	3.24	7.68	3.34	8.18	3.43	8.81	3.47
R^2	0.99		0.99		0.99		0.99		0.99		0.98	

Note that hv stands for heavy vehicles; pc stands for passenger cars; UL stands for 95% Upper Limit of the confidence interval ($\alpha = 0.05$) and LL stands for Lower Limit of the 95% confidence interval ($\alpha = 0.05$); T_c stands for critical headway and T_f means follow up headway; t stands for the t-statistic testing the significance of each regression coefficient; the t-statistic is the ratio of the estimated coefficient (est) to its standard error (s.e.); p-value was obtained in the t-test ($\alpha = 0.05$).

Table 6 Results of regressions for critical headways on the double-lane roundabout (left entry lane).

Estimation	Fleet									
	10% hv		20% hv		30% hv		100% pc		100% hv	
	T_{ce}	T_{ci}	T_{ce}	T_{ci}	T_{ce}	T_{ci}	T_{ce}	T_{ci}	T_{ce}	T_{ci}
est [s]	4.74	3.80	5.49	3.98	6.13	4.17	4.01	3.70	10.71	6.48
s.e. [s]	0.09	0.12	0.13	0.17	0.19	0.25	0.09	0.13	0.76	0.96
t	52.43	32.24	42.26	23.57	31.60	16.74	43.23	29.39	14.02	6.73
p-value	<.001	<.001	<.001	<.001	<.001	<.001	<.001	<.001	<.001	<.001
UL [s]	4.92	4.04	5.75	5.24	6.51	4.66	4.19	3.95	12.21	9.21
LL [s]	4.56	3.57	4.32	3.65	5.75	3.68	3.83	3.46	8.37	4.59
R^2	0.99		0.98		0.97		0.98		0.84	

Note that hv stands for heavy vehicles; pc stands for passenger cars; UL stands for 95% Upper Limit of the confidence interval (α = 0.05) and LL stands for Lower Limit of the 95% confidence interval (α = 0.05); T_{ce} stands for critical headway for the right entry lane; T_{ci} stands for critical headway for the left entry lane and T_f means follow up headway; t stands for the t-statistic testing the significance of each regression coefficient; the t-statistic is the ratio of the estimated coefficient (est) to its standard error (s.e.); p-value was obtained in the t-test (α= 0.05).

The trends which appear in the Tables, 4, 5 and 6, show that lower model parameters resulted when the percentages of heavy vehicles decreased from p=100 % to p=0% (where this last percentage is equivalent to 100% passenger cars). According to literature on the topic (see e.g. [29][57]), for both roundabouts the model parameters increase when the percentages of heavy vehicles increase from p=0 % to p=100%. In this regard, it should be noted that heavy vehicles reduce the vehicular capacity at roundabouts, especially with a higher entering volume of trucks. Moreover, the space and maneuvering requirements of most trucks entering a roundabout are restricted by size and operational features which, in turn, affect the driver gap acceptance behaviour.

3.1. PCEs calculation for the case study of single-lane roundabout

Once the parameters of the model were estimated through a non-linear regression analysis for different percentages of heavy vehicles and each one-lane entry of the case study of single-lane roundabout, calculation of PCEs was performed by using Eq. 2. Note that geometric design features of the single-lane roundabout have been already specified in chapter 4.

Since the capacity functions C_{car} and C_p are depending on the circulating flow, the equivalent factors E_t are a function of the circulating flow (see Fig. 2): indeed, E_t is depending on the circulating flow along the one-lane circulatory roadway.
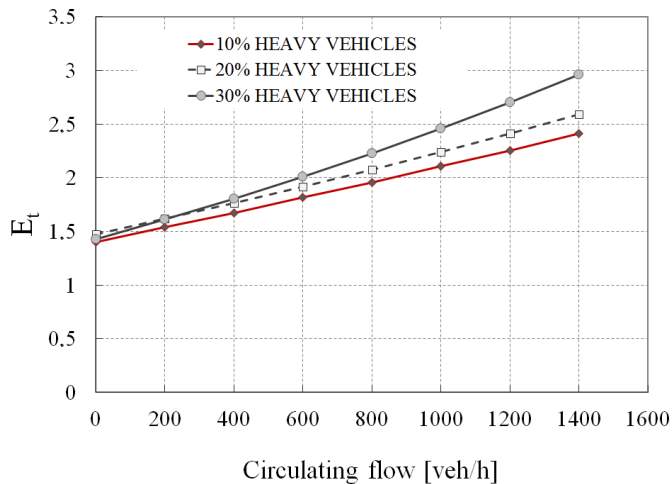
Figure 2 PCE estimations on 4-leg, at grade, single-lane roundabout

Figure 2 shows that, for the different mixed fleets (i.e. 10%, 20%, 30% of heavy vehicles), and for Q_c ranging from 0 to 600 veh/h, E_t is increasing, but it keeps values less than (or equal to) 2. For Q_c ranging from 600 to 800 veh/h, E_t is about 2 for a mixed fleet with 20% or 10% of heavy vehicles. For all fleets, E_t exceeds 2 when Q_c is increasing from (about) 900 veh/h onwards, or when traffic conditions for the circulating flow are close to the saturation level. The results confirmed that the impacts of heavy vehicles on the traffic streams at the single-lane roundabouts can be quite different from that on the uninterrupted flow facilities (including free- ways, multilane highways, weaving segments, and merge and diverge segments on freeways or multilane highways) and other interrupted flow facilities. Differently from HCM 2010 [2] which assumes a heavy vehicle to be equivalent to two passenger cars and sets as 2.0 the PCE for heavy vehicles for roundabouts, a higher PCE effect would be expected on the quality of traffic conditions when the traffic stream contains a high number of heavy vehicles. Based on these results:

- if one assumes E_t=2 according to Highway Capacity Manual [2], the impact of heavy vehicles on the traffic flow quality, even in usual operational conditions (i.e. a mixed fleet with 10% or 20% of heavy vehicles), can be overestimated with Q_c about below 800 veh/h;
- if one assumes E_t=2 as HCM [1] proposes, the impact of heavy vehicles is, in turn, underestimated with Q_c above 900 veh/h, since E_t exceeds 2 (E_t=3 is only reached for a mixed fleet with 30% of heavy vehicles in saturated conditions of the circulatory roadway).

However, it should be noted that heavy vehicles here considered (with a length less than 10 m) are only a part of heavy vehicles which were simulated to estimate the HCM PCE values [2].

3.2. PCE calculations for the case study of double-lane roundabout

With reference to the double-lane roundabout case study, again Et were calculated based on the criterion specified before (see section 2). Note that geometric design features of the double-lane roundabout have been already specified in chapter 4.

In order to represent E_t for double-lane roundabout by using Eq. 2, it should be noted that since the capacity functions C_{car} and C_p are depending on the circulating flow, for the right entry lanes, the equivalent factors shall also depend on the circulating flow Q_{ce} in the outer lane of the circulatory roadway. For the left entry lanes, in turn, the equivalent factors are depending on the inner circulating flow Q_{ci} and the outer circulating flow Q_{ce} on the two circulating lanes of the ring. Thus, in the case of the left entry lane, surface plots have been generated for graphing the PCEs versus Q_{ci} and Q_{ce} on the circulatory roadway.

Figure 3 shows the estimation of PCEs for the right entry lane for a percentage of heavy vehicles from 10% to 100%; note that since no significant difference was given between the PCEs for p=10%, 20% and 30%, only a mean curve corresponding to the three (mixed) traffic conditions before mentioned was plotted.
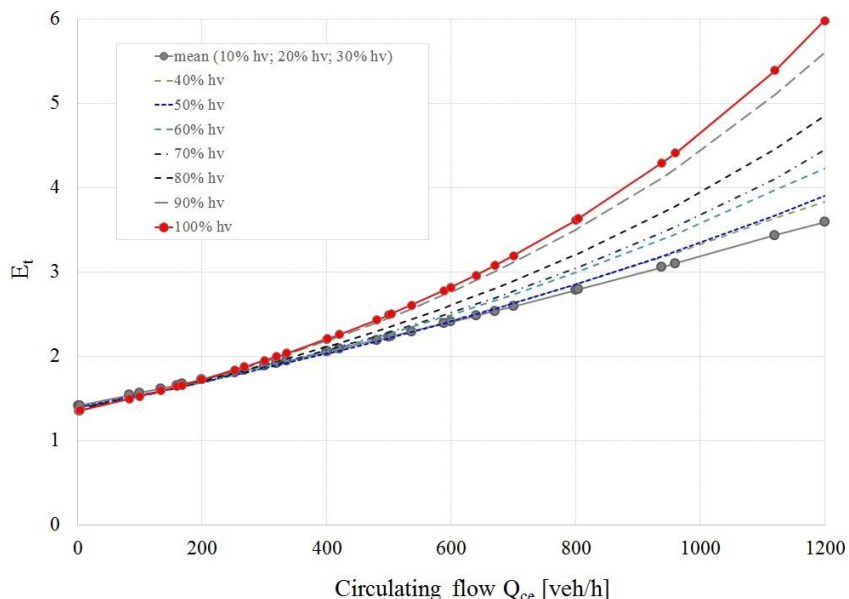

Figure 3 PCE estimations on double-lane roundabout – right entry lane.

Note that hv stands for heavy vehicles, while Q_{ce} stands for the circulating flow in the outer lane of the circulatory roadway; E_t stands for equivalent factor.

The results in Figure 3 show that E_t increases and keeps values of around 2 when Q_{ce} in the outer lane of the ring ranges from 0 to 400 veh/h. E_t goes up further as

Q_{ce} increases from 400 veh/h to 800 veh/h, but it resulted a little less than 4. E_t is increasing for Q_{ce} ranging from 800 veh/h on wards for the mixed fleet, but remains below 4 also for high values of the circulating flow in the outer lane of the ring, except for a percentage of heavy vehicles greater than 80%. In this latter case, in fact, PCEs reach values beyond the threshold of 4. Only for informative intention, the same Figure 3 also shows the plot of the PCEs versus Q_{ce} for the unrealistic situation of traffic demand with 100% heavy vehicles; in this case, higher values of PCEs are determined than usual operational conditions. Only for informative intention, the same Figure 3 also shows the plot of the PCEs versus Q_{ce} for less realistic situations of traffic demand with percentages of heavy vehicles under p = 40%-100%; in these cases, higher values of the equivalent factors were determined than usual operational conditions represented by the mean curve corresponding to the three mixed (more realistic) traffic conditions with p =10%, 20% and 30%. However, it should be noted that E_t increases and again keeps values of around 2 when Q_{ce} in the outer lane of the ring ranges from 0 to 400 veh/h. Et goes up further as Q_{ce} increases from 400 veh/h to 800 veh/h, but it keeps values of around 3 for the mixed fleets with a percentage of heavy vehicles less than or equal to p = 80%. E_t is increasing for Q_{ce} ranging from 800 veh/h onwards for the mixed fleets, but remains below 4 also for high values of the circulating flow in the outer lane of the ring (up to about Q_{ce} = 1000 veh/h) and high percentages of heavy vehicles (up to the percentage of heavy vehicles less than or equal to p = 80%). E_t goes up further as Q_{ce} increases from around 1000 veh/h onwards.

It is noteworthy that especially for high vehicular conflicting flows (and already when Q_{ce} reaches out beyond 400 veh/h), the effect of heavy vehicle on vehicular operations is a little more pronounced with a low heavy vehicles percentage than for right lane on single-lane roundabouts (see Fig .2).
In turn, Figures 4 and 5 depict the surface plots of the PCEs for the left entry lane on the double-lane roundabout. As in the case of the right entry lane, the results of E_t under p =10%, 20% and 30% are shown, since the mixed fleets with these percentages of heavy vehicles are more realistic and can occur frequently in traffic conditions on real-world. However, since a synthesis is also needed, the surface plots under p = 40%-100% were omitted. Specifically, Figure 4 shows the surface plot when the heavy vehicles percentage is set equal to 10%; in turn, Figure 5 shows the mean surface plot which was considered as representative for the traffic scenarios with p = 20% and 30%, given that no relevant difference resulted in PCE calculation when each of these two percentages was simulated with AIMSUN.
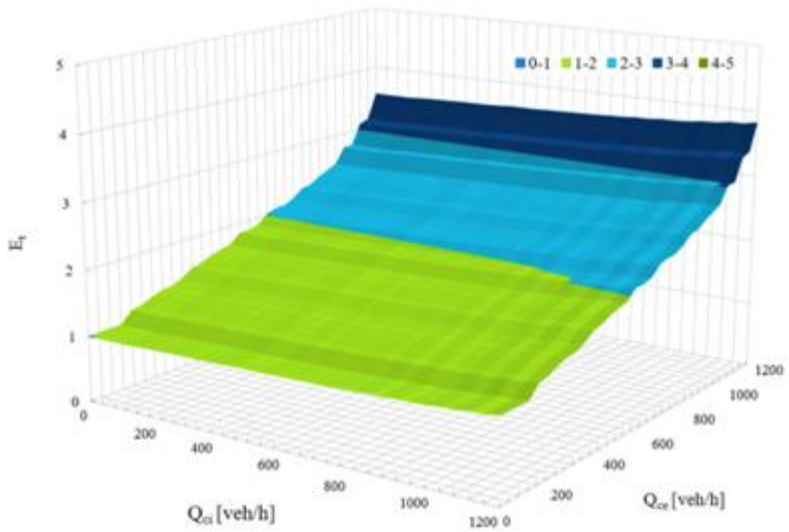
Figure 4 PCE estimations on double-lane roundabout – left entry lane (heavy vehicles percentage of 10 %)

Note Q_{ce} = circulating flow in the outer lane of the circulatory roadway; Q_{ci} = circulating flow in the inner lane of the circulatory roadway; E_t = equivalent factor.
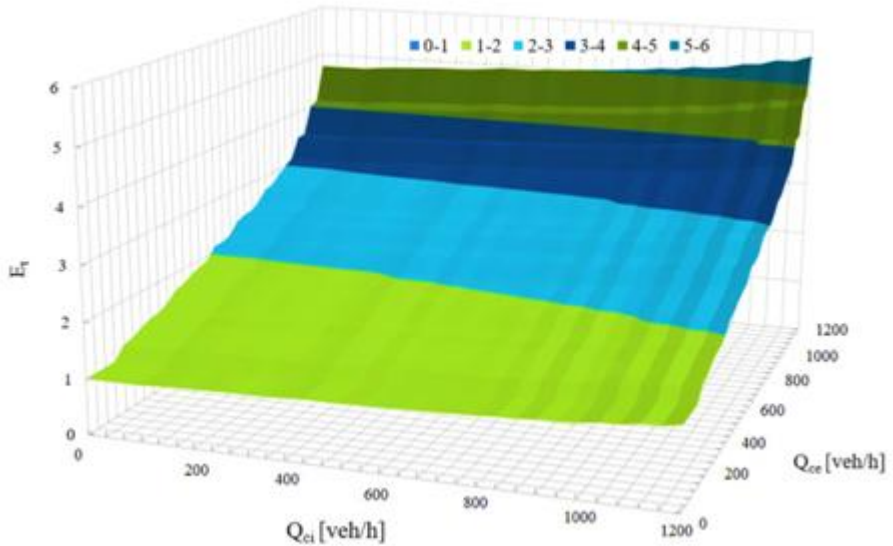

Figure 5 PCE estimations on double-lane roundabout – left entry lane (mean percentage of heavy vehicles between 20 % and 30%).

Note Q_{ce} = circulating flow in the outer lane of the circulatory roadway; Q_{ci} = circulating flow in the inner lane of the circulatory roadway; E_t = equivalent factor.

191

Figure 6 shows, for illustrative purpose only, the surface plot with reference to the percentage of heavy vehicles equal to 100 %; it is obvious that is corresponding to unrealistic traffic conditions and comments will be omitted.
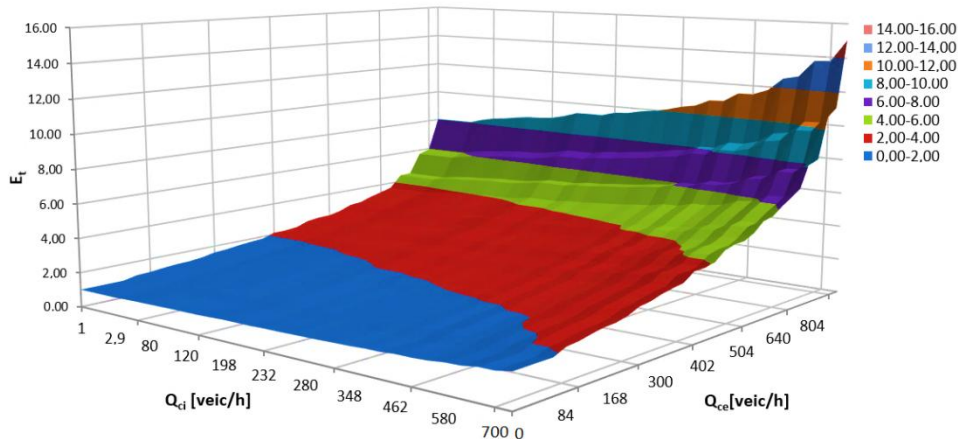

Figure 6 PCE estimations on double-lane roundabout – left entry lane (heavy vehicles percentage of 100%)

Note Q_{ce} stands for the circulating flow in the outer lane of the circulatory roadway, while Q_{ce} stands for the circulating flow in the inner lane of the circulatory roadway.

Specifically, Figure 4 shows the case when the percentage of heavy vehicles is equal to 10%, whereas Figure 5 shows the mean surface plot which was considered representative for the traffic scenarios with p = 20% and 30%; this choice was made given that no relevant difference resulted in PCEs when each of these two percentages was simulated with AIMSUN. Results in the above surface plots show that an E_t just under 4 can be reached with 10% of heavy vehicles (see Figure 4), while an E_t just over 5 can be reached with 20% or 30% of heavy vehicles (see Figure 5). Thus, keeping constant the value of Q_{ce}, the PCEs increase when Q_{ci} increases; in turn, keeping constant the value of Q_{ci}, one can observe a similar trend of PCEs when Q_{ce} increases.

As a consequence, if one set Et = 2 to adjust the flow rates for heavy vehicles as proposed by the HCM [2] for roundabouts, an underestimation of the effect of heavy vehicles on the quality of traffic flow may result. Such a result has been found to be consistent with the conclusions already drawn from [31] as discussed in Section 2; the Author, indeed, recommended values of passenger car equivalents different from what the HCM [2] proposes for roundabouts.

4. Conclusive comments

As a general remark, it should also be noted that a higher percentage of heavy vehicles reflected reduced values of the simulated capacity at entries. Heavy

vehicles contribute to reduce the vehicular capacity of each entry lane at entries and this effect is expected to be more pronounced with a higher entering volume of heavy vehicles. There is considerable evidence that unlike passenger cars, the space and manoeuvring requirements of most heavy vehicles approaching a roundabout are considerably restricted by their size and operational performances; this can affect gap acceptance behavior of the heavy vehicles that approach the roundabout and enter the circulatory roadway.

Differently from methods that propose constant values for the passenger car equivalents, the results highlighted that PCEs for heavy vehicles were depending on operations at the double-lane roundabout. Since the capacity depends on the circulating flow, PCEs also depend on the circulating flow. Specifically, for the right entry lane the PCEs depend on the circulating flow in the outer lane of the ring, while for the left lane the PCEs resulted dependent from the two circulating flows, one in the outer lane and one in the inner lane of the ring. A significant number of heavy vehicles in the traffic stream gave rise to an increase in the PCE values. For both entry lanes, analogous trends were observed; PCEs increased when the circulating flow increased, especially when the traffic streams contained a higher number of heavy vehicles. Thus, assuming constant values of PCEs for roundabouts as those provided by the HCM [2], the effect of trucks on traffic conditions could be interpreted improperly.

References

1. Roess, R.P. & Prassas, E.S. (2014). The Highway Capacity Manual: A Conceptual and Research History Vol. 1. Springer Tracts on Transportation and Traffic 5. London: Springer.

2. Highway Capacity Manual. (2010). Transportation Research Board. (5th ed). Washington DC: Transportation Reesarch Board.

3. AIMSUN Dynamic Simulator User Manual, Transport Simulation System (TSS) version 8, Barcelona, 2011.

4. Zhen (Sean), Q., Jia, L., Li, X., Zhang, M., Wang, H. (2017). Modeling heterogeneous traffic flow: A pragmatic approach. Transportation Research Part B: Methodological 99, 183-204.

5. Anwaar, A., Van Boxel, D., Volovski, M., Anastasopoulos, P.C., Labi, S., Sinha, K. C. (2011). Using Lagging Headways to Estimate Passenger Car Equivalents on Basic Freeway Sections. Journal of Transportation of the Institute of Transportation Engineers 2(1), 5–17.

6. Nassiri, H., Tabatabaie, S., Sahebi. S. (2017.) Delay-based Passenger Car Equivalent at Signalized Intersections in Iran. Promet- Traffic & Transportation 29(2), 135-142.

7. Al-Kaisy, A. (2006). Passenger car equivalents for heavy vehicles at freeways and multilane highways: some critical issues. ITE Journal 76(3), 40–43.

8. Sarraj, Y.R. (2014). Passenger car equivalents at signalized intersections for heavy and medium trucks and animal driven carts in Gaza, Palestine. International Journal of Emerging Technology and Advanced Engineering 4(2), 80-88.

9. Kimber, R.M., McDonald, M., Hounsell, N. (1985). Passenger car units in saturation flows: Concept, definition, derivation. Transportation Research Part B: Methodological 19(1), 39-61.

10. Benekohal, R., Zhao, W. (2000). Delay-Based Passenger Car Equivalents for Trucks at Signalized Intersections. Transportation Research Part A 34, 437–457.

11. Huber, M.J. (1982). Estimation of passenger-car equivalents of trucks in traffic stream. Transportation Research Record 869, 60–70.

12. Arasan, V. T., Arkatkar, S.S. (2010). Microsimulation study of effect of volume and road width on PCU of vehicles under heterogeneous traffic. Journal of Transportation Engineering 136(12), 1110–1119.

13. Mohan, M., Chandra, S. (2016). Concept of queue clearance rate for estimation of equivalency factors at priority junctions. Canadian Journal of Civil Engineering 43(7), 593-598.

14. Aumann, P., Whitehead, M. (2015). Austroads Guide to Road Design Part 4b - Roundabouts. Sydney, N.S.W. Austroads, December 2015. pp. 84.

15. AUSTROADS. (2011). VicRoads Supplement to Austroads Guide to Road Design – Part 4B roundabouts.

16. AUSTROADS (1993). Guide to traffic engineering Practice; Part 6 – Roundabouts, Sydney, Australia.

17. Benekohal, R., Zhao, W. (2000). Delay-Based Passenger Car Equivalents for Trucks at Signalized Intersections. Transportation Research Part A 34, 437–457.

18. Webster, N., Elefteriadou, L. (1999). A simulation study of truck passenger car equivalents (PCE) on basic freeway sections. Transportation Research Part B: Methodological 33(5), 323-336.

19. Al-Kaisy, A., Hall, F., Reisman, E. (2002). Developing Passenger Car Equivalents for Heavy Vehicles on Freeways During Queue Discharge Flow. Transportation Research Part A 36(8),725-742.

20. Keller, E.L., & Saklas. J.G. (1984). Passenger Car Equivalents from Network Simulation. Journal of Transportation Engineering 110(4), 397–411.

21. Kiran, S., Verma, A. (2016). Review of Studies on Mixed Traffic Flow: Perspective of Developing Economies. Transportation in Developing Economies, 2:5.

22. National Research Council, and Transportation Research Board. (2010). HCM 2010: Highway Capacity Manual. Washington, DC: Transportation Research Board.

23. FGSV Ed. (2015). Handbuch für die Bemessung von Straßenverkehrsanlagen (HBS) Edition 2015 [German Highway Capacity Manual]. Forschungsgesellschaft für Straßen und Verkehrswesen (FGSV) [Road and Transport Association]. Cologne, edition 2015.

24. Craus, J., Polus, A., Grinberg, I. (1980). A revised method for the determination of passenger car equivalencies. Transportation Research Part A: General 14(4), 241-246.

25. Geistefeldt, J. (2009). Estimation of passenger car equivalents based on capacity variability. Transportation Research Record: Journal of the Transportation Research Board 2130, 1–6.

26. Giuffrè, O., Granà, A., Giuffrè, T., Marino, R. (2012). Researching a capacity model for multilane roundabouts with negotiation of the right-of-way between antagonist traffic flows. Modern Applied Science 6(5), 2-12.

27. Giuffrè, O., Granà, A., Tumminello, M.L., Sferlazza, A. (2017). Estimation of Passenger Car Equivalents for single-lane roundabouts using a microsimulation-based procedure. Expert Systems with Applications 79, 333-347.

28. Giuffrè, O., Granà, A., Marino, S. & Galatioto, F. (2016a). Microsimulation-based passenger car equivalents for heavy vehicles driving turbo-roundabouts. Transport 31 (2), 295-303.

29. Dahl, J., Lee, C. (2012). Empirical estimation of capacity for roundabouts using adjusted gap-acceptance parameters for trucks. Transportation Research Record 2312, 34–45.

30. Yap, Y.H., Gibson, H.M., Waterson, B. J. (2013). An international review of roundabout capacity modelling. Transport Reviews 33(5), 593-616.

31. Lee C. (2015) Developing passenger-car equivalents for heavy vehicles in entry flow at roundabouts, Journal of Transportation Engineering 141(8): 1--1.

32. Troutbeck, R.J. (1988). Current and future Australian practice for the design of unsignalised intersections. In: W. Brilon (ed.) Intersections Wthout Traffc Signalis, Proceedings of an International Workshop, Bochum, West germany, Srnger-Verlag, Berlin, pp. 1-19.

33. List, G. F., Yang, B., Schroeder J.B. (2015). On the treatment of trucks in roundabout analyses. Transportation Research Record 2483, 140–147.

34. Otković, I. Tollazzi, T., Šraml, M. (2013). Calibration of microsimulation traffic model using neural network approach. Expert Systems with Applications 40(15), 5965-5974.

35. Valdez, M., Cheu, R.L., Duran, C. (2011). Operations of modern roundabout with unbalanced approach volumes. Transportation Research Record 2265, 234–243.

36. Kang, N., Nakamura, H. (2016). An analysis of heavy vehicle impact on roundabout entry capacity in Japan. Transportation Research Procedia 15, 308-318.

37. Sumner, R., Hill, D. & Shapiro, S. 1984. Segment Passenger Car Equivalent Values for Cost Allocation on Urban Arterial Roads. Transportation Research 18A (5/6), 399-406.

38. Macioszek, E. (2010). Analiza Wpływu Stopnia Obciążenia Ruchem na Wartość Współczynnika Przeliczeniowego dla Pojazdów Ciężkich na Skrzyżowaniach Typu Rondo [Analysis of the influence of the traffic load on the value of car equivalents for heavy vehicles on roundabouts]. Logistyka [Logistics] 6, 2071–2079 (in Polish).

39. Macioszek, E. (2012). Geometrical determinants of car equivalents for heavy vehicles crossing circular intersections. In: Mikulski J. (eds) Telematics in the Transport Environment, TST 2012. Communications in Computer and Information Science 329, 221-228. Springer, Berlin, Heidelberg.

40. Tanyel, S., Caliskanelli, S.P., Aydn M.M., Utku, S, B. (2013). An investigation of heavy vehicles effect on traffic circles. Digest 2013, 1675-1700.

41. List, G. F., Yang, B., Schroeder J.B. (2015). On the treatment of trucks in roundabout analyses. Transportation Research Record 2483, 140–147.

42. Lenters, M., Rudy, C. 2010. HCM Roundabout Capacity Methods and Alternative Capacity Models. *ITE Journal 80(7)*, 22-27.

43. Robinson, B. W., Rodegerdts, L., Kittelson, W. et al. (2000). Roundabouts. An informational Guide. Federal Highway Administration. United States Department of Transportation, Publication No. FHWA-RD-00-067 FHWA.

44. Kimber, R.M. (1989). Gap-Acceptance and Empiricism in Capacity Prediction. *Transportation Science* 23(2), 100-111.

45. Overton, R. (2016). Evaluation of Heavy Vehicles on Capacity Analysis for Roundabout Design. NEXTRANS Project No. 180TUY2.2. USDOT Region V Regional University Transportation Center Final Report.

46. Louah G. (1992). Panorama critique des modeles français de capacité des carrefours giratoires. Actes du séminaire international Giratoires '92 [*Roundabouts, 1992*], Nantes, France, 1992.

47. CERTU (1999). Carrefours urbains Guide, Lyon France 1999.

48. Guichet, B. (2005). Roundabouts in France and new use. TRB Transportation research, National Roundabout Conference proceedings 2005, Vail Colorado, USA, 22-25 May, 2005.

49. Akcelik, R. (2004). aaSIDRA user Guide. Akcelik and Associates Pty ltd, Melbourne, Australia.

50. Bovy, P.H. (1991). Zusammenfassung des Schweizerischen Kreiselhandbuchs [Summary of Swiss Roundabout Guide], In: Straße und Verkehr 3/1991, S. 129-139, in German.

51. Brilon, W., Stuwe, B. (1993). Capacity and design of traffic circles in Germany*. Transportation Research Record* 1398, 61-67

52. Wu, N. (2001). A universal procedure for capacity determination at unsignalized (priority-controlled) intersections. *Transportation Research Part B: Methodological* 35(6), 593–623.

53. Brilon, W. (2014). Roundabouts: A State of Art in Germany. In 4th International Conference on Roundabouts. Transportation Research Board, Seattle, April 2014.

54. Hagring, O., (1998). A further generalization of Tanner's formula. Transportation Research Part B: Methodological, 32(6), 423–429.

55. GenStat for Windows, 17th Edition, V.

56. Bethea R. M., Duran B. S.; Boullion T. L. (1985). Statistical Methods for Engineers and Scientists. New York: Marcel Dekker.

57. Giuffrè, O., Granà, A., Marino, S., Galatioto, F.: Microsimulation-based passenger car equivalents for heavy vehicles driving turbo-roundabouts, Transport 31(2): 295-303 (2016).

CHAPTER SIX

Surrogate safety measures at roundabouts in AIMSUN and VISSIM environment

1. Introduction

Roundabouts have been increasingly used in recent years either as new road infrastructures or as substitutes for unsignalized or signalized four-leg intersections, and have been chosen all over the world as effective engineering countermeasures for their innumerable advantages involving increased capacity and positive impact on the environment, and especially improvement in intersection safety performance than other intersection configurations and control mode. Nowadays modern roundabouts and, more recently, alternative roundabouts (as turbo roundabouts) are becoming increasingly attractive to transportation engineers which focus their attention on developing road safety measures and assessment tools for management purposes. To be able to predict as precisely as possible the number of crashes and even more to know the causes behind them is the challenge of many road engineers, since this can represent the starting point for building new, more safe infrastructures, or upgrading existing road facilities to highest levels of safety.

Crashes are complex events, being the result of the combination of several factors such as road, vehicle, human behavior, roadway environment, traffic conditions, and so on. Traditional approaches to estimate potential traffic conflicts are based on real crash data occurred on field; however, these techniques present a series of shortcomings essentially related to the availability of crash data that is in some case still limited by adequate or up-to-date databases.

It is well-known that crashes are rare events, and their on-field collection not only would require a long observation time, but does not take into account some information, such as the drivers' behavior preceding the crash, the causes behind it, traffic operating conditions at the time of the collision, and so on; moreover, minor crashes, with a small severity, are often not even recorded [1]. These lacunae in the observed crash data can be overcome by using *traffic conflict techniques* which analyze the road situations from the aspect of more observable traffic conflicts (and other events associated with safety and operations) than crashes [2], and surrogate measures of safety introduced most recently to explore the safety performance of any road facility through simulated vehicle trajectories exported from microscopic simulation models; see e.g. [3].

Based on this premise, the goal of the research activity described in this chapter was to explore safety performance of three different roundabout schemes (i.e. single-lane, double-lane and turbo roundabouts) through surrogate measures of safety. For each roundabout under examination, a comparison was performed based on the trajectory files derived from VISSIM [4] and AIMSUN [5]. Thus, these

traffic microsimulation models were used to build, for each roundabout, a model calibrated on the same empirical capacity function; the last function was based on a meta-analytic estimation of the critical and follow-up headways (see chapter 2). Furthermore, in order to explore the implications of various traffic volume distributions on the safety performance of the selected roundabouts, different traffic flow scenarios were simulated; for each roundabout, three origin-destination matrices were then developed by using an iterative process so as to ensure a pre-fixed saturation ratio at each entry [6]. For each roundabout, the simulated vehicle trajectories exported from AIMSUN and VISSIM were used to perform a conflict analysis through the Surrogate Safety Assessment Model (SSAM).

The SSAM results processed from the two traffic microsimulation models provided a very high number of potential conflicts especially when SSAM default filters were used. Since the output from the two software also resulted strongly different, it was deemed necessary to set iteratively some SSAM filters, in order to render the output from AIMSUN and VISSIM comparable.

In the following sections, after a brief literature review on safety measures and SSAM applications, the calibration of the microscopic traffic models here used will be described; thus, the assessment of safety performance through surrogate measures of safety for the roundabouts select as case studies (i.e single-lane, double-lane and turbo roundabouts) will be explained. Finally, the results in terms of surrogate measures of safety obtained by means of SSAM application will be commented on.

2. Literature review on safety measures and SSAM applications

As introduced above, a conflict can be defined as a situation in which two or more users move so close to each other in time and space that there could be a risk of collision if they do not take any action to change their position [2]. The traffic conflicts technique, developed at the beginning of the 1960s, utilizes field observers to identify crashes that have occurred and conflict events by watching dangerous maneuvers. The main criticism of the technique is that the subjectivity of field observers may cause additional uncertainty in the collection of accurate data on conflicts [3].

Furthermore, these methods do not allow future assessment about safety on new roads and intersections; besides, the influence that different traffic flow scenarios could have on the number of crashes is unknown.

An alternative approach recently used refers to the employment of surrogate safety measures that makes it possible to explore the safety performance of any road facility through simulated vehicle trajectories exported from traffic microsimulation models. These surrogate measures are based on the identification, classification, and evaluation of traffic conflicts that occur during microsimulation. This approach eliminates the subjectivity associated with the

conventional conflict analysis technique and makes it possible to assess the safety of a road infrastructure under a controlled environment, before a crash occurs. [2].

Recent advances in research and applications to road and highway design and transportation engineering have outlined the great potential for useful application of microscopic traffic simulation models to accurately account not only for traffic conditions, but also for analyzing the safety performance of roads and intersections. Indeed, they are able to capture the interactions of road traffic and simulate drivers' behavior, through a series of also complex algorithms describing car following, lane changing and gap acceptance as they occur in the real world. In this regard, Gettman & Head [4] used micro-simulation as a tool to analyze traffic safety conditions and obtained measures with much more detail than the subjective measures based on field observation. In turn, since the time for collection data is not limited, as happens on field, several operational scenarios can be simulated. Moreover, micro-simulation is able to reproduce changes that occur at the traffic-flow level and different choice of routes for vehicles. This means that the micro-simulation also takes into account a potential conflict that does not necessarily have a direct relationship with actual observed conflicts or with recorded crashes. On the other hand, it is also true that the effectiveness and the usefulness of microscopic traffic simulation models for analysis of traffic safety situations depends on the ability of these models to consider, during the simulation process, any behavioral relationships that could lead to crashes and establish a relationship between simulated safety measures and the likelihood of crash occurrence in real world. However, common micro-simulators have within several model parameters to set, and so many ways to model traffic in road networks, i.e. traffic arrival, priority rules, road geometry, and so on; thus, the conflicts estimated through micro-simulation models could be affected by these choices [7].

Micro-simulation outputs derived from the trajectory file in which the position of all vehicles in the network, for each simulation step, is identified, represent the starting point for carrying out a safety road analysis through surrogate safety measures. Safety road analysis through surrogate safety measures can be conducted by a software application. In this regard, one can remember the Surrogate Safety Assessment Model (SSAM) which reads trajectories files generated by micro-simulators. SSAM also calculates the number of potential conflicts and categorizes these in three types based on the directions of colliding path vehicles; for each pair of vehicles involved in the conflict, it evaluates the surrogate measures of safety.

In a recent research, SSAM was used for predict conflicts in three intersections, i.e. four-leg priority intersection, four-leg staggered intersection, and single-lane roundabout [2]. In this case, before performing the safety analysis, SSAM was validated with two methods: the output derived from SSAM were compared, firstly, with the number of the conflict calculated with crash prediction models

and then with conflicts observed on field. In turn, Essa& Sayed [7] used SSAM for evaluating surrogate safety measures of urban signalized intersections; they compared the conflicts estimated from two traffic microsimulation models (i.e. VISSIM [4] and PARAMICS [8] to crash data. Safety performance of freeway merge areas was also analyzed trough SSAM by using conflicts simulated from VISSIM micro-simulator [9]. The field-measured traffic conflict was used to improve the calibration of the microscopic traffic simulation models and for adjusting the threshold values in SSAM.
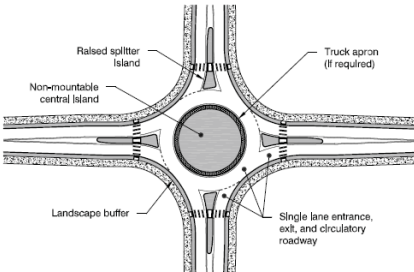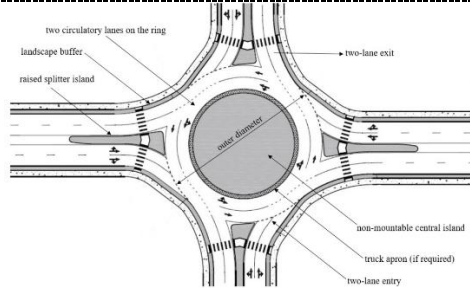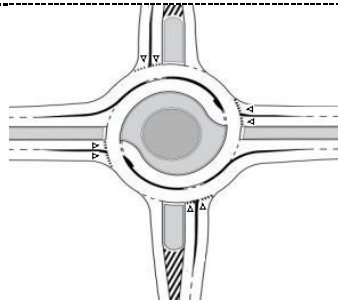
A comparison related to safety performance through surrogate measures of safety for roundabouts was conducted by Vasconcelos et al [10]. In this case, SSAM, after validation based on outputs of crash prediction models, was used to assess the safety performance of three roundabout selected as case studies, i.e. single-lane, double-lane and turbo roundabouts. The authors found that the safety performance was comparable for turbo-roundabouts and single-lane roundabouts.

Since the assessment of safety performance of any road facility, by means of surrogate safety measures, goes through the processing of trajectory files generated by a micro-simulator, it is clear that this safety analysis will depend strongly on microscopic traffic simulation models. In turn, the outputs of the micro-simulation, i.e. the trajectory file, not only depends on the choices made by the analyst in the building step of the microscopic traffic simulation model, but could also depend on the micro-simulator used.

3. Data descriptions and preliminary analysis

Three roundabouts were selected: a single-lane roundabout, a double-lane roundabout and a turbo roundabout, all of these with design characteristics based on current geometrical Italian standards [11, 12]. Note that the characteristics of the geometric design of the single-lane roundabout selected as study case are the same as those used in the GA-based calibration procedure in Chapter 4. The same goes for the study case of double-lane roundabout, in which both entries and exits are composed by two lanes and the width of the outer diameter placed this scheme among conventional roundabouts [11]. In turn, the turbo roundabout geometric design for the selected case study was chosen consistent to the turbo design proposed by Giuffrè et al. [13]. Table 1 shows the three roundabout layouts selected as study cases; the geometric characteristics are indicated for each of them.

Table 1 Geometric characteristics of three roundabout layout selected as case studies

Roundabouts layout designed in AIMSUN and VISSIM micro-simulators	outer diameter [m]	circulatory roadway width [m]	entry lane width [m]	exit lane width [m]
	39.00	7.00	3.75	4.50
	41.00	9.00	3.50	4.50
	just over of 40 m	inside lane width of 4.50 m, an outside lane width of 4.20 m	3.50	4.50

3.1. Calibration of microscopic traffic simulation models

In order to carry out a comparison of estimates produced by the SSAM software in terms of conflict frequencies simulated with AIMSUN and VISSIM, the starting point was to calibrate the two microscopic simulation models on the same input data. Since the network models of single-lane, double-lane and turbo roundabout were already calibrated in AIMSUN, the next task was to these roundabout models were built and calibrated in VISSIM. The calibration procedure in VISSIM was conducted manually and, as for AIMSUN, the calibration parameters were preliminarily identified by using a sensitivity analysis. Calibration of the

roundabout models built in VISSIM was performed comparing the simulated output of capacity with an empirical capacity function; this last function was the same used for calibrating the roundabout models built in AIMSUN (see chapter 4).

The VISSIM microscopic simulation package (version 8.0) was used for microscopic modelling of the single-lane, double-lane and turbo roundabouts, each of these having the same geometric characteristic as the models built in AIMSUN (see Table 1). The first step for building each microscopic model consisted in represent the roundabouts both graphically and from an operational and functional point of view. In the VISSIM micro-simulator, roadway networks are usually represented by graphs with nodes located at intersections and links placed on road segments [4]. The links are joined to each other by connectors for merging, crossing, and splitting the traffic flows. Each link has certain properties including e.g. the planar coordinates of its alignment, the number of lanes with lane widths, and some optional properties describing the characteristics of the road. Thus, once the roundabouts, according to the layouts selected as case studies (see Fig. 1), were represented with a succession of links and connectors, the next step was to attribute the yield-rule to the entry lanes.
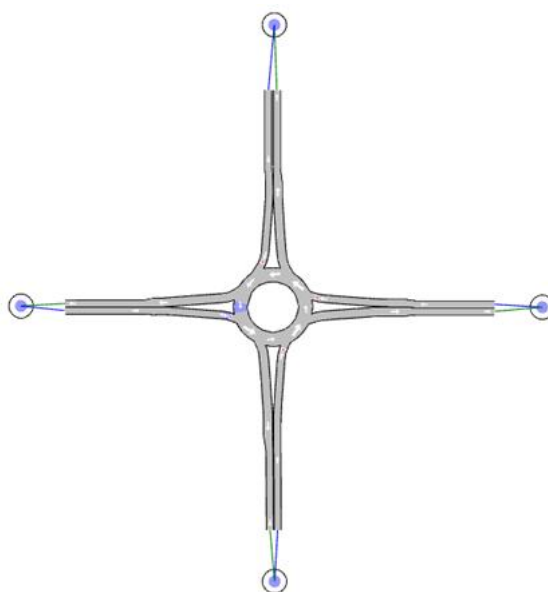

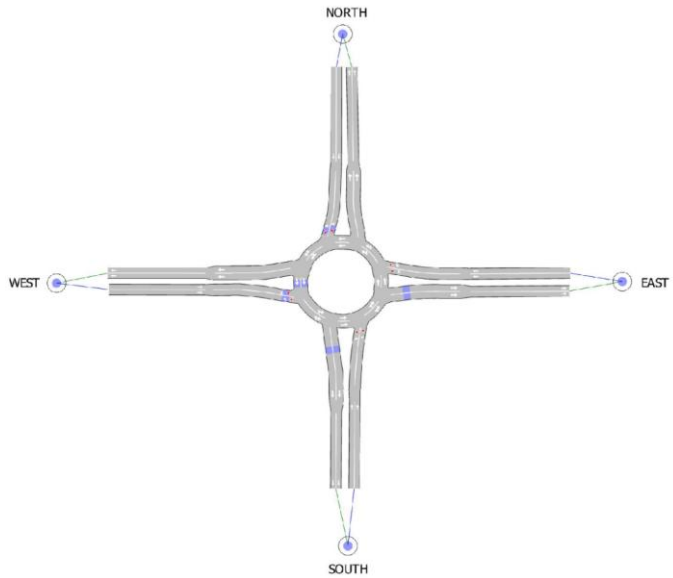**Figure 1** The AIMSUN model of the single-lane roundabout

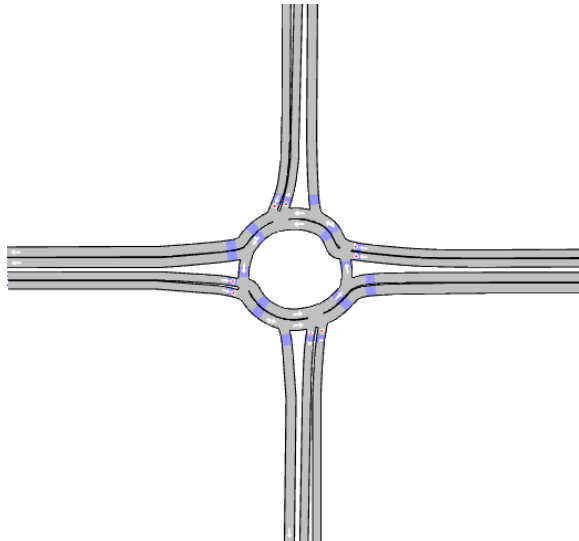**Figure 2** The AIMSUN model of the double-lane roundabout

Figure 3 The AIMSUN model of the turbo roundabout

Table 2 Default and set values of parameters used in manual calibration for the single-lane roundabout

Aimsun parameters	Default values	Set Value
Reaction time [s]	0.80	0.86
Minimum Headway [s]	0.00	1.58
Speed Acceptance:	1.10	1.00

Table 3 Default and set values of parameters used in manual calibration for the double-lane roundabout

Aimsun parameters	Entry lane	Default values	Set Value
Reaction time [s]	*Right*	0.80	0.94
	Left	0.80	0.95
Minimum Headway [s]	*Right*	0.00	1.00
	Left	0.00	1.33
Speed Acceptance:	*Right*	1.10	0.95
	Left	1.10	0.97

Table 4 Default and set values of parameters used in manual calibration for the turbo roundabout

Aimsun parameters	Default values	Set Value
Reaction time [s]	1.35	1.00
Minimum Headway [s]	0.00	1.70

The traffic sign, located at the entry lane of each roundabout, reproduced the typical yield-rule of this type of intersection, in which vehicles approaching the roundabout must give way to the circulating traffic flow. Then, detectors were opportunely located at the entries and on circulating lanes, for checking, at any simulation step, the total number of vehicles travelling in a section, included their speed. After that, the type of vehicles travelling on the infrastructure was chosen. In VISSIM, the class of private transport vehicles is classified in categories like trucks, cars, bikes, and pedestrians; for each of them specific features - like vehicle length, width, acceleration and deceleration rates, maximum speed and so on- can be specified. In this case, the car class was selected as a category of vehicles travelling on the roundabouts. As is well-known, VISSIM works with two microscopic traffic simulation models including *car following* and *lane change* logic; each of them has many parameters that affect vehicle interactions and thus the simulation results (for more details see e.g. [4]). In these case studies, the *car following* model was used for calibration of all roundabouts models and in particular the *Wiedemann 74* model was selected because it is more suitable for urban traffic. Since there are various parameters that users can set in this model, a sensitive analysis was conducted to establish which had more influence on simulation outputs. Finally, three parameters proved more sensitive and therefore were used for the calibration of the models: 1) *average standstill distance*, which is defined as the average desired distance between stopped cars; 2) *additive part of desired safety distance*"; 3) "*multiplicative part of desired safety distance*", which are parameters having a major influence on the safety distance and thus affecting the saturation flow rate.

Once the three roundabouts were represented in VISSIM, O/D matrices were assigned from all entries with due consideration to the directions of turn, in order

to reproduce a circulating flow (facing the subject entry) from 0 to 1400 veh/h, with step of 200 veh/h. A saturated condition was reached at each entry lane; the corresponding maximum number of vehicles approaching the roundabout, read through detectors appropriately positioned, gave the entry lane capacity.

Finally, manual calibration of the models built in VISSIM was performed by running the simulation many times, comparing the outputs of simulated capacity with the empirical capacity function, iteratively adjusting the model parameters. In order to obtain the calibrated models built in VISSIM, as close as possible to the AIMSUN ones, the empirical capacity function taken into account for calibrating the models with VISSIM software was the same as used during the calibration process of the models built in AIMSUN. Therefore, to perform this empirical capacity function the Hagring's model was used based on the meta-analytical estimation of the critical and the follow-up headways (see Chapter 4). Then, in order to establish a criterion for acceptance (or otherwise rejection) the model, the GEH index was used; this index makes it possible to compare the empirical capacities with the simulated capacity outputs from VISSIM. According to the definition of this index [15], a model can be considered calibrated if the deviation among simulated and observed values - in this case represented by the empirical capacities - is smaller than 5 in at least 85% of the cases (for more details see Chapter 4).

Figures 4, 5 and 6 show the microscopic models of the roundabouts built in VISSIM; for each roundabout the default values and set values of the model parameters used in the manual calibration procedure are listed in Tables 5, 6, 7
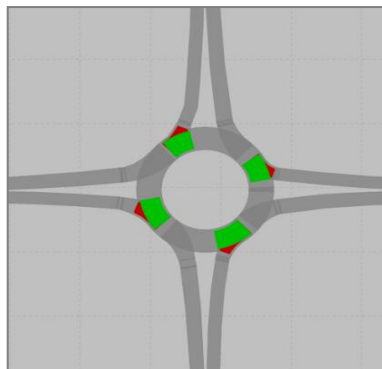

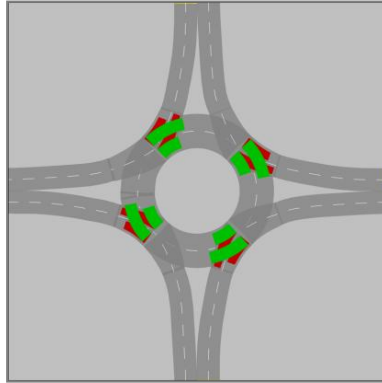**Figure 4** The VISSIM model of the single-lane roundabout

Figure 5 The VISSIM model of the double-lane roundabout

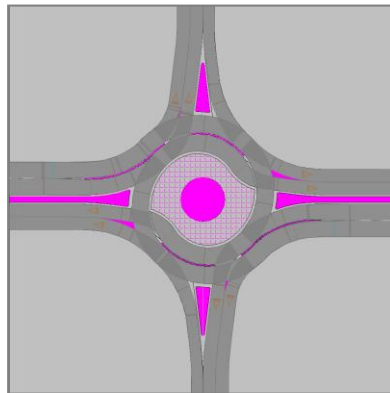**Figure 6** The VISSIM model of the turbo roundabout

Table 5 Default and set values of parameters used in manual calibration for the single-lane roundabout

VISSIM parameters	Default values	Set Value
Average Standstill Distance	2.00	5.10
Additive Part Of Desired Safety Distance	2.00	3.60
Multiplicative Part Of Desired Safety Distance	3.00	1.80

Table 6 Default and set values of parameters used in manual calibration for the double-lane roundabout

VISSIM parameters	Entry lane	Default values	Set Value
Average Standstill Distance	*Right*	2.00	1.80
	Left	2.00	4.50
Additive Part Of Desired Safety Distance	*Right*	2.00	3.05
	Left	2.00	5.00
Multiplicative Part Of Desired Safety Distance	*Right*	3.00	4.75
	Left	3.00	5.00

Table 7 Default and set values of parameters used in manual calibration for the turbo roundabout

VISSIM parameters	Default values	Set Value
Average Standstill Distance	2.00	5.00
Additive Part Of Desired Safety Distance	2.00	3.10
Multiplicative Part Of Desired Safety Distance	3.00	1.50

Therefore, for a single-lane roundabout a GEH index equal to 87.5% was obtained; the same result was achieved for the right entry lane of the double-lane roundabout, while for left entry lane, a GEH index of 100% was reached. Finally, for the turbo-roundabout, using the same calibration values both entry lane, the GEH index resulted equal to 87% and 75%, for the right entry lane and left entry lane, respectively. It should be noted that although, in the latter case the GEH index was below the percentage of 85%, each individual GEH_i value was just slightly higher than 5. Despite this last result, the models could be accepted as significantly able to reproduce the empirical data of capacity. This correspondence can also be seen from Figures 7 to 9 showing the simulated capacity obtained with manually calibrated VISSIM parameters and the empirical capacity.
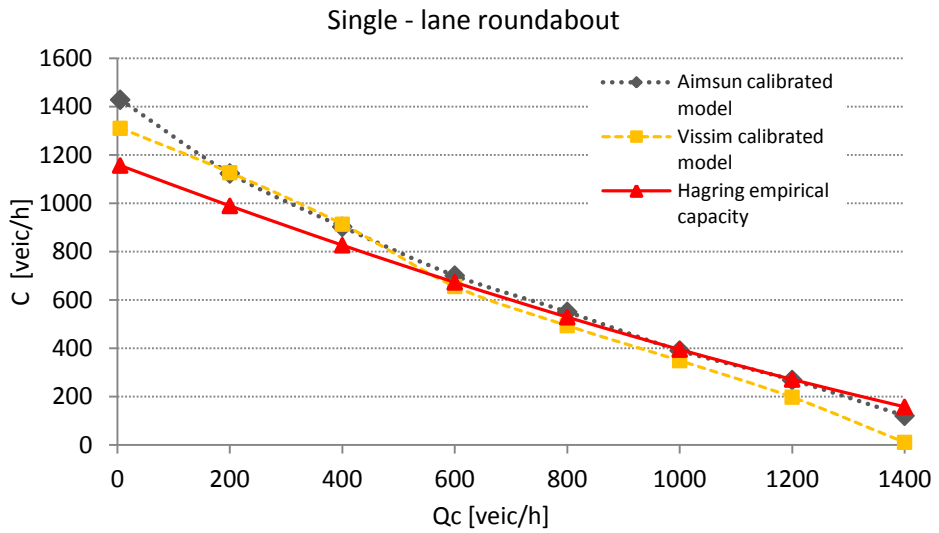
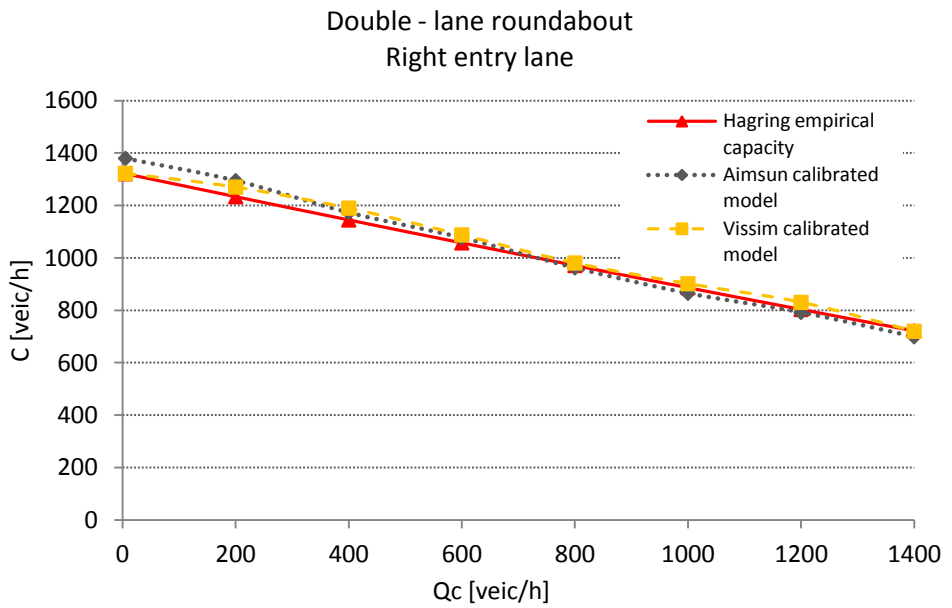**Figure 7** Simulated capacity from AIMSUN and VISSIM vs the empirical capacity function

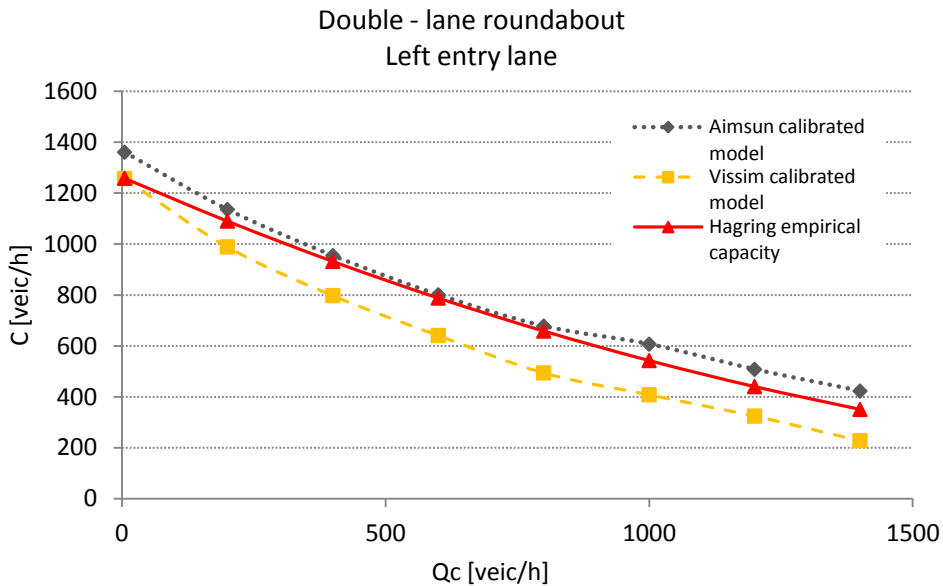**Figure 8** Simulated capacity from AIMSUN and VISSIM vs the empirical capacity function

209

Figure 9 Simulated capacity from AIMSUN and VISSIM vs the empirical capacity function

3.2. Development of traffic demand data input

In order to explore the influence that several traffic operational conditions could have on road safety, different traffic scenarios were simulated for each calibrated model by using three origin-destination matrices. These data were developed using an iterative process so as to ensure reproduction of a pre-fixed saturation ratio at each entry [12].

The three traffic situations here considered, corresponding to the three O/D matrices of traffic flow percentages, were the following (Tables 8, 9 and 10):

- case a) all percentages of turning and crossing traffic flow were assumed balanced;
- case b) crossing flow movements from and to major entries were assumed predominant over the other turning movements that were imposed in an equal percentage among left and right turn; in turn, left and right turning movements from minor to major entries were assumed predominant over through movements from and to minor entries with a prevalence for left turning movements over the right one;case c) similar to case b), left and right turning movements from minor to major entries were assumed, also this time, predominant over through movements from and to minor entries with the percentage of left and right turning movements now inverted in comparison to the case b).

Table 8 percentage origin/destination matrix for case a)

O/D	South	East	North	West
South	0	0.33	0.33	0.33
East	0.33	0	0.33	0.33
North	0.33	0.33	0	0.33
West	0.33	0.33	0.33	0

Table 9 percentage origin/destination matrix for case b)

O/D	South	East	North	West
South	0	0.30	0.05	0.65
East	0.05	0	0.05	0.90
North	0.05	0.65	0	0.30
West	0.05	0.90	0.05	0

Table 10 percentage origin/destination matrix for case c)

O/D	South	East	North	West
South	0	0.65	0.05	0.30
East	0.05	0	0.05	0.90
North	0.05	0.30	0	0.65
West	0.05	0.90	0.05	0

The next step consisted in implementing an iterative procedure to calculate the total capacity of the three roundabouts in order to ensure a pre-fixed saturation ratio at each entry; this research activity was developed based on the procedure introduced by Mauro [6]. The capacity at each entry was computed using the capacity formula used and referred by Brilon et al [16]:

$$C = A - B \cdot Q_c \quad (pcu/h) \tag{1}$$

in which the capacity is a simple linear relationship among the circulating flow, Q_c and two parameters, A and B, which depend on the number of circulating lanes and entry lanes as shown in the following Table 11:

Table 11 Values of the parameters referred by Brilon et al [16].

Circle lane number	Entry lane number	A	B	Sample size
3	2	1409	0.42	295
2	2	1380	0.50	4574
2-3	1	1250	0.53	879
1	1	1218	0.74	1504

It should be noted that for calculating the entry capacity at single-lane roundabout, the values of parameters A and B equal to 1218 and 0.74 were considered respectively, while for the double-lane roundabout selected as a study case the selected values for A e B parameters were 1380 and 0.50, respectively. Finally, for turbo-roundabouts, some assumptions were made. Since the major road was composed by two entry lanes facing only one circulating flow, the operation of both entry lanes could be associated with a single-lane roundabout; thus, A and B values were assumed equal to 1218 and 0.74, respectively. Instead, the minor road of the turbo roundabout was composed by two entry lanes where entering vehicles from the left-lane faced two antagonist circulating flows, and entering vehicles from the right-lane faced one circulating stream. Consequently, the values of parameters A and B, for calculating the entry capacity at the turbo roundabout, were specified according to the operation of each entry lane, i.e. assuming that operation was assimilable to a single-lane roundabout entry for the right-lane and a double-lane entry for the left-lane.

Once the formula for calculating capacity and the origin/destination matrix percentage were specified, in order to obtain the entering flows under the condition of under-saturation of the entries, the iterative procedure described in Mauro [12] was followed. This procedure starts by assigning in a totally arbitrary way a traffic demand, which represents an initial condition, through the following flow vector:

$$\left[Q_{ei}^{(1)}\right] = \left[Q_{e1}^{(1)} \ Q_{e2}^{(1)} \ Q_{e3}^{(1)} \ Q_{e4}^{(1)}\right]$$

A percentage origin/destination matrix $P_{O/D}$ should be also assigned.

After these assumptions, the iterative procedure is articulated in the following steps:

1. for entry "1", the antagonist circulating traffic flow is determined, $Q_{c1}^{(1)}$ as a function of the first attempt flow vector $\left[Q_{ei}^{(1)}\right]$ and of the matrix $\left[P_{ij}\right]$, and then, by using the capacity formula (1), there is found a new value of the entering flow at entry "1" $\left[Q_{e1}^{(1)^*}\right]$;

2. for entry "2", the method is the same as described in the first step, but in this case the circulating traffic antagonist for the entry "2", $Q_{c2}^{(1)}$, will be calculated as a function of the new update flow vector: $\left[Q_{ei}^{(1)}\right] = \left[Q_{e1}^{(1)^*} \ Q_{e2}^{(1)} \ Q_{e3}^{(1)} \ Q_{e4}^{(1)}\right]$ in which the value of the entering flow at entry "1" is replaced with that calculated at the previous step, i.e. with $\left[Q_{e1}^{(1)^*}\right]$. Then, applying the capacity formula (1), the entering flow at leg "2" is determined. Thus, at the end of this second step, the update flow vector will be $\left[Q_{ei}^{(1)}\right] = \left[Q_{e1}^{(1)^*} \ Q_{e2}^{(1)^*} \ Q_{e3}^{(1)} \ Q_{e4}^{(1)}\right]$;

3. for entries "3" and "4", the steps described above are repeated; thus at the end of the first iteration we should have the following vector of the entering flow: $\left[Q_{ei}^{(2)}\right] = \left[Q_{e1}^{(1)^*} \quad Q_{e2}^{(1)^*} \quad Q_{e3}^{(1)^*} \quad Q_{e4}^{(1)^*}\right]$, i.e. a first attempt vector of the entering flow;

4. the second iteration starts, considering as a vector of the entering flow the flow achieved at the end of the previous iteration, i.e. $\left[Q_{ei}^{(2)}\right]$ and then in order to obtain a vector of the entering flows, of the second attempt, the steps from one to three described above have to be followed. The iterations will end when convergence is achieved, until for two successive steps we obtain two equal vectors of the entering flows, i.e., $\left[Q_{ei}^{(k-1)}\right] = \left[Q_{ei}^{(k)}\right]$.

Finally the elements of the origin/destination traffic demand $M_{O/D}$ were obtained by multiplying each element of row "i" of matrix $P_{O/D}$ by the corresponding element of the entering flow vector $\left[Q_{ei}^{(k)}\right]$.

It is to be noted that for all steps the capacity formula used for calculating the entering flows was multiplied by a saturation ratio that was fixed equal to 0.6.

Appling this iterative process, and considering a saturation ratio equal to 0.6, for the three roundabouts being studied and for all cases of the traffic percentage matrix, the origin-destination matrices were obtained.

Since the equation (1) does not provide a capacity calculation for turbo-roundabouts, as was specified above, some assumptions were made: all entry lanes of the major road and the right-entry lane of the minor road were treated as the entry lanes of a single-lane roundabout, and the left-entry lane of the minor road as a left entry lane of a double-lane roundabout. In addition, considering that this capacity formula is particularized according to the number of entry and circulating lanes, then two different demand matrices were calculated, i.e. one valid for the entry lanes of the major road and right entry lane of the minor road of the turbo roundabout and another one valid for the left entry lane of the minor road of the turbo roundabout. These matrices were appropriately combined with each other in order to obtain one matrix valid for all the entries of the turbo roundabout. The following Tables 12 to 20 show the traffic demand $M_{O/D}$ for the three roundabouts here studied.

Table 12 Single-lane roundabout demand data for case a)

O/D	South	East	North	West
South	0	168	168	168
East	168	0	168	168
North	168	168	0	168
West	168	168	168	0

Table 13 Single-lane roundabout demand data for case b)

O/D	South	East	North	West
South	0	111	18	240
East	30	0	30	542
North	18	240	0	111
West	30	542	30	0

Table 14 Single-lane roundabout demand data for case c)

O/D	South	East	North	West
South	0	261	20	120
East	33	0	33	589
North	20	120	0	261
West	33	589	33	0

Table 15 Double-lane roundabout demand data for case a)

O/D	South	East	North	West
South	0	211	211	211
East	211	0	211	211
North	211	211	0	211
West	211	211	211	0

Table 16 Double-lane roundabout demand data for case b)

O/D	South	East	North	West
South	0	157	26	341
East	35	0	35	637
North	26	341	0	157
West	35	637	35	0

Table 17 Double-lane roundabout demand data for case c)

O/D	South	East	North	West
South	0	365	28	168
East	38	0	38	682
North	28	168	0	365
West	38	682	38	0

Table 18 Turbo roundabout demand data for case a)

O/D	South	East	North	West
South	0	180	224	224
East	210	0	210	210
North	224	224	0	180
West	210	210	210	0

Table 19 Turbo roundabout demand data for case b)

O/D	South	East	North	West
South	0	129	31	404
East	36	0	36	643
North	31	404	0	129
West	36	643	36	0

Table 20 Turbo roundabout demand data for case c)

O/D	South	East	North	West
South	0	279	34	205
East	36	0	36	643
North	34	205	0	279
West	36	643	36	0

In order to extract trajectory files, traffic demand matrices thus obtained, were insert into AIMSUN and VISSIM, and for each calibrated model, fifteen replications of simulation, one hour each, were made. From all these replications five simulations among the ones that best replicated the O/D matrices were chosen.

4. Comparison Surrogate Safety Measures from AIMSUN and VISSIM micro-simulator

As introduced in section 1, Surrogate Safety Assessment Model (SSAM) software was used in this step. SSAM makes it possible to carry out a safety analysis of any road facility, by means surrogate safety measurement [17]; combining micro-simulation and automated conflict analysis, it allows to evaluate the safety performance of any road facilities by means of surrogate measures. Through the

vehicle trajectory file (TRJ.file from here on), generated by common traffic micro-simulators, SSAM analyzes the interactions among vehicles moving in the modelled road networks and determines whether or not each interaction satisfies the criteria to be deemed to involve a conflict. Thus, it calculates many surrogate measures of safety and classifies conflicts in three main categories. The following flowchart in Figure 10 shows the input and output data for SSAM.
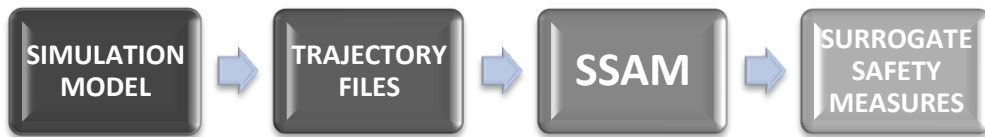

Figure 10 Flowchart: input and outputs data for SSAM

The SSAM software uses a series of algorithms to identify, classify, and evaluate surrogate measures of traffic conflicts that occur in the simulation model i.e. in the trajectory files. The technique to identify conflicts is explained briefly below; for more details, refer to the specific literature [3, 6]. The procedure starts with the definition of the width and height of the rectangular analysis area. The dimension of the area is determined basing on the trajectory file size. Then SSAM creates, for each trajectory file, a zone grid to cover the entire rectangular analysis area. For a single time step of a trajectory file, SSAM reads the speed of each vehicle located in the analysis region, and basing on this speed, projects over the next 10 seconds of trajectory data its future position; e.g. the future path for a generic vehicle A is composed of sequential segments each with two points representing the successive positions of the vehicle A (see Fig.11)
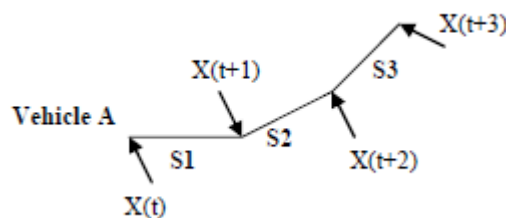

Figure 11 the future path for a generic vehicle A [3]

At this point, SSAM represents each vehicle with a rectangular perimeter delineating its location and orientation at its projected future position. Thus, it puts this rectangle (vehicle) on the grid and calculates which zones (rectangular) in the grid will contain at least some portion of that vehicle (see Fig.12).
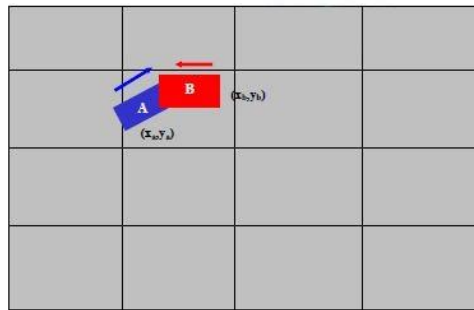
Figure 12 Checking Conflict Between Two Vehicles [3]

Whenever a new vehicle is added on the grid, it checks if that vehicle, represented by its rectangle, overlaps wholly or partly, another rectangle. If that happens, it means that a conflict has been identified among these two vehicles. Therefore, each time, SAAM updates a database listing all conflicts registered for each pair of vehicles, including type of conflict and its surrogate measures that are [3]:

- *minimum time-to-collision (TTC)*: defined as the minimum time-to-collision value observed during the conflict, i.e. the time between two vehicles that will collide with each other if they do not change their respective trajectories;
- *minimum post-encroachment time (PET)*: the time spent between the end of the crossing vehicle passage and the time at which the through vehicle actually reaches the collision potential point;
- *initial deceleration rate (DR)*: is the initial deceleration rate of the second vehicle, recorded as the instantaneous acceleration rate. If the vehicle brakes (i.e., reacts), this is the first negative acceleration value observed during the conflict. If the vehicle does not brake, this is the lowest acceleration value observed during the conflict;
- *maximum deceleration rate (MaxD)*: the maximum deceleration of the second vehicle, recorded as the minimum instantaneous acceleration rate observed during the conflict. A negative value indicates deceleration. A positive value indicates that the vehicle did not decelerate during the conflict;
- *maximum speed (MaxS):* the maximum speed of either vehicle throughout the conflict;
- *maximum speed differential (DeltaS):* defined as the magnitude of the difference in vehicle velocities (or trajectories), such that if v_1 and v_2 are the velocity vectors of the first and second vehicles respectively, then *DeltaS = |v_1 - v_2|*.

For better understand the meaning of the aforementioned surrogate safety measures, one can refer to the following Figure 13.
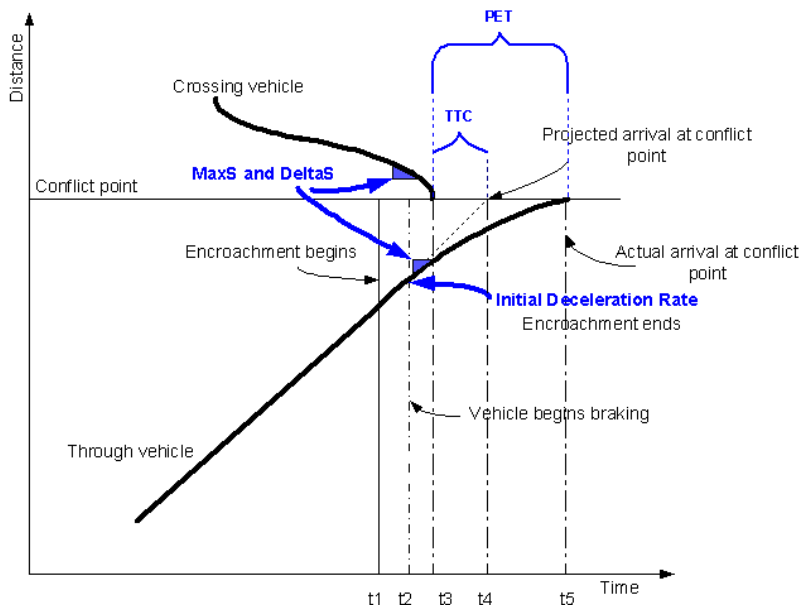
Figure 13 SSAM Safety Measures. Source: FHWA

In order to achieve the goal of this research activity, for each calibrated model (i.e. for the single-lane roundabout, the double-lane roundabout and the turbo roundabout), five simulation replications were run in AIMSUN and VISSIM so that the relative vehicles trajectory files were processed separately with the SSAM application for estimating surrogate measures.

In what follows, in order to distinguish the results of the SSAM obtained with the TRJ.file coming from the two micro-simulators chosen for this comparison, i.e. AIMSUN and VISSIM, we will call "SSAM-AIMSUN" the results of the SSAM software obtained elaborating the TRJ.file, coming from AIMSUN, whereas with "SSAM-VISSIM" we will refer to the SSAM results obtained with the TRJ.file coming from VISSIM.

Once the trajectory files were developed from the simulation process, the first step is represented by the loading of the trajectory file related to each simulation into the SSAM software. The SSAM software is made up of six folders: *Configuration, Conflict, Summary, Filter, Ttest* and *Map*, each of them with a specific function. TRJ.files were loaded in the "Configuration" folder, in which the analyst can set some conflict thresholds such as the *time to collision*, the *post-encroachment time*, the *rear-end* and *crossing conflict angle.* In this regard, it is useful to remember that the SSAM software, basing on the "conflict angle", i.e. the angle that the directions of two vehicles form during their conflict, classifies conflicts in: i) rear-end when this angle is between 0° and 30°; ii) lane-changing when it is between 30° and 85°; iii) crossing when this angle is greater than 85° (Fig. 14).
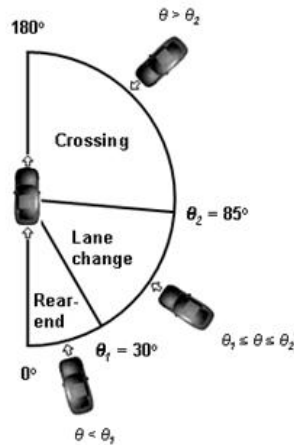
Figure 14 SSAM Conflict angle diagram

No threshold filter was initially applied; the maximum TTC value of 1.5 sec and the maximum PET value of 5 sec were left unchanged, that is were the default ones. The trajectory files were processed, and in the "Conflict" folder all the conflicts and the relevant surrogate safety measures recorded in all TRJ.files were listed. In the "Summary" folder, for each type of surrogate measure, the mean value, the maximum and minimum value and the variance of them, calculated based on all conflicts recorded, are shown. In other words, in the "Summary" folder the statistics for each surrogate measure (i.e. mean, max, min, and variance value), calculated according to conflicts listed in the "Conflict" folder, are shown. Moreover, the "Summary" folder shows both the number of the total conflicts - classified for typology (i.e. rear-end, crossing and lane-change) - recorded in all trajectory files and the number of the conflicts recorded in each single TRJ.file. In the "Filter" folder it is also possible to set the value thresholds to the surrogate measures registered by the SSAM, i.e. it is possible to filter the results obtained. It is noteworthy that, since the aim, at least in this first phase, was to make a comparison between the results of the "SSAM-AIMSUN" and "SSAM-VISSIM" leaving the SSAM default filters, no threshold filter was applied in the "Filter" folder. Finally, in the "Map" folder it was possible to see not only the location of conflicts on each roundabout but, through icons of different shapes and colours, it was also possible to identify immediately the position of the different types of conflicts.

Therefore, five trajectory files coming from the two micro-simulators and related to each roundabout, were elaborated by SSAM, obtaining thus, for each of them the surrogate safety measures.
The results obtained by the comparison between "SSAM-AIMSUN" and "SSAM-VISSIM" show a significant difference in the number of conflicts detected by SSAM processing TRJ.files as derived from the two micro-simulators. As can be seen

from the following histograms in Figures 15, 16 and 17, that show the mean values of normalized total conflicts provided by AIMSUN and VISSIM, this difference between the output derived from the two micro-simulator is more evident for the double-lane and turbo roundabouts. In fact, for the single-lane roundabout the percentage of total conflicts varies between 12% and 35%, depending on the traffic scenarios considered (i.e. case a, b or, c in Tables 8-10); this percentage reaches up to 90% for the turbo roundabout; see "case a" in Figure 17.

In addition, for both software, the number of potential conflicts seems to be quite high for a one-hour simulation. Indeed, especially with TRJ. file coming from AIMSUN, SSAM found a higher number of conflicts at the turbo roundabout for the traffic scenarios identified as cases a) and b), than the double-lane roundabout.
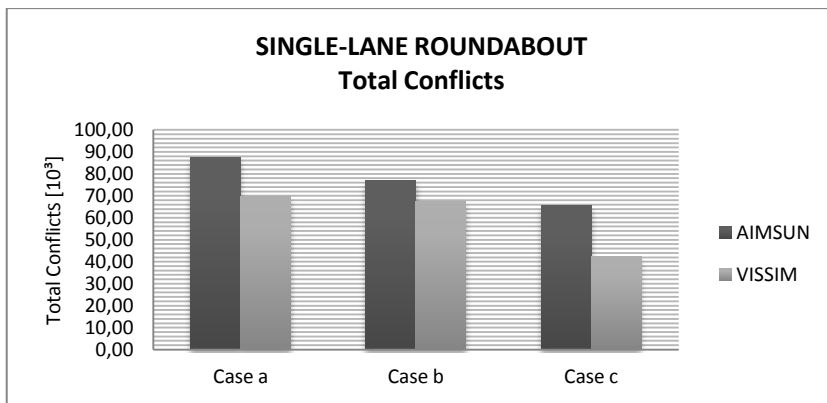

Figure 15 - Comparison AIMSUN vs. VISSIM, total conflicts - in different traffic scenario at single-lane roundabout - elaborated with SSAM default filters
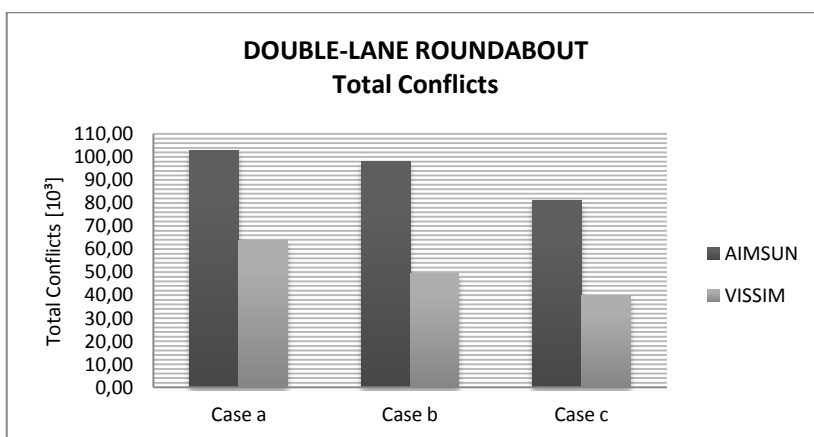

Figure 16 Comparison AIMSUN vs. VISSIM, total conflicts - in different traffic scenario at double-lane roundabout elaborated - with SSAM default filters
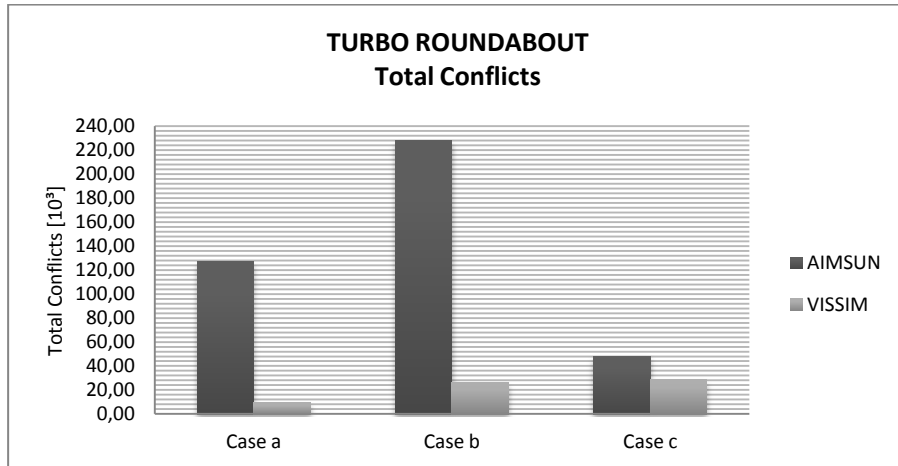
Figure 17 Comparison AIMSUN vs. VISSIM, total conflicts - in different traffic scenario at turbo roundabout - elaborated with SSAM default filters

Based on the above results, it was considered necessary to set the SSAM software modifying the thresholds of the filters, to make the safety analysis independent of the micro-simulator used. In this case, a sensitive analysis was also conducted to identify which filters have an influence on SSAM results. According to several researches about this issue [18-22], there are two main SSAM parameters that affect the results: *"Time To Collision"* (TTC) and *"Post-Encroachment Time"* (PET), whose meaning has already been specified above.

TTC and PET are both indicators of collision likelihood; a smaller value of these, during a conflict event, indicates a higher probability of a collision. The *"Max Speed"*, defined as the maximum speed of either vehicle throughout the conflict, was identified as parameter that affects SSAM results [18].

In order to select adequately a threshold value for TTC and PET, several studies was take into account on the subject. Many researchers agree that conflicts with a TTC value of less than 1.5 sec indicate a high probability of collision and therefore consider this value as the maximum threshold [17, 18]. By contrast, there are few references about the critical PET threshold, but in any case, it is clear that a low value of this parameter indicates a higher probability of an accident; moreover, by definition, the value of PET should be greater than the TTC.

Thus, after several trials, in the "Configuration" folder TTC and PET threshold values were set respectively of 1.5 and 2.5 sec, for all study cases. In addition, a more restrictive value for PET was applied for all traffic scenarios considered (i.e. cases a, b and c of the double-lane roundabout scheme only).

For all traffic scenarios examined at double-lane roundabouts, a maximum value of 1.9 was set for conflicts processed with VISSIM trajectory files. This maximum value of PET is nothing other than the one recorded by SSAM with the AIMSUN trajectory files.

By contrast, the *"Max Speed"* threshold value was specified on the basis of the roundabout layouts considered. A minimum threshold value of the *"Max Speed"* was applied for all traffic scenarios examined at single-lane and turbo roundabouts, specifically equal to 1.0 and 1.18, respectively. No filter of the *"Max Speed"* was applied to double-lane roundabouts.

It should be noted that in the "filter" folder, if SSAM registered a minimum value of TTC and PET equal a zero, these thresholds were increased up to 0.1. Indeed, according to [18,23], zero values of TTC and PET represent a mere processing error and for this reason it is necessary to delete them. Moreover, comparing conflicts placed in the network, obtained with input data from AIMSUN and VISSIM, it was realized that VISSIM identified conflicts that were very far from the intersection area, i.e. several conflicts were also identified on the legs of the roundabout, upstream of the intersection. For this reason, a filter around the area of interest was applied. Thus, the comparison - about the number of conflicts detected by the SSAM with TRJ input file coming from AIMSUN and VISSIM - only provided conflicts that fell within a 30-meter radius of each roundabout entry.

As one can see in the following Figures 18-20, by applying the aforementioned filters, a good fit was obtained for the frequency of conflicts derived from AIMSUN and VISSIM. Indeed, the percentage difference of total conflicts reported with files from the two micro-simulators does not exceed, in any traffic scenario examined, the percentage of 30%.
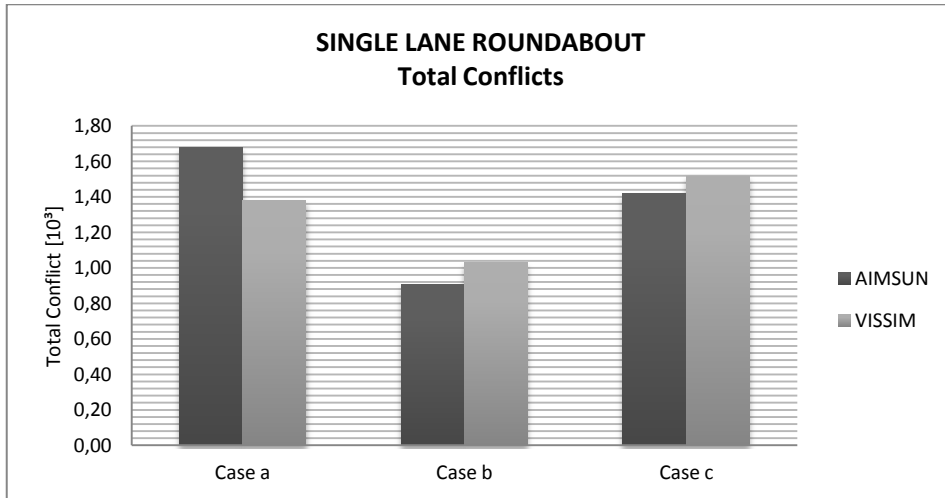

Figure 18 Comparison AIMSUN vs. VISSIM, total conflicts - in different traffic scenario at single-lane roundabout - elaborated with the thresholds of the SSAM filters modificated
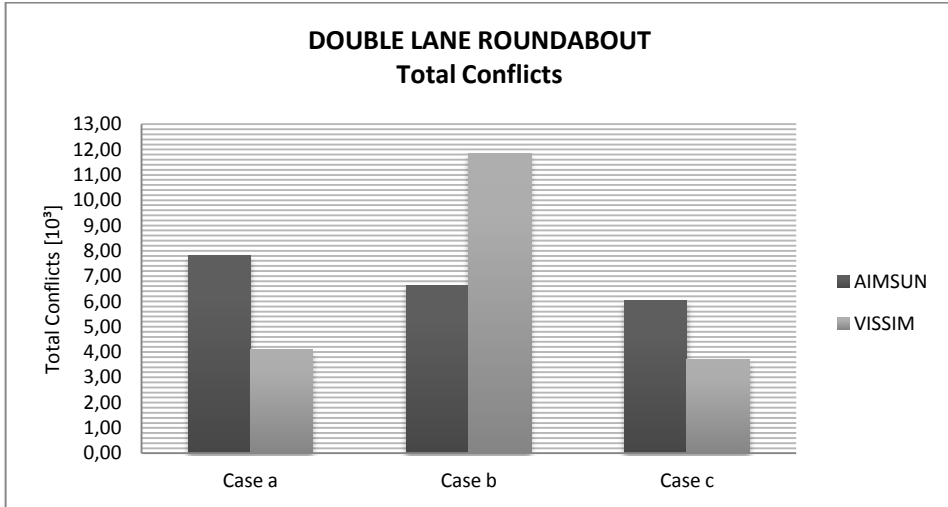
Figure 19 Comparison AIMSUN vs. VISSIM, total conflicts - in different traffic scenario at double-lane roundabout - elaborated with the thresholds of the SSAM filters modificated
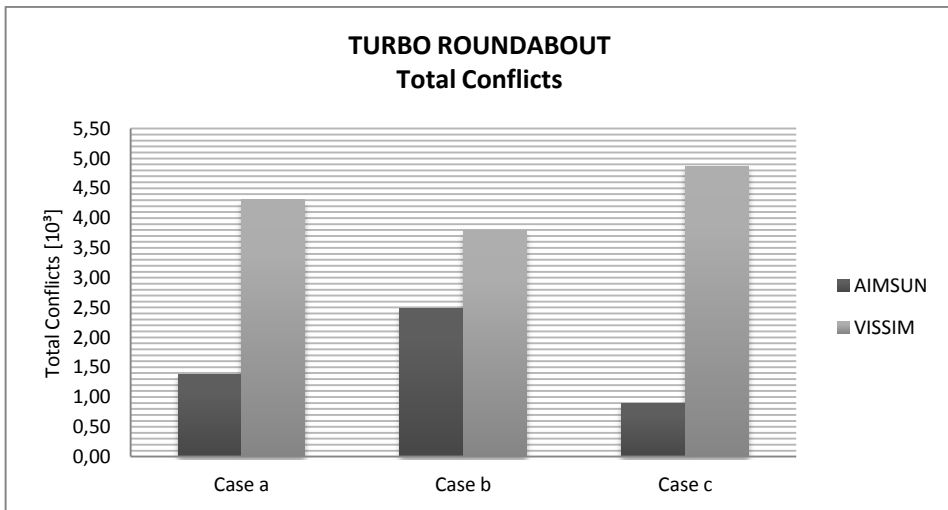
Figure 20 Comparison AIMSUN vs VISSIM, total conflicts - in different traffic scenario at turbo roundabout - elaborated with the thresholds of the SSAM filters modificated

A comparison of the total conflicts by using the T-Student distribution for hypothesis testing was also made. The Student's T Test, in generally way, compares two average values and allows to establish if these are different from each other, i.e. if the samples come from the same population. In this case, the two samples were represented by the result of elaborating SSAM on five TRJ file from AIMSUN and VISSIM. Therefore, under the hypothesis that the two sample, N1 and N2, of magnitude equal to 5, were extracted from a Normal population with the same mean-square deviation $\sigma^1 = \sigma^2$, a statistic T-test was performed only

223

for all the total conflicts as recorded by SSAM with TRJ. coming from VISSIM and AIMSUN for each roundabout under different traffic conditions.

T-test was conducted with two levels of significance, α=0.01 and α=0.05; thus based on the hypothesis H_0: $\mu_1=\mu_2$, i.e. the two sample means are equal each other, if the result of the test will lead to accept the hypothesis H_0, then there will be no significance in the difference between the sample averages; otherwise, it will be said that the difference between the two sample means is significant. Furthermore, the SSAM application is able to make this test automatically, loading two files in the "T-test" folder. The results of the T-test, showed in the following Tables 21-23 highlight that the T-test was no significant for all the case a), b) and c) at single-lane roundabouts, that means that there is no significant difference between the means μ_1 and μ_2 of the two samples (i.e. SSAM-VISSIM and SSAM-AIMSUN results); the same result was achieved for the turbo roundabout. Since the T-test resulted significant for all case at double-lane roundabout, especially when α=0.05, one can say that there is a significant different between the means of the two samples.

Table 21 Vissim-Aimsun T-test result for single-lane roundabout, case studies a), b), c).

	AIMSUN		VISSIM			T-student α=0.05		T-student α=0.01	
	Mean	Var.	Mean	Var.	T-Value	T Critical	Significant	T Critical	Significant
CASE A	3,40	2,30	2,80	0,20	0,85	2,31	NO	3,36	NO
CASE B	1,75	0,25	2,00	1,00	0,45	2,31	NO	3,36	NO
CASE C	3,00	2,00	3,20	0,70	0,30	2,31	NO	3,36	NO

Table 22 Vissim-Aimsun T-test result for double-lane roundabout, case studies a), b), c).

	AIMSUN		VISSIM			T-student α=0.05		T-student α=0.01	
	Mean	Var.	Mean	Var.	T-Value	T Critical	Significant	T Critical	Significant
CASO A	19,60	13,30	23,80	0,20	2,56	2.31	YES	3.36	NO
CASO B	16,20	1,70	22,60	0,30	10,12	2.31	YES	3.36	YES
CASO C	16,00	10,00	19,60	12,80	1,68	2.31	NO	3.36	NO

Table 23 Vissim-Aimsun T-test result for turbo roundabout, case studies a), b), c).

	AIMSUN		VISSIM			T-student α=0.05		T-student α=0.01	
	Mean	Var.	Mean	Var.	T-Value	T Critical	Significant	T Critical	Significant
CASE A	3,40	2,80	2,60	3,80	0,70	2.31	NO	3.36	NO
CASE B	6,20	1,20	6,00	11,00	0,13	2.31	NO	3.36	NO
CASE C	2,20	0,70	3,00	3,50	0,90	2.31	NO	3.36	NO

Since a safety analysis of any road facility trough surrogate safety measurements can be conducted by a lot of common micro simulators like AMSUN, VISSIM, PARAMICS etc, setting filters in SSAM is strictly necessary in order to have similar output data, in term of number of conflicts. Overall, a good correlation between

the simulated conflicts by AIMSUN and VISSIM were obtained after adjusting some SSAM parameters, especially setting lower values of the Time-To-Collision and Post Encroachment Time than default ones and also eliminating those conflicts that provided a zero value them.

This result is in part confirmed by T-test, in order to compare the SSAM-VIISM and SSAM-AIMSUN results for all roundabouts under examination and each of them also for all traffic condition that was take into account (i.e. case a, b, c). Indeed, the statistic T-test resulted no significant for the single-lane and turbo roundabout, on the contrary this test for double-lane roundabout had turned out significant, especially for a level significance equal to 0.05. Finally, concerning to implications that different scenarios could have on safety performance at roundabouts, it is possible to state that a different flow distribution at roundabouts provides a different number of conflicts; thus, for the same roundabout scheme exists a traffic scenario that provides less potential crashes than another traffic scenario.

The comparison about the surrogate safety measures at roundabouts based on the simulated trajectories as derived from the two traffic microsimulation models here used, has allowed to set SSAM filters in order to have a comparable frequency of conflicts. The results are sufficiently encouraging to suggest that this line of research should continue, with a view to that use of simulated conflicts is a viable, promising approach for estimating the roundabout safety performance. Moreover, the outcome of this research activity could represent the starting point to address, in the near future, issues associated with the development of safety prediction models for roundabouts.

References

1. Amundsen, F. and Hyden, C. Traffic conflicts. Proceedings of first workshop on traffic conflicts. 1977. Oslo: Institute of Transport Economics.
   Available at the website: http://www.ictct.org/wp-content/uploads/LIB_Amundsen_Hyden_1977.pdf
2. Vasconcelos L., Leto L., Seco A.M., Silva B.S. Validation of Surrogate safety Assessment Model For Assessment of intersection safety. Transportation Research Record: Journal of the Transportation Research Board, No. 2432, Transportation Research Board of the National Academies, Washington, D.C., 2014, pp. 1–9.
3. Gettman D.,Pu L., Sayed T.,Shelby S. Surrogate Safety Assessment Model and Validation: Final Report. June 2008.
4. PTV VISSIM User Manual. PTV Planung Transport Verkehr AG, Karlsruhe, 2012.
5. AIMSUN Dynamic Simulator User Manual, Transport Simulation System (TSS) version 8, Barcelona, 2011.
6. Gettman D. & Head L. Surrogate Safety Measures from Traffic Simulation Models Transportation Research Record 1840 Paper No. 03-2958_200.
7. Essa M & Sayed T. Transferibility of calibration microsimulation model parameters for safety assessment using simulated conflicts. Accident Analysis and Prevention 84 (2015) 41–53.
8. Quadstone Paramics: (2015). [Online] QuadstoneParamics. Accessed Feb 2015.
9. Chen P.,. Zeng W, Yu G. and Wang Y. Surrogate Safety Analysis of Pedestrian-Vehicle Conflict at Intersections Using Unmanned Aerial Vehicle Videos. Hindawi Journal of Advanced Transportation Volume 2017.
10. Vasconcelos L., Silva B.S., Seco A. Safety analysis of turbo-roundabouts using SSAM tecnique. CITTA 6th Annual Conference on Planning Research Responsive Transports For Smart Mobility.
11. Norme funzionali e geometriche per la costruzione delle intersezioni stradali [Functional and geometric standards for the construction of road intersections] (2006) Ministero Infrastrutture e Trasporti [Minister of Infrastructure and Transport], in Italian.
12. Mauro, R. 2010. *Calculation of Roundabouts: Capacity, Waiting Phenomena and Reliability*. Berlin Heidelberg: Springer.
13. O. Giuffrè, A. Granà, S. Marino, F. Galatioto, Microsimulation-based passenger car equivalents for heavy vehicles driving turbo-roundabouts, Transport 31 (2) (2016) 295-303.
14. O. Hagring, A further generalization of Tanner's formula, Transportation Research Part B: Methodological 32(6) (1998) 423–429.

15. Barceló J. Fundamentals of Traffic Simulation. International Series in Operations Research & Management Science. Volume 145. DOI 10.1007/978-1-4419-6142-6 Springer New York Dordrecht Heidelberg London (2010).

16. Brilon W., Wu, N. and Bondzio, L. (1997). Unsignalized Intersections in Germany – A State of the Art 1997, Proceedings of the Third International Symposium on Intersections Without Traffic Signals, pp. 61–70, Portland, Oregon, USA, July 1997.

17. Surrogate Safety Assessment Model (SSAM)–SOFTWARE USER MANUAL Publication Number: FHWA-HRT-08-050, May 2008, available at: https://www.fhwa.dot.gov/publications/research/safety/08050/

18. Saleem T., Persaud B., Shalaby A., Ariza A. Can Microsimulation Be Used to Estimate Intersection Safety? Case Studies Using VISSIM and Paramics. Transportation Research Record: Journal of the Transportation Research Board, No. 2432, Transportation Research Board of the National Academies, Washington. D.C., 2014, pp. 142–148.

19. Duong D.D.Q., Saccomanno F.F. Hellinga B.K.. Calibration of microscopic traffic model for simulating safety performance. Compendium of papers of the 89th Annual TRB Conference held Jan. 10 – 14, 2010 in Washington, DC. Revised November 15, 2009.

20. Fan R., Yu H., Liu P., Wang W.Using Vissim simulation model and Surrogate Safety Assessmnet Model for estimating field measured traffic conflicts. IET Intell. Transp. Syst., 2013, Vol. 7, Iss. 1, pp. 68–77.

21. Ozbay J. J et al.Derivation and Validation of a New Simulation based surrogate safety measure Transportation Research Part C_2014 Elsevier.

22. Sobhani A. Young W. Sarvi M. A simulation based approch to assess the safety performance of road locations. Transportation Research Part C 32 (2013) 144-138 Elsevier.

23. Saulino G., Persaud B., Bassani M. Calibration and application of crash prediction models for safety assessment of roundabouts based on simulated conflicts. Transportation Research Board 94th Annual Meeting Compendium of Papers, 2015.

CONCLUSION
Findings and Future Developments

Several studies and researches have shown that modern roundabouts are safe and effective as engineering countermeasures for traffic calming. The increasing use of roundabouts around the world and, more recently, turbo roundabouts, has induced a great variety of experiences in the field of intersection design, capacity modeling and traffic safety. As for unsignalized intersections, which represent the starting point to extend knowledge about the operational analysis to roundabouts, the general situation in capacity estimation is still characterized by the discussion between gap acceptance models and empirical regression. However, capacity modeling must contain both the analytical construction and then solution of the model, and the implementation of driver behavior. Thus, issues on a realistic modeling of driver behavior by the parameters that are included into the operational analysis are always of interest for practitioners and analysts in road infrastructure engineering. In turn, safety issues at roundabouts as for any road entity, concern the use of direct measures of road safety and, more recently, surrogate measures of safety. It is well-known that crash frequency and severity are direct measures of road safety; in turn, road safety analysis has traditionally been undertaken using crash data. However, there are well-known problems associated with availability and quality of crash data. To name but a few, crash data are not always sufficient due to small sample sizes or incomplete set of recorded data. In relation to certain critical elements such as the lack of details to improve understanding of crash failure mechanism and the driver crash avoidance behavior, crash analysis can lead to inconclusive results. The use of crash records for safety analysis represents a reactive approach: a significant number of crashes needs to be recorded before an action can be taken. This also reduces the ability to examine the safety effects of a recently implemented safety countermeasure, although the Highway Safety Manual (2010) gives a comprehensive approach to measure road safety. Because of these issues, road safety analysis can benefit from reliable analysis methods that utilize observable non-crash traffic events and other surrogate data instead of road crashes.

It should be noted that microscopic traffic simulation models have become increasingly useful tools for the advanced analysis of transport systems and have proven to be an active field of research in computer science and transportation engineering. As introduced in the Chapters of this PhD thesis, advances in research and current application to road and highway planning and design over the last few years have outlined their great potential to assess operational performances and safety effects on road facilities, since they can support the evaluation of road policy and infrastructure changes before implementing them in the real world. However, traffic microsimulation models normally include a large number of parameters that must be calibrated before the model can be used as a tool for

prediction. Several methodologies for calibrating such models has been recently proposed in the literature, but there have been no attempts to identify general calibration principles based on a collective experience in transportation engineering.

Starting from these considerations, firstly, this PhD thesis presents a literature review about the key methodological issues in the operational and safety analysis of modern roundabouts. Focus is made on the aspects associated with the gap acceptance behavior, the derivation of the analytical-based models, and the calculation of parameters included into the capacity equations, as well as steady-state conditions and uncertainty in entry capacity estimation. And after, the issue of calibration of microscopic traffic simulation models has been given a big role; indeed, this PhD thesis focused on calibration of microscopic traffic simulation models since they can represent useful tools to evaluate operational and safety performances at roundabouts. Case studies of roundabouts are selected and built in AIMSUN and then VISSIM in order to perform the calibration process appropriately.

With that said, based on what has been outlined in the Foreword of this PhD thesis and through the successive chapters, the main findings of the thesis are as follows:

 – *based on a systematic literature review on estimations of critical and follow-up headways at roundabouts a meta-analysis of effect sizes was performed as part of the literature review through the random-effects model (see Chapter 2). Since several studies and researches developed worldwide were examined, and then the effect size varied from study to study, the dispersion in effects across studies was assessed and the summary effect for each of the parameters under examination was computed. Calculations were made both for single-lane and double-lane roundabouts, as well as for turbo roundabouts. Compared to the results of individual studies, the single (quantitative) meta-analytic estimate provided an accurate and reliable synthesis on the specific issue here addressed. Thus, this research activity highlighted that the meta-analysis gives, with greater power of the individual reviewed studies, a comprehensive measure for the parameters of interest.*

 – *Based on the use of the Monte Carlo simulation to get the distribution of entry capacity at roundabouts and then Crystal Ball software to perform the random sampling from the probability density functions of each contributing parameter (i.e. the critical headway and the follow up headway), the entry capacity distributions at roundabouts were presented (see Chapter 3). The results of the analysis performed in this research activity were expressed probabilistically, meaning that the probability distributions of capacity rather than the simple point estimates should be obtained. The comparison of the capacity values based on a meta-analytic estimation of each contributing parameter and the capacity functions*

based on the probability distributions of the model parameters, gave more insights in managing uncertainty in capacity estimations and developing an appropriate approach to capacity modeling at roundabouts.

– *The research activity in Chapter 4 focused on the genetic algorithm-based calibration procedure for a microscopic traffic simulation model for single-lane and double-lane roundabouts. For both case studies, the genetic algorithm tool in MATLAB® was applied in order to reach the convergence between the outputs from Aimsun microscopic simulator and the empirical capacity functions once again based on the meta-analytic estimation of critical and follow up headways. The automatic interaction with AIMSUN was implemented through an original external Python script. Results showed that the genetic algorithm-based calibration procedure gave a better match to the empirical capacity functions than simple manual calibration and the efficiency of the calibration efforts resulted significantly improved.*

– *The calibrated model was then applied to calculate the Passenger Car Equivalents (PCEs) for heavy vehicles driving roundabouts, since they represent the starting point for operational analysis of road and intersections (see Chapter 5). In this regard, a criterion is proposed which implies a comparison between the capacity that would occur with a traffic demand of passenger cars only and the capacity reached starting from a traffic demand with a certain percentage of heavy vehicles. Traffic microsimulation was used to evaluate the variation of the traffic quality in presence of mixed fleets, varying the percentage of trucks in traffic demand. Simulation experiments were conducted in AIMSUN using the calibrated model to produce the base capacity function and the mixed capacity functions for each entry lane. Based on the output of multiple simulation runs, the capacity functions for each entry lane of the roundabouts were developed and PCEs for heavy vehicles were calculated by comparing results for a fleet only made of passenger cars with those of the mixed fleets under different percentages of heavy vehicles. However, for all entry lanes, analogous trends were observed: PCEs increased when the circulating flow increased (i.e. the circulating flow on the ring at the single-lane roundabout, and the outer lane of the ring for the right entry lane at double-lane roundabout; two circulating flows - one in the outer lane and one in the inner lane of the ring – were identified for the left lane of the double-lane roundabout for which surface plots of the PCEs were obtained); besides, PCEs increased when the traffic streams contained a higher number of heavy vehicles. The differences between the values of PCEs estimated in this chapter and the HCM values for PCEs were briefly described: if one assumes $E_t = 2$ according to the Highway Capacity Manual (2010), the impact of heavy vehicles on the traffic flow quality, even in usual operational conditions (i.e. a mixed fleet with 10%, 20% or 30*

230

% of heavy vehicles), can be misunderstood. Although the results of this research activity have been found to be consistent with the conclusions already drawn from literature (as discussed in Chapter 5), and the knowledge that they can be influenced by the assumptions with regard to user behaviour and the single class of heavy vehicles only used, this study gave some indication of the application of the proposed criterion for the capacity-based calculation of PCEs at roundabouts.

- *At last, issues on safety analysis through microscopic traffic simulation models are also addressed (see chapter 6). Two traffic microsimulation models ere applied, since safety assessment of any road entity can be very different depending on the micro-simulator which is used Specifically, the safety performance of single-lane, double-lane and turbo roundabouts through surrogate measures of safety was explored. For each roundabout under examination, a comparison was performed based on the outcome derived from VISSIM and AIMSUN. Thus, AIMSUN and VISSIM were used to built, for each roundabout, a calibrated model which was able to fit the same empirical capacity function (one for each roundabout), based on a meta-analytic estimation of the critical and follow-up headways. Furthermore, in order to explore the implications of various traffic volume distributions on the safety performance of the selected roundabouts, different traffic flow scenarios were simulated. For each roundabout, base dont the simulated vehicle trajectories exported from AIMSUN and VISSIM, a conflict analysis through the Surrogate Safety Assessment Model (SSAM was performed). The SSAM results processed from the two traffic microsimulation models provided a very high number of potential conflicts when the SSAM default filters were used. Since the output from the two software resulted strongly different, some SSAM filters were set iteratively. The comparison about the surrogate safety measures based on the simulated trajectories derived from AIMSUN and VISSIM, allowed to set SSAM filters in order to have a comparable frequency of conflicts as confirmed by statistical tests.*

Despite this research presented in this PhD thesis is the first analysis for roundabouts that I made, it should be noted that, in order to automate the calibration process, the formulation of AIMSUN calibration as an optimization problem and the GA-based approach here proposed appeared to be effective. The comparison between the empirical data and the simulation results gave insights into the performance of the calibration procedure, consistently with the sensitivity analysis and manual calibration that had highlighted no further need of a higher number of calibration parameters. However, given the nature of this analysis, a positive finding would probably not be definitive, but would address a direction for additional research.

Another important aspect in the research is the method proposed to evaluate the impact of heavy vehicles on traffic conditions, since it is an essential component in the estimation of the roundabout capacity. It should be noted that the case in which the heavy vehicle composition in the traffic flow consisted only of a subject type of heavy vehicle might be more elucidative to better understand the effect of this group of heavy vehicles on the operational performance of the intersection; by the way, analysts often have difficulties in finding roundabouts in operation or any other locations with extensive heavy truck traffic. Moreover, the method developed and tested to estimate PCEs for roundabouts, it is quite general and applicable to other intersercion layouts. The criterion proposed for PCE calculation could be applied to other case studies of more complex multi-lane roundabouts and/or roundabouts at ramp terminals and suggest how to address further problems that practitioners usually face using traffic microsimulation in professional life; however, the same criterion of PCE calculation should be specified to explore in the near future more classes of heavy vehicles.

At last, the comparison about the surrogate safety measures at roundabouts based on the output derived from the two traffic microsimulation models here used, has allowed to set SSAM filters in order to have a comparable frequency of conflicts. With the understanding that there is still very to do regarding safety modeling through traffic microsimulation models, The results are sufficiently encouraging to suggest that this line of research should continue, with a view to that use of simulated conflicts is a viable, promising approach for estimating the roundabout safety performance. Moreover, the outcome of this research activity could represent the starting point to address, in the near future, issues associated with the development of safety prediction models for roundabouts.

Since modern roundabouts are not only capable of improving traffic flow but they can as well cut down vehicular emissions and fuel consumption by reducing the vehicle idle time at intersections and thereby creating a positive impact on the environment, future research objectives could regard the study of the impact of roundabouts in cutting down vehicular emissions. This could create a broader framework when the benefit–cost analysis method, used for most public works and transportation projects, should be applied to aid decision about the best suitable solution for a (selected) location based on the type of problem susceptible to correction by the roundabout alternative.